Durham E-Theses

The role of L-ascorbic acid in S-nitrosothiol decomposition and aspects of the nitrosation of thiones

Holmes, Anthony J.

The Role of L-Ascorbic Acid in *S*-Nitrosothiol Decomposition and Aspects of the Nitrosation of Thiones

Anthony J. Holmes BSc GRSC

Thesis submitted for the degree of

Doctor of Philosophy

University of Durham

September 2000

Abstract

Ascorbic acid has been found to promote nitrosothiol decomposition *via* two pathways. In the first, ascorbic acid acts as a reducing agent for added or adventitious copper (II), producing copper (I). This reacts with the nitrosothiol, giving nitric oxide and disulfide as the ultimate products. The reaction requires only small quantities of ascorbic acid, and is catalytic in copper.

The second pathway requires higher concentrations of ascorbic acid, the stoichiometry being one mole of ascorbic acid to two moles of nitrosothiol. The products are nitric oxide and thiol, and the reaction has been interpreted in terms of rate limiting nucleophilic attack by ascorbate at the nitroso nitrogen, followed by decomposition of the O-nitroso ascorbate formed to nitric oxide and dehydroascorbic acid. The rate equation is first order in both the nitrosothiol and ascorbic acid, and the entropy of activation is significantly negative. pH – rate profiles reveal the ascorbate dianion is much more reactive than the monoanion, and that the neutral form has negligible reactivity.

Nitrosation of thione-containing nitrogen heterocycles by nitrous acid leads to the equilibrium formation of $=SNO^+$ species; large equilibrium constants are observed. The reactions exhibit many of the features generally observed in nitrosation, including catalysis by halides and thiocyanate, and some participation by dinitrogen trioxide as a nitrosating agent. The nitrosation rate constants are large, approaching values representing the encounter-controlled limit.

The $=SNO^+$ species are generally unstable, decomposing under acidic conditions to nitric oxide and a disulfide. Decomposition of *S*-nitrosated 4-thiopyridine showed hydrolysis occurs at pH 7.4, re-forming the thione. The nitroso species reacts rapidly with ascorbate, forming nitric oxide and thione.

Declaration

The work in this thesis was carried out in the Chemistry Department at the University of Durham between 1st October 1997 and 30th September 2000. It has not been submitted for any other degree and is the author's own work, except where acknowledged by reference.

Copyright

Acknowledgements

I would like to thank my supervisor, Professor Lyn Williams, for his help during my PhD studies. I acknowledge the financial support received from the EPSRC, and the University of Durham and ICI for graduate scholarships.

I feel I should probably thank all my lab colleagues for giving me plenty to laugh at over the last three years, especially Darren, Paul, Dave, Andy, Seve, Lynsey and Linda. I would put in some silly nicknames for them all, but Two Pint Wonder Darren would hit me. Ah, too late. Dave must be cursed for his persistence in leading me into public houses (hope you're not superstitious Dave). Thank you also to Colin Greenhalgh, for keeping all the equipment running.

A special thank you is due to my fiancée ♥Kathryn♥ for all her support, including the unfortunate task of proof reading this vast white elephant. May chicken dippers be on the menu for the many years of married life to come!

I would also like to thank my family for all their support throughout my PhD studies and the rest of my education. Indeed, the whole of my life. I will contemplate joining the real world eventually. Thanks also to Kathryn's parents for their kindness and hospitality. I would also like to thank my friend Craig, who hasn't really seen much of me over the last three years, and when he has we've been too drunk to recognise each other. That bit was a joke, by the way…

A special thank you is extended to one Anthony J. Holmes, who wrote this thing. I bet you all wished he hadn't!

I hope I haven't offended anybody during the above, other than those people I intended to.

There are many other people I would like to thank, but there isn't space.

Actually, there is a little bit of space. Just enough to praise the brilliance of the Goons, Fawlty Towers, Monty Python (but not the circus), Mr. Bean (I want to *be* him), Black Adder, Just a Minute, the News Quiz, the NOW! Show, and the other ones. In addition, I must say: Hooray! for glue, pens, paper, chairs, tables, food, and all of those other little objects we all use and take for granted every day.

There's still a bit of space left so I suppose I should really use it to thank the people I said I would thank if I had enough space to do so. Well, here goes. Thank you to

To the view along the East Coast and Midland Mainlines,
without which this would have been completed sooner

Chapters 3 – 6

Ascorbic Acid in the Decomposition Reactions of S-Nitrosothiols

Chapters 7 – 9

S-Nitrosation of Thione – Thiol Tautomeric Systems

Appendices

Introduction – the Chemistry of Nitrosation

Chapter 1 Introduction – The Chemistry of Nitrosation

Nitrosation is the addition of NO^+ to a chemical entity, alcohols, amines and thiols being amongst the most commonly used substrates. Nitrosation reactions are important in a number of industrial processes, including the formation of diazonium ions (which are important intermediates, for example in azo dye production), the manufacture of hydroxylamine and the production of alkyl nitrites for medicinal use. A comprehensive text covering the many aspects of nitrosation has been published.[1]

Any species capable of donating NO^+ is potentially useful as a nitrosating agent. Examples of species that have been utilised for this purpose are nitrous acid, dinitrogen trioxide and nitrosyl halides. These and other nitrosating agents and substrates are discussed in the following sections.

1.1 Reagents for Use in Nitrosation

1.1.1 Acidified Nitrous Acid and the Nitrosonium Ion

Acidified solutions of nitrous acid (easily prepared by acidifying nitrite salts such as sodium nitrite) have been widely used in nitrosation. Nitrous acid exists in *cis* and *trans* forms (Figure 1.1), microwave and infrared spectroscopy revealing the *trans* form to be favoured.[2] The relatively high energy barrier to rotation around the N–OH bond (45.2 kJ mol⁻¹) suggests that this bond has significant double bond character.
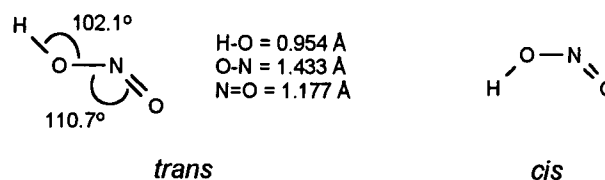
Figure 1.1 Structure of nitrous acid

Nitrous acid has not been isolated due to its instability, its decomposition in solution is rapid and occurs according to Scheme 1.1,[3] but it has been observed in the vapour phase.

$$3\,HNO_2 \rightleftharpoons 2\,NO + HNO_3 + H_2O$$
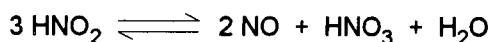
Scheme 1.1 Decomposition of nitrous acid

Nitrous acid exhibits a characteristic UV spectrum, consisting of a five-fingered band centred around 360 nm ($\varepsilon \approx 50$ dm^3 mol^{-1} cm^{-1}). The species is a weak acid, dissociating to nitrite. The pK_a for this process has been subject to uncertainty, but a value of 3.15 is generally accepted as the more accurate figure.[4]

Under very acidic conditions, nitrous acid exists in equilibrium with the nitrosonium ion (NO^+), the conversion being essentially quantitative in 60 % sulfuric acid (Scheme 1.2). The UV spectrum of NO^+ exhibits a peak at 260 nm,[5] and the ion possesses a Raman line [6] at 2 300 cm^{-1}.

$$H_3O^+ + HNO_2 \rightleftharpoons NO^+ + 2\,H_2O$$
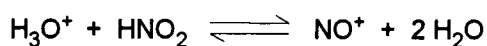
Scheme 1.2 Formation of NO^+ from nitrous acid

Nitrosation by acidified nitrous acid solutions proceeds according to the rate law given in Equation 1.1, which was first observed in 1958 for the diazotisation of anilines.[7] [S] represents the substrate concentration.

$$Rate = k[HNO_2][H^+][S] \qquad \text{Equation 1.1}$$

Two mechanistic interpretations have been proposed to explain the rate law in Equation 1.1. One involves the pre-equilibrium formation of $H_2NO_2^+$ (the nitrous acidium ion) which acts as the nitrosating agent, reacting with the substrate in the rate-determining step.[8] Alternatively, formation of NO^+ according to Scheme 1.2, followed by a direct reaction between NO^+ and the substrate in a slow step, also yields the rate law in Equation 1.1.[9] These two mechanistic interpretations are shown in Scheme 1.3.

$$HNO_2 + H^+ \rightleftharpoons H_2NO_2^+$$

$$H_2NO_2^+ \rightleftharpoons NO^+ + H_2O$$

$$H_2NO_2^+ + S \xrightarrow{\text{slow}} \text{Product}$$

$$NO^+ + S \xrightarrow{\text{slow}} \text{Product}$$
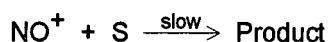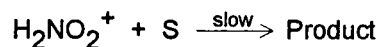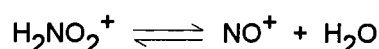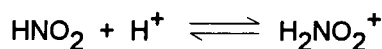
Scheme 1.3 Nitrosation of substrate S by acidified nitrous acid / NO^+

There has been contention regarding which mechanism is operating. There has been no direct observation of the nitrous acidium ion, though some ^{18}O exchange experiments have been interpreted in terms of $H_2NO_2^+$ being the active species under moderately acidic conditions.[10]   Under highly acidic conditions the nitrosonium ion is observed, and is therefore almost certainly the active nitrosating species. It has also been suggested that the nitrous acidium ion is best regarded as water solvated NO^+.[11]

Deviations from the rate law in Equation 1.1 have been observed during studies of nitrosations in acidified nitrous acid solutions, and can be explained by the formation of another active nitrosating agent, dinitrogen trioxide.

1.1.2 Dinitrogen Trioxide

The structure of N_2O_3 is given in Figure 1.2.[2]
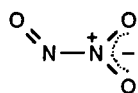
Figure 1.2 Structure of N_2O_3

In solution, dinitrogen trioxide (N_2O_3) exists in equilibrium with nitrous acid (Scheme 1.4). N_2O_3 is blue, exhibiting an absorption maximum at 625 nm.[12] The value of $K_{N_2O_3}$ in Scheme 1.4 has been the subject of some debate, but most commentators now regard a value of 3.0×10^{-3} dm^3 mol^{-1} as reasonable.[13]

$$2\,HNO_2 \rightleftharpoons N_2O_3 + H_2O \qquad K_{N_2O_3} = \frac{[N_2O_3]}{[HNO_2]^2}$$
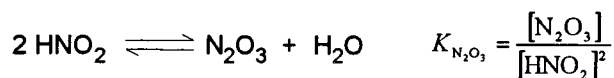
Scheme 1.4 Formation of N_2O_3 from nitrous acid

N_2O_3 dissociates into nitric oxide and nitrogen dioxide in the gas phase, as represented by Scheme 1.5.

$$N_2O_3 \rightleftharpoons NO + NO_2$$
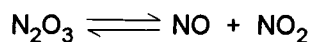
Scheme 1.5 Gas phase dissociation of N_2O_3

Nitrosation by acidified nitrous acid in which N_2O_3 becomes the active nitrosating agent gives rise to the rate law Equation 1.2 or Equation 1.3, depending upon the conditions and the nature of the substrate.

$$Rate = k_2 K_{N_2O_3}[HNO_2]^2[S] \qquad \text{Equation 1.2}$$

$$Rate = k_{N_2O_3}[HNO_2]^2 \qquad \text{Equation 1.3}$$

The above equations are readily interpreted in terms of Scheme 1.6, which includes the equilibrium formation of N_2O_3 from nitrous acid, followed by a direct reaction between the substrate and N_2O_3. Under conditions where the reaction between the substrate and N_2O_3 is rate limiting, Equation 1.2 prevails. With very reactive substrates, the reaction between the substrate and N_2O_3 can become faster than the hydrolysis of and the formation of N_2O_3, resulting in rate limiting N_2O_3 formation. Equation 1.3 then applies. The value of $k_{N_2O_3}$ has been estimated to be *ca.* 9 dm^3 mol^{-1} s^{-1} at 25 °C.[14]

$$2\,HNO_2 \underset{k_{-N_2O_3}}{\overset{k_{N_2O_3}}{\rightleftharpoons}} N_2O_3 + H_2O \qquad K_{N_2O_3} = \frac{k_{N_2O_3}}{k_{-N_2O_3}}$$

$$N_2O_3 + S \overset{k_2}{\longrightarrow} S\text{-}\overset{+}{N}O + NO_2^-$$
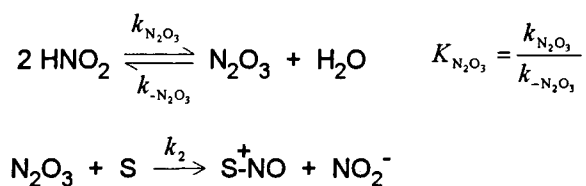
Scheme 1.6 Nitrosation with nitrous acid in which N_2O_3 becomes the active nitrosating agent

Many substrates, for example anilines, are believed to react with N_2O_3 at rates approaching the encounter limit (*ca.* 10^{10} dm^3 mol^{-1} s^{-1}), evidence being the

observation of activation energies [15] $\approx$ 20 kJ mol^{-1}, the predicted value for encounter controlled reactions.[16]

1.1.3 Dinitrogen Tetroxide, Nitrogen Dioxide, Nitric Oxide and Peroxynitrite

Dinitrogen tetroxide, N_2O_4, exists in equilibrium with nitrogen dioxide (Scheme 1.7).

$$2\,NO_2 \rightleftharpoons N_2O_4$$
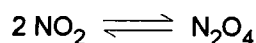
Scheme 1.7 Formation of N_2O_4 from NO_2

The solid state structure of N_2O_4 is given in Figure 1.3a.[2] The chemistry of this species is often described in terms of the ionic structure in Figure 1.3b, and the Raman line at 2 300 cm^{-1} observed for N_2O_4 in sulphuric acid clearly indicates the presence of the nitrosonium ion.[17] The solid, in fact, possesses a very long N–N bond.

N–N = 1.75 Å
N–O = 1.21 Å
$\angle$ O–N–O = 135°

$ON^+\ NO_3^-$

a   b
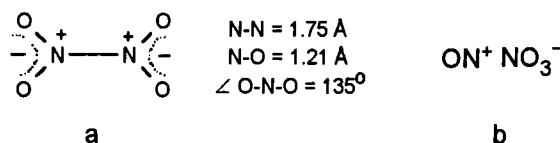
Figure 1.3 The structure of N_2O_4

N_2O_4 has been extensively used in nitrosation, substrates include amines, alcohols and thiols; the formation of nitro- compounds as side products is also known.[18] NO_2 has also been shown to be effective in nitrosation, the reaction occurring *via* N_2O_4 formation.[19]

There have been reports of direct nitrosation by nitric oxide,[e.g. 19] however NO is not expected to be an effective electrophilic nitrosating agent. Rigorous exclusion of oxygen prevents the reactions in most cases, and therefore it is likely that species derived from the oxidation of NO, such as N_2O_3, are the effective reagents.

Catalysts such as Cu^{2+}, Ag^+ and I_2 do permit nitrosation by nitric oxide, even under anaerobic conditions. In the case of Cu^{2+} [18] and I_2 [20] the reactions are believed to proceed *via* reaction between the catalyst and NO, forming the active nitrosating agent. With Ag^+ and amines the reaction probably proceeds by reaction between

Ag^+ and the amine to form an $N^{+\bullet}$ radical cation: this then reacts with NO, forming a nitrosamine.[21]

The biological relevance of peroxynitrite (ONOO-) and nitroso species has given rise to interest in whether peroxynitrite could effect nitrosation *in vivo*. As in the case of nitric oxide, there has been some contention regarding whether direct nitrosation by peroxynitrite takes place. An hypothesis article discussed the possibilities and arrived at the conclusion that direct nitrosation by peroxynitrite is unlikely.[22] A more likely mechanism is the decomposition of peroxynitrous acid to NO or NO_2, which under aerobic conditions can form effective nitrosating agents such as N_2O_3.[22, 23] There have been reports of direct nitrosation of thiols by peroxynitrite, but the yields were very low (around 1%).[24]

1.1.4 Nitrosyl Halides and Nitrosyl Thiocyanate

Nitrosyl halides (XNO where X = F, Cl, Br, I) are readily made by reacting the halogen with nitric oxide (Scheme 1.8). The resultant molecules are gases at room temperature and pressure. FNO is colourless, ClNO orange / yellow and BrNO is red.[2]

$$X_2 + 2\,NO \rightleftharpoons 2\,XNO$$
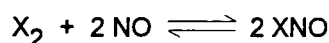
Scheme 1.8 Formation of nitrosyl halides

The nitrosyl halides of F, Cl and Br have been extensively studied, and nitrosyl iodide has been detected in the gas phase. A recent study has reported the photolytic isomerisation of ClNO and BrNO to their respective isonitrosyl halides (XON) in an argon matrix at 10 K.[25]

Decomposition of nitrosyl halides back to the halogen and nitric oxide occurs readily, as does their hydrolysis, forming nitrous acid. Electrophilic nitrosation by nitrosyl halides is easily achieved and these reagents have the advantage that they can be used in organic solvents, providing a useful alternative to nitrous acid for substrates with low water solubility.[18]

Nitrosation by nitrous acid is strongly catalysed by Cl⁻, Br⁻ and I⁻. The reactions proceed *via* pre-equilibrium formation of the nitrosyl halide, which then reacts with the substrate, regenerating the catalyst (Scheme 1.9).[18]

$$HNO_2 + X^- + H^+ \underset{k_{-XNO}}{\overset{k_{XNO}}{\rightleftharpoons}} XNO + H_2O \qquad K_{XNO} = \frac{k_{XNO}}{k_{-XNO}}$$

$$S + XNO \underset{k_{-2}}{\overset{k_2}{\rightleftharpoons}} X^- + \overset{+}{S}\text{-NO}$$

$$\overset{+}{S}\text{-NO} \overset{k_3}{\longrightarrow} products$$
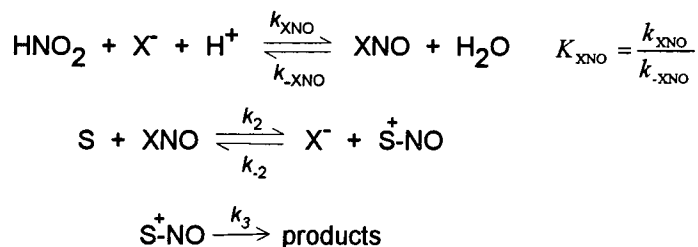
Scheme 1.9 Halide catalysis in nitrosation by nitrous acid

When the equilibrium for XNO formation is established faster than the nitrosyl halide reacts with the substrate, the rate law is given by Equation 1.4: this is the usual the case.[26] Knowledge of K_{XNO} enables k_2 to be determined, and this has been achieved for a range of substrates with Br⁻ and Cl⁻ as catalysts.[18] The instability of nitrosyl iodide with respect to iodine formation has prevented the accurate determination of K_{INO}, hence extensive kinetic analysis of I⁻ catalysis has not been carried out.

$$Rate = k' [H^+][HNO_2][S][X^-] - k_{-2}[SNO^+][X^-] \text{ where } k' = k_2 K_{XNO}$$

Equation 1.4

The relative electronegativities of Br and Cl predict that nitrosyl chloride will be more electrophilic than the corresponding bromide, hence values of k_2 in Scheme 1.9 are expected to be higher when X = Cl, and this is generally observed experimentally.[18] However, the product $k_2 K_{XNO}$ is larger for Br⁻ than for Cl⁻ because of the large difference in K_{XNO} values (K_{ClNO} = 1.1 × 10⁻³ dm⁶ mol⁻² and K_{BrNO} = 5.1 × 10⁻² dm⁶ mol⁻² at 25 °C in water)[26] hence catalysis by bromide is always more effective.

If $k_{-2}[X^-][SNO^+]$ is a lot greater than $k_3[SNO^+]$ then no catalysis is observed. Rate limiting proton loss (i.e. the step with rate constant k_3 in Scheme 1.9) also results in the absence of catalysis, and has been observed for amides, 2,4-dinitroaniline and *N*-acetyl tryptophan when [X⁻] is large. [18,27]

Thiocyanate (⁻SCN) catalysis of nitrosation by nitrous acid exhibits many of the same features as catalysis by halides. Thiocyanate is a more effective nitrosation catalyst than the halides because of the larger value of K_{XNO} when X is ⁻SCN ($K_{ONSCN} = 30$ dm⁶ mol⁻² at 25 °C in water).[28]

Rate limiting formation of nitrosyl thiocyanate has been observed in thiocyanate catalysed nitrosations, for example the nitrosation of aniline,[29] azide,[30] and thioglycolic acid.[31] Under these circumstances the rate law becomes that given in Equation 1.5 and is zeroth order in the substrate concentration.

$$Rate = k_{XNO}[HNO_2][X^-][H^+] \qquad \text{Equation 1.5}$$

1.1.5 Nitrosonium Salts

Numerous nitrosonium salts are known, for example nitrosonium tetrafluoroborate ($NO^+BF_4^-$) and nitrosonium hexafluorophosphate ($NO^+PF_6^-$). The salts have been used as effective nitrosating agents, but their rapid hydrolysis (to nitrous acid) necessitates their use under anhydrous conditions. The reagents have been successfully used to nitrosate some of the less reactive substrates for which other nitrosating agents have proved unsuitable, for example aromatic amides.[18]

1.1.6 Nitrosation by Nitroso Compounds

Nitroso compounds have also found uses as reagents in nitrosation. Alkyl nitrites (RONO), derived from alcohols, have been used as nitrosating agents. Like the nitrosyl halides, they can be particularly useful for substrates with low water solubility because they can be used in a range of non-aqueous solvents.

1.2 Substrates for Nitrosation

Many of the salient features observed in nitrosation reactions have been discussed in Section 1.1. Some substrate specific points are presented in the following sections.

1.2.1 *N*-Nitrosation

The discussion on *N*-nitrosation will concentrate on the nitrosation of amines. Nitrosation of other nitrogen containing compounds has been studied and reviewed, including the nitrosation of amides, hydroxylamines, sulfamic acid and ammonia.[32]

Reaction of primary amines with nitrosating agents results in the formation of a diazonium ion (RN_2^+), formed by proton transfer and loss of water from the intermediate primary nitrosamine (RNHNO), Scheme 1.10.[32] Spectroscopic techniques have enabled primary aromatic nitrosamines to be observed,[33] and a small number of these species have been isolated.[32]
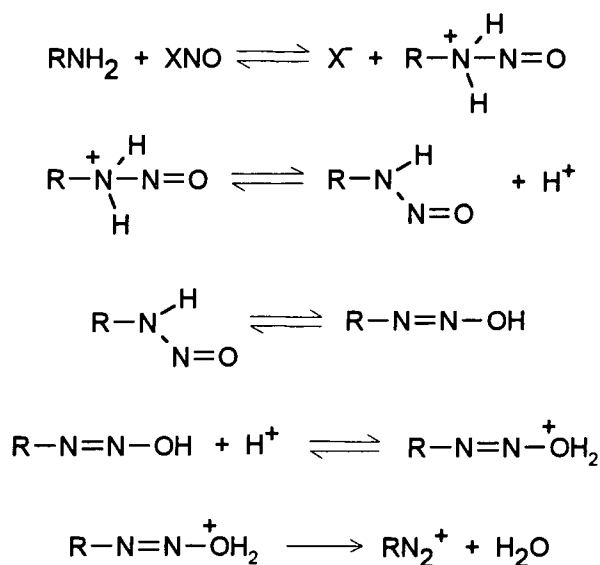
Scheme 1.10 Formation of diazonium ions from primary amines

Diazonium ions react with a wide range of nucleophiles, including water and halides, and are therefore useful precursors for a range of organic compounds such as phenols. Attack at both nitrogen atoms in diazonium ions is known.

Aryl diazonium ions are widely used in the synthesis of azo dyes, in which the diazonium partakes in an electrophilic aromatic substitution reaction (Scheme 1.11). The highly conjugated π-system formed in these reactions gives rise to the colour properties of the compounds. The colour can be 'fine-tuned' by using aromatic compounds with different substituents and ring systems. Aryl diazonium ions can

be isolated as salts, but these are generally unstable and prone to explode, so are rarely isolated in practice.
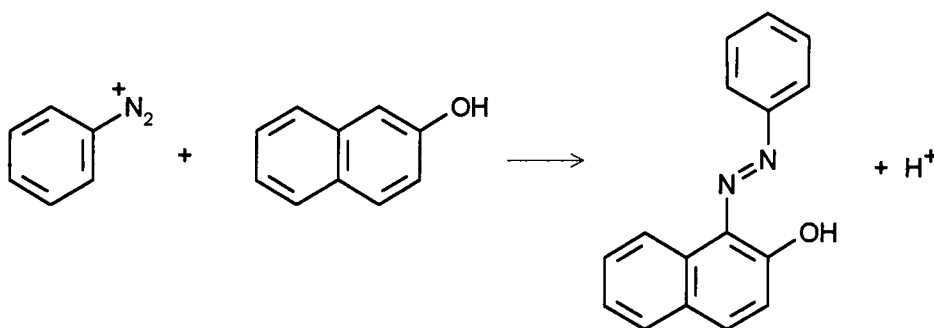
Scheme 1.11 Azo dye formation

Diazonium ions formed from primary aliphatic amines do not benefit from stabilisation from the π-system as for aryl diazonium ions and therefore rapidly lose nitrogen, forming carbocations, which then react with low selectivity to form a range of products.[32]

Secondary amines undergo nitrosation to form nitrosamines (R_2NNO). The absence of a proton on the nitrogen adjacent to the NO moiety precludes the subsequent formation of diazonium ions and the nitrosamines produced are stable. The reactions are reversible, and the back reactions have been studied by using nitrous acid traps to prevent the re-formation of the nitrosamine.

The formation and the removal of nitrosamines have become important areas of research, given the carcinogenic nature of the compounds.[34] This is seen as particularly relevant because of the presence of nitrite in many foods (added as a preservative) and the possibility of its conversion to nitrosating agents under the acidic conditions of the stomach.

The kinetics of N-nitrosation exhibit many of the features outlined in Section 1.1.[35] Characteristics of particular interest are:

- The apparent upper limit for k in Equation 1.1 for the nitrosation of reactive amines by nitrous acid. This value of around 6 000 dm^6 mol^{-2} s^{-1} (referring to reaction of the free base form of the amine) is believed to represent reaction occurring at the encounter limit.[36]

- Most of the reactions occur through the free base form of the amine. However, at higher acidities (0.1 – 6.5 M perchloric acid), reaction proceeding *via* the protonated form of anilines has been observed: the rate equation is Equation 1.6. Acid catalysis is even observed beyond the point at which the amine is essentially fully protonated, and has been explained in terms of a π-complex forming between the aryl ring and the nitrosonium ion (Scheme 1.12).[37] Complexes of this type have been isolated.[38]

$$Rate = k \left[arNH_3{}^+ \right] \left[NO^+ \right] h_o \qquad \text{Equation 1.6}$$
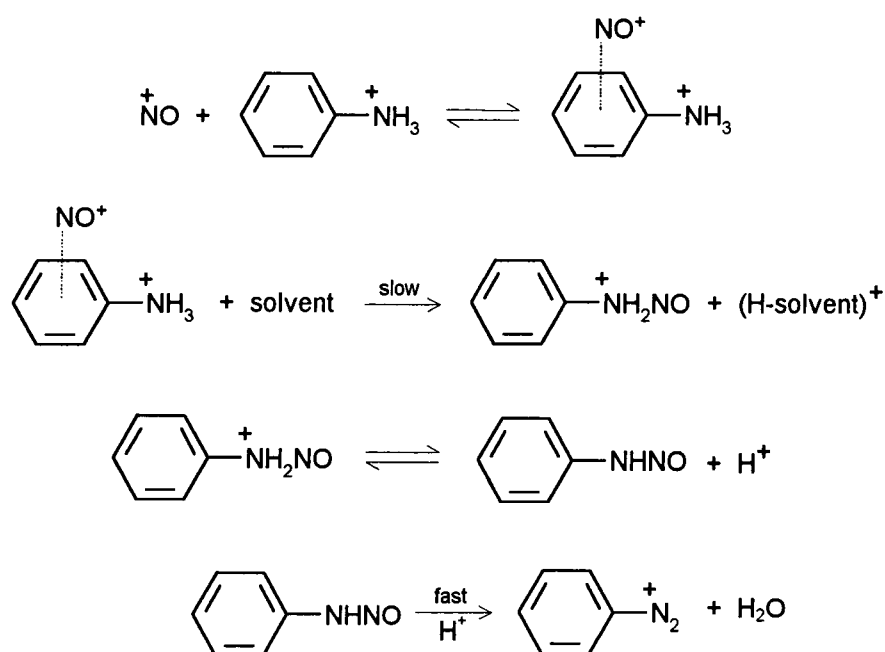
Scheme 1.12 π-complex involvement in the nitrosation of anilines

- In very concentrated acids (greater than 60% sulfuric acid) the proton loss from the initial $arNH_2NO^+$ becomes rate limiting. This reduces the rate of diazotisation and can lead to competition between diazotisation and intramolecular rearrangement to the *para-* *C*-nitroso aniline (Fischer-Hepp rearrangement).[32]

1.2.2 *C*-Nitrosation

C-Nitrosation can be divided into two types: nitrosation occurring at aliphatic and alicyclic carbons, and nitrosation at aromatic carbon centres.

1.2.2.1 Aliphatic and Alicyclic *C*-Nitrosation

C-Nitrosation of aliphatic and alicyclic compounds can give rise to various products including monomeric *C*-nitroso compounds, dimeric *C*-nitroso compounds, and oximes.[39] The monomers are generally less stable than the other products, but are easily identified by their blue or green colour when formed.

Upon dimerisation, forming both the Z and E forms, the nitroso species become colourless (Scheme 1.13). The E isomers are usually more stable than the Z isomers. Dissociation to the monomers can be achieved by heating.
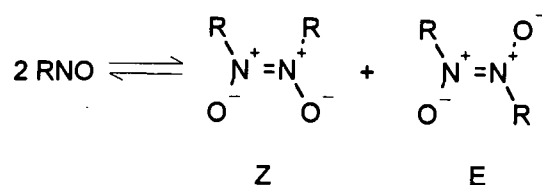
Scheme 1.13 Dimerisation of *C*-nitroso compounds

The nitrosation of ketones occurs readily, forming the corresponding oximes.[39] The usual range of nitrosating agents are effective. Whilst mono nitrosation and subsequent oxime formation is usually observed with aliphatic ketones, reaction with alicyclic ketones proceeds through dinitrosation, yielding dioximes.[40] The mechanism of oxime formation proceeds via enolisation of the ketone, followed by *C*-nitrosation and rearrangement to the oxime (Scheme 1.14).[41] Conditions under which the enolisation of the ketone is rate limiting and conditions under which the nitrosation step is rate limiting have both been observed.
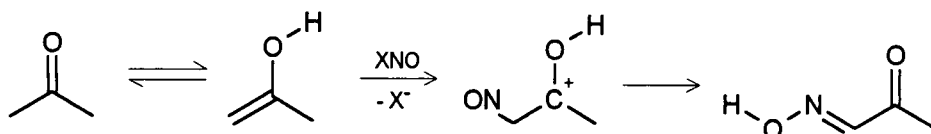
Scheme 1.14 Oxime formation from ketones

When the nitroso group is formed on a tertiary carbon atom, where stable oxime formation is not possible, or where several electron-withdrawing groups are present, C–C bond cleavage occurs.[40]

The reaction of alkenes with the nitrosating agent nitrosyl chloride results in the initial formation of nitroso chloride adducts.[42] These are mostly unstable and the final products are therefore nitroso dimers or oximes (Scheme 1.15). Both *syn* and *anti* addition have been observed, the preference being dependent upon the alkene and solvent used.[39]
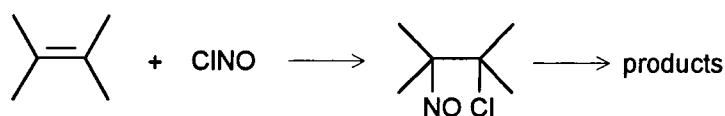
Scheme 1.15 Reaction of alkenes with nitrosyl chloride

Alkanes also undergo reaction with nitrosyl chloride in a free radical process initiated by irradiation with UV or visible light.[43] The immediate products are nitroso compounds, which then go on to form a variety of products including the oximes. An example of a commercially useful nitrosation of an alkane is the production of caprolactam from cyclohexane.[39]

1.2.2.2 Aromatic *C*-Nitrosation

C-nitrosation of aromatic compounds has been subject to less study than their *C*-nitration because the reactions require considerable activation by electron donating groups to proceed at reasonable rates.[44]

Nitrosation of phenols by nitrous acid is readily achieved, phenol itself forms predominantly *p*-nitroso phenol, which is tautomeric as indicated in Scheme 1.16.[45]
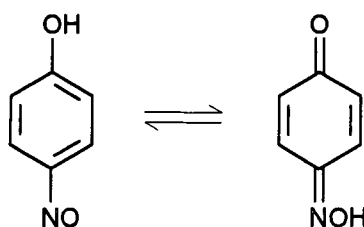
Scheme 1.16 Tautomerisation of *p*-nitroso phenol

Nitrosation of tertiary aromatic amines also gives *C*-nitroso products, the *para* isomers predominating.   Secondary aromatic amines usually undergo initial *N*-nitrosation, the product of which can rearrange in the Fischer-Hepp rearrangement to the *para C*-nitroso compound.[44]

C-nitrosation proceeds *via* an A-S$_E$2 mechanism where the electrophilic nitrosating agent reacts with the aromatic compound, forming a Wheland intermediate which then undergoes deprotonation to form the products (Scheme 1.17).[44]   The rate determining step in these reactions depends upon the conditions employed.
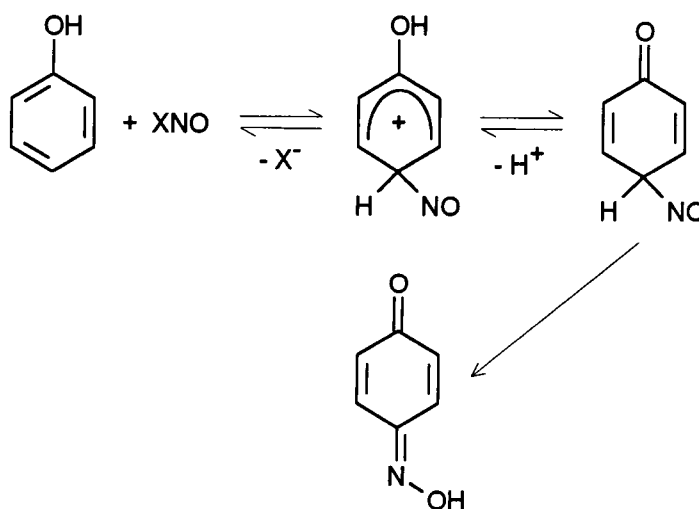
Scheme 1.17 A-S$_E$2 mechanism of aromatic *C*-nitrosation

Under very acidic conditions, the reactions can also proceed *via* initial π-complex formation between the aromatic compound and the nitrosonium ion. Stabilisation of the often unstable *C*-nitroso products by complex formation between the nitroso product and the nitrosonium ion has also been observed in the nitrosations of *o*-xylene, *m*-xylene, toluene and anisole (Scheme 1.18).[46, 47]
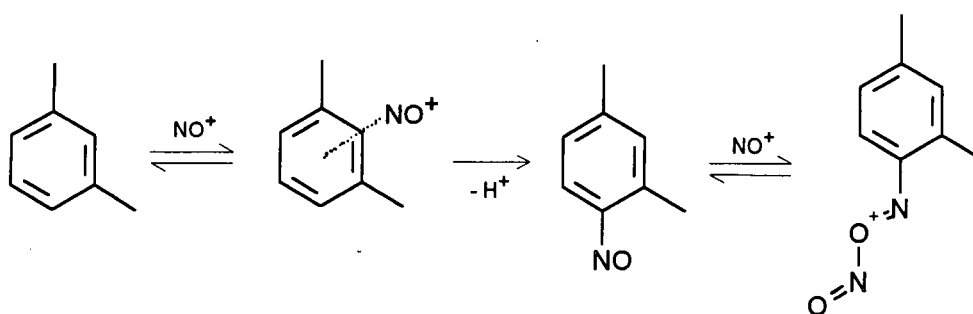
Scheme 1.18 Formation of complexes in the nitrosation of *m*-xylene

Nitrous acid catalysis is important in some aromatic *C*-nitrations, and can proceed *via* nitrosation. Treating aromatic compounds with excess nitrous acid often gives nitro products. Many of these reactions proceed *via* initial nitrosation, followed by oxidation of the product by nitrous acid, forming the nitro product.[44] Carrying out the reactions under nitric oxide can reduce the oxidation to the nitro products if desired.[46]

An alternative mechanism for nitrous acid catalysed nitration has been identified in which electron transfer between NO^+ and the aromatic compound occurs, yielding NO and a radical cation. The radical cation then reacts with NO_2 or NO^+ to yield the nitro product. Nitrous acid catalysed nitrosations that have been interpreted in terms of this mechanism include the nitration of *N,N*-dimethylaniline,[44,48] phenols,[49] and phenyl ethers.[50]

1.2.3 *O*-Nitrosation

The most commonly encountered form of *O*-nitrosation is the nitrosation of alcohols to form alkyl nitrites (RONO), which have themselves been used as nitrosating agents. The formation and decomposition of alkyl nitrites is discussed briefly here, followed by a focus on the nitrosation of ascorbic acid.

Alcohols are readily nitrosated using the reagents described in Section 1.1, and the substrates are generally very reactive. When nitrous acid is used as the nitrosating agent, there is no catalysis by halides.[51] The generic mechanism for the nitrosation of alcohols is given in Scheme 1.19.

$$R-OH + ONX \rightleftharpoons R-\overset{+}{O}\overset{NO}{\underset{H}{\diagup}} + X^-$$

$$R-\overset{+}{O}\overset{NO}{\underset{H}{\diagup}} \rightleftharpoons R-ONO + H^+$$
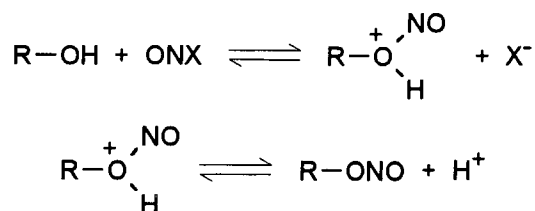
Scheme 1.19 Nitrosation of alcohols

Alkyl nitrite formation in significantly reversible, and equilibrium constants for the nitrosation of several alcohols, defined by Equation 1.7, have been measured.[52,53]

Typical values are: ethyl nitrite, ~ 1 dm³ mol⁻¹; isopropyl nitrite, ~ 0.5 dm³ mol⁻¹ and tertiarybutyl nitrite, < 0.05 dm³ mol⁻¹.[52,53]

$$K = \frac{[RONO]}{[ROH][HNO_2]} \qquad \text{Equation 1.7}$$

Hydrolysis of alkyl nitrites is subject to both acid and base catalysis.[51] Under acidic conditions the hydrolysis is facile and proceeds according to Scheme 1.20. Re-nitrosation is possible because of the production of nitrous acid, and this must be removed using a nitrous acid trap if the hydrolysis is to reach completion.
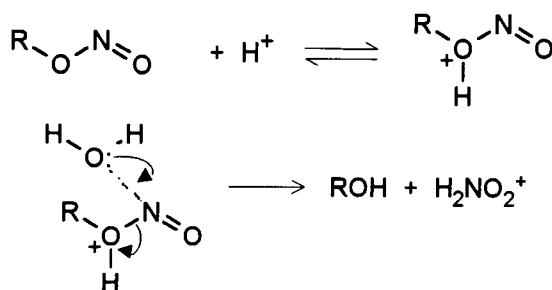
Scheme 1.20 Acid catalysed hydrolysis of alkyl nitrites

Base hydrolysis proceeds as outlined in Scheme 1.21 and has been shown by the absence of oxygen exchange to be a concerted reaction, i.e. there is no contribution from an addition elimination mechanism.[54] The hydrolysis is irreversible under basic conditions because the nitrous acid produced rapidly deprotonates to form nitrite, which is not effective in nitrosation.
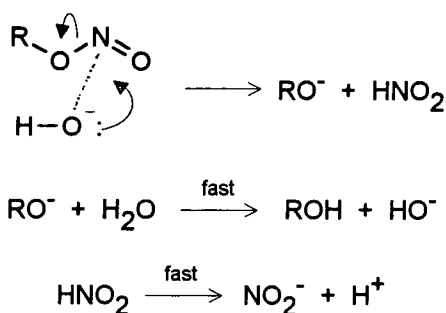
Scheme 1.21 Base catalysed hydrolysis of alkyl nitrites

1.2.3.1 Nitrosation of Ascorbic Acid

The reaction between ascorbic acid and nitrous acid was first reported in 1934 by Karrer and Bendas.[55] The products of the reaction are dehydroascorbic acid and nitric oxide, as shown in Scheme 1.22. Extensive study into the mechanism of the oxidation reaction has been carried out, and many similarities with nitrosations at nitrogen and oxygen were observed.[56-62]
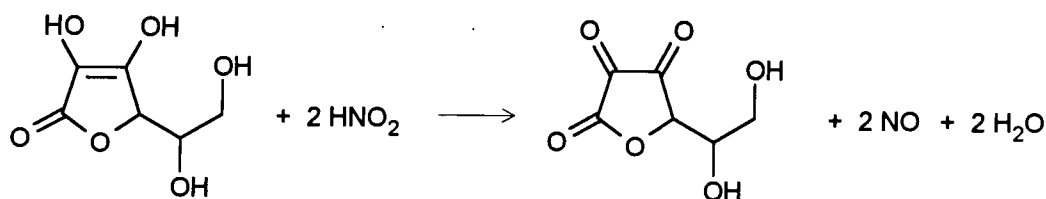
Scheme 1.22 Reaction between ascorbic acid and nitrous acid

At moderate acidities (0.1 – 1 M perchloric acid), the reaction between ascorbic acid and nitrous acid proceeds according to the rate law Equation 1.8. This can therefore be interpreted in terms of the pre-equilibrium formation of either the nitrous acidium ion or the nitrosonium ion, which then reacts with the ascorbic acid in the rate-determining step (see Scheme 1.3, Section 1.1.1). This reaction was found to be subject to halide catalysis, as described in Section 1.1.4. At these acidities, the reactive ascorbic acid species is the neutral form of the molecule (pK_a values 4.25 and 11.75).

$$Rate = k[HNO_2][H^+][\text{ascorbic acid}] \qquad \text{Equation 1.8}$$

When much lower acidities were employed (pH 3 – 4), the reactions were found to be zeroth order in ascorbic acid, the rate equation being Equation 1.9. This is due to the active nitrosating agent being N_2O_3, the formation of which is rate determining (see Scheme 1.6, Section 1.1.2).

$$Rate = k_{N_2O_3}[HNO_2]^2 \qquad \text{Equation 1.9}$$

At intermediate acidities the situation is more complicated, with the rate law being given by a combination of terms, as shown in Equation 1.10. The first term represents reaction *via* nitrous acidium / nitrosonium ion and the last represents reaction *via* N_2O_3. The kinetic form of the last term indicates that rapid pre-equilibrium formation of N_2O_3 occurs, followed by rate limiting attack upon the

N_2O_3 by ascorbic acid. The reaction of ascorbic acid with N_2O_3 was shown to occur through both the monoanionic and neutral forms of the ascorbic acid.

$$Rate = k[H^+][HNO_2][\text{ascorbic acid}] + k_2 K_{N_2O_3}[HNO_2]^2[\text{ascorbic acid}]$$ Equation 1.10

The observation of nitric oxide and dehydroascorbic acid as products led to the proposal of Scheme 1.23 to explain the reaction.
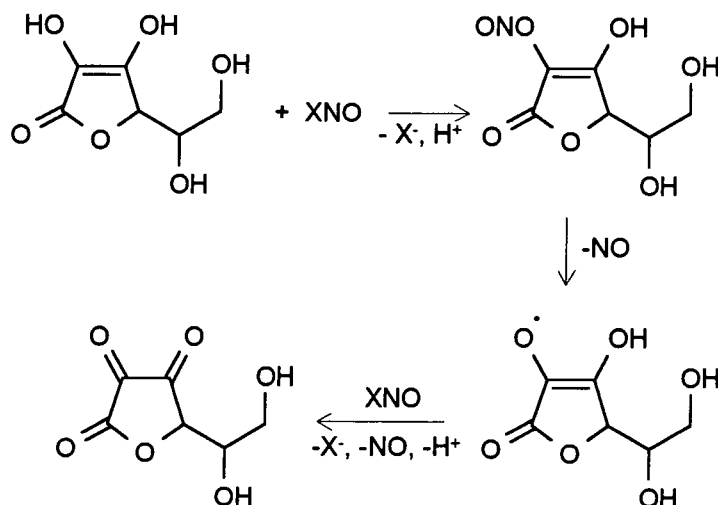
Scheme 1.23 Reaction scheme for the nitrosation of ascorbic acid

The kinetics described above were all obtained by following the ascorbic acid concentration spectrophotometrically, and therefore gave no information regarding the kinetics of the subsequent steps after the formation of the initial product in Scheme 1.23. Later work gave more information regarding these later steps, and is summarised below.[63]

When the reaction between ascorbic acid and nitrous acid was studied in air saturated, 0.01 – 0.10 M acid solutions with equimolar concentrations of the reactants, first order kinetics were observed. This was attributed to the rapid re-formation of nitrous acid by the autoxidation of nitric oxide (Scheme 1.24); hence, the concentration of nitrous acid did not change enough for non-first-order kinetics to be observed. These results indicate that the steps following the initial nitrosation (i.e. the steps leading to nitric oxide production) must have been more rapid than the initial nitrosation.

$$2\,NO + O_2 \longrightarrow 2\,NO_2$$

$$H_2O + NO_2 + NO \rightleftharpoons 2\,HNO_2$$
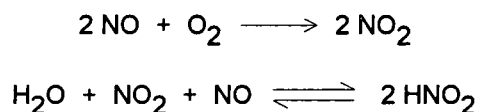
Scheme 1.24 Autoxidation of nitric oxide and subsequent nitrous acid formation

In the same study, conditions were also used where [ascorbic acid] $\gg$ [HNO$_2$]. Complete decomposition of the ascorbic acid was observed, indicating that the nitric oxide was re-forming nitrous acid, and the traces were, after the initial consumption of one mole of ascorbic acid and nitrous acid, zeroth order in ascorbic acid. Autoxidation of NO had become rate limiting under these conditions.

1.2.4 *S*-nitrosation

The most commonly encountered substrates in *S*-nitrosation are thiols. As might be expected, the nitrosation of thiols has similarities with the nitrosation of alcohols, and exhibits many of the features described in Section 1.1. The nitrosation of thiols has previously been reviewed.[64]

Nitrosation of thiols by acidified solutions of nitrous acid proceeds rapidly, and for some substrates rate constants approaching values believed to represent encounter controlled reactions are observed.[65] Halide and thiocyanate catalysis in these nitrosations has been observed.[64, 65] Other nitrosating reagents are effective, including N$_2$O$_3$, N$_2$O$_4$, and alkyl nitrites.[64]

The products of thiol nitrosations are *S*-nitrosothiols (RSNO), and the instability of these compounds has made the nitrosation of thiols more difficult to study than the corresponding reactions of alcohols. The instability of nitrosothiols arises from the ease of homolysis of the S–N bond, resulting in disulfide formation.[66] Some nitrosothiols, particularly those with bulky groups close to the nitroso moiety, are less prone to bond cleavage. In fact, some have been crystallised and crystal structures obtained, e.g. for *S*-nitroso *N*-acetyl penicillamine.[67]

Scheme 1.25 shows the nitrosation of thiols and the subsequent decomposition of the products. The properties and reactions of the nitrosothiol products are discussed in depth in Chapter 2.

$$RSH + XNO \rightleftharpoons RSNO + X^- + H^+$$

$$2\,RSNO \longrightarrow RSSR + 2\,NO$$
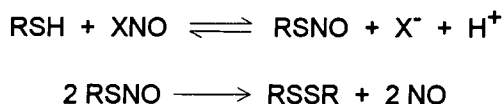
Scheme 1.25 Nitrosation of thiols

Thiols appear to be more reactive towards nitrosating agents than alcohols and amines.[31]　The greater nucleophilicity of S relative to O and N explains this observation.[67] When thiols containing an amino group as well as a thiol group, such as cysteine, are nitrosated, the reaction preferentially occurs at the sulfur atom.[31] Migration of the nitroso group to the nitrogen, followed by diazotisation and intramolecular attack by sulfur upon the diazonium ion, as shown in Scheme 1.26, has been reported.[68]
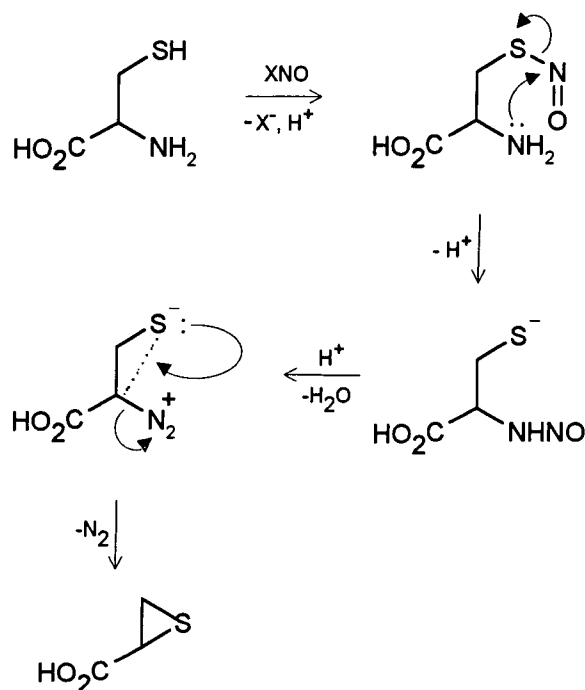
Scheme 1.26 Cysteine nitrosation

It was thought that the nitrosation of thiols contrasted with that of alcohols in that it was effectively irreversible. This was attributed to the larger rate constants for the forward reaction for thiols, because of the greater nucleophilicity of S relative to O, and to the less basic nature of S relative to O causing the back reaction, which requires protonation of the S, to be less favoured. It has since been demonstrated that the reactions are slightly reversible,[67] and this turns out to be important in the

Cu^{2+} catalysed decomposition of nitrosothiols (see Section 2.2.2.3). Typical values for the equilibrium constant for nitrosothiol formation, defined by Equation 1.11, are: *S*-nitroso penicillamine, $\sim 3 \times 10^5$ dm³ mol⁻¹; *S*-nitroso cysteine $\sim 6 \times 10^5$ dm³ mol⁻¹.[67]

$$K = \frac{[\text{RSNO}]}{[\text{RSH}][\text{HNO}_2]} \qquad \text{Equation 1.11}$$

1.2.4.1 Nitrosation of Thiones

Thiones are sulfur analogues of ketones, containing the >C=S functional group. Some nitrosation reactions of thiones have been studied, particularly the nitrosation of thiourea (Figure 1.4)[69] and its derivatives.[70] The nitrosation of thiourea can occur either at nitrogen or at sulfur, and nitrosations at both of these centres have been observed.[69]
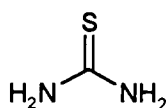
Figure 1.4 Thiourea

Early work on the reaction of thiourea with nitrous acid was carried out by Werner,[71] who observed two reactions, yielding the products shown in Scheme 1.27.

$$\text{HNO}_2 + (\text{NH}_2)_2\text{CS} \longrightarrow \text{H}^+ + \text{SCN}^- + \text{N}_2 + 2\,\text{H}_2\text{O}$$

via N-nitrosation

$$2\,\text{HNO}_2 + 2\,\text{H}^+ + 2\,(\text{NH}_2)_2\text{CS} \longrightarrow (\text{NH}_2)_2\overset{+}{\text{C}}\text{SS}\overset{+}{\text{C}}(\text{NH}_2)_2 + 2\,\text{NO} + 2\,\text{H}_2\text{O}$$

via S-nitrosation
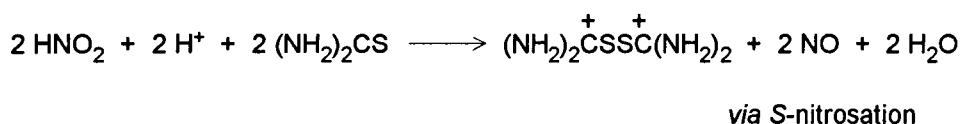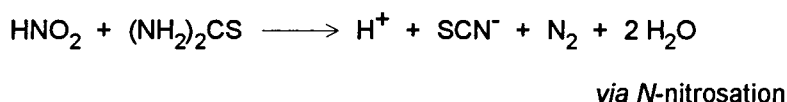
Scheme 1.27 Reaction of thiourea with nitrous acid

The second reaction, producing *C,C*-dithiodiformamidinium,[72] is favoured at high acidities whereas the first reaction predominates at low acidities.[71] The second reaction was observed to proceed *via* the formation and rapid decay of a red species. Further studies showed that the transient species was actually more yellow than red when observed at low concentration, and formed in equilibrium with equimolar concentrations of H^+, HNO_2 and thiourea.[69]

The fact that the nitrosonium ion tends towards being a soft electrophile led to the assertion that the yellow species forms through *S*-nitrosation, and the structure of the yellow species is therefore that given in Figure 1.5.[70] This *S*-nitrosation can also be accompanied by nitrosation at a nitrogen centre.

$$H_2N \diagdown$$
$${\diagup}{=}{\overset{+}{S}NO}$$
$$H_2N \diagup$$
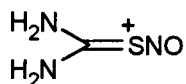
Figure 1.5 *S*-nitrosation on thiourea

The kinetics of *S*-nitrosation and the equilibrium constants for the formation of the yellow species have been measured for a range of thiourea derivatives, and the value of the equilibrium constants correlated with the pK_a values.[70] Studies have also been made into the decomposition of the nitroso products.[73, 74]

The nitrosation and decomposition of the products of the heteroaromatic thione pyridine-2(*1H*)-thione (2-thiopyridine) exhibits many similarities to that of thiourea.[75] These are discussed with the results of studies on the nitrosation of other heteroaromatic thiones in Chapter 7 and 8.

1.3 References

1. D. L. H. Williams, 'Nitrosation', Cambridge University Press, Cambridge, 1988.

2. N. N. Greenwood and A. Earnshaw, 'Chemistry of the Elements', Chapter 11, Pergamon Press, Oxford, 1984.

3. F. A. Cotton and G. Wilkinson, 'Advanced Inorganic Chemistry', Fourth Edition, Wiley, New York, 1980.

4. J. Tummavuori and P. Lumme, *Acta. Chem. Scand.*, **22**, 2003 (1968).

5. K. Singer and P. A. Vamplew, *J. Chem. Soc.*, 3971 (1956).

6. W. R. Angus and A. H. Leckie, *Proc. Roy. Soc. (A)*, **150**, 615 (1935).

7. E. D. Hughes, C. K. Ingold and J. H. Ridd, *J. Chem. Soc.*, 77 (1958).

8. E. D. Hughes, C. K. Ingold and J. H. Ridd, *J. Chem. Soc.*, 88 (1958).

9. D. J. Benton and P. Moore, *J. Chem. Soc. (A)*, 3179 (1970).

10. C. A. Bunton and G. Stedman, *J. Chem. Soc.*, 3466 (1959).

11. F. Steel and R. Winkler, *Z. Phys. Chem.*, **25**, 217 (1960).

12. J. Mason, *J. Chem. Soc.*, 1288 (1959)

13. G. Y. Markovits, S. E. Schwartz and L. Newman, *Inorg. Chem.*, **20**, 445 (1981).

14. M. S. Garley and G. Stedman, *J. Inorg. Nucl. Chem.*, **43**, 2863 (1981).

15. J. Casado, A. Castro, J. R. Leis, M. A. Lopez Quintela and M. Mosquera, *Montash Chem.*, **114**, 639 (1983).

16. S. R. Logan, 'Fundamentals of Chemical Kinetics', p. 78, Longman, Harlow, 1996.

17. D. J. Millen, *J. Chem. Soc.*, 2600 (1950).

18. D. L. H. Williams, 'Nitrosation', Chapter 1, Cambridge University Press, Cambridge, 1988.

19. W. A. Pryor, D. F. Church, C. K. Govindan, G. Crank, *J. Org. Chem.*, **47**, 156 (1982).

20. B. C. Challis and J. R. Outram, *J. Chem. Soc., Perkin Trans. 1*, 2768 (1979).

21. B. C. Challis and J. R. Outram, *J. Chem. Soc., Chem. Commun.*, 707, (1978).

22. D. L. H. Williams, *Nitric Oxide: Biol. Chem.*, **1**, 522 (1997).

23. R. M. Uppu, J. N. Lemercier, G. L. Squadrito, H. W. Zhang, R. M. Bolzan and W. A. Pryor, *Arch. Biochem. Biophys.*, **358**, 1 (1998).

24. A. van der Vliet, P. A. Chr. 't Hoen, P. S.-Y. Wong, A. Bast and C. E. Cross, *J. Biol. Chem.*, **273**, 30255 (1998).

25. G. Maier, H. P. Reisenauer and M. DeMarco, *Chem. Eur. J.*, **6**, 800 (2000).

26. H. Schmid, *Chem. Ber.*, **70**, 421 (1937).

27. A. Castro, E. Iglesias, J. R. Leis, M. E. Peña, J. V. Tato, D. L. H. Williams, *J. Chem. Soc., Perkin Trans. 2*, 1165 (1986).

28. G. Stedman and P. A. E. Whincup, *J. Chem. Soc.*, 5796 (1963).

29. C. A. Bunton, D. R. Llewellyn and G. Stedman, *J. Chem. Soc.*, 568 (1959).

30. G. Stedman, *J. Chem. Soc.*, 2949 (1959).

31. D. L. H. Williams, 'Nitrosation', Chapter 7, Cambridge University Press, Cambridge, 1988.

32. D. L. H. Williams, 'Nitrosation', Chapter 4, Cambridge University Press, Cambridge, 1988.

33. E. Müller and H. Haiss, *Chem. Ber.*, **96**, 570 (1963).

34. 'The Dictionary of Compounds and Their Effects', 2nd ed., Vol. 5, Ed. S. Gangolli, Royal Society of Chemistry, Cambridge, 1999.

35. J. H. Ridd, *Quart. Rev.*, **15**, 418 (1961).

36. J. H. Ridd, *Adv. Phys. Org. Chem.*, **16**, 1 (1978).

37. B. C. Challis and J. H. Ridd, *J. Chem. Soc.*, 5208 (1962).

38. E. K. Kim and J. K. Kochi, *J. Org. Chem.*, **54**, 1692 (1989)

39. D. L. H. Williams, 'Nitrosation', Chapter 2, Cambridge University Press, Cambridge, 1988.

40. O. Touster, *Organic Reactions*, **7**, 327 (1953).

41. J. R. Leis, M. E. Peña and D. L. H. Williams, *J. Chem. Soc., Chem. Commun.*, 45 (1987).

42. W. A. Tilden and W. A. Stenstone, *J. Chem. Soc.*, 554 (1877).

43. H. Mitzger and E. Müller, *Chem. Ber.*, **90**, 1179 (1957).

44. D. L. H. Williams, 'Nitrosation', Chapter 3, Cambridge University Press, Cambridge, 1988.

45. S. Veibel, *Ber.*, **63**, 1577 (1930).

46. J. H. Atherton, R. B. Moodie and D. R. Noble, *J. Chem. Soc., Perkin Trans. 2*, 699 (1999).

47. J. H. Atherton, R. B. Moodie and D. R. Noble, *J. Chem. Soc., Perkin Trans. 2*, 229 (2000).

48. J. C. Giffney and J. H. Ridd, *J. Chem. Soc., Perkin Trans. 2*, 618 (1979).

49. U. Al-Obaidi and R. B. Moodie, *J. Chem. Soc., Perkin Trans. 2*, 467 (1985).

50. L. Main, R. B. Moodie and K. Schofield, *J. Chem. Soc., Chem. Commun.*, 48 (1982).

51. D. L. H. Williams, 'Nitrosation', Chapter 6, Cambridge University Press, Cambridge, 1988.

52. J. Casado, F. M. Lorenzo, M. Mosquera and M. F. R. Prieto, *Can. J. Chem.*, **62**, 136 (1984).

53. S. E. Aldred, D. L. H. Williams and M. Garley, *J. Chem. Soc., Perkin Trans. 2*, 777 (1982).

54. S. Oae, N. Asai and K. Fujimori, *Tet. Lett.*, **24**, 2103 (1977).

55. P. Karrer and H. Bendas, *Helv. Chim. Acta*, **17**, 743 (1934).

56. C. A. Bunton, H. Dahn and L. Loewe, *Nature*, **183**, 163 (1959).

57. H. Dahn, L. Loewe, E. Lüscher and R. Menassé, *Helv. Chim. Acta*, **43**, 287 (1960).

58. H. Dahn and L. Loewe, *Helv. Chim. Acta*, **43**, 294 (1960).

59. H. Dahn, L. Loewe and C. A. Bunton, *Helv. Chim. Acta*, **43**, 303 (1960).

60. H. Dahn and L. Loewe, *Helv. Chim. Acta*, **43**, 310 (1960).

61. H. Dahn, L. Loewe and C. A. Bunton, *Helv. Chim. Acta*, **43**, 317 (1960).

62. H. Dahn, L. Loewe and C. A. Bunton, *Helv. Chim. Acta*, **43**, 320 (1960).

63. B. D. Beake, R. B. Moodie and D. Smith, *J. Chem. Soc., Perkin Trans. 2*, 1251 (1995).

64. D. L. H. Williams, *J. Chem. Soc. Rev.*, **14**, 171 (1985).

65. L. R. Dix and D. L. H. Williams, *J. Chem. Soc., Perkin Trans. 2*, 109 (1984).

66. N. Arulsamy, D. S. Bohle, J. A. Butt, G. J. Irvine, P. A. Jordan and E. Sagan, *J. Am. Chem. Soc.*, **121**, 7115 (1999).

67. P. H. Beloso and D. L. H. Williams, *J. Chem. Soc., Chem. Commun.*, 89 (1997).

68. C. D. Maycock and R. J. Stoodley, *J. Chem. Soc., Chem. Commun.*, 234 (1976).

69. K. Al-Mallah, P. Collings and G. Stedman, *J. Chem. Soc., Dalton Trans.*, 2469 (1974).

70. P. Collings, K. Al-Mallah and G. Stedman, *J. Chem. Soc., Perkin Trans. 2*, 1734 (1975).

71. E. A. Werner, *J. Chem. Soc.*, **101**, 2180 (1912).

72. O. Foss, J. Johnson and O.Tuedten, *Acta Chim. Scand.*, **12**, 1782 (1958).

73. P. Collings, M. Garley and G. Stedman, *J. Chem. Soc., Dalton Trans.*, 331 (1981).

74. M. S. Garley, G. Stedman and H. Miller, *J. Chem. Soc., Dalton Trans.*, 1959 (1984).

75. S. Amado, A. P. Dicks and D. L. H. Williams, *J. Chem. Soc., Perkin Trans. 2*, 1869 (1998).

Introduction – the Chemistry and Physiology of Nitric Oxide and S-Nitrosothiols

Chapter 2 The Chemistry and Physiology of Nitric Oxide and *S*-Nitrosothiols

2.1 Nitric Oxide

2.1.1 Physical Properties of Nitric Oxide

Nitric oxide is a paramagnetic molecule, possessing one unpaired electron. However, it is not EPR active at room temperature, in solution or in the solid state, at normal microwave frequencies.[1] The bonding in nitric oxide can be represented in valence bond terms by the resonance canonicals depicted in Figure 2.1.

$$\overset{\cdot}{\underset{}{N}}{}^{+}\!-O^{-} \longleftrightarrow \overset{\cdot}{N}=O \longleftrightarrow \overset{\cdot}{\underset{}{N}}{}^{-}\!-O^{+} \longleftrightarrow N-O^{\cdot}$$
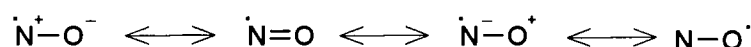
Figure 2.1 Valence bond descriptions of nitric oxide

The molecular orbital description of the bonding for the 2S and 2P levels, in order of increasing energy, is: σ_{N-O} (2 e⁻), n_O (2 e⁻), $2 \times \pi_{N-O}$ (4 e⁻), n_N (2 e⁻), π^{*}_{N-O} (1 e⁻), σ^{*}_{N-O} (empty).[1] The total bond order for the molecule is ~ 2.5 and the bond length ~ 1.15 Å,[1] with ν_{str} = 1 840 cm⁻¹. The unpaired electron is delocalised in the π^{*} orbital, with about 60% of the spin density located on the nitrogen atom.[2] This fact has been used to rationalise why nitric oxide has a low tendency to dimerise in solution, namely that the lone electron is stabilised by extensive delocalisation, and that dimerisation leaves the bond order virtually unchanged.[3] In the solid state, the loosely bound dimer $(NO)_2$ is formed and has been observed using X-ray crystallography.[4]

Nitric oxide boils at –159 °C and melts at –163 °C under atmospheric pressure, and at standard temperature and pressure is a colourless gas.[3] The liquid and solid forms of nitric oxide are also colourless, though a blue coloration is often observed due to contamination by N_2O_3.[3]

The solubility of nitric oxide in water is approximately 2×10^{-3} mol dm⁻³ at 25 °C and atmospheric pressure, which is comparable with the solubility of oxygen and carbon dioxide.[1] This aqueous solubility is virtually unchanged over pH values ranging from 2 –13.[3]

2.1.2 The Chemistry of Nitric Oxide

The chemistry of nitric oxide centres on the free radical nature of the species, and can be divided into three main categories: reaction with other free radical species; redox processes; and reaction with transition metals, i.e. its co-ordination chemistry. Clearly all of these reactivities are potentially relevant in the physiological environment. The chemistry of nitric oxide is also important in understanding atmospheric processes.

2.1.2.1 Reactivity as a Free Radical

Nitric oxide is, when compared to other free radicals, relatively stable; some of the reactions it undergoes are outlined below.[1]

- **Reaction with Dioxygen**

Perhaps the most well studied reaction of nitric oxide is its reaction with molecular oxygen. Many people have seen a demonstration where a gas jar filled with nitric oxide is opened to the atmosphere, resulting in the immediate formation of brown fumes: nitrogen dioxide. The generally accepted mechanism for this reaction is given in Scheme 2.1. The pre-equilibrium formation of N_2O_2 must have a negative $\Delta H°$ in order to satisfy the observation that the rate constant for oxidation decreases with increasing temperature.[3]

$$2\,NO \rightleftharpoons N_2O_2$$
$$N_2O_2 + O_2 \longrightarrow 2\,NO_2$$
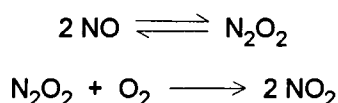
Scheme 2.1 Gas phase oxidation of nitric oxide

The rate law for the reaction is given by Equation 2.1.

$$Rate = k[NO]^2[O_2] \qquad \text{Equation 2.1}$$

In solution, the rate law for the reaction of nitric oxide with oxygen is the same as that for the gas phase reaction, and the product is nitrite. The generally accepted mechanism for nitrite formation is given in Scheme 2.2.[3] The third order rate constant is $\approx 1 \times 10^4$ mol^{-2} dm^6 s^{-1} at 25 °C [5] and is unchanged over the pH range 1 – 13.[6] The rate equation for the oxidation has important implications when

considering the solution state chemistry of nitric oxide. Even in solutions saturated with NO and O_2 (concentrations $\sim 1 \times 10^{-3}$ M), nitric oxide is relatively long lived because the large rate constant gives a low rate of reaction when multiplied by the concentration terms.[1] *In vivo*, NO oxidation would be very slow, however other nitric oxide decomposition reactions are active, for example the reaction of nitric oxide with superoxide.

$$2\,NO + O_2 \longrightarrow 2\,NO_2$$
$$NO_2 + NO \rightleftharpoons N_2O_3$$
$$N_2O_3 + H_2O \rightleftharpoons 2\,HNO_2$$
$$HNO_2 \rightleftharpoons H^+ + NO_2^-$$
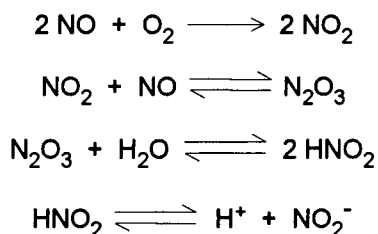
Scheme 2.2 Oxidation of nitric oxide in solution

The important point to note from Scheme 2.2 is the production solely of nitrite, rather than nitrate (which would be produced by the hydrolysis of NO_2). It has been shown using pulse radiolysis that the reaction between NO_2 and NO is very much faster than the hydrolysis of NO_2, with the rate constant being close to the diffusion controlled limit.[3]

- **Reaction with Superoxide**

Nitric oxide reacts with superoxide, yielding peroxynitrite, Scheme 2.3.[7] At physiological pH, peroxynitrite forms peroxynitrous acid, which is unstable and decays with a half life of a couple of seconds.[7] Under normal physiological conditions the decay of peroxynitrite results in concentrations that are too low to exert significant toxic effects, but in some cases, when peroxynitrite and nitric oxide concentrations are higher, steady state concentrations of peroxynitrite may be high enough to be toxic. Indeed, peroxynitrite has been detected during the activation of macrophages and has been shown to exhibit bactericidal action.[8, 9]

$$NO + O_2^{\cdot-} \longrightarrow ONOO^-$$
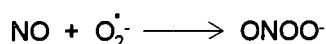
Scheme 2.3 Formation of peroxynitrite from nitric oxide and superoxide

- ## Reaction with Hydrogen Peroxide

The reaction of nitric oxide with hydrogen peroxide, which is present in higher concentrations in biological media than superoxide, yields singlet oxygen (Scheme 2.4),[10] which is highly reactive and could contribute to cell damage during the activation of macrophages.[1]

$$2\ NO\ +\ H_2O_2\ \longrightarrow\ {}^1O_2\ +\ H_2O\ +\ N_2O$$
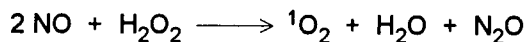
Scheme 2.4 Reaction of nitric oxide with hydrogen peroxide

- ## Hydrogen Atom Abstraction

Nitric oxide is much less efficient than the hydroxyl radical at abstracting H atoms from neutral molecules. Nevertheless, a few examples have been reported.[11,12]

2.1.2.2 Co-ordination Chemistry of Nitric Oxide

Much work has been carried out on the co-ordination chemistry of nitric oxide and the nature of the complexes it forms with transition metals.[13] Such complexes are called nitrosyl complexes, and examples are known with a wide range of metals, including Fe, Cr, Co, Ni, Pt, Ru, V, Te and W.[3]

Nitric oxide has several modes of co-ordination, with linear, bent and bridging forms known (Figure 2.2).

$$M{=}N{=}O$$
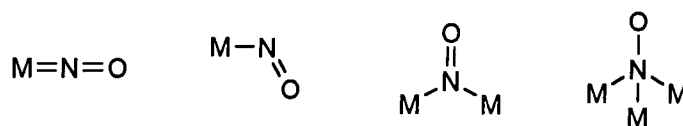
Figure 2.2 Co-ordination modes of nitric oxide with transition metals

Nitric oxide generally forms strong bonds to metals, often involving back bonding between the metal and the ligand: the resulting complexes are therefore often intensely coloured. The bonding in these complexes has been extensively studied using a range of spectroscopic techniques, including X-ray crystallography, photoelectron spectroscopy, ESR and ^{15}N nmr. Their synthesis is usually achieved by direct combination of the metal with nitric oxide, though other reagents can be used, such as nitrosonium salts.[1]

The extensive interest in metal nitrosyls has principally been because of their potential for use as homogeneous catalysts. Several nitrosyl complexes have also been used as electrophilic nitrosating agents.[14] Complexation of nitric oxide by transition metal containing enzymes and proteins, particularly the iron containing haemoglobin and guanylate cyclase are now widely studied.

2.1.2.3 The Atmospheric Chemistry of Nitric Oxide

The production of nitric oxide in vehicle exhausts leads to the generation of dangerous low level ozone and nitrogen dioxide, both components of the photochemical smog common in many large cities. Nitrogen dioxide can be photolysed in sunlight to give nitric oxide and an excited state oxygen atom. This oxygen atom then reacts with molecular oxygen, generating ozone (Scheme 2.5).

$$2\,NO + O_2 \longrightarrow 2\,NO_2$$

$$NO_2 \xrightarrow{h\nu} NO + O^*$$

$$O_2 + O^* \longrightarrow O_3$$
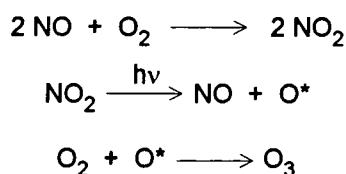
Scheme 2.5 Formation of low level ozone by nitric oxide

In the upper atmosphere nitric oxide participates in the formation of HNO_3, which is precipitated as acid rain. Nitric oxide is one of the most active ozone depleting compounds (Scheme 2.6) due to its being regenerated in a reaction with excited state oxygen atoms. Note the contrast with the action of nitric oxide in the lower atmosphere; this arises from the lower frequency of collisions between nitric oxide and O_2 in the upper atmosphere).

$$NO + O_3 \longrightarrow NO_2 + O_2$$

$$NO_2 + O^* \longrightarrow NO + O_2$$
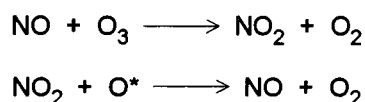
Scheme 2.6 Ozone depletion by nitric oxide in the upper atmosphere

The major sources of atmospheric nitric oxide are fertilisers, aircraft emissions, vehicle exhausts, lightning and microbial processes.

2.1.3 Physiology of Nitric Oxide

The molecule once seen as an environmental nuisance is now recognised as a species of fundamental importance in a range of functions in animals and plants. Nitric oxide was named "Molecule of the Year" in 1992,[15] and studies of its functions now proliferate in the biological literature. The 1998 Nobel Prize for Physiology and Medicine was awarded jointly to Furchgott, Ignarro and Murad for their pioneering work on the biological aspects of nitric oxide; in fact, Alfred Nobel benefited from the nitric oxide releasing drug glyceryl trinitrate, both financially and medically.

In animals, nitric oxide is crucial in a wide range of processes including vasodilation, neurotransmission and immune defence. For plants, the nitric oxide story is only just beginning to unravel. It is now believed that the majority of plants produce their own nitric oxide, and it is involved in defence against pathogens, leaf expansion and root growth.[16]

The non-specialised nature of nitric oxide and its toxicity render its biological action somewhat surprising. Unlike many important biological molecules, it is not a complex molecule with spatial and electronic characteristics tailored to interact at specific sites. However, the small size of this molecule, coupled with the fact that it is neutral, gives it the ability to cross cell membranes.

The wide range of functions in which nitric oxide assists has led some researchers to suggest that other simple, small molecules should also be investigated to establish whether they have physiological roles. Examples are hydrogen sulfide [17] and carbon monoxide.[18]

2.1.3.1 Biosynthesis of Nitric Oxide

Nitric oxide is synthesised *in vivo* from L-arginine by the enzyme class nitric oxide synthases (NOS), producing L-citrulline as the by-product (Scheme 2.7.).[19] Labelling studies have shown that the source of oxygen in both nitric oxide and citrulline is molecular oxygen, and the enzymes are therefore dioxygenases.[3] The synthesis of nitric oxide is specific to L-arginine, with a number of similar species, including D-arginine, inhibiting the process. [20]
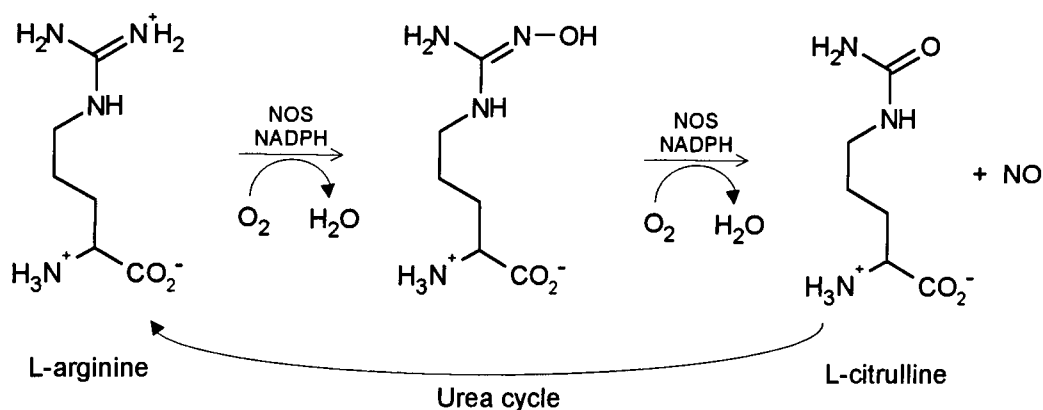
Scheme 2.7 Biosynthesis of nitric oxide from L-arginine

Several different NOS isoforms have been discovered: the constitutive endothelial (eNOS) and neuronal (nNOS) synthases, and the inducible (iNOS) synthase.[21] The eNOS in endothelial cells, where nitric oxide acts as a vasodilator, and the neuronal nNOS, being constitutive, are always present. These enzymes are able to respond rapidly, releasing nitric oxide in picomolar amounts over a short time. Conversely, in macrophages where nitric oxide assumes a cytotoxic function, the action of the inducible iNOS is subject to a delay of several hours, and nitric oxide is released by the enzyme in nanomolar quantities over a long period of time. Unlike eNOS and nNOS, iNOS is not dependent upon calmodulin, an enzyme that binds calcium ions.[20]

Nitric oxide production in many plants is also through the L-arginine pathway catalysed by nitric oxide synthases.[22] However, plants that lack the nitric oxide synthase enzymes also produce nitric oxide.[16] It is possible that, at least in plants, other enzymatic pathways might be important: recently nitrate reductase has been shown to reduce nitrite to nitric oxide in a process requiring NADPH.[22]

In certain physiological environments, the chemical reduction of nitrite might also be a mechanism for nitric oxide production. Nitric oxide is produced by non-NOS pathways in acidic environments such as the stomach and skin surface.[23] The source of the nitric oxide is probably the decomposition of nitrous acid derived from nitrite produced by nitrate reductase or by bacteria on the skin.

2.1.3.2 Vasodilation

Vasodilation, the widening of blood vessels, is caused by the relaxation of the smooth muscle surrounding the vessels. This process does not simply involve the absence of contraction, but is a process which requires activation of the iron containing enzyme guanylate cyclase (GC), and the conversion of guanosine triphosphate (GTP) into cyclic guanosine monophosphate (cGMP), Figure 2.3.[3]
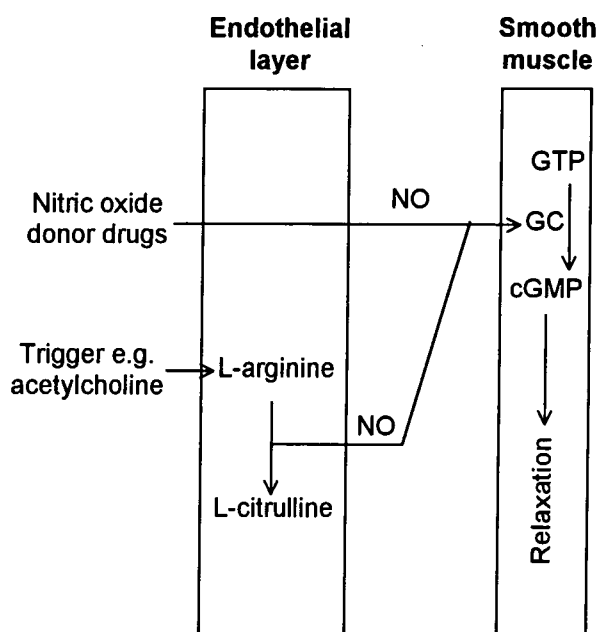
Figure 2.3 Schematic of the processes leading to smooth muscle relaxation and vasodilation

The process is triggered by several substances, including acetyl choline, bradykinin and adenine.[20] These triggers do not act directly at the smooth muscle sites, but at the endothelial cells that line the blood vessels.[24] When triggered, the endothelial cells release a messenger that diffuses across the cell membranes and into the smooth muscle. This messenger is known as the Endothelial Dependent Relaxation Factor (EDRF), and has been shown, amid some controversy,[19,20,25] to be nitric oxide.[26,27]

Amongst the evidence which proved critical in identifying nitric oxide as the EDRF was the fact that nitric oxide and the EDRF act identically; that superoxide dismutase (SOD) prolongs the action of the EDRF, by removal of superoxide; that superoxide reduces the action of the EDRF; and that haemoglobin, which binds nitric oxide very strongly, destroys the action of the EDRF.[20]

The process of smooth muscle relaxation proceeds as follows.[3] Ca^{2+} / calmodulin activates NOS in the endothelial cells, which produces nitric oxide from L-arginine. The nitric oxide then diffuses from the endothelial layer into the smooth muscle, where it activates soluble guanylate cyclase, possibly by binding to the iron centre,[28] converting GTP to cGMP. The cGMP then initiates the relaxation of the smooth muscle. Sheer stress caused by increased blood flow also activates the release of nitric oxide from the endothelial layer, leading to vasodilation and relieving the stress.

The failure of smooth muscle relaxation can lead to health problems such as hypertension, and various nitric oxide donor compounds, such as glyceryl trinitrate and amyl nitrite, have been administered to relieve such complaints. These compounds act by releasing nitric oxide directly to the smooth muscle, bypassing the endothelial cells. The thiol dependent metabolism of these compounds can lead to the development of tolerance.

2.1.3.3 Platelet Aggregation

Platelets are small cell fragments present in blood that are able to adhere to each other and to the walls of blood vessels, allowing blood clotting and providing vital protection in the event of injury. Nitric oxide inhibits the aggregation of platelets and actively promotes their dissagregation.[20] The action of nitric oxide in this respect was found to be mediated *via* a cGMP mechanism, the nitric oxide source being both the endothelial cells and the platelets themselves. Inhibition of platelet aggregation is essential within blood vessels to prevent blockages, which can lead to heart failure.

2.1.3.4 Immune Defence

Nitric oxide is active in immune defence, being involved in macrophage activity, antiparisitic activity and the action of neutrophils.[20]

Macrophages are cells that provide a non-specific immune response, protecting against foreign substances and cells without relying upon fully identifying the substances.[3] Macrophages must be activated by substances called cytokines in order to respond.[20] The macrophage acts by engulfing the matter (a process known as phagocytosis) and then killing it using cytotoxic substances.

The cytotoxicity of activated macrophages has been shown to depend upon the presence of L-arginine,[20] and this action is accompanied by the formation of nitrite and citrulline, showing that nitric oxide is involved.[29] The NOS involved in the production of the nitric oxide here is inducible, resulting in the production of relatively high levels of nitric oxide, when it becomes cytotoxic.

If a region of the body suffers a large infection this is accompanied by high levels of macrophage activity, and the nitric oxide produced causes vasodilation, and sometimes a critical drop in blood pressure (hypotension). This condition is known as septic shock.

2.1.3.5 Apoptosis

The role of nitric oxide in apoptosis, the process by which cells commit suicide, provides a good example of the two sides of nitric oxide's physiological nature; it exhibits both pro- and anti- apoptosic properties.

Nitric oxide produced by the eNOS inhibits apoptosis in several types of cell, including endothelial cells and lymphocytes.[29] The precise mechanism by which nitric oxide inhibits apoptosis is not yet clear, though several possibilities have been identified. Nitric oxide can influence gene transcription and enzyme activity, and can alter the redox balance in cells through reaction with oxygen radicals, and it is possible that these factors could be important in apoptosis.

Nitric oxide produced in larger quantities by the iNOS can induce the biochemical features of apoptosis in various cell types. Once again, the precise mechanism involved is unknown, but it seems likely that nitric oxide induces DNA damage,

leading to the production of caspases which will promote fragmentation of DNA and hence death of the cell. The method by which nitric oxide induces DNA damage is also speculative. Some studies suggest that peroxynitrite, formed from the reaction of nitric oxide with superoxide, causes the damage,[30] but others failed to find evidence for this and instead suggest that nitric oxide acts directly in this respect.[21]

2.1.3.6 Neurotransmission

Messages are transmitted within the brain and around the body along nerves. The information is passed along each nerve cell in the form of tiny electrical impulses until it reaches the boundaries between cells, which are called synapses. Here the electrical impulse is converted into a chemical messenger, which diffuses to adjacent cells, passing on the information. The main chemical messengers in this process are the amino acids aspartic acid and glutamic acid.

Neurotransmission of this type is known to be associated with elevated cGMP levels,[20] and the process is also dependent upon Ca^{2+} / calmodulin. The similarity in the dependencies found with smooth muscle relaxation led researchers to investigate the possibility that nitric oxide was involved. It was then that the dependence upon L-arginine, and the production of citrulline was discovered. In the late 1980s it was reported that cultured brain cells produced a substance that was like EDRF,[31] and an enzyme that catalyses the formation of nitric oxide from L-arginine was isolated from the rat forebrain.

Nitric oxide appears to act in two ways in the nervous system. In the first, it acts in the brain as a retrograde messenger, being formed in the postsynaptic nerve cell following activation by an amino acid neurotransmitter. Nitric oxide then diffuses into neighbouring cells, including the presynaptic nerve cell, acting upon guanylate cyclase, and strengthening the connection across the synapse. It is possible that nitric oxide aids the development of long-term memory in this way.

2.1.3.7 Other Processes

Nitric oxide is involved in numerous other physiological processes, including the re-adsorption and re-deposition of bone,[32] antioxidant action,[33] and is possibly a carcinogen.[3]

2.1.3.8 Nitric Oxide in Medicine

Nitric oxide donor drugs and drugs that act upon pathways producing or utilising nitric oxide have potential uses in relieving a number of conditions, including angina, male erectile dysfunction, asthma, and use in surgery, for example to reduce blood clotting.

Nitric oxide has been administered directly in gaseous form, for example to relieve high blood pressure in the lungs of babies.[34] A number of drugs used to treat hypertension work by releasing nitric oxide, including glyceryl trinitrate and amyl nitrite.[3]

Pfizer's impotency drug Viagra (sildenafil citrate) acts by inhibiting the enzyme phosphodiesterase type 5 (PDE5). This enzyme is responsible for the degradation of cGMP in the corpus cavernosum, so the drug works by allowing cGMP levels to rise, causing an increased response to nitric oxide and enhancing vasodilation.[35]

Future possibilities for nitric oxide based therapy are drugs based upon diazeniumdiolates, or NONOates, which release nitric oxide in water (Figure 2.4).[36] Sensors used in intensive care to continuously monitor compounds in the blood stream have been coated with silicone rubber incorporating NONOates to prevent potentially fatal blood clots developing. The coating works by releasing nitric oxide, which inhibits platelet aggregation and reduces clotting.[37]
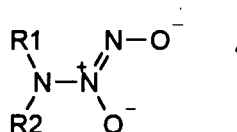
Figure 2.4 Generic structure of the NONOates

2.2 *S*-Nitrosothiols

2.2.1 Physical Properties of *S*-Nitrosothiols

S-Nitrosothiols are formed from the nitrosation of thiols (see Section 1.2.4) and have the general structure R-S-N=O. The terms primary, secondary and tertiary are often used to categorise nitrosothiols, and this refers to the structure at the carbon α to the nitroso group (Figure 2.5).
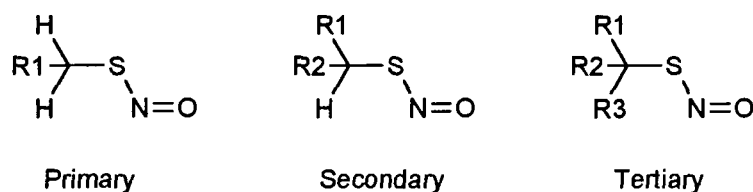
Figure 2.5 Primary, secondary and tertiary nitrosothiols

Nitrosothiols are coloured: primary and secondary species are red/pink whilst the tertiary compounds are green. The colour arises from the visible absorption maximum at 545 nm (primary and secondary species) or 590 nm (tertiary species), which is due to the weak $n_N \rightarrow \pi^*_{NO}$ transition ($\varepsilon \approx 20$ dm^3 mol^{-1} cm^{-1}). A more intense absorption maximum ($\varepsilon \approx 1\ 000$ dm^3 mol^{-1} cm^{-1}) is also exhibited by nitrosothiols at 340 nm, and this is due to the $n_O \rightarrow \pi^*_{NO}$ transition.[38]

Infra-red and Raman spectroscopic investigations have been carried out on *S*-nitrosothiols, showing complete loss of the S–H stretch at 2 600 cm^{-1} seen for thiols and the appearance of two new bands at $\approx 1\ 500$ cm^{-1} (N=O stretch) and ≈ 650 cm^{-1} (N–S stretch).[39]

^{1}H and ^{13}C nmr spectra have been obtained and used to distinguish between nitrosothiols and their corresponding thiols.[40] Resonances of protons on the α carbon are shifted to lower frequency by about 1 ppm upon nitrosation. Protons on the β carbon only undergo significant shifts upon nitrosation for tertiary nitrosothiols: this could relate to the preferred conformers of these nitrosothiols relative to primary and secondary species (see below). The ^{13}C spectra show shifts to higher frequency of around 10 ppm for the α carbons, whereas the β carbons exhibit shifts to lower frequency of about 5 ppm upon nitrosation.

[15]N nmr studies on *S*-nitrosothiols have also been carried out, and the chemical shifts correlated with the visible absorption maxima and reduction potentials of the nitrosothiols, and also the pK_{SH} of the parent thiol.[41] The ^{15}N nmr shift for primary and secondary nitrosothiols is around 730 ppm whereas that for tertiary species is around 790 ppm (referenced to ^{15}N spectrum of Na[15]NO$_2$),[41] indicating the electron density on the nitroso nitrogen is lower for the latter class of nitrosothiols: this could explain their greater reactivity in reactions with nucleophiles.

Many nitrosothiols are not sufficiently stable to isolate as solids, but some have been crystallised, for example *S*-nitrosoglutathione,[42] *S*-nitroso *N*-acetyl penicillamine,[43] *S*-nitroso captopril,[44,45] some *S*-nitroso thiosugars,[46,47] and *S*-nitroso triphenylmethane thiol.[39] Crystal structures have been obtained for some of these nitrosothiols, including *S*-nitroso *N*-acetyl penicillamine[43] and *S*-nitroso captopril.[44]

Theoretical studies and the analysis of crystallographic data provide information about the preferred conformations of nitrosothiols.[39,45] The *syn* conformer (Figure 2.6) is predicted to be preferred on electronic grounds for all nitrosothiols, and this is observed for the primary and secondary species.[45] For tertiary nitrosothiols a competing steric effect causes a preference for the *anti* conformer. The energy difference between the *syn* and *anti* forms is around 4 kJ mol^{-1} for tertiary nitrosothiols, the value being obtained by variable temperature ^{15}N nmr.[45] The energy barrier for inter-conversion has been calculated for MeSNO to be about 60 kJ mol^{-1},[39] the barrier arising from the significant double bond character of the S–N bond.
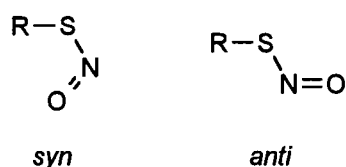
Figure 2.6 *Syn* and *anti* conformers of a nitrosothiol

2.2.2 The Chemistry of *S*-Nitrosothiols

The reactions of *S*-nitrosothiols have aroused considerable interest in recent years because of the potential for nitric oxide release from these compounds. Studies have been undertaken with a view to understanding the medical potential and

physiological action, which is similar to that of nitric oxide, of nitrosothiols. Much of the chemistry of these compounds has been reviewed.[48,49,50]

2.2.2.1 Thermal and Photochemical Decomposition

Nitrosothiols undergo thermally and photochemically induced homolytic cleavage of the S–N bond, producing nitric oxide and the corresponding disulfide as the final products.[51] The photochemical process has been studied in detail for *S*-nitroso glutathione decomposition and can be induced by irradiation with light of 340 nm or 545 nm wavelength.[52] The process is approximately first order in [RSNO],[52] and proceeds *via* production of thiyl radicals which were detected using EPR techniques.[53] The mechanism in Scheme 2.8 has been proposed for this reaction.[54]

$$RSNO \xrightarrow{h\nu / \Delta} RS^\bullet + {}^\bullet NO$$

$$RS^\bullet + RSNO \longrightarrow RSSR + {}^\bullet NO$$

$$RS^\bullet + O_2 \longrightarrow RSOO^\bullet$$

$$RSOO^\bullet + RSNO \longrightarrow RSSR + {}^\bullet NO + O_2$$
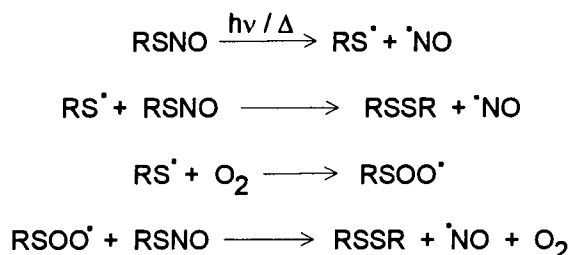
Scheme 2.8 Mechanism of the photochemical and thermal degradation of nitrosothiols

Some nitrosothiols, especially tertiary ones, are less susceptible to photochemical decomposition than others, and this has been attributed mainly to steric effects rather than differences in the strength of the S–N bond.[55]

Interesting work has recently been reported in which a monolayer of the thiol dithiothreitol was formed on a gold surface, and nitrosated by transnitrosation from *S*-nitroso dithiothreitol using a continuous flow system.[56] Exposure of the derivatised surface to visible light caused loss of nitric oxide and the formation of disulfide on the surface. This could have possible future medical applications for the delivery of nitric oxide with high spatial selectivity.

2.2.2.2 Hg²⁺ / Ag⁺ Promoted Decomposition

The hydrolysis of nitrosothiols (Scheme 2.9) has been studied under acidic conditions in the presence of a nitrous acid trap, ensuring no re-formation of the

nitrosothiol.[51] The reaction is promoted by Hg^{2+} and Ag^{+}. Reaction with Hg^{2+} has found application in the Saville assay for quantitative determination of nitrosothiols.[57]

$$H_2O + RSNO + H^+ \rightleftharpoons RSH + HNO_2 + H^+$$

nitrous acid trap
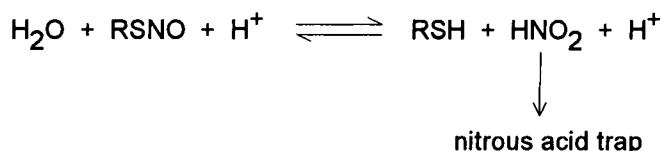
Scheme 2.9 Hydrolysis of nitrosothiols

The mechanism of the reaction has been thoroughly studied,[58] and Hg^{2+} appears to be more effective than Ag^{+}. With Hg^{2+} the hydrolysis is first order in both [RSNO] and [Hg^{2+}] and the rate constant shows little variation with nitrosothiol structure. The reaction has been interpreted in terms of complexation between the metal ion and the nitrosothiol sulfur atom, followed by attack by water in the rate determining step, yielding nitrous acid and the {RSHg}$^+$ complex.

The high affinity of thiols for Hg^{2+} leads to the mercury ion becoming effectively trapped in the {RSHg}$^+$ complex, so stoichiometric quantities of Hg^{2+} are required. $Hg(NO_3)_2$ was more effective in the reaction than $HgCl_2$, and this was attributed to the fact that the latter species exists predominantly in its undissociated form in aqueous solution.

Decomposition by Ag^+ occurs by a different mechanism than for Hg^{2+}, being first order in [RSNO] and 2.5 order in [Ag^+]. Precipitation of the RSAg complex produced in the reaction is observed.

2.2.2.3 Cu^+ Catalysed Decomposition of *S*-Nitrosothiols

Nitrosothiol decomposition was found to occur in the presence of low concentrations of Cu^{2+}, the amount present adventitiously in buffer solutions often being sufficient to effect decomposition.[59] The failure to observe any change in the Cu^{2+} EPR signal during the reaction suggested Cu^{2+} was the active species.[59] However, this was later shown to be incorrect, and use of the specific Cu^+ chelator neocuproine, and the effect of reducing agents, proved the active species to be Cu^+.[60]

Other metal ions such as Zn^{2+}, Mg^{2+}, Ni^{2+} and Fe^{3+} were investigated and found to be ineffective.[59] Whilst some contention exists regarding the ability of Fe^{2+} to catalyse nitrosothiol decomposition,[59,61] Cu^+ is certainly the most effective catalyst.

The products of the Cu^+ catalysed decomposition reactions are the disulfide and nitric oxide,[59] which makes the reaction interesting from a physiological perspective. The reaction can be completely halted by the addition of metal chelators such as EDTA and the specific Cu^+ chelator neocuproine.[59, 60]

The Cu^+ ions essential for the decomposition are produced by reduction of the Cu^{2+} by thiolate.[60] Small amounts of thiolate are present in nitrosothiol solutions because of the reversibility of nitrosation and, possibly, through alkaline hydrolysis of the nitrosothiol.[60,62]

The kinetics of the Cu^+ catalysed decomposition exhibit a variety of characteristics.[59,60,62] First order decomposition of the nitrosothiols is usually observed, and in these situations plots of k_{obs} versus $[Cu^{2+}]$ are linear, showing the reaction to be first order in $[Cu^{2+}]$.[59] Induction periods are often observed, which get shorter as more Cu^{2+} or thiol is added.[62] These result from the requirement to form sufficient Cu^+ initially to allow reaction to occur at rates faster than the re-oxidation and disproportionation of the Cu^+. In some circumstances zeroth order decomposition traces have been observed, and have been interpreted in terms of rate limiting Cu^+ formation.[60]

When first order decomposition traces are observed, adding thiol initially leads to increasing k_{obs} values, and plots of k_{obs} versus thiolate are linear. However, for some thiols such as *N*-acetyl penicillamine, k_{obs} reaches a maximum as [thiol] is increased, whereupon k_{obs} then decreases. This has been attributed to complexation of Cu^{2+} by the thiol, probably through the carboxylate groups.[60]

The observations described above are consistent with the mechanism given in Scheme 2.10.[60] The reaction is catalytic in Cu^{2+}, and produces thiolate, therefore only small amounts of thiol need to be present initially. For GSNO decomposition, the rapid formation of a Cu^{2+}-GSH complex, followed by Cu^+ release and GSNO decomposition, has been observed.[63]

$$RSH \rightleftharpoons RS^- + H^+$$

$$2\,RS^- + 2\,Cu^{2+} \longrightarrow 2\,Cu^+ + RSSR$$

$$RSNO + Cu^+ \longrightarrow RS^- + NO + Cu^{2+}$$
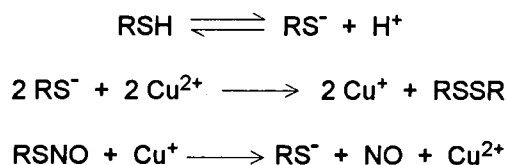
Scheme 2.10 Copper catalysed decomposition of nitrosothiols

When nitrosothiol solutions are prepared in acid solution using excess nitrous acid, the nitrosation equilibrium is forced further to the nitrosothiol product, and less thiol is therefore present, resulting in slower decomposition in the Cu^+ catalysed pathway, eventually halting the reaction.[62] Similarly, in nitrosothiol solutions which have been left standing prior to adding copper, the thiol undergoes aerial oxidation and slower decomposition is then observed.[62] Nitrosothiol solutions kept under acidic conditions are stable, presumably because the thiolate anion, the active reducing agent, is now protonated.

Values of rate constants for the Cu^+ catalysed decomposition of nitrosothiols, despite their continued quotation in the literature, are essentially meaningless because the true quantities of both Cu^{2+} and thiol are always unknown. However, it was clear from the early studies [59] that some nitrosothiols have greater apparent reactivity than others do. The observation that nitrosothiols with β-amino groups were very reactive led to the proposal that intermediates like that shown in Figure 2.17 are important in the reaction.[59]
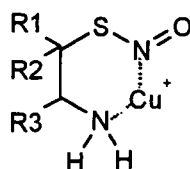
Figure 2.17 Complex between a nitrosothiol and Cu^+

GSNO was first thought to have low reactivity,[59] but recent work following nitric oxide formation rather than GSNO decomposition, revealed rapid decomposition of GSNO in the Cu^+ catalysed reaction.[64] The difference between this study and the earlier work was the relative concentrations of the nitrosothiol and Cu^{2+}: for the early work [GSNO] >> [Cu^{2+}], whereas for the later work the reverse was true. The limited decomposition when [GSNO] >> [Cu^{2+}] has been attributed to strong

complexation of the copper by the disulfide, GSSG,[65] produced in the reaction (Figure 2.8): this was confirmed by showing nitric oxide release from GSNO was slower and gave lower yields when GSSG was added.[64]
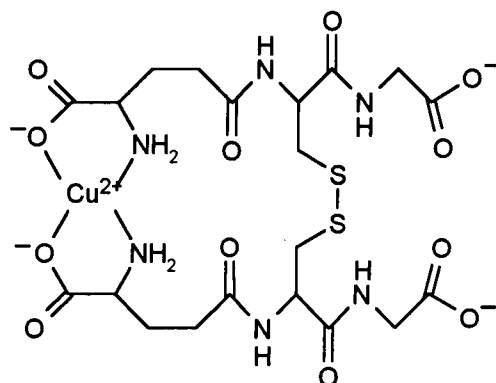
Figure 2.8 Complexation of Cu^{2+} by GSSG

In the *in vivo* situation, very little copper is actually present as free (hydrated) Cu^{2+}: most of the copper is bound to proteins. It was therefore necessary to investigate whether protein-bound Cu^{2+} sources catalyse nitrosothiol decomposition. Studies using Cu^{2+} bound to the tripeptide Gly-Gly-His, to two histidine molecules, or to human serum albumin, showed that nitrosothiol decomposition still occurred *via* the Cu^+ catalysed pathway, albeit at lower rates.[66]

One of the major copper containing enzymes in mammals is the copper zinc-containing form of superoxide dismutase (CuZn-SOD).[67] The enzyme catalyses the conversion of superoxide to hydrogen peroxide. Given that superoxide reacts rapidly with nitric oxide, the enhancement of nitric oxide-dependent vasodilation by CuZn-SOD could arise from the removal of superoxide.[68] However, the possibility that the copper in the enzyme enhances vasodilation by releasing nitric oxide from nitrosothiols also exists. The enzyme has been shown to mediate nitrosothiol decomposition in a process that is enhanced by reducing agents such as glutathione, suggesting the reaction occurring involves the Cu^+ pathway.[67] Reaction of the enzyme with hydrogen peroxide, producing superoxide and Cu(I)Zn-SOD has also been observed, and this too mediates *S*-nitroso glutathione decomposition.

2.2.2.4 Decomposition by Seleno Compounds

Selenium is an essential element in mammalian diets. Selenium deficiency has been linked to several types of heart disease, and the selenium containing enzyme glutathione peroxidase has been linked to processes involving nitric oxide.[69]

Studies on S-nitroso N-acetyl penicillamine and GSNO decomposition showed that nitric oxide release from the nitrosothiols was stimulated by selenium containing compounds, including selenocystamine and selenocystine.[69] In the case of GSNO only, glutathione peroxidase was also effective. The reactions require the presence of thiols, an observation that led to the proposal of the mechanism in Scheme 2.11, which falls short of fully explaining what happens to the nitrosothiol. The addition of selenols (R'SeH) in the absence of added thiol also caused decomposition, providing evidence for the last step in the scheme.

$$R'Se\text{-}SeR' + RSH \rightleftharpoons RS\text{-}SeR' + R'SeH$$

$$RS\text{-}SeR' + RSH \rightleftharpoons RS\text{-}SR + R'SeH$$

$$RSNO + R'SeH \longrightarrow NO + products$$
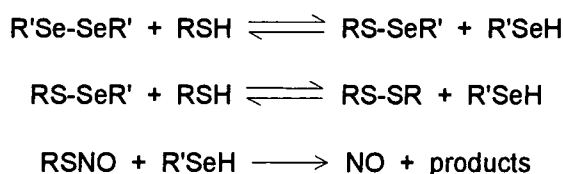
Scheme 2.11 Seleno decomposition of S-nitrosothiols

2.2.2.5 Reactions of Nitrosothiols with Thiols

The reactions between nitrosothiols and thiols can be categorised into two types: reaction between between the nitrosothiol RSNO and a different thiol, R'SH; and the reaction of RSNO with the thiol from which it is derived, RSH.

- **Reaction of RSNO with a different thiol, R'SH**

The earliest studies on the reactions between nitrosothiols and different thiols gave three disulfides as the isolated products, RSSR, R'SSR and R'SSR'.[70] These products are consistent with the decomposition of the nitrosothiol RS'NO as well as the nitrosothiol initially present, and therefore indicate that nitrosation of R'SH occurs. Spectrophotometric studies have confirmed that some RSNO is converted to R'SNO.[71] Two possible mechanisms exist: spontaneous decomposition of RSNO to NO, which then oxidises to a nitrosating reagent such as N_2O_3; or a direct transfer of NO^+ from RSNO to R'SH (transnitrosation).

Reactions between thiomalic acid and *S*-nitroso cysteine and between thioglycolic acid and *S*-nitroso *N*-acetyl penicillamine were studied, and under conditions where [R'SH] >> [RSNO] first order kinetics were observed.[71] The change in k_{obs} with pH followed a sigmoidal curve with a point of inflexion at p$K_{R'SH}$, indicating a reaction *via* R'S⁻. The observation that the formation of R'SNO is much faster than the spontaneous decomposition of RSNO proves that the reaction occurs by direct NO⁺ transfer.

The rate equation is first order in both the nitrosothiol and the thiolate concentrations, and some rate constants have been reported.[71,72] The process is reversible, and some equilibrium constants have been obtained at pH 7.4.[73] The reaction occurring is therefore that shown in Scheme 2.12.

$$R'SH \rightleftharpoons R'S^- + H^+$$

$$RSNO + R'S^- \rightleftharpoons RS'NO + RS^-$$
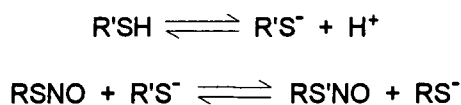
Scheme 2.12 Transnitrosation from nitrosothiols to thiols

- **Reactions between RSNO and RSH**

Several studies have investigated the process occurring when nitrosothiols are reacted with the thiol from which they are derived. When low concentrations of the thiol are present, and no metal chelator is used, the nitrosothiol can decompose to nitric oxide and the disulfide *via* the copper catalysed pathway (Section 2.2.3).

When higher concentrations of thiol are used ([RSH] >> [RSNO]), the decomposition of the nitrosothiol is unaffected by the addition of Cu^{2+} or metal ion chelators,[74,75] indicating that the decomposition is not *via* the Cu^+ catalysed route.

Analysis of the products showed that the nitrogenous products are ammonia,[74,75,76] nitrous oxide,[74,76] and some nitrite.[74] The reduction in nitrite yield under anaerobic conditions was interpreted in terms of prior formation of nitric oxide, followed by oxidation.[74] For thiol concentrations approximately equal to the nitrosothiol concentration, nitrite is the principal nitrogen containing product,[74,75] however as the thiol to nitrosothiol ratio is increased the major nitrogen product becomes ammonia. [74,75]

The main sulfur containing product is the disulfide.[74,75]   Suggestions that the sulfinamide ($RS(O)NH_2$) forms have also been advanced,[76] though the evidence for this is not conclusive.

The rate equation for these reactions is given in Equation 2.2.[75,77]   The rate constants for the reactions [75] are several orders of magnitude lower than those for thiol – nitrosothiol transnitrosations.[72]   pH dependence studies revealed that the reactive form of the thiol is the thiolate anion.[75]

$$Rate = k[RSNO][RSH] \qquad \text{Equation 2.2}$$

One of the reaction schemes proposed for these reactions is given in Scheme 2.13.[74,75]
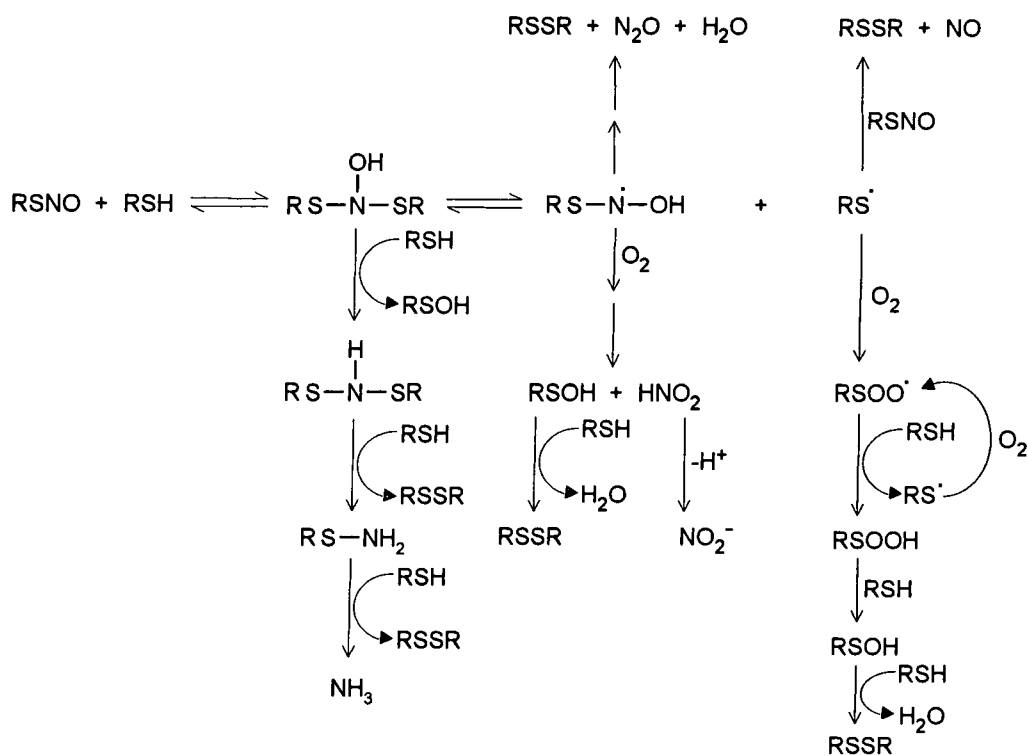
Scheme 2.13 A possible mechanism for the reaction of RSNO with RSH

Some contribution from direct nucleophilic attack at the nitrosothiol sulfur atom by thiolate, yielding the disulfide and NO⁻ has also been proposed.[76,77]   The NO⁻ then rapidly reacts with itself, forming nitrous oxide (Scheme 2.14). Some evidence for the formation of NO⁻ has been reported.[76]

$$2\,NO^- + 2\,H^+ \longrightarrow N_2O + H_2O$$
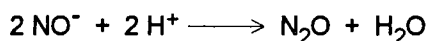
Scheme 2.14 Formation of nitrous oxide from NO⁻

2.2.2.6 Nitrosothiol Decomposition by Other Sulfur Nucleophiles

The reactions between nitrosothiols and a number of sulfur centred nucleophiles have been studied, including sulfite, thiocyanate, thiomethoxide and sulfide.[78] In most cases the reactions were first order in the nitrosothiol concentration and first order in the nucleophile concentration. The reactions with sulfide exhibited more complicated kinetics, which were not fully evaluated.

The most reactive of these nucleophiles was sulfite, followed by thiomethoxide. For example, the second order rate constant for the reaction of sulfite with *S*-nitroso cysteine at pH 7.4 and 25 °C is 650 dm³ mol⁻¹ s⁻¹. Sulfite was shown to react through SO_3^{2-} rather than HSO_3^-. The reaction produced the thiol and another species shown not to be nitric oxide or nitrite, and presumed to be hydroxylamine disulfonate, which is the usual product of sulfite nitrosation.[79]

2.2.2.7 Reaction Between Nitrosothiols and Nitrogen Nucleophiles

Nitroso compounds such as alkyl nitrites have been used as nitrosating agents, and it is possible that nitrosothiols could find similar application. The nitrosation of amines by nitrosothiols has been reported,[80,81] and in the case of secondary amines where the reaction yields stable nitrosamines the reaction could have physiological significance given the carcinogenic nature of the products.

Kinetic and mechanistic studies on the reaction between nitrogen nucleophiles, particularly amines, and the nitrosothiol *S*-nitroso penicillamine have been carried out.[81] The reaction with secondary amines produces nitrosamines, whereas for primary amines diazotisation leading to de-amination occurs. The observed rate equation for these reactions is given in Equation 2.3, and indicates that the reactive species is the free base form of the amine: significant reactivity is therefore only observed at high pH.

$$Rate = \frac{kK_a[\text{amine}]_t[\text{RSNO}]}{K_a + [\text{H}^+]}$$

Equation 2.3

The reaction occurring was shown to be a direct nitrosation because it was unaffected by the removal of oxygen from the solutions. For secondary amines a correlation between $\log k$ and the pK_a of the amine was observed, though this correlation did not extend to include the primary amines studied. A fairly reasonable correlation between $\log k$ and the Ritchie N^+ parameter [82,83] was observed,* including primary and secondary amines, and other nucleophiles such as azide. This observation is in line with the results of studies where nitrogen nucleophiles were reacted with nitroso sulfonamide [84,85] and both these and the nitrosothiol study also revealed that $\log k$ did not correlate with the Pearson nucleophilicity parameter n.[86]

The reactions of primary amines and ammonia revealed that, under conditions where $[RNH_2]_\tau \gg [RSNO]$, k_{obs} values reached a plateau value at high $[RNH_2]_\tau$. This was interpreted in terms of the prior formation of an inactive complex between the amine and the nitrosothiol, for which some spectroscopic evidence was obtained. A possible structure for this complex is given in Figure 2.9.
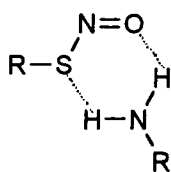
Figure 2.9 Possible complex between a primary amine and a nitrosothiol

2.2.2.8 Reaction of Nitrosothiols with Hydrogen Peroxide and Superoxide

Hydrogen peroxide has been shown to react with nitrosothiols, forming peroxynitrite.[88] At physiological pH the formation of the peroxynitrite is too slow for its concentration to build up to observable levels before decomposing. At high pH (*ca.* 13) peroxynitrite was identified by its characteristic UV absorption at 302 nm.[89]

---

* Ritchie observed that for reactions of nitrogen nucleophiles with a given cation, $\log k = \log k_o + N^+$, where k_o is a parameter relating to the cation used and N^+ depends upon the nucleophiles and the solvent. Some of Kice's data showed that the relationship could be extended to include the reaction of nitrogen nucleophiles with neutral electrophiles if the initial attack by the nucleophiles is rate limiting.[87]

The reaction was found to be first order in both the nitrosothiol and hydrogen peroxide concentrations, and pH dependence studies identified the hydroperoxide anion as the reactive species.[88] The reaction mechanism outlined in Scheme 2.15 was proposed. Subsequent oxidation of the thiol by peroxynitrite probably occurs.

$$H_2O_2 \rightleftharpoons HOO^- + H^+ \qquad pK_a = 11.5$$

$$HOO^- + RSNO \longrightarrow RS^- + ONOOH$$

$$ONOOH \rightleftharpoons ONOO^- + H^+$$

$$ONOOH \longrightarrow NO_3^- + H^+$$

$$ONOO^- \longrightarrow NO_2^- + \tfrac{1}{2}O_2$$
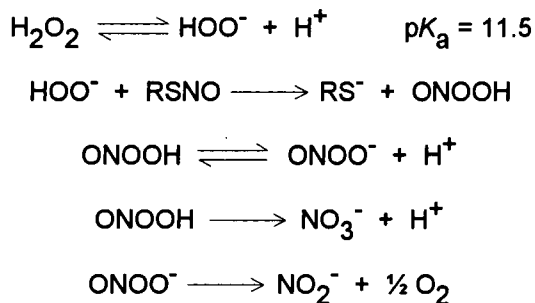
Scheme 2.15 Mechanism of the reaction between nitrosothiols and hydrogen peroxide

The decomposition of nitrosothiols by superoxide (O_2^-), produced from the reaction between xanthine and xanthine oxidase, has also been reported.[90] Whilst it is possible that the reaction could proceed *via* hydrogen peroxide formation and its subsequent reaction with the nitrosothiol, the inability of catalase (which destroys hydrogen peroxide) to affect the reaction suggests that the reactive species is superoxide.   The stoichiometry of the reaction was found to be two moles of superoxide to one mole of nitrosothiol. The mechanism of the reaction was not elucidated, but it was suggested that the stoichiometry could be explained if superoxide reacted with the nitrosothiol to produce nitric oxide, which would then rapidly react with superoxide to produce peroxynitrite.

2.2.2.9 Ascorbic Acid and Nitrosothiol Decomposition

Several investigations have reported that ascorbic acid (Vitamin C) can promote *S*-nitrosothiol decomposition.[47,91,92,93]   Some of the work was carried out in physiological media.[92] The decomposition has been partly explained in terms of Cu^{2+} reduction by ascorbic acid,[47,92] though evidence of a copper independent reaction was also presented.[91,92,93]   These studies are discussed in detail in Chapters 3 – 5 alongside the results obtained from further studies into these reactions.

2.2.3 *S*-Nitrosothiol Physiology

S-nitrosothiols and *S*-nitrosoproteins have been detected *in vivo* including in human airways, blood, plasma and in the brain.[94,95,96,97] Typical concentrations appear to be in the micro-molar range.[95] The most prevalent *in vivo S*-nitroso compounds are *S*-nitroso glutathione, *S*-nitroso albumins and *S*-nitroso haemoglobin,[96] which has been characterised.[98,99]

The mechanisms of *S*-nitrosothiol formation *in vivo* have not yet been elucidated. Under most biological conditions, conventional nitrosation by acidified nitrite is not feasible. Several suggestions have been made regarding the *in vivo* formation mechanisms, including formation from thiols and nitric oxide, formation from thiols and nitric oxide catalysed by copper ions or the copper protein ceruloplasmin,[100,101] formation mediated by inducible nitric oxide synthase,[102] and transnitrosation from other species.

Nitrosothiols exhibit many of the physiological properties that nitric oxide does, which has led many researchers to assume that the physiological action of nitrosothiols occurs *via* nitric oxide release. This assumption has been challenged on the grounds that the *in vitro* stability of nitrosothiols with respect to spontaneous nitric oxide release does not correlate with their potency in physiological environments.[49,95] However, several pathways exist for the release of nitric oxide from nitrosothiols (Section 2.2.2) and those which operate *in vivo* are not fully established, so the lack of correlation in not necessarily evidence that prior nitric oxide release does not occur during nitrosothiol activation.

The role of naturally occurring (endogenous) nitrosothiols is not yet fully understood. Endogenous nitrosothiols and many synthetic nitrosothiols have been shown to induce vasodilation in both veins and arteries,[46,49,103] inhibition of platelet aggregation, and have been implicated in the nervous system[49] and cell death.[49] Deficiency of nitrosothiols in airways has been implicated in asthmatic respiratory failure.[104] There is some evidence that nitrosothiols might also cleave DNA in the presence of hydrogen peroxide.[105] It has been suggested that nitrosothiols might act as storage systems for nitric oxide in the body,[96] and that stable nitrosothiols might transfer their NO moiety to other thiols, forming less stable species, which then release nitric oxide.[94,106]

Research has been carried out into the medical potential of nitrosothiols, and the subject has been recently reviewed.[95] Where the treatment of angina is concerned, nitrosothiols might offer advantages over the widely used glyceryl trinitrate because nitrosothiol therapy is not prone to the drug tolerence.[107] *S*-nitroso glutathione is used to inhibit platelet aggregation during some operations,[50] and the possibility of targeting nitrosothiols to kill cancerous cells is being explored.[108]

2.3 References

1. M. Fontecave, and J.-L. Pierre, *Bull. Soc. Chim. Fr.*, **131**, 620 (1994).

2. R. Beringer, E. Rawson and A. Henry, *Phys. Rev.*, **94**, 343 (1954).

3. A. R. Butler and D. L. H. Williams, *Chem. Soc. Rev.*, 233 (1993).

4. W. J. Dulmange, E. A. Meyers and W. N. Lipscomb, *Acta Cryst.*, **6**, 760 (1953).

5. H. Tsukahara, T. Ishida and M. Mayumi, *Nitric Oxide: Biol. Chem.*, **3**, 191 (1999).

6. P. C. Ford, D. A. Wink and D. M. Stanbury, *FEBS Lett.*, **326**, 1 (1993).

7. J. S. Beckman, M. Carson, C. D. Smith and W. H. Koppen, *Nature*, **364**, 584 (1993).

8. H. Ischiropoulos, L. Zhu and J. S. Beckman, *Arch. Biochem. Biophys.*, **298**, 446 (1992).

9. L. Zhu, C. Gum and J. S. Beckman, *Arch. Biochem. Biophys.*, **298**, 452 (1992).

10. A. A. Noronha, M. M. Epperlein and N. Woolf, *FEBS Lett.*, **321**, 59 (1993).

11. E. G. Janzen, A. L. Wilcox and V. Monoharan, *J. Org. Chem.*, **58**, 3597 (1993).

12. A. L. Wilcox and E. G. Lanzen, *J. Chem. Soc., Chem. Comm.*, 1377 (1993).

13. M. P. Doyle, S. M. Mahapatro, R. D. Broene and J. K. Guy, *J. Am. Chem. Soc.*, **110**, 593 (1980).

14. G. B. Richter-Addo and P. Legzdins, 'Metal Nitrosyls', Oxford University Press, New York, 1992.

15. E. Culotta, D. E. Coshland Jr., *Science*, **258**, 1862 (1992).

16. J. Durner and D. F. Klessig, *Current Opinion in Plant Biology*, **2**, 369 (1999).

17. 'This Week', *New Scientist*, 11 April, 13 (1998).

18. S. H. Snyder and D. S. Bredt, *Scientific American*, **226**, 28 (1992).

19. P. R. Myers, R. L. Minor, R. Guerra, J. N. Bates and D. G. Harrison, *Nature*, **345** 161 (1990).

20. S. Moncada, R. M. J. Palmer and E. A. Higgs, *Pharm. Rev.*, **43**, 109 (1991).

21. S. Dimmeler and A. M. Zeiher, *Nitric Oxide: Biol. Chem.*, **1**, 275 (1997).

22. H. Yamasaki, Y. Sakihama and S. Takahashi, *Trends in Plant Science*, **4**, No. 4, 128 (1999).

23. E. Weitzberg and J. O. N. Lundberg, *Nitric Oxide: Biol. Chem.* **2**, 1 (1998).

24. R. F. Furchgott and J. V. Zawadzki, *Nature*, **228**, 373 (1980).

25. M. Feelisch, M. T. Poel, R. Zamra, A. Deussen and S. Moncada, *Nature*, **368**, 62 (1994).

26. R. M. J. Palmer, A. G. Ferrige and S. Moncada, *Nature*, **327**, 524 (1987).

27. L. J. Ignarro, G. M. Buga, K. S. Wood, R. E. Byrns and G. Chaudhuri, *Proc. Natl. Acad. Sci. USA*, **84**, 9265 (1987).

28. A. R. Butler, F. W. Flitney and D. L. H. Williams, *TiPS*, **16**, 18 (1995).

29. M. A. Marletta, S. Yoon, R. Igengov, C. D. Leat and J. S. Wishnok, *Biochem.*, **27**, 8706 (1988).

30. M. G. Salgo, E. Bermudez, G. L. Squadrito and W. A. Pryor, *Arch. Biochem. Biophys.*, **322**, 500 (1995).

31. R. G. Knowles, M. Palacios, R. M. J. Palmer and S. Moncada, *Proc. Natl. Acad. Sci. USA*, **86**, 9030 (1989).

32. P. V. Hauschka and P. D. Damoulis, *Biochem. Soc. Trans.*, **26**, 39 (1998).

33. J. Kanner, S. Harel and R. Granit, *Arch. Biochem. Biophys.*, **289**, 130 (1991).

34. S. Young, *New Scientist*, 13 March, 36 (1993).

35. Viagra U.S. Prescribing Information, *http://www.pfizer.com*, Pfizer, 2000.

36. J. Saavedra and L. Keefer, *Chem. Br.*, July, 31 (2000).

37. New Scientist, 1 April, 11 (2000).

38. J. Barrett, D. F. Debenham and J. Glauser, *J. Chem. Soc., Chem. Commun.*, 248 (1965).

39. N. Arulsamy, D. S. Bole, J. A. Butt, G. J. Irvine, P. A. Jordan and E. Sagan, *J. Am. Chem. Soc.*, **121**, 7115 (1999).

40. B. Roy, A. du Moulinet d'Hardemare and M. Fontecave, *J. Org. Chem.*, **59**, 7019 (1994).

41. K. Wang, Y. Hou, W. Zhang, M. B. Ksebati, M. Xian, J.-P. Cheng and P. G. Wang, *Bioorg. Med. Chem. Lett.*, **9**, 2897 (1999).

42. T. W. Hart, *Tet. Lett.*, **26**, 2013 (1985).

43. L. Field, R. V. Dilts, R. Ravichandran, P. G. Lenhert and G. E. Carnahan, *J. Chem. Soc., Chem. Comm.*, 249 (1978).

44. L. Jia, X. Youngs and W. Guo, *J. Pharm. Sci.*, **88**, 981 (1999).

45. M. D. Bartberger, K. N. Houk, S. C. Powell, J. D. Mannion, K. Y. Lo, J. S. Stamler and E. J. Toone, *J. Am. Chem. Soc.*, **122**, 5889 (2000).

46. A. R. Butler, R. A. Field, I. R. Greig, F. W. Flitney, S. K. Bisland, F. Khan and J. F. Belch, *Nitric Oxide: Biol. Chem.*, **1**, 211 (1997).

47. A. P. Munro and D. L. H. Williams, *Can. J. Chem.*, **77**, 550 (1999).

48. D. L. H. Williams, *J. Chem. Soc., Chem. Comm.*, 1085 (1996).

49. A. R. Butler and P. Rhodes, *Anal. Biochem.*, **249**, 1 (1997).

50. D. L. H. Williams, *Acc. Chem. Res.*, **32**, 869 (1999).

51. D. L. H. Williams, *J. Chem. Soc. Rev.*, **14**, 171 (1985).

52. D. J. Sexton, A. Muruganandam, D. J. McKenney and B. Mutus, *Photochem. Photobiol.*, **59**, 463 (1994).

53. R. J. Singh, N. Hogg, J. Joseph and B. Kalyanaraman, *J. Biol. Chem.*, **271**, 18596 (1994).

54. P. D. Wood, B. Mutus, R. W. Redmond, *Photochem. Photobiol.*, **64**, 518 (1996).

55. N. Bainbrigge, A. R. Butler and C. H. Gorbitz, *J. Chem. Soc., Perkin Trans. 2*, 351 (1997).

56. R. Etchenique, M. Furman and J. A. Olabe, *J. Am. Chem. Soc.*, **122**, 3967 (2000).

57. B. Saville, *Analyst*, 670 (1958).

58. H. R. Swift and D. L. H. Williams, *J. Chem. Soc., Perkin Trans. 2*, 1933 (1997).

59. S. C. Askew, D. J. Barnett, J. McAninly and D. L. H. Williams, *J. Chem. Soc., Perkin Trans. 2*, 741 (1995).

60. A. P. Dicks, H. R. Swift, D. L. H. Williams, A. R. Butler, H. H. Al-Sa'doni and B. G. Cox, *J. Chem. Soc., Perkin Trans. 2*, 481 (1996).

61. A. F. Vanin, I. V. Malenkova and V. A. Serezhenkov, *Nitric Oxide: Biol. Chem.*, **1**, 191 (1997).

62. A. P. Dicks, P. H. Beloso and D. L. H. Williams, *J. Chem. Soc., Perkin Trans. 2*, 1429 (1997).

63. A. C. F. Gorren, A. Schrammel, K. Schmidt and B. Mayer, *Arch. Biochem. Biophys.*, **330**, 219 (1996).

64. D. R. Noble, H. R. Swift and D. L. H. Williams, *J. Chem. Soc., Chem. Comm.*, 2317 (1999).

65. K. Varnagy, I. Sovago and H. Kozlowski, *Inorg. Chim. Acta*, **151**, 117 (1988).

66. A. P. Dicks and D. L. H. Williams, *Chem. Biol.*, **3**, 655 (1996).

67. D. Jourd'heuil, F. S. Laroux, A. M. Miles, D. A. Wink and M. B. Grisham, *Arch. Biochem. Biophys.*, **361**, 323 (1999).

68. R. J. Gryglewski, R. M. J. Palmer and S. Moncada, *Nature*, **320**, 454 (1986).

69. Y. Hou, Z. Guo, J. Li and P. G. Wang, *Biochem. Biophys. Res. Comm.*, **228**, 88 (1996).

70. S. Oae, Y. H. Kim, D. Fukushima and K. Shinhama, *J. Chem. Soc., Perkin Trans. 1*, 913 (1978).

71. D. J. Barnett, J. McAninly and D. L. H. Williams, *J. Chem. Soc., Perkin Trans. 2*, 1131 (1994).

72. D. J. Barnett, A. Ríos and D. L. H. Williams, *J. Chem. Soc., Perkin Trans. 2*, 1279 (1995).

73. D. J. Meyer, H. Kramer, N. Özer, B. Coles and B. Ketterer, *FEBS Lett.*, **345**, 177 (1994).

74. S. P. Singh, J. Wishnok, M. Keshive, W. M. Deen and S. R. Tannenbaum, *Proc. Natl. Acad. Sci. USA*, **93**, 14428 (1996).

75. A. P. Dicks, E. Li, A. P. Munro, H. R. Swift and D. L. H. Williams, *Can. J. Chem.*, **76**, 789 (1998).

76. P. S.-Y. Wong, J. Hyun, J. M. Fukuto, F. N. Shirota, E. G. DeMaster, D. W. Shoeman and H. T. Nagasawa, *Biochem.*, **37**, 5362 (1998).

77. T. Komiyama and K. Fujimori, *Bioorg. Med. Chem. Lett.*, **7**, 175 (1997).

78. A. P. Munro and D. L. H. Williams, *J. Chem. Soc., Perkin Trans. 2*, 1794 (2000).

79. S. B. Oblath, S. S. Markiwitz, T. Novakin and S. G. Chang, *J. Phys. Chem.*, **86**, 4853 (1982).

80. S. Oae and K. Shinhama, *Org. Prep. Proc. Int.*, **15**, 165 (1983).

81. A. P. Munro and D. L. H. Williams, *J. Chem. Soc., Perkin Trans. 2*, 1989 (1999).

82. C. D. Ritchie, *Acc. Chem. Res.*, **5**, 348 (1972).

83. C. D. Ritchie, *J. Am. Chem. Soc.*, **97**, 1170 (1975).

84. L. García-Río, E. Iglesias, J. R. Leis, M. E. Peña and A. Ríos, *J. Chem. Soc., Perkin Trans. 2*, 29 (1993).

85. J. R. Leis, M. E. Peña and A. M. Ríos, *J. Chem. Soc., Perkin Trans. 2*, 587 (1995).

86. R. G. Pearson, H. Sobel and J. Songstad, *J. Am. Chem. Soc.*, **90**, 319 (1968).

87. J. L. Kice and E. Legan, *J. Am. Chem. Soc.*, **95**, 3912 (1973).

88. P. J. Coupe and D. L. H. Williams, *J. Chem. Soc., Perkin Trans. 2*, 1057 (1999).

89. M. N. Hughes and H. G. Nicklin, *J. Chem. Soc. (A)*, 457 (1968).

90. S. Aleryani, E. Milo, Y. Rose and P. Kostka, *J. Biol. Chem.*, **273**, 6041 (1998).

91. M. Kashiba-Iwatsuki, M. Yamaguchi and M. Inoue, *FEBS Lett.*, **389**, 149 (1996).

92. M. Kashiba-Iwatsuki, K. Kitoh, E. Kasahara, H. Yu, M. Nisikawa, M. Matsuo and M. Inoue, *J. Biochem.*, **122**, 1208 (1997).

93. J. N. Smith and T. P. Dasgupta, *Nitric Oxide: Biol. Chem.*, **4**, 57 (2000).

94. M. Kashiba, E. Kasahara, K. Chien and M. Inoue, *Arch. Biochem. Biophys.*, **363**, 213 (1999).

95. H. Al-Sa'Doni and A. Ferro, *Clinical Sc.*, **98**, 507 (2000).

96. J. S. Stamler, O. Jaraki, J. Osborne, D. I. Simon, J. Keaney, J. Vita, D. Singel, C. R. Valeri and J. Loscalzo, *Proc. Natl. Acad. Sci. USA*, **89**, 7674 (1992).

97. B. Gaston, J. Reilly, J. M. Drazen, J. Fackler, P. Ramdev, D. Arnelle, M. E. Mullins, D. J. Sugarbaker, C. Chee, D. J. Singel, J. Loscalzo and J. S. Stamler, *Proc. Natl. Acad. Sci. USA*, **90**, 10957 (1993).

98. R. P. Patel, N. Hogg, N. Y. Spencer, B. Kalyanaraman, S. Matalon and V. M. Darley-Usmar, *J. Biol. Chem.*, **274**, 15487 (1999).

99. M. Wolzt, R. J. MacAllister, D. Davis, M. Feelisch, S. Moncada, P. Vallance and A. J. Hobbs, *J. Biol. Chem.*, **274**, 28983 (1999).

100. K. Inoue, T. Akaike, Y. Miyamoto, T. Okamoto, T. Sawa, M. Otagiri, S. Suzuki, T. Yoshimura and H. Maeda, *J. Biol. Chem.*, **274**, 27069 (1999).

101. G. Stubauer, A. Giuffrè and P. Sarti, *J. Biol. Chem.*, **274**, 28128 (1999).

102. G. Mamone, N. Sannolo, A. Malorni and P. Ferranti, *FEBS Lett.*, **462**, 241 (1999).

103. A. R. Butler, H. H. Al-Sa'doni, I. L. Megson and F. W. Flitney, *Nitric Oxide: Biol. Chem.*, **2**, 193 (1998).

104. B. Gaston, S. Sears, J. Woods, J. Hunt, M. Ponaman, T. McMahon and J. S. Stamler, *Lancet*, **351**, 1317 (1998).

105. J.-W. Park and H. K. Kim, *Biochem. Biophys. Res. Comm.*, **200**, 966 (1994).

106. Z. Liu, A. Ridd, J. E. Freeman and J. Loscalzo, *J. Pharmacol. Exp. Therapeutics*, **284**, 526 (1998).

107. I. L. Megson, M. J. Roseberry, M. R. Miller, F. A. Mazzei, A. R. Butler and D. J. Webb, *Br. J. Pharmacol.*, **126**, Suppl. S, 78P (1999).

108. Y. Hou, J. Wang, P. R. Andreana, G. Cantauria, S. Tarasia, L. Sharp, P. G. Braunschweiger and P. G. Wang, *Bioorg. Med. Chem. Lett.*, **9**, 2255 (1999).

Identification of Two Pathways for Ascorbic Acid Mediated S-Nitrosothiol Decomposition

Chapter 3 Identification of Two Pathways for Ascorbic Acid Mediated
S-Nitrosothiol Decomposition

3.1 Introduction

3.1.1 Structure and Properties of Ascorbic Acid

L-Ascorbic acid § (Figure 3.1) is a compound of some considerable importance, especially in its physiological role as Vitamin C. Other names for the compound include cevitamic acid and L-*threo*-2,3,4,5,6-pentahydroxyhex-2-enoic acid-4-lactone. The importance of the Vitamin as a flour improver and food preservative has led to its being assigned an additive number: E300.
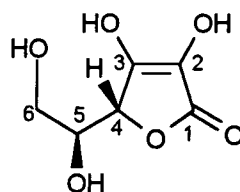
Figure 3.1 The structure of L-ascorbic acid

Vitamin C was first isolated from the adrenal cortex of cattle by Albert Szent – Györgyi in 1922, avoiding the difficulties involved in separating the compound from the sugars in fruit juices. Following analysis to establish the formula mass and molecular formula, the work was published in 1928 naming the newly isolated compound a hexuranic acid.[1]

Work carried out by Haworth on samples provided by Szent – Györgyi resulted in the accurate determination of the structure of ascorbic acid.[2] This was achieved by studying the chemical reactions of the compound, coupled with some UV and X-ray studies.[3,4] The compound was renamed ascorbic acid [5] after being identified as the species whose deficiency causes scurvy. In 1937 Szent – Györgyi and Haworth were awarded the Nobel Prizes for physiology and for chemistry respectively for their pioneering work on ascorbic acid.

Crystals of ascorbic acid are white, melting with decomposition at 190 – 192 °C. X-ray crystallographic studies reveal monoclinic spheroidal crystals, with four molecules of ascorbic acid per unit cell.[3] These molecules are almost completely

---

§ Hereafter use of the name ascorbic acid implies a reference to L-ascorbic acid

flat. The optical rotation of L – ascorbic acid is + 23° in water at 20 °C. Ascorbic acid is highly soluble in water (0.3 g cm^{-3} at 20 °C), less soluble in alcohols and insoluble in benzene, ether and fats.

The UV / visible spectrum of ascorbic acid exhibits λ_{max} = 243 nm at pH 2 in water (ε = 10 000 dm^3 mol^{-1} cm^{-1}). This transition arises from $\pi \rightarrow \pi^*$ excitation in the conjugated carbon – carbon double bond of the lactone ring.[6]

The pK_a values of ascorbic acid are 4.25 (OH group on C$_3$) and 11.75 (OH group on C$_2$). The acidity of the C$_3$ OH group is readily explained in terms of the stabilisation of the O$^-$ anion by conjugative resonance with the carbonyl group on C$_1$. This assertion is backed up experimentally by X-ray studies,[6] which show significant shortening of the C$_3$-O and C$_1$-C$_2$ bonds and lengthening of the C$_1$=O and C$_2$=C$_3$ bonds in sodium ascorbate relative to the neutral acid (Table 3.1). The red shift of the UV λ_{max} to 265 nm upon formation of the ascorbate monoanion is further testimony to this.

Bond	Length in ascorbic acid / Å	Length in sodium ascorbate / Å
C$_1$=O	1.216	1.233
C$_1$-C$_2$	1.452	1.416
C$_2$=C$_3$	1.338	1.373
C$_3$-O	1.326	1.287

Table 3.1 X-ray data for ascorbic acid and sodium ascorbate[6]

3.1.2 Redox Chemistry of Ascorbic Acid

It is the redox chemistry of ascorbic acid that gives rise to the physiological importance of the molecule. This, in turn, has resulted in intense interest in all aspects of its redox properties, particularly those involving iron, copper, thiols and reactive free radicals of biological relevance. A full understanding of the redox chemistry of this important compound remains elusive because of its complexity.

Ascorbic acid (H$_2$A) can act as a two – electron reducing agent, forming dehydroascorbic acid (DHA, Figure 3.2). Loss of one electron from ascorbic acid

results in the formation of the ascorbyl radical HA•, or more accurately the ascorbate radical A•⁻, the species being deprotonated over most of the pH range (pK_a = - 0.45 [6]). This radical is stabilised by delocalisation over the π - system, and has been observed using EPR techniques.[6] Ascorbate radicals undergo disproportionation, yielding H_2A and DHA.[7]
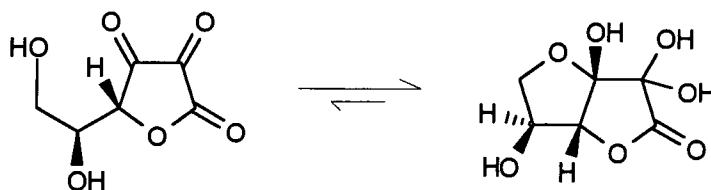
Figure 3.2 Dehydroascorbic acid, showing equilibrium with its most stable (> 99%) bicyclic hemiketal form

3.1.2.1 Autoxidation

The term autoxidation refers to the oxidation of a species by molecular oxygen, in the absence of catalysts. The autoxidation of ascorbic acid to dehydroascorbic acid is slow, being virtually negligible at pH values [7] below 7. The rate of autoxidation increases with pH and calculations show that, even at physiological pH (pH 7.4) where > 99% of the ascorbic acid is present as the monoanion, the reaction occurs principally *via* the dianion.[7]

Irradiation of solutions of ascorbic acid has also been found to cause oxidation. This occurs under both aerobic and anaerobic conditions and proceeds *via* a photochemical free radical pathway. UV, *X*-ray and *γ*-ray sources are active in this respect.[6]

3.1.2.2 Catalysis by Transition Metal Ions

Ascorbic acid oxidation is readily catalysed by transition metal ions, particularly Fe^{3+} and Cu^{2+}, and also Pd^{2+} and Hg^{2+}. [8-12] It is clear that the processes involved are complex, and despite decades of research there is still no consensus regarding the mechanisms involved. There have been several reviews about the transition metal catalysed oxidation.[10,13]

The variety of mechanisms proposed for the catalysed oxidation of ascorbic acid arises in part from the variation in kinetic features observed in different studies. A range of conditions has been employed, so there is a possibility that the mechanism of oxidation is not the same in all cases. Some differences have been observed between the mechanisms involving Cu^{2+} and Fe^{3+}, even under similar conditions.[10]

The discussion that follows concentrates mainly upon the Cu^{2+} catalysed oxidation, given that this produces Cu^+ which is of particular relevance to *S*-nitrosothiol chemistry (Section 2.2.2.3). It has generally been found that the kinetic order with respect to [ascorbic acid] is one,[8,10,14] however the order with respect to other components is less clear. The order in $[Cu^{2+}]$ has often been determined as one,[9,10,12] though other values have been observed including 0.5,[15] and 0.9.[16]

Similarly, the kinetic order in the partial pressure of oxygen is also found to differ, typically decreasing from one as the oxygen pressure is decreased.[10] The oxidation becomes more facile as the pH is increased, indicating the involvement of the ascorbate mono- and di- anions.[8,10,12]

A mechanism that has been invoked in several studies involves the initial reduction of Cu^{2+} by ascorbate, forming the ascorbate radical, which then reacts with Cu^{2+}.[8,10] Reformation of the catalyst is by oxidation of Cu^+ by oxygen, producing hydrogen peroxide (Scheme 3.1).

$$H_2A \rightleftharpoons HA^- + H^+$$

$$HA^- + Cu^{2+} \rightleftharpoons HA^\bullet + Cu^+$$

$$HA^\bullet \rightleftharpoons A^{\bullet -} + H^+$$

$$A^{\bullet -} + Cu^{2+} \longrightarrow DHA + Cu^+$$

$$2\,Cu^+ + 2\,H^+ + O_2 \longrightarrow H_2O_2 + 2\,Cu^{2+}$$
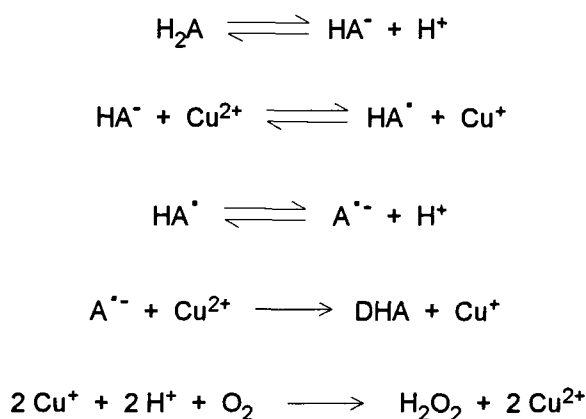
Scheme 3.1 One possible mechanism for the oxidation of ascorbic acid by Cu^{2+}

The formation of complexes comprising ascorbate, Cu^{2+} and O_2 has also been proposed,[12,17] as have chain mechanisms such as that given in Scheme 3.2.[10]

$$H_2A \rightleftharpoons A^- + H^+$$

$$\text{Initiation} \quad 2\,Cu^{2+} + HA^- \longrightarrow DHA + 2\,Cu^+ + H^+$$

$$Cu^+ + O_2 \longrightarrow Cu^{2+} + O_2^-$$

$$O_2^- + H^+ \longrightarrow HO_2^\bullet$$

$$HO_2^\bullet + HA^- \longrightarrow HO_2^- + HA^\bullet$$

$$HA^\bullet + Cu^{2+} \longrightarrow Cu^+ + DHA + H^+$$

$$\text{Termination} \quad Cu^+ + HO_2^\bullet + H^+ \longrightarrow Cu^{2+} + H_2O_2$$
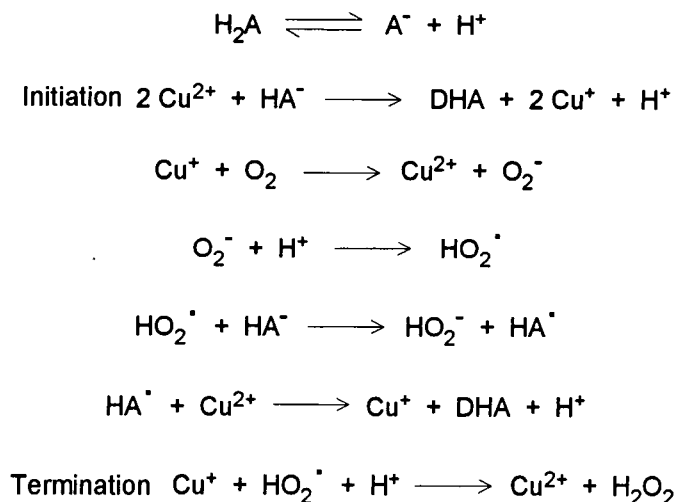
Scheme 3.2 Chain mechanism for the Cu^{2+} catalysed oxidation of ascorbic acid

Cu^{2+} catalysed oxidation of ascorbic acid might also proceed anaerobically, the catalyst being reformed by the disproportionation of Cu^+. Oscillatory behaviour with respect to the ascorbic acid concentration has also been observed,[18] believed to be a consequence of the interplay between the various reaction steps, critically involving the disproportionation of the ascorbate radical to ascorbic acid and dehydroascorbic acid. The metal ion catalysed oxidation of ascorbic acid is also promoted by Cl^-.[11]

Most reports demonstrate that the addition of metal chelators such as ethylenediaminetetraacetic acid (EDTA) inhibits the metal ion catalysed oxidation of ascorbic acid.[2,17,19] There have been suggestions of catalysis by these complexes, though it appears the copper complex is not effective in this regard, whereas the iron complex might be.[7,20]

3.1.2.3 Ascorbic Acid and Thiols: Redox Interactions

Low molecular mass thiols such as cysteine and the tripeptide glutathione are found *in vivo* and, like Vitamin C, act as antioxidants. There has been some contention regarding the interplay of the redox properties of ascorbic acid and these thiols. Suggestions have been made that ascorbic acid maintains glutathione (GSH) in its

reduced state, and paradoxically that the opposite is true.[6] It is possible for both of these situations to be true in physiology, providing that one of them operates *via* an indirect pathway. This seems likely for the former process, in which Vitamin C stimulates processes that can subsequently aid glutathione disulfide (GSSG) reduction.[6]

Early work failed to find any evidence that glutathione could reduce dehydroascorbic acid, however later reports show unambiguously that the process does occur, given sufficiently high [GSH].[21,22] An enzymatic pathway for reduction of dehydroascorbic acid by glutathione, involving dehydroascorbate reductase, has also been identified.[23] The recovery of ascorbic acid from its oxidised form is not always complete because of the irreversible decomposition of dehydroascorbic acid.[6]

Mutual inhibition of the Cu^{2+} catalysed oxidation of glutathione and ascorbic acid has been observed in mixtures.[24] The oxidation of ascorbic acid is inhibited by the sequestering of copper ions by thiols and their disulfides. Glutathione complexes Cu^{+},[24] and glutathione disulfide complexes Cu^{2+},[25] reducing the availability of copper ions to catalyse ascorbic acid oxidation. The oxidation of glutathione is in turn inhibited by ascorbic acid reducing thiyl radicals formed during the process,[10] and possibly by complexation of copper by ascorbic acid.[6] Other thiols, e.g. imidazolethiones, have also been found to inhibit ascorbic acid oxidation in a similar manner.[23]

3.1.3 Physiology of Ascorbic Acid

Ascorbic acid is classed as a vitamin because humans are unable to synthesise it and must therefore obtain it from dietary sources. This makes us somewhat unusual in that virtually the entire living world can synthesise ascorbic acid, the exceptions being primates, guinea pigs and some microorganisms.[26] A constant intake is required because we possess no storage mechanism for the vitamin. The recommended daily allowance of ascorbic acid is 25 – 75 mg, rising to 200 – 600 mg for therapeutic doses.[27] Typical concentrations of Vitamin C in the body are: 9 mg kg^{-1} (blood), 100 – 150 mg kg^{-1} (brain, liver), 70 mg kg^{-1} (lungs), 55 mg kg^{-1} (hearts, kidney).[28] The best dietary sources of ascorbic acid are fruit and vegetables, particularly broccoli and green pepper.[6]

The principal role of Vitamin C in physiology is to act as an antioxidant and a reductant. Ascorbic acid will scavenge many biologically dangerous free radicals, such as $HO^{\bullet}$, $ROO^{\bullet}$ and the reactions involved are highly favourable both thermodynamically and kinetically.[7] The process substitutes relatively harmless ascorbate radicals for the damaging ones. There is no reaction between oxygen and the ascorbate radical under physiological conditions, so no formation of damaging peroxyl radicals. There is some production of superoxide radicals, but these are removed by superoxide dismutase.

The antioxidant activity of Vitamin E (tocopherol) is enhanced by ascorbic acid. Vitamin E is the principal antioxidant in lipid layers, and the molecule is found within the lipid – aqueous interface, enabling ascorbic acid to reduce the tocopheroxyl radical back to Vitamin E.[7]

The best known Vitamin C deficiency symptom is the development of scurvy. The disease produces haemorrhaging into tissue, bleeding gums, loosening of teeth, anaemia and weakness.[6] It was during the many arduous naval voyages of the sixteenth and seventeenth centuries that this disease became recognised as a problem, and the importance of fruits and vegetables in preventing scurvy was recognised at this time.

It is possible to overdose on many vitamins, but there is no known state of hypervitaminosis for Vitamin C, even with daily doses as high as six grams.[26] There have been suggestions that prolonged exposure to high doses of ascorbic acid might increase the risk of developing certain cancers, and that the oxalic acid produced from dehydroascorbic acid degradation could increase kidney stone formation.[6] However, on balance there are probably no major risks associated with large Vitamin C intakes, though nor is there any significant benefit.

3.1.4 Aims

There is currently much interest in advancing the understanding of decomposition reactions of *S*-nitrosothiols, in particular those reactions that might have biological significance, e.g. production of nitric oxide. Studies of such reactions provide important information for researchers investigating the physiology and medical potential of nitrosothiols.

The reduction of Cu^{2+} by ascorbic acid is potentially important, given the known Cu^+ catalysed decomposition of nitrosothiols [29] and the widespread occurrence of ascorbic acid and copper sources *in vivo*. Studies in the biological literature have reported that ascorbic acid mediates nitrosothiol decomposition *in vitro* [30] and in plasma, liver and kidney fractions.[31] Evidence was presented implicating a pathway that did not involve metal ions.[31] Scorza showed that some reducing agents, including ascorbic acid, enhanced nitric oxide release from *S*-nitroso albumin.[32]

The aims of the ascorbic acid work were to identify the decomposition pathways for nitrosothiols in which ascorbic acid is involved at physiological pH, and to acquire kinetic and mechanistic information relating to these reactions.

3.2 Initial Studies

The effect of adding ascorbic acid to a solution containing *S*-nitroso glutathione, GSNO,§ is shown in Figure 3.3. Increasing the concentration of ascorbic acid results in faster decomposition of the GSNO (monitored at 340 nm, one of the absorbance maxima of GSNO). Trace D is unusual in that the absorbance initially decreases, but then increases again, making it impossible to establish whether all of the GSNO has decomposed.

---

§ Structures of all the nitrosothiols used are given in Appendix 2
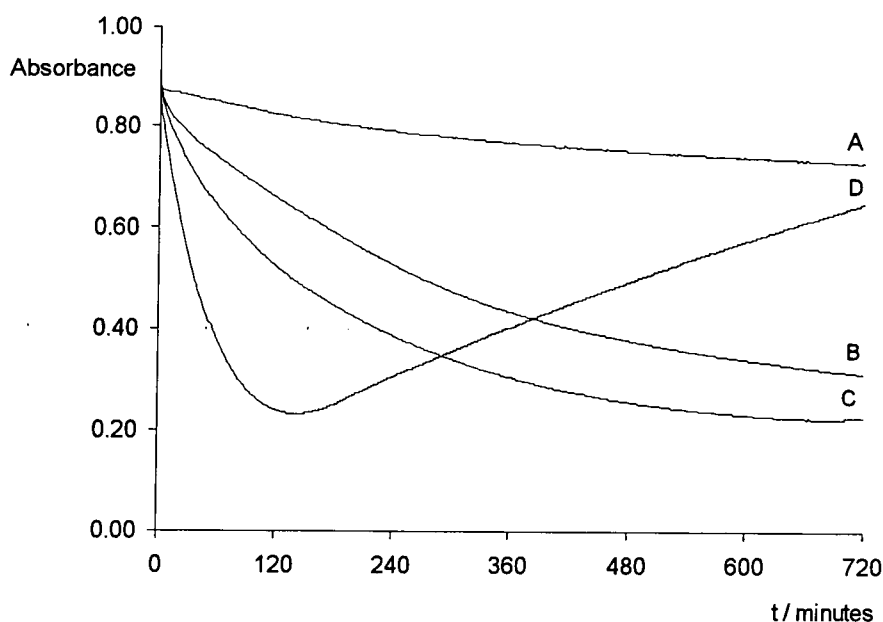
Figure 3.3 Decomposition of GSNO (1×10^{-3} M) in the presence of ascorbic acid (A = no ascorbic acid, B = 1×10^{-4} M, C = 1×10^{-3} M, D = 1×10^{-2} M), at pH 7.4, 25 °C

Following the decomposition at 545 nm, the other absorbance maximum of GSNO, revealed that complete decomposition does occur with higher ascorbic acid concentrations (Figure 3.4). The absorbance increase in Figure 3.3 must be due to the absorbance of one of the reaction products (see section 3.2.3.1). The lower extinction coefficient of the nitrosothiol at this wavelength ($\sim$ 20 dm^3 mol^{-1} cm^{-1} compared with $\sim$ 1000 dm^3 mol^{-1} cm^{-1} at 340 nm) requires the measurement of much smaller absorbance changes.
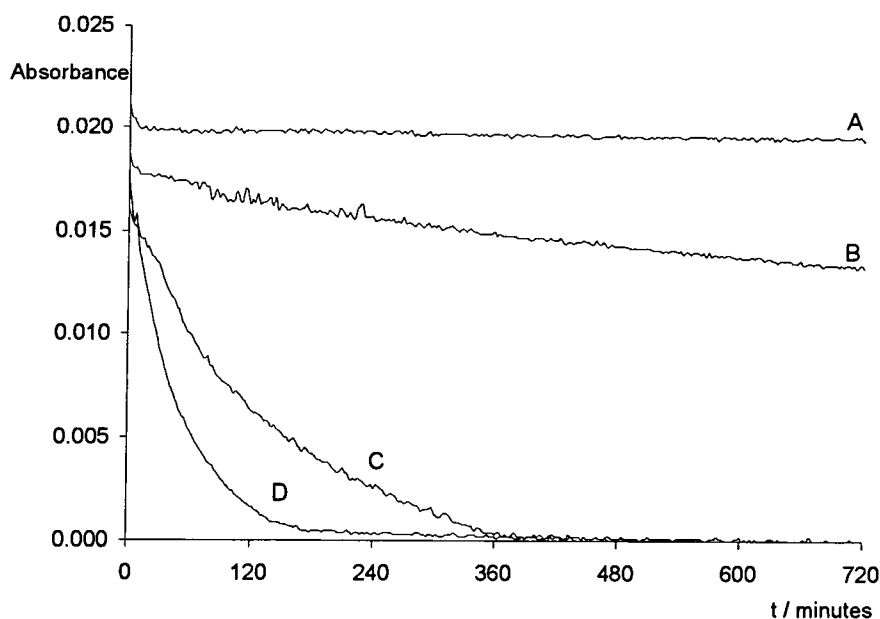
Figure 3.4　As per Figure 3.3, except the reaction was followed at 545 nm

3.2.1　Effect of Metal Chelation

To ascertain if the ascorbic acid promoted decomposition of GSNO involves metal ions, ethylenediaminetetraacetic acid, EDTA (Figure 3.5), was added. EDTA strongly chelates metal ions, and has been widely used to effectively remove them from solution. It forms a 2:1 EDTA – Cu^{2+} complex,[33] and will disproportionate and chelate Cu^+, therefore halting the Cu^+ catalysed decomposition of nitrosothiols.[34]
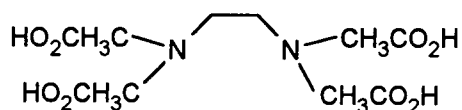
Figure 3.5　Structure of EDTA

Figure 3.6 shows the effect of adding EDTA upon the decomposition of GSNO in the presence of added copper (present as $CuSO_4$) and a low concentration of ascorbic acid. In the absence of EDTA the decomposition proceeds to completion, whereas the addition of EDTA, either before the start of reaction or during the reaction, completely halts the decomposition. The marked change in absorbance when the EDTA was added (trace B) results from the volume change upon addition.

70
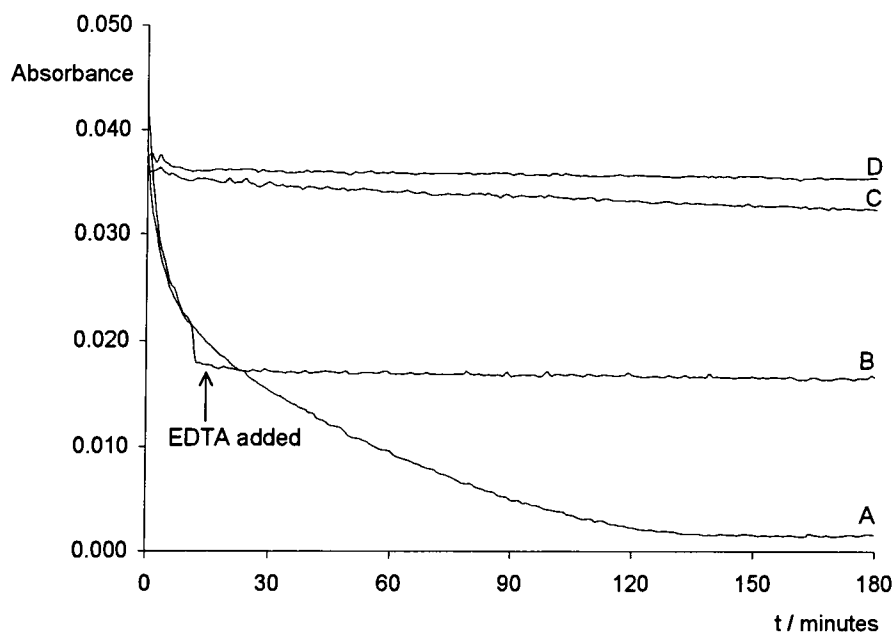
Figure 3.6 Effect of EDTA upon the decomposition of GSNO (2×10^{-3} M) with Cu^{2+} (1×10^{-4} M) and ascorbic acid (1×10^{-4} M, except D which contains no ascorbic acid). A = no EDTA, B = 1×10^{-3} M EDTA added after 14 minutes, C and D = 1×10^{-3} M EDTA present from start time. 25 °C and pH 7.4

Studying *S*-nitroso *N*-acetyl penicillamine (SNAP) in the presence of higher concentrations of ascorbic acid demonstrated that decomposition can still occur when EDTA is present, Figure 3.7. The Figure clearly shows a pathway exists for nitrosothiol decomposition by ascorbic acid that is independent of metal ions. The traces also clearly indicate that the addition of copper greatly enhances the rate of decomposition of this nitrosothiol.
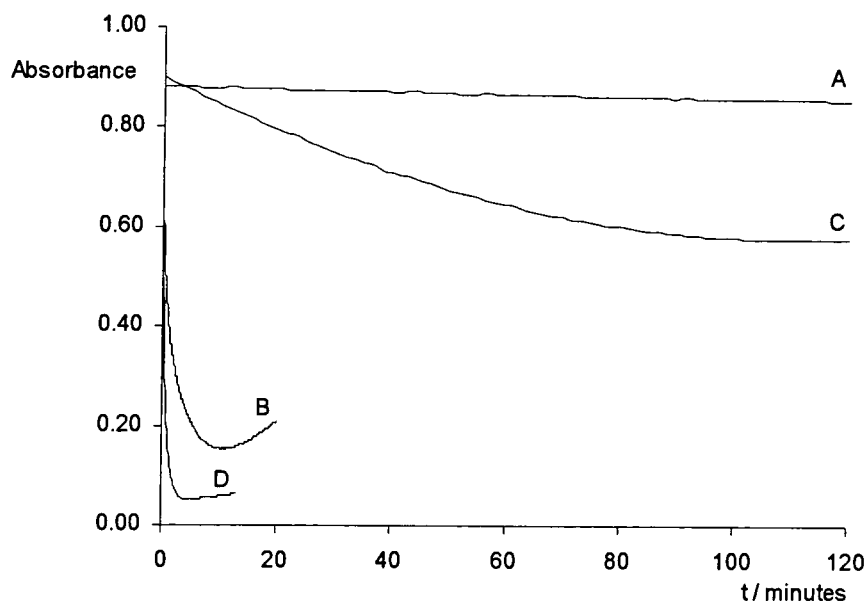
Figure 3.7 SNAP (1×10^{-3} M) with: A = 0.01 M ascorbic acid, 1×10^{-3} M EDTA; B = 0.01 M ascorbic acid, 1×10^{-5} M Cu^{2+}; C = 0.10 M ascorbic acid, 1×10^{-3} M EDTA; D = 0.10 M ascorbic acid, 1×10^{-5} M Cu^{2+}. 25 °C and pH 7.4

Nitrosothiol decomposition mediated by ascorbic acid appears to proceed *via* two pathways: one involving metal ions and the other independent of metal ions. Given that Cu^+ is the only effective metal ion to promote nitrosothiol decomposition,[34] it is reasonable to assume that the metal dependent pathway involves the reduction of Cu^{2+} to Cu^+ by ascorbic acid.

The copper independent reaction is not specific to SNAP decomposition, as shown in Figure 3.8, which shows the repeat scan spectra obtained for the decomposition of *S*-nitroso penicillamine *via* the copper independent pathway. The loss of the nitroso group is evident from the decreasing absorbance at 340 nm.
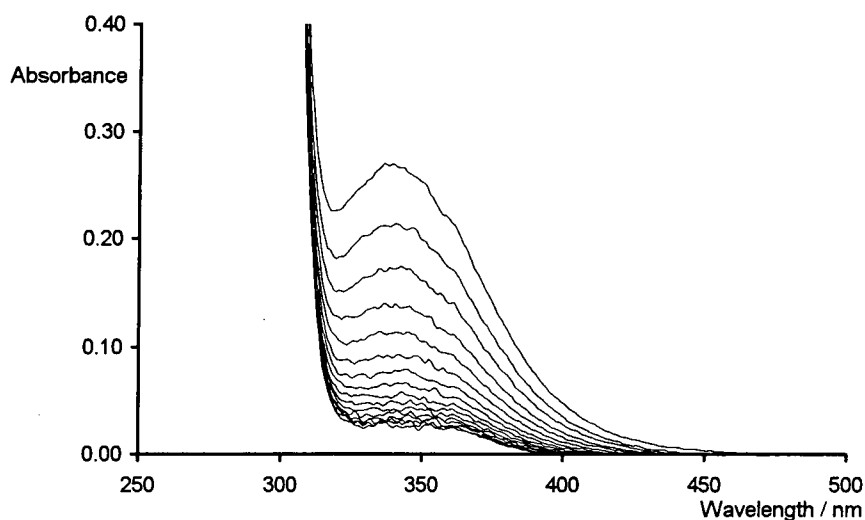
Figure 3.8 S-nitroso penicillamine (5×10^{-4} M) decomposition in the presence of 5×10^{-3} M ascorbic acid and 1×10^{-3} M EDTA. Spectra taken every 30 seconds. 25 °C and pH 7.4

3.2.2 Establishing the Stoichiometry

The copper reaction is known to be catalytic in copper ions,[34] and Figure 3.6 confirms this. This also reveals that only small quantities of ascorbic acid are required, suggesting that the reaction yields either Cu^+ or a reducing agent capable of reducing Cu^{2+}.

To establish the stoichiometry of the copper independent reaction, the decomposition of S-nitroso cysteine (SNCys) was followed at 545 nm in the presence of various ascorbic acid concentrations and EDTA (1×10^{-3} M). The nitrosothiol was prepared using a two − fold excess of nitrous acid to ensure essentially complete conversion of the thiol to its nitroso derivative. Table 3.2 gives the extent of decomposition observed in each nitrosothiol sample.

[H$_2$A] / mol dm^{-3}	[SNCys] / mol dm^{-3}	Ratio [SNCys] to [H$_2$A]	Initial absorbance	Final absorbance	Δ absorbance
0.002	0.010	5.0	0.168	0.105	0.063
0.003	0.010	3.3	0.164	0.071	0.093
0.004	0.010	2.5	0.165	0.055	0.110
0.005	0.010	2.0	0.166	0.045	0.121
0.007	0.010	1.4	0.168	0.036	0.129
0.010	0.010	1.0	0.163	0.038	0.125

Table 3.2 Absorbance change at 545 nm for SNCys decomposition at pH 7.4 and 25 °C with various [ascorbic acid] and 1 × 10^{-3} M EDTA

The plot of percentage nitrosothiol decomposition (calculated assuming a final absorbance of 0.036 represents complete decomposition) versus the ratio of SNCys to ascorbic acid concentrations in Figure 3.9 has a break point at a ratio of 2 SNCys : 1 H$_2$A. For samples where the ascorbic acid concentration is greater than or equal to half the nitrosothiol concentration the reaction reaches completion.
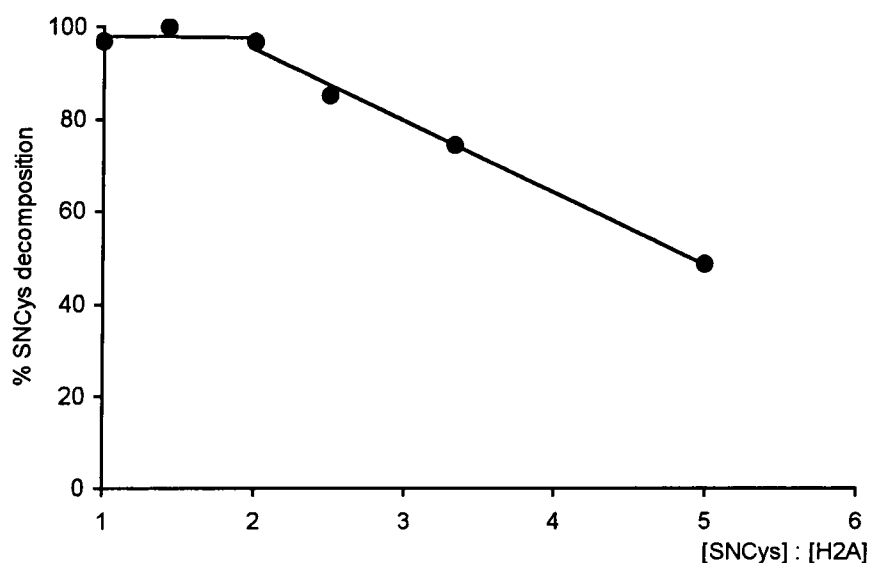
Figure 3.9 Graph of the data in Table 3.2 illustrating the stoichiometry of the copper independent reaction of SNCys with ascorbic acid

Data from a similar experiment using *S*-nitroso penicillamine (SNPen) also reveal that the stoichiometry of the copper independent reaction between nitrosothiols and ascorbic acid is 2 mol nitrosothiol to 1 mol ascorbic acid (Table 3.3). These results are in agreement with studies carried out on GSNO decomposition by

Kashiba-Iwatsuki *et al.*[30]   Smith *et al* reported [35] 1:1 stoichiometry for the GSNO reaction, but the mechanism advanced in their study predicts 2:1 stoichiometry. No interpretation was proffered to account for this apparent anomaly.

$[H_2A]$ / mol dm^{-3}	$[SNPen]$ / mol dm^{-3}	Ratio [SNPen] to $[H_2A]$	Δ absorbance	% SNPen decomposition
0.001	0.010	10	0.027	24
0.002	0.010	5.0	0.047	43
0.004	0.010	2.5	0.083	76
0.006	0.010	1.7	0.106	97
0.008	0.010	1.3	0.105	96
0.010	0.010	1.0	0.109	100

Table 3.3 Extent of SNPen decomposition with various ascorbic acid concentrations at pH 7.4 and 25 °C in the presence of EDTA (1×10^{-3} M)

3.2.3 Product Studies

3.2.3.1 Source of the Increasing Absorbance at 340 nm

The increasing absorbance observed at 340 nm for some of the decompositions discussed so far must be due to a species forming in the cell during the reaction. The thiols and disulfides corresponding to the nitrosothiols (Section 3.2.3.2) do not absorb at 340 nm. Ascorbic acid is therefore a more likely source of the absorbing species.

The spectrum of ascorbic acid (1×10^{-2} M) in pH 7.4 phosphate buffer was obtained every two hours for 14 hours, Figure 3.10. The sample was maintained at 25 °C in the spectrometer throughout this time, thus reproducing the conditions prevailing during the decomposition experiments. An absorbance increase is clearly visible at 340 nm.
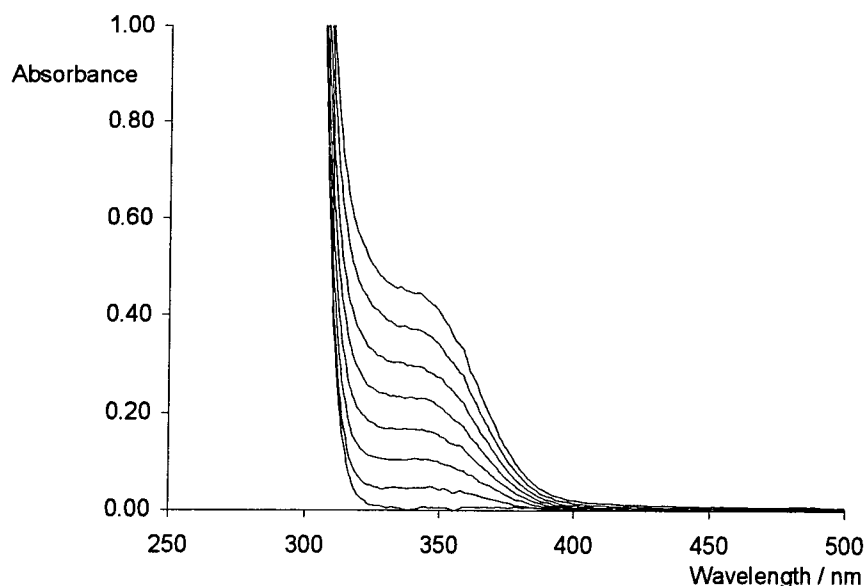
Figure 3.10 Spectra of an ascorbic acid solution $(1 \times 10^{-2}$ M) acquired every 2 hours at pH 7.4, 25 °C

Repeating the experiment in the presence of EDTA $(1 \times 10^{-3}$ M) resulted in the extent of the absorbance increase at 340 nm being considerably reduced (absorbance at 340 nm after 14 hours was *ca.* 0.3). This suggests the involvement of ascorbic acid oxidation, which is catalysed by metal ions, and yields dehydroascorbic acid (DHA).

The stability of a solution of authentic dehydroascorbic acid $(1 \times 10^{-3}$ M) at pH 7.4 and 25 °C was followed by obtaining repeat scans every two hours (Figure 3.11). The dehydroascorbic acid exhibits a peak at 265 nm, but no significant absorbance at 340 nm. A sample of 1×10^{-2} M dehydroascorbic acid (as would be formed by the oxidation of all the ascorbic acid in Figure 3.10) would absorb strongly enough at 340 nm, but not sufficiently at 310 nm, to explain the spectra in Figure 3.10.

The dehydroascorbic acid decomposes over time, initially resulting in increasing absorbance at 345 and 265 nm. The absorbance at 265 nm then decreases whilst that at 345 nm remains almost constant. Accounting for the spectra in Figure 3.10 requires that only a small quantity of dehydroascorbic acid be formed and decomposed, given that a significant quantity of ascorbic acid would remain to account for the absorbance below 310 nm.
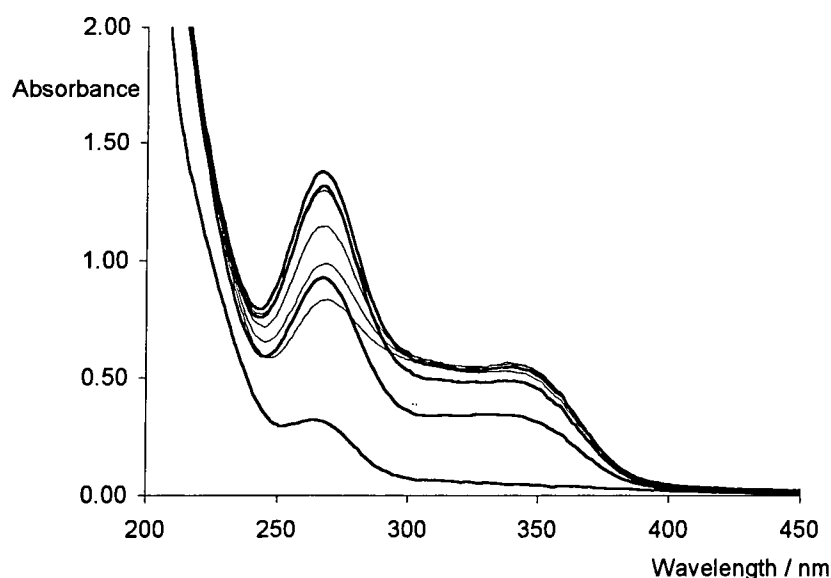
Figure 3.11 The decomposition of dehydroascorbic acid (1×10^{-3} M) at pH 7.4, 25 °C. Thicker lines represent the initial absorbance increases at 345 and 265 nm. Thinner lines show the subsequent absorbance decrease at 265 nm. Spectra obtained every 2 hours

Figure 3.11 shows all of the features reported by Herbert *et al* during their study of the structure of ascorbic acid in 1933.[2] The decomposition of dehydroascorbic acid proceeds *via* hydrolysis of the lactone ring and subsequent decomposition, resulting in the formation of oxalic and L-threonic acids (Scheme 3.3). [6]
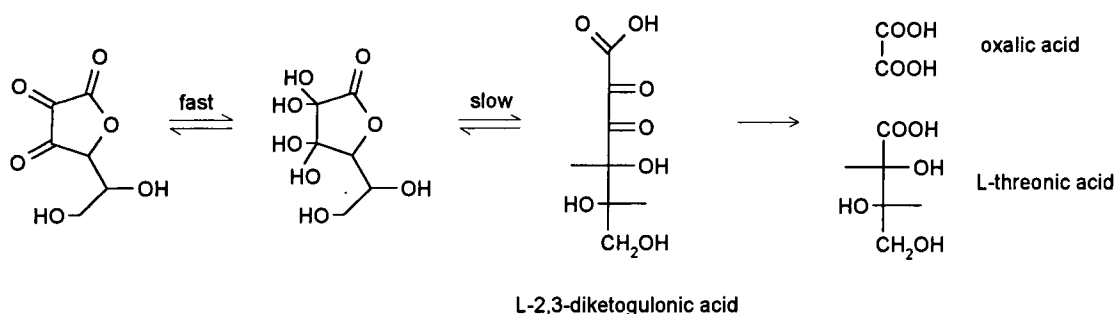
Scheme 3.3 The decomposition of dehydroascorbic acid

3.2.3.2 Determination of Sulfur Containing Products

- **Thiol analysis**

Samples from both the copper dependent and independent reactions were analysed for thiol content upon the decompositions reaching completion. The nitrosothiol chosen for the analyses was *S*-nitroso cysteine because it is possible to ensure both pathways are complete in a short time (~ 15 minutes), thus reducing the oxidation

77

to disulfide of any cysteine produced in the reaction. This oxidation is relatively slow at pH 7.4 given the involvement of the thiolate ion in the oxidation[36] (pK_a = 8.4).

Detection of thiol was carried out using the Ellman method,[37] in which the aromatic disulfide 5,5'-dithiobis(2-nitrobenzoic acid), DTNB, reacts with the thiol to produce a mixed disulfide and 2-nitro-S-thiobenzoic acid, TNB^{2-} (Scheme 3.4). The latter species is detected by its absorbance at 412 nm, and is most stable at pH 7.2, making the technique ideal for the analysis of samples at physiological pH.
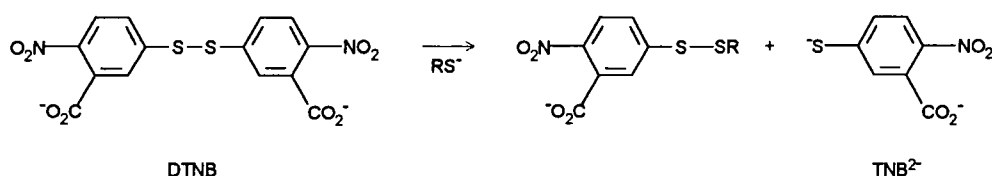
Scheme 3.4 The reaction involved in the Ellman procedure for thiol analysis

On each occasion the Ellman procedure was used, a calibration curve was constructed by measuring the maximum absorbance due to TNB^{2-} for samples of known thiol concentration. Typical calibration data are given in Table 3.4 and Figure 3.12. The plot of absorbance against [cysteine] is linear, giving ε_{412nm} = 13 900 ± 260 $dm^3\ mol^{-1}\ cm^{-1}$, which is in good agreement with the value published [37] by Ellman: 13 600 $dm^3\ mol^{-1}\ cm^{-1}$. The small intercept is due to the absorbance of the large excess of DTNB present in the samples.

[Cysteine] / mol dm^{-3}	[DTNB] / mol dm^{-3}	Absorbance at 412 nm
1.00×10^{-5}	4.96×10^{-4}	0.219
2.00×10^{-5}	4.96×10^{-4}	0.374
3.00×10^{-5}	4.96×10^{-4}	0.514
4.00×10^{-5}	4.96×10^{-4}	0.643
5.00×10^{-5}	4.96×10^{-4}	0.782

Table 3.4 Calibration data for the Ellman analysis for thiol, carried out at pH 7.4, 25 °C
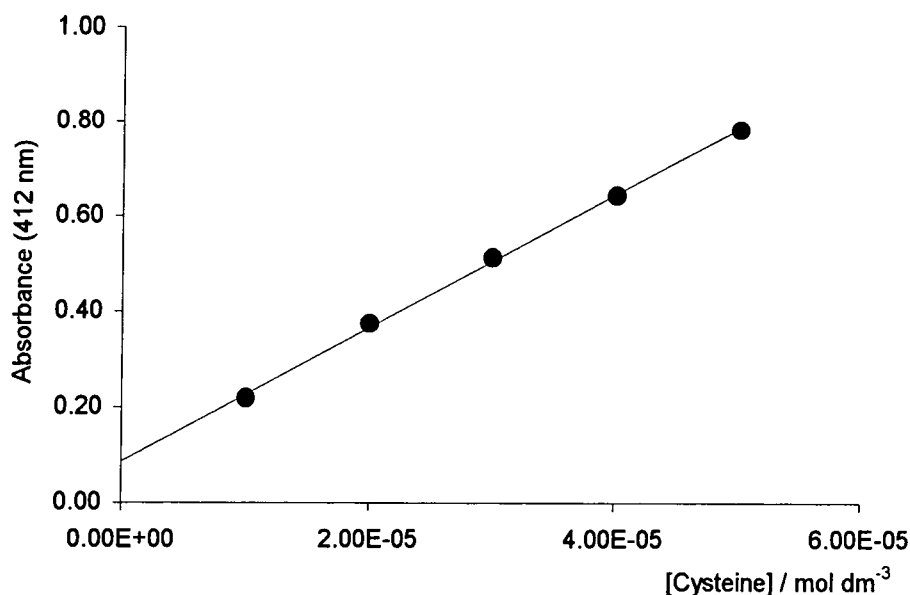
Figure 3.12 The calibration curve from the data in Table 3.4

The copper independent decomposition of S-nitroso cysteine was analysed for thiol after the reaction reached completion (progress of the reaction was monitored at 545 nm). The reaction solution contained 1×10^{-3} M nitrosothiol, 0.10 M ascorbic acid and 1×10^{-3} M EDTA, and was maintained at pH 7.4 and 25 °C. 0.10 cm^3 aliquots were then taken and added to a cell containing DTNB (final concentration 4.96×10^{-4} M) and phosphate buffer, giving a total volume of 2.50 cm^3. The results of the analysis are given in Table 3.5. A control containing 4×10^{-3} M ascorbic acid and 4.96×10^{-4} M DTNB showed no TNB^{2-} production over 30 minutes, discounting reduction of DTNB by ascorbic acid.

Absorbance at 412 nm	[Cysteine] in analyte / mol dm^{-3}	∴ [Cysteine] in reaction sample / mol dm^{-3}	% sulfur recovered as thiol
0.54	3.25×10^{-5}	8.13×10^{-4}	81
0.58	3.54×10^{-5}	8.85×10^{-4}	89

Table 3.5 Results of the thiol analysis carried for the copper independent pathway.

The results show over 80 % of sulfur from the nitrosothiol was recovered as thiol in the metal independent reaction. The true figure will probably be higher, given that some of the thiol might have autoxidised, and that dehydroascorbic acid will oxidise thiols.

Analysis of the copper dependent reaction, in which S-nitroso cysteine (1×10^{-3} M) was allowed to decompose in the presence of ascorbic acid (1×10^{-5} M) and Cu^{2+} (1×10^{-5} M) gave the results in Table 3.6. 0.50 cm³ aliquots were used in this analysis.

Absorbance at 412 nm	[Cysteine] in analyte / mol dm⁻³	∴ [Cysteine] in reaction sample / mol dm⁻³	% sulfur recovered as thiol
0.18	6.62×10^{-6}	3.31×10^{-5}	3.3
0.14	3.74×10^{-6}	1.87×10^{-5}	1.9

Table 3.6 Thiol analysis for the copper dependent decomposition pathway

The major sulfur-containing product of the metal independent reaction is thiol, whereas that of the copper dependent reaction is not. The most likely product of this latter reaction is disulfide, and this is demonstrated in the following section.

- **Disulfide Detection**

Cystine, the disulfide of cysteine, is insoluble in water at pH values close to neutrality, and therefore will precipitate if formed in significant quantity during S-nitroso cysteine decomposition.

50 cm³ of 0.020 M S-nitroso cysteine (nitrosated using a two – fold excess of nitrous acid) was added to an equal volume of pH 7.4 buffer containing 2×10^{-3} M ascorbic acid, 1×10^{-4} M Cu^{2+} and sufficient NaOH to neutralise the acid used for nitrosation. After the colour due to S-nitroso cysteine completely faded, an aliquot was tested for thiol using DTNB: none was detected. Several hours later a precipitate had formed. This was recovered by filtration, washed with water and dried *in vacuo*. The solid decomposed between 242 and 246 °C, similar to the literature values for cystine, 234 – 239 °C. [38] A sample of authentic cystine decomposed at 248 – 252 °C. Based on the mass of solid obtained the percentage of sulfur from S – nitroso cysteine recovered as cystine was about 50 %.

Two control experiments were carried out. In the first, S-nitroso cysteine (0.010 M) was allowed to decompose with Cu^{2+} (1×10^{-4} M) and the residual thiol from a 1:1 nitrosation. A solid was recovered, giving a sulfur yield of around 50%. In the second control experiment S – nitroso cysteine was reacted with ascorbic acid (0.10

M) in the presence of EDTA (1×10^{-4} M). In this case, no precipitate was observed and DTNB gave a positive reaction.

The production of disulfide in the copper dependent reaction was verified using HPLC analysis. GSNO (2×10^{-3} M) was reacted with Cu^{2+} (2×10^{-4} M) and ascorbic acid (2×10^{-4} M) at pH 7.4, 25 °C, the extent of decomposition being monitored at 545 nm. When the reaction was complete a sample was analysed using reverse – phase HPLC [39] with a C-18 Spherisorb ODS2 column and a mobile phase comprising 90% pH 2.5 phosphate buffer / 10% MeOH (v/v). Detection was by UV spectrophotometry at 220 nm. Details of the reaction and control samples analysed are tabulated below.

Sample composition	Retention time/ minutes	Peak area / arbitrary units	assignment
Glutathione disulfide (GSSG) 1×10^{-3} M	6.15	135 095	GSSG
GSSG 1×10^{-3} M	6.11	105 895	GSSG
Glutathione (GSH) 2×10^{-3} M	5.06	87 463	GSH
	6.11	20 070	GSSG
GSSG 1×10^{-3} M	5.07	64 745	GSH
GSH 2×10^{-3} M	6.14	94 860	GSSG
Ascorbic acid (H_2A) 2×10^{-4} M	4.48	17 950	H_2A
GSNO 2×10^{-3} M	8.86	436 183	GSNO
Reaction sample 1	5.07	13 570	GSH
	6.12	105 440	GSSG
	8.86	35 795	GSNO
Reaction sample 2	5.10	9 302	GSH
	6.12	140 790	GSSG

Table 3.7 Results of the HPLC analysis of the products from the copper dependent decomposition of GSNO

To compensate for the variation in injection volume between runs, but in the absence of a suitable compound for use as an internal standard, authentic samples of known [GSSG] : [GSH] were analysed, and a response ratio calculated. The response ratio, GSSG response : GSH response, was 2.9. Adopting the reasonable assumption that the sulfur in GSNO is converted to either the thiol or the disulfide during the reaction, this response ratio can be used to calculate the percentage disulfide produced. These results are tabulated below (Table 3.8).

Sample	% sulfur in GSNO present as GSSG	% sulfur in GSNO present as GSH
Reaction sample 1	84	16
Reaction sample 2	91	9

Table 3.8 Sulfur containing product distribution for the copper decomposition of GSNO

3.2.3.3 Determination of Nitrogen Containing Products

• **Nitric oxide**

A specific nitric oxide electrode was utilised to establish whether the two pathways for nitrosothiol decomposition yielded nitric oxide. The principles of operation of the electrode are discussed in Appendix 3.

Calibration of the electrode was established daily using either the ascorbic acid / $NaNO_2$ or the H_2SO_4 / KI / $NaNO_2$ methods described in Section A3.3. Both methods give quantitative conversion of $NaNO_2$ to NO. A typical calibration result is given in Table 3.9 and Figure 3.13. In this case the response was 1.85 nA μM^{-1}. The small intercept is presumed to be due to the potential difference between the meter and the calibration solution.

[NO] / $\mu mol\ dm^{-3}$	I / nA
2.47	5.18
4.16	8.35
6.22	12.0
8.27	16.5
10.3	19.4

Table 3.9 NO electrode calibration data, using the ascorbic acid / $NaNO_2$ method and the WPI Mk I NO electrode
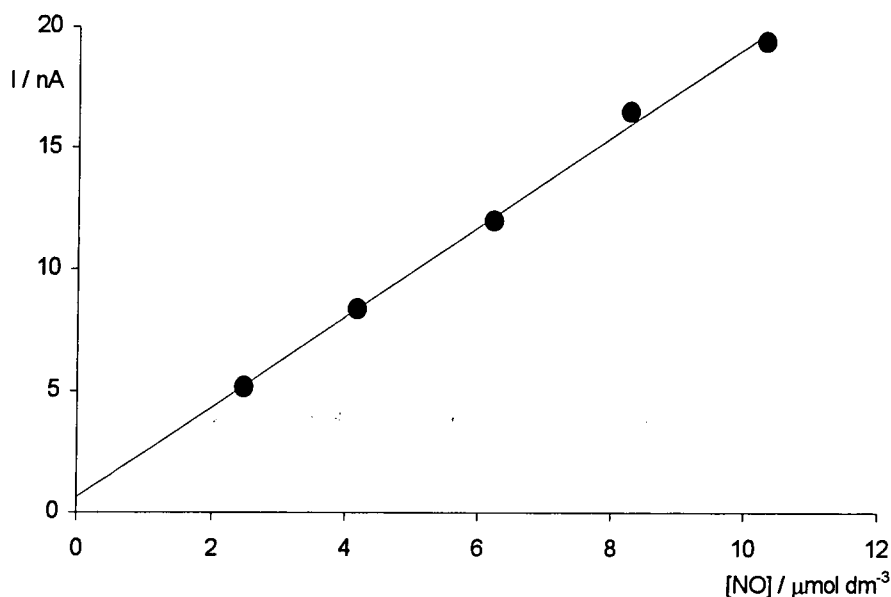
Figure 3.13 Calibration curve for the data in Table 3.9

The decomposition of S-nitroso cysteine (8.33×10^{-6} M) was studied at pH 7.4 and 25 °C. In the copper independent decomposition the ascorbic acid concentration was 0.010 M and the EDTA concentration 1×10^{-3} M. For the copper dependent reaction the solution contained 5×10^{-6} M ascorbic acid and 5×10^{-6} M Cu^{2+}. In both cases, the nitrosothiol was prepared with a two – fold excess of nitrous acid. The results of the analysis are given in Table 3.10. Given that some nitric oxide will undergo oxidation or be lost to the headspace these results indicate quantitative conversion of the nitrosothiol to nitric oxide.

Pathway	I / nA	NO yield / %
Copper dependent	14.0	87
Copper independent	12.7	78

Table 3.10 NO yield from the two decomposition pathways

3.2.3.4 Summary of Products

The results from the previous sections establish the products as summarised in Table 3.11. The products of the copper pathway are disulfide and nitric oxide, and those of the copper independent pathway thiol and nitric oxide. These findings are

consistent with those of other investigators.[30]   The results from Section 3.2.3.1 suggest that the ascorbic acid is converted to dehydroascorbic acid.

Pathway	% S recovered as thiol	% S recovered as disulfide	NO yield / %
Copper dependent	2.6	88	87
Copper independent	85	--	78

Table 3.11 Summary of reaction products analysis for the decomposition of S – nitroso cysteine by ascorbic acid

3.3 Further Studies on the Copper Dependent Pathway

Some further studies of the copper dependent reaction were carried out, and these are discussed here. There is little value in conducting detailed kinetic studies given that (a) the precise concentration of copper is always unknown due to the traces of metal ions present in buffer solutions; (b) the salient features have been previously indentified.[29] The copper independent pathway does lend itself to detailed study as little is known about this pathway: the findings of these studies are presented in Chapter 4.

3.3.1 Varying the Copper Concentration

Figure 3.14 shows the absorbance traces obtained when GSNO decomposition (2 × 10^{-3} M, nitrosated with a two – fold excess of nitrous acid) was followed in the presence of 5 × 10^{-4} M ascorbic acid and various concentrations of Cu^{2+}. The results show that increasing [Cu^{2+}] led to faster decomposition, up to 1.2 × 10^{-4} M Cu^{2+}. Still higher copper concentrations gave rise to no further increase in the rate of decomposition.
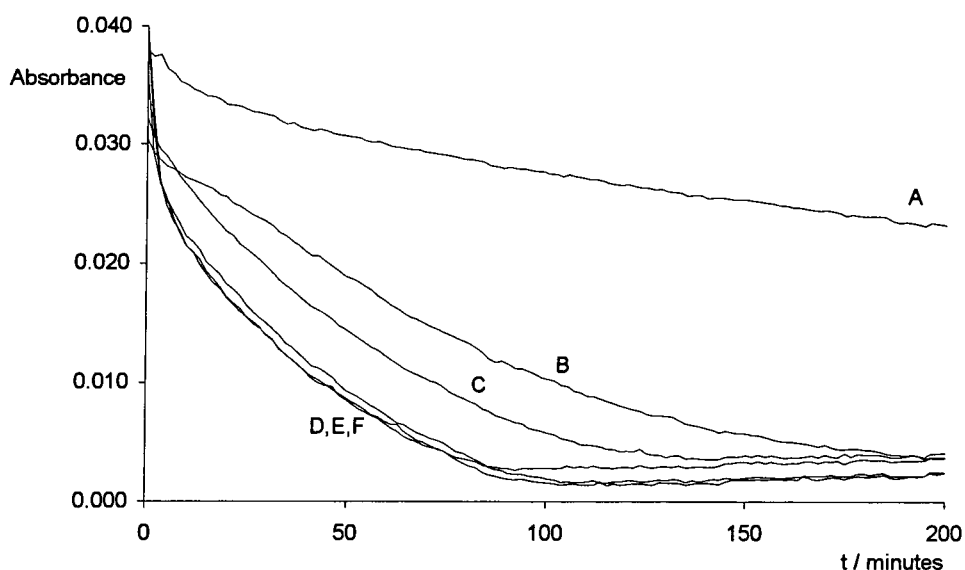
Figure 3.14 GSNO (2×10^{-3} M) with ascorbic acid (5×10^{-4} M) and copper at pH 7.4 and 25 °C, followed at 545 nm. [Cu^{2+}]: A = none, B = 3×10^{-5} M, C = 6×10^{-5} M, D = 1.2×10^{-4} M, E = 1.5×10^{-4} M, F = 1.8×10^{-4} M.

3.3.2 Varying the Ascorbic Acid Concentration

Figure 3.15 shows the effect of changing the ascorbic acid concentration upon the decomposition of SNAP. The nitrosothiol was prepared using a two – fold excess of nitrous acid, reducing the residual thiol to negligible levels and halting the copper reaction (trace A). Addition of ascorbic acid gave rise to decomposition, which became faster when more ascorbic acid was present.
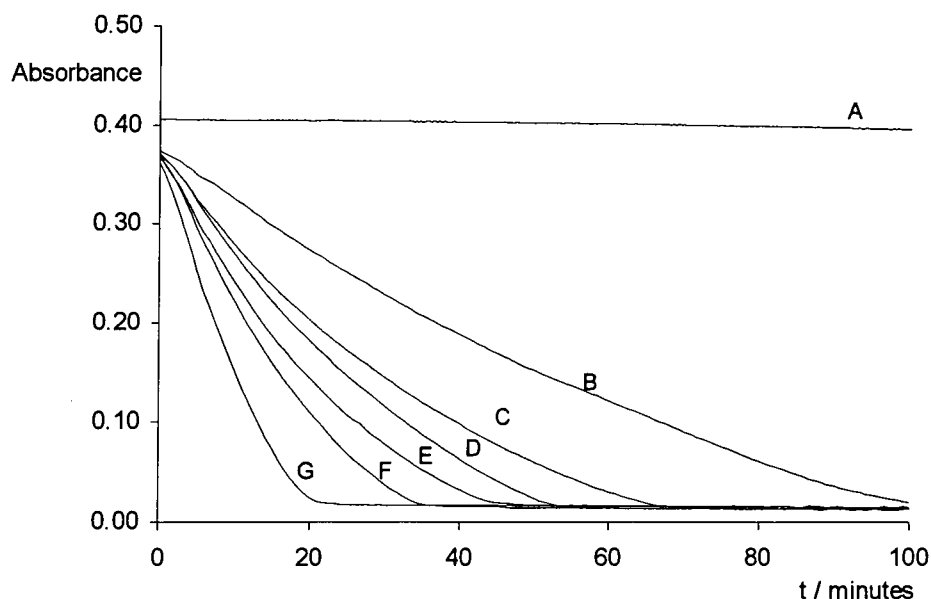
Figure 3.15 SNAP (4×10^{-4} M), Cu^{2+} (5×10^{-6} M) at pH 7.4 and 25 °C, followed at 340 nm. [Ascorbic acid]: A = none, B = 5×10^{-6} M, C = 8×10^{-6} M, D = 1×10^{-5} M, E = 1.5×10^{-5} M, F = 2×10^{-5} M, G = 3×10^{-5} M.

3.3.3 Reversal of GSSG Inhibition of GSNO Decomposition

The Cu^+ mediated decomposition of GSNO, one of the most important S – nitrosothiols biologically, is somewhat atypical. The earliest work [34] found GSNO to be only slightly reactive *via* the copper pathway. Further studies revealed that, when studied spectrophotometrically with GSNO concentrations $\sim$ 1 mM, and certainly in excess of [Cu^{2+}], decomposition often failed to reach completion.[29] Despite this fact, GSNO has been successfully used as a nitric oxide donor in medical research.[40] Addition of more copper, or more thiol to reduce Cu^{2+}, brought about further decomposition.

It is now recognised that the product of the copper promoted decomposition of GSNO, GSSG, complexes copper, halting the reaction.[41] A complex absorbing at 265 and 625 nm has been identified, the proposed structure of this 1:1 complex is given in Figure 3.16.[42] A 2:1 Cu^{2+} – GSSG complex has also been isolated at higher copper concentrations.
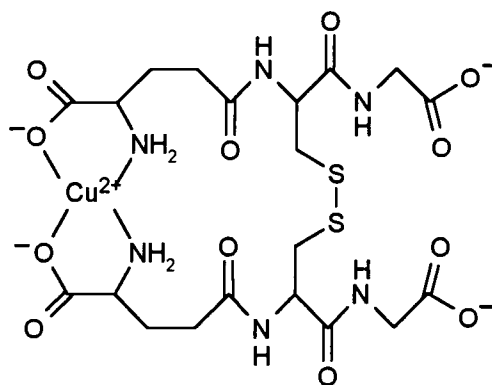
Figure 3.16 Structure of the 1:1 Cu^{2+} – GSSG complex

When GSNO decomposition is studied using the nitric oxide electrode the GSNO concentration is typically in the micromolar range, of the same order or less than that of the copper concentration. In such situations, complete and rapid GSNO decomposition has been observed, the addition of GSSG slowing and eventually halting the reaction.[41] These conditions are probably more relevant to the *in vivo* situation than those prevailing in the spectrophotometric experiments.

The decomposition of GSNO was studied in the presence of added GSSG, Figure 3.17. Trace A shows that very little decomposition occurred when no ascorbic acid was present because of the complexation of the copper by the disulfide. Adding ascorbic acid caused decomposition to occur, necessarily *via* the copper reaction because of the low ascorbic acid concentration used. It is interesting to note that the highest ascorbic acid concentration did not give rise to the fastest decomposition. This is perhaps tentative evidence that ascorbic acid, or one of its oxidation products, can complex out copper and inhibit the copper reaction.
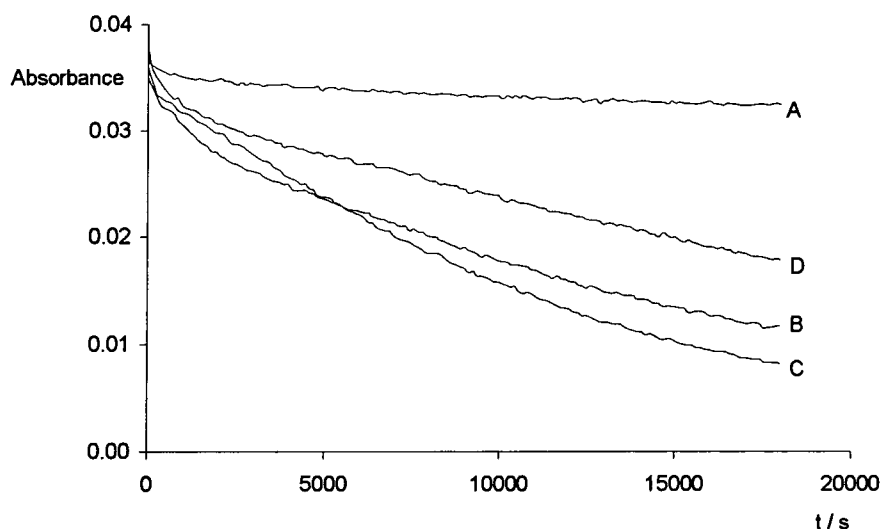
Figure 3.17 GSNO (2×10^{-3} M), added Cu^{2+} (1×10^{-5} M), GSSG (1×10^{-4} M) and varying ascorbic acid concentrations at pH 7.4 and 25 °C, followed at 545 nm. [Ascorbic acid]: A = none, B = 5×10^{-5} M, C = 1×10^{-4} M, D = 5×10^{-4} M.

The production of nitric oxide from a GSNO solution containing copper and GSSG with varying ascorbic acid concentrations is shown in Figure 3.18. The yield of nitric oxide and the rate of its production are clearly increased by the addition of ascorbic acid. Trace F, in the presence of EDTA, shows that all of the nitric oxide production is *via* the copper pathway.
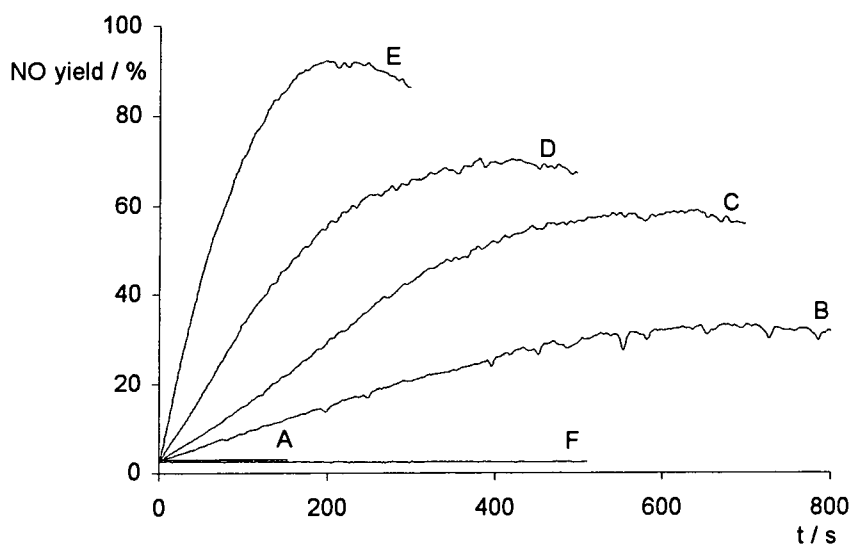
Figure 3.18 Reversal of the disulfide inhibition of GSNO decomposition by ascorbic acid. [GSNO] = 3.12×10^{-6} M, [Cu^{2+}] = 1×10^{-5} M, [GSSG] = 1×10^{-4} M. [Ascorbic acid]: A = 0 M; B = 5.32×10^{-7} M; C = 9.98×10^{-7} M; D = 3×10^{-6} M; E = 1.33×10^{-5} M; F = 1.33×10^{-5} M and 1×10^{-4} M EDTA

There are at least two possible routes by which ascorbic acid could reverse the inhibition by GSSG. One is that ascorbic acid might be reducing GSSG to GSH; the other involves ascorbic acid competing with GSSG for the Cu^{2+}, reducing it in the process and stimulating GSNO decomposition.

The Ellman method was utilised to test case one above. The composition of the samples analysed is given in Table 3.12. TNB^{2-} was detected at 412 nm, the samples were maintained at pH 7.4 and 25 °C. The results reveal that reduction of GSSG is not occurring.

Sample composition	[DTNB] / mol dm^{-3}	Maximum absorbance at 412 nm§
5×10^{-5} mol dm^{-3} GSH	5×10^{-4}	0.654
2.5×10^{-5} mol dm^{-3} GSSG	5×10^{-4}	0.026
2.5×10^{-5} M H$_2$A	5×10^{-4}	0.020
2.5×10^{-5} M GSSG, 2.5×10^{-5} M H$_2$A	5×10^{-4}	0.021
2.5×10^{-5} M GSSG, 1×10^{-4} M H$_2$A	5×10^{-4}	0.028

§ Cells initially incubated for 5 minutes prior to DTNB addition. Absorbance then monitored for 30 minutes.

Table 3.12 Results of the Ellman analysis carried out upon solutions containing GSSG and ascorbic acid

The specific Cu^+ chelator neocuproine [43] was used to test whether ascorbic acid would release Cu^+ from the GSSG – Cu^{2+} complex. The specificity of this chelator is believed to arise from the different preferred geometries of Cu^{2+} and Cu^+. The Cu^{2+} square planar 2 : 1 complex is destabilised by steric buttressing of the methyl groups. This influence is not present in the tetrahedral Cu^+ complex (Figure 3.19).

Steric strain in the Cu^{2+} complex
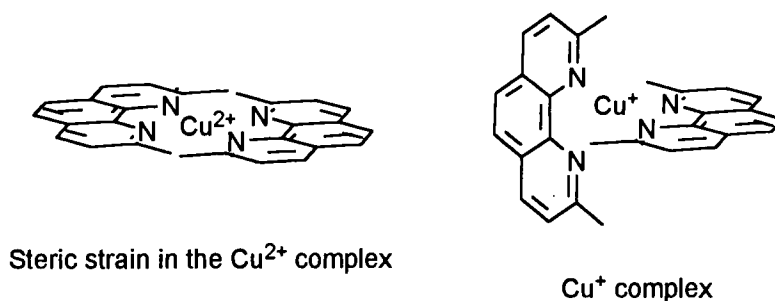
Cu^+ complex

Figure 3.19 Structure comparison for the complexation of Cu^{2+} and Cu^+ by neocuproine

The neocuproine – Cu^+ complex absorbs at 450 nm (ε = 7 950 dm^3 mol^{-1} cm^{-1}, isoamyl alcohol).[43] The composition of the samples and the absorbance values at 450 nm are in Table 3.13. The spectrum obtained for the first sample also showed the distinctive absorbance at 265 nm due to the GSSG – Cu^{2+} complex.[44] These data demonstrate that ascorbic acid releases and reduces Cu^{2+} from the GSSG – Cu^{2+} complex, thus enabling GSNO decomposition to take place.

Sample composition	[neocuproine] / mol dm^{-3}	Maximum absorbance at 450 nm
4×10^{-4} M GSSG, 2×10^{-5} M Cu^{2+}	---	0.00
4×10^{-4} M GSSG, 2×10^{-5} M Cu^{2+}	1×10^{-4} M	0.00
4×10^{-4} M GSSG, 2×10^{-5} M Cu^{2+}, 1×10^{-5} M H_2A	1×10^{-4} M	0.12
2×10^{-5} M Cu^{2+}, 1×10^{-5} M H_2A	1×10^{-4} M	0.10

Table 3.13 Detection for Cu^+ using neocuproine

3.4 Conclusion

The results identify two pathways for *S*-nitrosothiol decomposition in which ascorbic acid is involved. One is dependent upon the presence of Cu^{2+}, which is reduced to Cu^+ by the ascorbic acid. The other pathway is completely independent of metal ions and, unlike the former pathway, requires stoichiometric quantities of ascorbic acid, the stoichiometry being two nitrosothiol molecules to one of ascorbic acid. The products of the copper dependent pathway are nitric oxide and disulfide, whereas those of the copper independent pathway are nitric oxide and thiol.

Further study of the copper dependent reaction has revealed that nitrosothiol decomposition can be enhanced by the addition of both Cu^{2+} and ascorbic acid. The glutathione disulfide inhibition of *S* – nitroso glutathione decomposition is reversed by the addition of ascorbic acid, which acts by releasing Cu^+ from the GSSG – Cu^{2+} complex.

Further studies of the copper independent reaction, including detailed kinetic analysis, are reported in Chapter 4. A mechanism can be advanced for the copper dependent reaction that is an extension of the mechanism already established,[29] and

this is given in Scheme 3.5 Conclusions regarding both decomposition pathways can be found in Chapter 5.

$$H_2A + 2\,Cu^{2+} \longrightarrow DA + 2\,Cu^+$$

$$Cu^+ + RSNO \longrightarrow RS^- + Cu^{2+} + NO$$

$$2\,RS^- + 2\,Cu^{2+} \longrightarrow RSSR + 2\,Cu^+$$
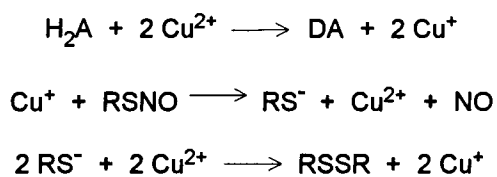
Scheme 3.5 Proposed mechanism for the copper dependent decomposition of $S-$ nitrosothiols by ascorbic acid

3.5 References

1. A. Szent-Györgyi, *Biochem. J.* **22**, 1387 (1928).

2. R. W. Herbert, E. L. Hirst, E. G. V. Percival, R. J. W. Reynolds and F. Smith, *J. Chem. Soc.*, 1270 (1933).

3. E. G. Cox, *Nature*, **130**, 206 (1932).

4. E. G. Cox and T. H. Goodwin, *J. Chem. Soc.*, 769 (1936).

5. A. Szent-Györgyi and W. H. Haworth, *Nature*, **131**, 24 (1933).

6. M. B. Davies, J. Austin and D. A. Partridge, 'Vitamin C: Its Chemistry and Biochemistry', The Royal Society of Chemistry, Cambridge (1991).

7. G. R. Buettner and B. A. Jurkiewicz, 'Handbook of Antioxidants', Chapter 5, Ed. E. Cadenas and L. Packer, Marcel Dekker, New York (1996).

8. J. Xu and R. B. Jordan, *Inorganic Chemistry*, **29** No. 16, 2933 (1990).

9. L. Mi and A. D. Zuberbühler, *Helv. Chim. Acta.*, **75**, 1547 (1992).

10. S. P. Mushran and M. C. Agrawal, *J. Scient. Ind. Res.*, **36**, 274 (1977) and references therein.

11. M. J. Sisley and R. B. Jordan, *J. Chem. Soc., Dalton Trans.*, 3883 (1997).

12. M. M. Taqui Khan and A. E. Martell, *J. Am. Chem. Soc.*, **89**, 4176 (1967).

13. M. B. Davies, *Polyhedron*, **11** No. 3, 285 (1992).

14. D. E. Hughes, *Anal. Chem.*, **57**, 555 (1985).

15. M. A. Joslyn and J. Miller, *Food Res.*, **14**, 325 (1949).

16. A. O. Dekker and R. G. Dickson, *J. Am. Chem. Soc.*, **62**, 2165 (1940).

17. R. F. Jameson and N. J. Blackburn, *J. Chem. Soc., Dalton Trans.*, 9 (1982).

18. J. Young, B. Franzus and T. T.-S. Huang, *Int. J. Chem. Kinet.*, **14**, 749 (1982).

19. E. V. Shtamm, A. P. Purmal and Y. I. Skurlav, *Int. J. Chem. Kinet.*, **11**, 461 (1979).

20. A. Pirie and R. Van Heyningen, *Nature*, **173**, 873 (1954).

21. H. Borsook, H. W. Davenport, C. E. P. Jeffreys and R. C. Warner, *J. Biol. Chem.*, **117**, 237 (1936).

22. F. G. Hopkins and E. J. Morgan, *Biochem. J.*, **30**, 1446 (1936).

23. R. C. Smith and J. Z. Gore, *Biochim. Biophys. Acta*, **1034**, 263 (1990).

24. Y. Ohta, N. Shiraishi, T. Nishikawa and M. Nishikima, *Biochem. Biophys. Acta*, **1471**, 378 (2000).

25. W. L. Baker, *Arch. Biochem. Biophys.*, **252** No. 2, 451 (1987).

26. H. R. Rosenberg, 'Chemistry and Physiology of the Vitamins', Interscience (1945).

27. 'Martindale: The Extra Pharmacopoeia', Pharmaceutical Press, 26th Ed. (1972).

28. L. A. S. Brown and D. P. Jones, 'Handbook of Antioxidants', Chapter 6, Ed. E. Cadenas and L. Packer, Marcel Dekker, New York (1996).

29. A. P. Dicks, H. R. Swift, D. L. H. Williams, A. R. Butler, H. H. Al-Sa'doni and B. G. Cox, *J. Chem. Soc., Perkin Trans. 2*, 481 (1996).

30. M. Kashiba-Iwatsuki, M. Yamaguchi and M. Inoue, *FEBS Lett.*, **389**, 149 (1996).

31. M. Kashiba-Iwatsuki, K. Kitoh, E. Kasahara, H. Yu, M. Nisikawa, M. Matsuo and M. Inoue, *J. Biochem.*, **122**, 1208 (1997).

32. G. Scorza, D. Pietraforte and M. Minetti, *Free Radical Biol. Med.*, **22** No. 4, 633 (1997).

33. P. Hemmerich, 'The Biochemistry of Copper', Ed. J. Peisach, D. Aisen and W. E. Blumberg, Academic Press, New York, 1996.

34. S. C. Askew, D. J. Barnett, J. McAninly and D. L. H. Williams, *J. Chem. Soc., Perkin Trans. 2*, 741 (1995).

35. J. N. Smith and T. P. Dasgupta, *Nitric Oxide: Biol. Chem.*, **4**, 57 (2000).

36. P. C. Jocelyn, 'Biochemistry of the SH Group', Chapter 4, Academic Press, London (1972).

37. G. L. Ellman, *Arch. Biochem. Biophys.*, **82**, 70 (1959).

38. B. S. Axelsson, K. J. O'Toole, P. A. Spencer and D. W. Young, *J. Chem. Soc., Perkin Trans. 1*, 807 (1994).

39. J. S. Stamler and M. Feelisch, 'Methods in Nitric Oxide Research', Chapter 36, Ed. M. Feelisch and J. S. Stamler, Wiley, Chichester (1996).

40. A. de Belder, C. Lees, J. Martin and S. Moncada, *Lancet*, **345**, 124 (1995).

41. D. R. Noble, H. R. Swift and D. L. H. Williams, *J. Chem. Soc, Chem. Commun.*, 2317 (1999).

42. K. Varnagy, I. Sovago and H. Kozlowski, *Inorg. Chim. Acta*, **151**, 117 (1988).

43. G. F. Smith and W. H. McCurdy, *Anal. Chem*, **24**, 371 (1952).

44. A. R. Amundsen, J. Whelan and B. Bosnich, *J. Am. Chem. Soc.*, **99**, 6730 (1977).

Kinetics and Mechanism of the Copper Independent Reaction

Chapter 4 Kinetics and Mechanism of the Copper Independent Reaction

4.1 Introduction

Evidence for the existence of two pathways for ascorbic acid promoted *S*-nitrosothiol decomposition was presented in Chapter 3. Some of the features of the copper catalysed reaction were explored, and analysis of the products and stoichiometry of both pathways was given. This chapter outlines the results of detailed kinetic studies into the copper independent reaction. Such analyses are essential for establishing the mechanism of the reaction and allow comparison with other studies.

4.2 Kinetics of *S*-Nitrosothiol Decomposition

Reactions were followed spectrophotometrically, monitoring the absorbance due to the nitrosothiol at a suitable wavelength. Choice of wavelength was such that the increasing absorbance due to dehydroascorbic acid decomposition was avoided (Section 3.2.3.1). For some substrates it was possible to monitor the absorbance at wavelengths around the 340 nm λ_{max}, giving better absorbance changes; for most substrates the less intense 545/590 nm peak had to be used.

The reaction solutions were maintained at 25 °C and pH 7.4 (phosphate buffer). EDTA was added to eliminate contributions from the copper dependent reaction. The nitrosothiols were prepared using a two – fold excess of nitrous acid to ensure complete nitrosation. Full details of the experimental procedures are in Chapter 6. The structures of the nitrosothiols studied are tabulated in Section 4.2.3.

4.2.1 Establishing the Rate Equation

- **Experiments using *S*-nitroso penicillamine**

The decomposition of *S*-nitroso penicillamine (SNPen) by ascorbic acid was followed at 340 nm. A large excess of ascorbic acid over the SNPen concentration was employed. Figure 4.1 shows the effect of different ascorbic acid concentrations upon the decomposition.
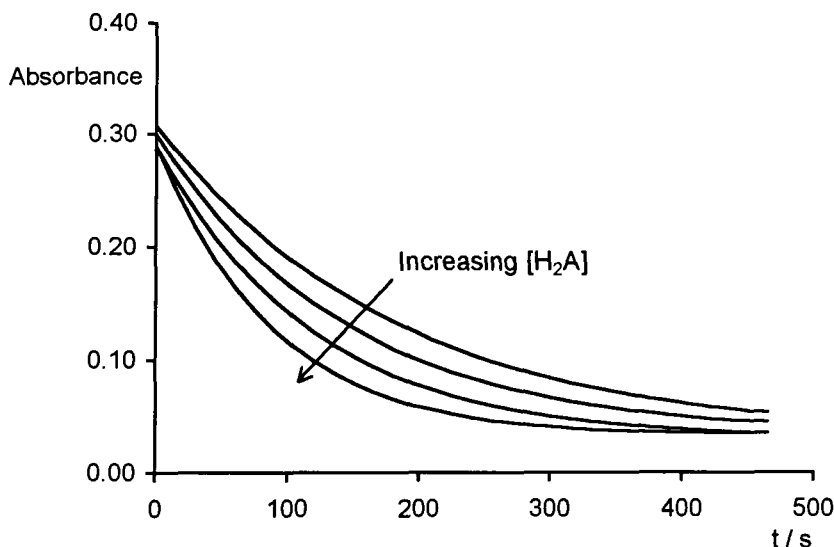
Figure 4.1 Decomposition of SNPen (4×10^{-4} M) by [H$_2$A] (4×10^{-3} M, 5×10^{-3} M, 6×10^{-3} M, 8×10^{-3}M). [EDTA] = 1×10^{-3} M. 25 °C, pH 7.4.

The traces obtained for SNPen decomposition were first order, indicating that the decomposition is first order with respect to [SNPen]. This is demonstrated in Figure 4.2, which shows the data from Figure 4.1 for the reaction with 8×10^{-3} M ascorbic acid. The data were fitted to the first order rate equation given in Equation 4.1 by applying a non – linear least squares method using the Scientist [1] package.
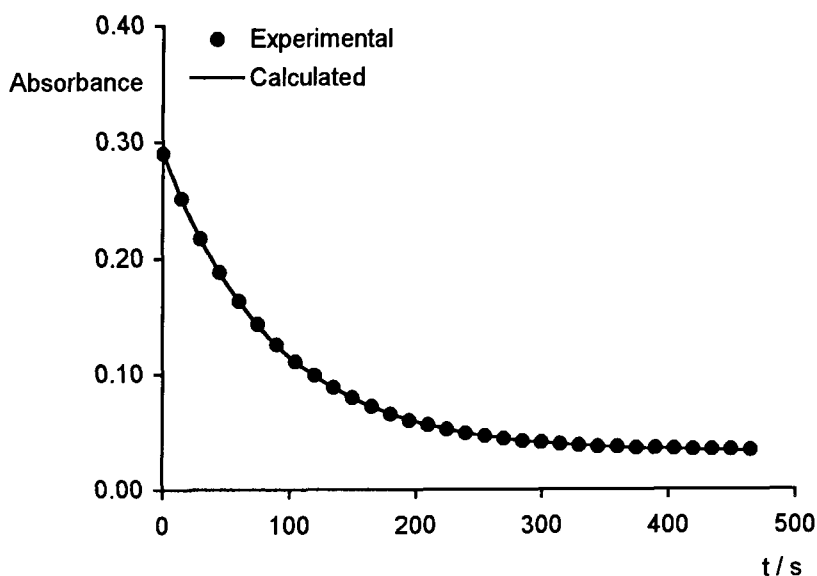
Figure 4.2 A first order decomposition trace for the reaction of SNPen (4×10^{-4} M) with ascorbic acid (8×10^{-3} M), with the theoretical curve superimposed. $k_{obs} = 0.0112 \pm 1 \times 10^{-4}$ s^{-1}.

$$Absorbance = A_0 \exp(-k_{obs}t) + c \qquad \text{Equation 4.1}$$

Values of the observed first order rate constants, k_{obs}, obtained for SNPen decomposition in the presence of a range of ascorbic acid concentrations are shown in Table 4.1.

$[H_2A]$ / mol dm^{-3}	k_{obs} / s^{-1}
4.00×10^{-3}	$5.58 \times 10^{-3} \pm 2 \times 10^{-5}$
5.00×10^{-3}	$7.13 \times 10^{-3} \pm 2 \times 10^{-5}$
6.00×10^{-3}	$8.67 \times 10^{-3} \pm 4 \times 10^{-5}$
8.00×10^{-3}	$1.12 \times 10^{-2} \pm 1 \times 10^{-4}$
1.00×10^{-2}	$1.37 \times 10^{-2} \pm 2 \times 10^{-4}$

Table 4.1 Kinetic data for the reaction between SNPen (4×10^{-4} M) and ascorbic acid

The reaction order with respect to [SNPen] has already been established as one, and the change in k_{obs} with $[H_2A]$ requires the order with respect to $[H_2A]$ to be greater than zero. The rate law can therefore be expressed in the general form of Equation 4.2, where $n > 0$.

$$Rate = k[\text{SNPen}] \cdot [H_2A]^n \qquad \text{Equation 4.2}$$

Pseudo first order conditions prevail when $[H_2A] >> [\text{SNPen}]$, therefore Equation 4.3 holds. From Equations 4.2 and 4.3 one can write Equation 4.4. Taking logarithms of both sides of Equation 4.4 yields Equation 4.5, from which it can be recognised that a plot of $\log(k_{obs}$ / s$^{-1})$ versus $\log([H_2A]$ / mol dm$^{-3})$ should be linear, with gradient n.

$$Rate = k_{obs}[\text{SNPen}] \qquad \text{Equation 4.3}$$

$$k_{obs} = k[H_2A]^n \qquad \text{Equation 4.4}$$

$$\log k_{obs} = \log k + n\log[H_2A] \qquad \text{Equation 4.5}$$

Figure 4.3 shows a plot of $\log(k_{obs}$ / s$^{-1})$ versus $\log([H_2A]$ / M) for the data in Table 4.1. As predicted, the plot gives a straight line. The gradient is 0.98, indicating $n = 1$ and the order with respect to $[H_2A]$ is one. SNPen decomposition by ascorbic acid *via* the copper independent pathway therefore has the rate law described by Equation 4.6, where k_2 is the second order rate constant for the reaction.
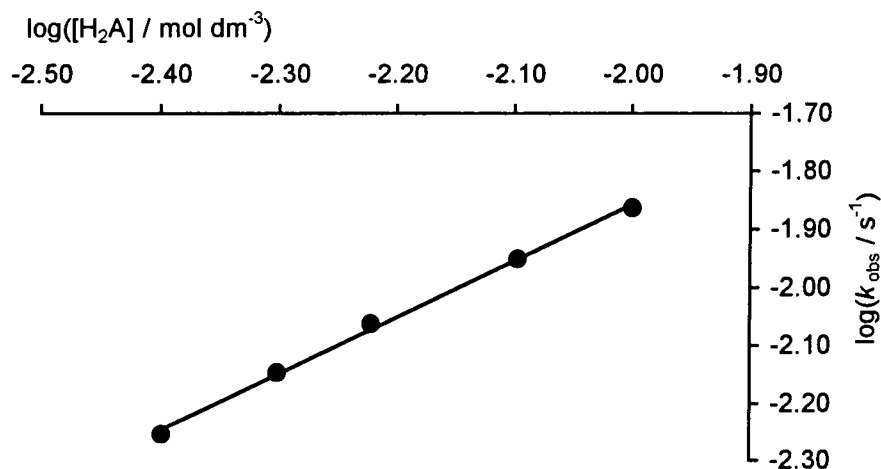
Figure 4.3 log (k_{obs} / s^{-1}) versus log ([H$_2$A] / mol dm^{-3}) for SNPen decomposition, data from Table 4.1

$$Rate = k_2 [\text{SNPen}] \cdot [\text{H}_2\text{A}]$$
        Equation 4.6

With n in Equation 4.4 equal to one, a graph of k_{obs} versus [H$_2$A] should be linear, the line passing through the origin. k_2 is readily obtained from the gradient. Such a plot is given in Figure 4.4, which uses the data in Table 4.1. Using the linear regression function in Excel[2] k_2 was determined as:

$k_2 = 1.40 \pm 0.11$ dm^3 mol^{-1} s^{-1}
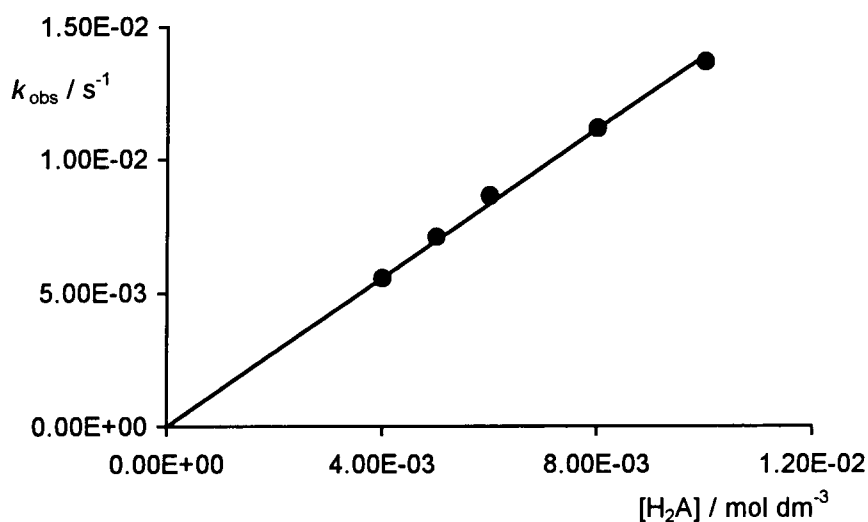
Figure 4.4 Plot of k_{obs} versus [H$_2$A] for SNPen decomposition, data from Table 4.1

• Experiments on S-nitroso 2-thioethanesulfonic acid

Data for the decomposition of S-nitroso 2-thioethanesulfonic acid are given in Table 4.2. These reactions are slow (several hours duration), but the observation of first order traces indicates that the concentration of ascorbic acid remains effectively constant throughout the reaction, hence there must be little oxidative decomposition of the ascorbic acid. This is presumably because of the strong complexation of metal ions by the EDTA, reduction of dehydroascorbic acid by the thiol product, and the low availability of oxygen in the sealed cells.

$[H_2A]$ / mol dm^{-3}	k_{obs} / s^{-1}
2.00×10^{-2}	$1.81 \times 10^{-4} \pm 1 \times 10^{-6}$
3.00×10^{-2}	$2.50 \times 10^{-4} \pm 2 \times 10^{-6}$
4.00×10^{-2}	$3.07 \times 10^{-4} \pm 2 \times 10^{-6}$
5.00×10^{-2}	$3.93 \times 10^{-4} \pm 4 \times 10^{-6}$
7.00×10^{-2}	$5.00 \times 10^{-4} \pm 4 \times 10^{-6}$
1.00×10^{-1}	$7.25 \times 10^{-4} \pm 6 \times 10^{-6}$

Table 4.2 Kinetic data for decomposition of S-nitroso 2-thioethanesulfonic acid
$(2 \times 10^{-3}$ M) obtained at 545 nm

The graph of k_{obs} versus $[H_2A]$ for the data in Table 4.2 is linear, but with a small positive intercept, indicating a decomposition reaction independent of $[H_2A]$ (Figure 4.5). The cause of this intercept is probably the thermal decomposition, and possibly some hydrolysis, of the nitrosothiol, which become observable on the time-scales employed for this substrate.
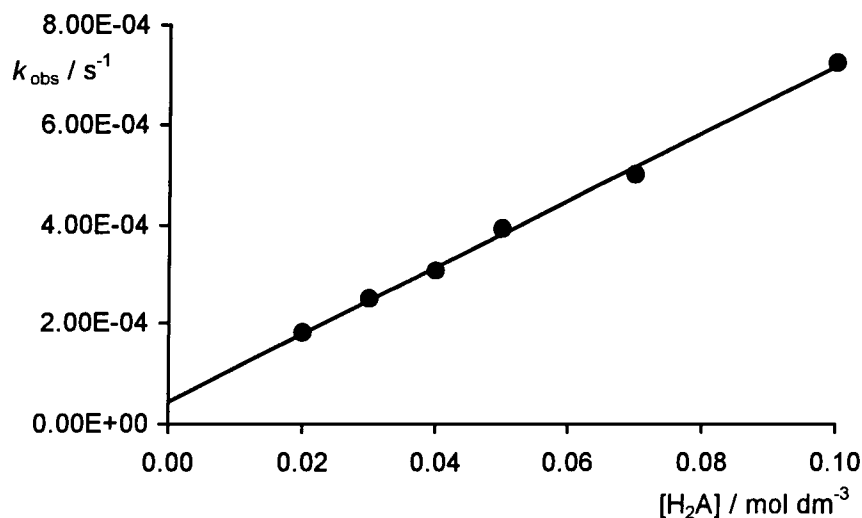
Figure 4.5 Plot of k_{obs} versus [H$_2$A] for S-nitroso 2-thioethanesulfonic acid decomposition

The full form of the rate equation for the copper independent decomposition of nitrosothiols is given by Equation 4.7, where k' represents the sum of contributions from the ascorbic acid independent processes, and [RSNO] represents the nitrosothiol concentration.

$$Rate = k_2[RSNO]\cdot[H_2A] + k'[RSNO] \qquad \text{Equation 4.7}$$

$$k_{obs} = k_2[H_2A] + k' \text{ when } [H_2A] \gg [RSNO] \qquad \text{Equation 4.8}$$

Regression analysis on the data in Table 4.2 gives

$k_2 = 6.73 \times 10^{-3} \pm 3.5 \times 10^{-4} \text{ dm}^3 \text{ mol}^{-1} \text{ s}^{-1}$

$k' = 4.5 \times 10^{-5} \pm 2 \times 10^{-5} \text{ s}^{-1}$

The rate law indicates that the rate – determining step is bimolecular, involving one molecule each of nitrosothiol and ascorbic acid. The simplest type of mechanism that can be envisaged to explain the rate equation is a concerted nucleophilic substitution process, S_N2. However, the mechanism must be more complicated than a single step S_N2 reaction because such a reaction would not give rise to thiol and nitric oxide as the products, nor the stoichiometry observed (Section 3.2.2). pH and temperature dependence studies should provide more evidence to assist in proposing a mechanism for the reaction: these are reported in sections 4.3 and 4.4. Reviewing all of the evidence together allows the postulation of a suitable mechanism, and this forms the basis of Section 4.5.

The copper independent decomposition of nitrosothiols is clearly first order in both the nitrosothiol and the ascorbic acid concentrations, which agrees with work carried out on the reaction between S-nitroso glutathione and ascorbic acid.[3] This is also in accord with the results obtained for similar reactions including the reaction between ascorbic acid and alkyl nitrites [4,5] and the ascorbic acid mediated decomposition of oral anticancer Pt^{IV} compounds.[6]

4.2.2 Determination of k_2 for a Range of S-Nitrosothiols

The reactions between ascorbic acid and a range of nitrosothiols were studied to obtain structure – reactivity information. The kinetic data obtained for each substrate are below. In all cases, the temperature was 25 °C and the pH was 7.4. The values of k_2 were obtained from plots of k_{obs} versus [H$_2$A], all of which gave good straight lines upon visual inspection. The correlation coefficients, r^2, obtained from the regression analysis are included. Intercepts with a standard error greater than the value of the intercept were deemed not statistically significant.

- S-Nitroso cysteamine

[H$_2$A] / mol dm^{-3}	k_{obs} / s^{-1}
5.00×10^{-3}	$1.32 \times 10^{-3} \pm 2.0 \times 10^{-5}$
6.00×10^{-3}	$1.56 \times 10^{-3} \pm 2.5 \times 10^{-6}$
8.00×10^{-3}	$1.98 \times 10^{-3} \pm 3.0 \times 10^{-5}$
1.00×10^{-2}	$2.40 \times 10^{-3} \pm 3.1 \times 10^{-6}$
1.50×10^{-2}	$3.47 \times 10^{-3} \pm 3.0 \times 10^{-5}$
2.00×10^{-2}	$4.60 \times 10^{-3} \pm 1.0 \times 10^{-4}$

$$[RSNO] = 5.0 \times 10^{-4} \text{ mol dm}^{-3}$$
$$\lambda = 400 \text{ nm}$$

Table 4.3 Kinetic data for the reaction of ascorbic acid with S-nitroso cysteamine

$k_2 = 0.217 \pm 3.0 \times 10^{-3}$ dm^3 mol^{-1} s^{-1}; $k' = 2.4 \times 10^{-4} \pm 4 \times 10^{-5}$ s^{-1}; $r^2 = 0.99$.

- **S-Nitroso 2-(dimethylamino)ethane thiol**

$[H_2A]$ / mol dm^{-3}	$^a k_{obs}$ / s^{-1}	$^b k_{obs}$ / s^{-1}
5.00×10^{-3}	$3.40 \times 10^{-3} \pm 4.7 \times 10^{-5}$	$2.94 \times 10^{-3} \pm 4.0 \times 10^{-5}$
6.00×10^{-3}	$4.02 \times 10^{-3} \pm 4.9 \times 10^{-5}$	$3.30 \times 10^{-3} \pm 6.0 \times 10^{-5}$
7.00×10^{-3}	-----	$3.96 \times 10^{-3} \pm 1.2 \times 10^{-4}$
8.00×10^{-3}	$5.47 \times 10^{-3} \pm 6.5 \times 10^{-5}$	$4.43 \times 10^{-3} \pm 5.0 \times 10^{-5}$
1.00×10^{-2}	$6.65 \times 10^{-3} \pm 1.1 \times 10^{-4}$	$6.37 \times 10^{-3} \pm 1.2 \times 10^{-4}$
1.50×10^{-2}	$9.95 \times 10^{-3} \pm 1.6 \times 10^{-4}$	$9.11 \times 10^{-3} \pm 2.0 \times 10^{-4}$
2.00×10^{-2}	$1.21 \times 10^{-2} \pm 3.6 \times 10^{-4}$	$1.19 \times 10^{-2} \pm 8.0 \times 10^{-5}$

$$[RSNO] = 5.0 \times 10^{-4} \text{ mol dm}^{-3}$$
$$\lambda = 400 \text{ nm}$$

[a] Gives $k_2 = 0.59 \pm 0.05$ dm^3 mol^{-1} s^{-1}; no statistically significant intercept; r^2 = 0.99
[b] Gives $k_2 = 0.60 \pm 0.02$ dm^3 mol^{-1} s^{-1}; no statistically significant intercept; r^2 = 0.99

Table 4.4 Kinetic data for the decomposition of S-nitroso 2-(dimethylamino)ethane thiol

These data give an average value of $k_2 = 0.59 \pm 1 \times 10^{-2}$ dm^3 mol^{-1} s^{-1}.

- **S-Nitroso 2-(diethylamino)ethane thiol**

$[H_2A]$ / mol dm^{-3}	$^a k_{obs}$ / s^{-1}	$^b k_{obs}$ / s^{-1}
5.00×10^{-3}	$3.11 \times 10^{-3} \pm 2.0 \times 10^{-5}$	-----
6.00×10^{-3}	$3.85 \times 10^{-3} \pm 6.0 \times 10^{-5}$	$4.52 \times 10^{-3} \pm 1.0 \times 10^{-4}$
7.00×10^{-3}	$4.21 \times 10^{-3} \pm 1.2 \times 10^{-4}$	-----
7.50×10^{-3}	-----	$5.62 \times 10^{-3} \pm 1.6 \times 10^{-4}$
9.00×10^{-3}	-----	$6.29 \times 10^{-3} \pm 1.0 \times 10^{-4}$
1.00×10^{-2}	$4.81 \times 10^{-3} \pm 6.0 \times 10^{-5}$	-----
1.50×10^{-2}	$6.70 \times 10^{-3} \pm 2.0 \times 10^{-4}$	$8.40 \times 10^{-3} \pm 4.0 \times 10^{-4}$
2.00×10^{-2}	$8.68 \times 10^{-3} \pm 4.0 \times 10^{-5}$	-----
2.10×10^{-2}	-----	$1.06 \times 10^{-2} \pm 6.0 \times 10^{-4}$
3.00×10^{-2}	-----	$1.50 \times 10^{-2} \pm 2.0 \times 10^{-4}$

$$[RSNO] = 5.0 \times 10^{-4} \text{ mol dm}^{-3}$$
$$\lambda = 400 \text{ nm}$$

[a] Gives $k_2 = 0.35 \pm 0.03$ dm^3 mol^{-1} s^{-1}; $k' = 1.5 \times 10^{-3} \pm 4 \times 10^{-4}$ s^{-1}; r^2 = 0.99
[b] Gives $k_2 = 0.42 \pm 0.03$ dm^3 mol^{-1} s^{-1}; $k' = 2.3 \times 10^{-3} \pm 5 \times 10^{-4}$ s^{-1}; r^2 = 0.99

Table 4.8 Kinetic data for the decomposition of S-nitroso 2-(diethylamino)ethane thiol

These data give an average value of $k_2 = 0.38 \pm 0.09$ dm^3 mol^{-1} s^{-1}.

- *S*-Nitroso 1-amino-2-methyl-2-propanethiol

$[H_2A]$ / mol dm^{-3}	k_{obs} / s^{-1}
5.00×10^{-3}	$6.80 \times 10^{-3} \pm 4.0 \times 10^{-5}$
6.00×10^{-3}	$8.46 \times 10^{-3} \pm 6.0 \times 10^{-5}$
7.00×10^{-3}	$9.06 \times 10^{-3} \pm 8.0 \times 10^{-5}$
8.00×10^{-3}	$1.04 \times 10^{-2} \pm 8.0 \times 10^{-5}$
1.00×10^{-2}	$1.21 \times 10^{-2} \pm 1.6 \times 10^{-4}$
1.20×10^{-2}	$1.52 \times 10^{-2} \pm 2.0 \times 10^{-4}$
1.50×10^{-2}	$1.75 \times 10^{-2} \pm 1.6 \times 10^{-4}$
2.00×10^{-2}	$2.28 \times 10^{-2} \pm 2.0 \times 10^{-4}$

$$[RSNO] = 5.0 \times 10^{-4} \text{ mol dm}^{-3}$$
$$\lambda = 400 \text{ nm}$$

Table 4.7 Kinetic data for the decomposition of *S*-nitroso-1-amino-2-methyl-2-propane thiol

$k_2 = 1.05 \pm 0.06$ dm^3 mol^{-1} s^{-1}; $k' = 1.9 \times 10^{-4} \pm 6 \times 10^{-5}$ s^{-1}; r$^2 = 0.99$.

- *S*-Nitroso cysteine (SNCys)

$[H_2A]$ / mol dm^{-3}	k_{obs} / s^{-1}
5.00×10^{-3}	$1.38 \times 10^{-3} \pm 2.0 \times 10^{-6}$
6.00×10^{-3}	$1.61 \times 10^{-3} \pm 6.0 \times 10^{-6}$
8.00×10^{-3}	$2.09 \times 10^{-3} \pm 8.0 \times 10^{-6}$
1.00×10^{-2}	$2.59 \times 10^{-3} \pm 8.0 \times 10^{-6}$
2.00×10^{-2}	$4.97 \times 10^{-3} \pm 2.0 \times 10^{-5}$

$$[RSNO] = 5.0 \times 10^{-4} \text{ mol dm}^{-3}$$
$$\lambda = 340 \text{ nm}$$

Table 4.8 Kinetic data for the reaction of ascorbic acid with SNCys

$k_2 = 0.24 \pm 2 \times 10^{-2}$ dm^3 mol^{-1} s^{-1}; $k' = 1.8 \times 10^{-4} \pm 2 \times 10^{-5}$ s^{-1}; r$^2 = 1$.

Figure 4.6 shows the plots of k_{obs} versus [H₂A] that were obtained for the substrates *S*-nitroso cysteine (●), *S*-nitroso 2-(dimethylamino)ethane thiol (○), *S*-nitroso 2-(diethylamino)ethane thiol (■), *S*-nitroso 1-amino-2-methyl-2-propane thiol (◆) and *S*-nitroso cysteine (◊).
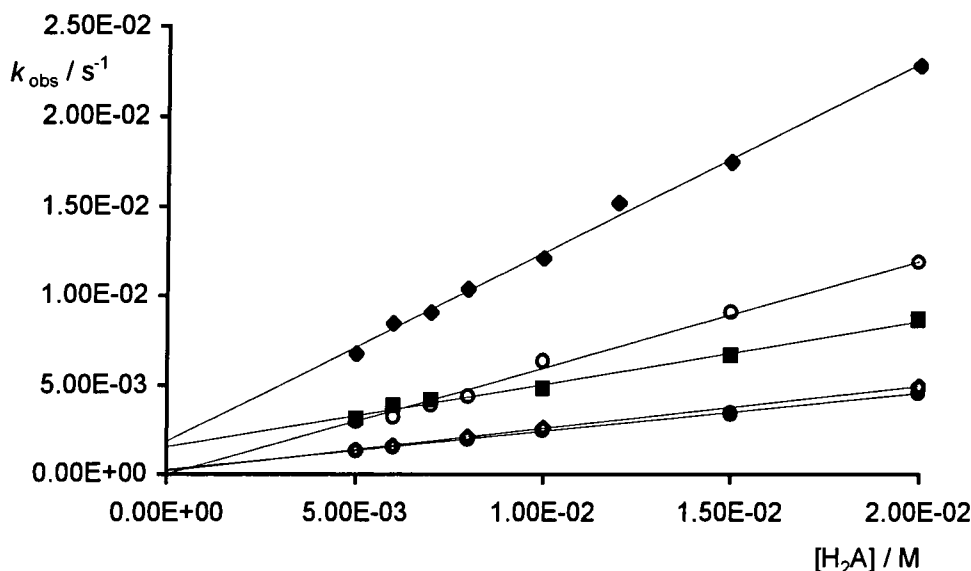
Figure 4.6 k_{obs} versus [H₂A] for various *S*-nitrosothiols (see text for details)

- ## *S*-Nitroso 2-thioethanesulfonic Acid

[H₂A] / mol dm⁻³	k_{obs} / s⁻¹
2.00×10^{-2}	$1.32 \times 10^{-4} \pm 1 \times 10^{-6}$
3.00×10^{-2}	$1.92 \times 10^{-4} \pm 1 \times 10^{-6}$
4.00×10^{-2}	$2.66 \times 10^{-4} \pm 1 \times 10^{-6}$
5.00×10^{-2}	$3.33 \times 10^{-4} \pm 2 \times 10^{-6}$
7.00×10^{-2}	$4.55 \times 10^{-4} \pm 2 \times 10^{-6}$
1.00×10^{-1}	$6.57 \times 10^{-4} \pm 4 \times 10^{-6}$

$$[RSNO] = 2.0 \times 10^{-3} \text{ mol dm}^{-3}$$
$$\lambda = 545 \text{ nm}$$

Table 4.6   Kinetic data for *S*-nitroso 2-thioethanesulfonic acid decomposition

$k_2 = 6.6 \times 10^{-3} \pm 1 \times 10^{-4}$ dm³ mol⁻¹ s⁻¹; no statistically significant intercept, $r^2 = 0.99$.

Considering the data in Section 4.2.1 for the same compound, an average value of $k_2 = 6.7 \times 10^{-3} \pm 2 \times 10^{-4}$ dm³ mol⁻¹ s⁻¹ can be calculated.

- ### *S*-Nitroso glutathione (GSNO)

$[H_2A]$ / mol dm^{-3}	k_{obs} / s^{-1}
1.50×10^{-2}	$3.04 \times 10^{-4} \pm 4 \times 10^{-7}$
2.00×10^{-2}	$4.11 \times 10^{-4} \pm 1 \times 10^{-6}$
4.00×10^{-2}	$8.45 \times 10^{-4} \pm 2 \times 10^{-6}$
6.00×10^{-2}	$1.29 \times 10^{-3} \pm 6 \times 10^{-6}$
8.00×10^{-2}	$1.55 \times 10^{-3} \pm 4 \times 10^{-6}$
1.00×10^{-1}	$2.00 \times 10^{-3} \pm 1 \times 10^{-5}$

$$[RSNO] = 1.0 \times 10^{-3} \text{ mol dm}^{-3}$$
$$\lambda = 400 \text{ nm}$$

Table 4.4 Kinetic data for the reaction of ascorbic acid with GSNO

$k_2 = 2.02 \times 10^{-2} \pm 1.0 \times 10^{-3}$ dm^3 mol^{-1} s^{-1} ; no statistically significant intercept; r^2 = 0.99.

- ### *S*-Nitroso *N*-acetyl cysteamine

$[H_2A]$ / mol dm^{-3}	k_{obs} / s^{-1}
3.00×10^{-2}	$1.69 \times 10^{-4} \pm 4.0 \times 10^{-6}$
4.00×10^{-2}	$1.95 \times 10^{-4} \pm 2.0 \times 10^{-6}$
5.00×10^{-2}	$2.55 \times 10^{-4} \pm 2.0 \times 10^{-6}$
7.00×10^{-2}	$3.22 \times 10^{-4} \pm 2.0 \times 10^{-6}$
1.00×10^{-1}	$4.76 \times 10^{-4} \pm 2.0 \times 10^{-6}$
1.20×10^{-1}	$5.39 \times 10^{-4} \pm 4.0 \times 10^{-6}$

$$[RSNO] = 2.0 \times 10^{-3} \text{ mol dm}^{-3}$$
$$\lambda = 545 \text{ nm}$$

Table 4.6 Kinetic data for the decomposition of *S*-nitroso *N*-acetyl cysteamine

$k_2 = 4.3 \times 10^{-3} \pm 3 \times 10^{-4}$ dm^3 mol^{-1} s^{-1} ; $k' = 4 \times 10^{-5} \pm 2 \times 10^{-5}$ s^{-1} ; r^2 = 0.99.

- ### *S*-Nitroso *N*-acetylcysteine (SNAC)

$[H_2A]$ / mol dm^{-3}	k_{obs} / s^{-1}
1.00×10^{-1}	$3.50 \times 10^{-4} \pm 1 \times 10^{-5}$
1.25×10^{-1}	$4.27 \times 10^{-4} \pm 2 \times 10^{-5}$
1.50×10^{-1}	$5.02 \times 10^{-4} \pm 1 \times 10^{-5}$
2.00×10^{-1}	$6.39 \times 10^{-4} \pm 3 \times 10^{-5}$
2.50×10^{-1}	$7.35 \times 10^{-4} \pm 3 \times 10^{-4}$
3.00×10^{-1}	$9.18 \times 10^{-4} \pm 5 \times 10^{-5}$

$$[RSNO] = 2.0 \times 10^{-3} \text{ mol dm}^{-3}$$
$$\lambda = 545 \text{ nm}$$

Table 4.11 Kinetic data for the reaction of ascorbic acid with SNAC

$k_2 = 2.7 \times 10^{-3} \pm 2 \times 10^{-4}$ dm³ mol⁻¹ s⁻¹; $k' = 8.3 \times 10^{-5} \pm 4 \times 10^{-5}$ s⁻¹; r² = 0.99.

- ### *S*-Nitroso cysteine ethyl ester

$[H_2A]$ / mol dm^{-3}	k_{obs} / s^{-1}
1.60×10^{-2}	$6.06 \times 10^{-3} \pm 4.0 \times 10^{-5}$
3.20×10^{-2}	$1.06 \times 10^{-2} \pm 4.0 \times 10^{-5}$
4.80×10^{-2}	$1.54 \times 10^{-2} \pm 2.0 \times 10^{-5}$
6.40×10^{-2}	$2.11 \times 10^{-2} \pm 4.0 \times 10^{-5}$
8.00×10^{-2}	$2.32 \times 10^{-2} \pm 6.0 \times 10^{-5}$
9.60×10^{-2}	$2.87 \times 10^{-2} \pm 1.0 \times 10^{-4}$

$$[RSNO] = 1.0 \times 10^{-3} \text{ mol dm}^{-3}$$
$$\lambda = 400 \text{ nm}$$

Table 4.12 Kinetic data for the decomposition of *S*-nitroso cysteine ethyl ester

$k_2 = 0.28 \pm 0.03$ dm³ mol⁻¹ s⁻¹; $k' = 2 \times 10^{-3} \pm 2 \times 10^{-3}$ s⁻¹; r² = 0.99.

- ### *S*-Nitroso *N*-acetyl-D,L-penicillamine (SNAP)

$[H_2A]$ / mol dm^{-3}	k_{obs} / s^{-1}
1.00×10^{-1}	$3.09 \times 10^{-4} \pm 1.4 \times 10^{-6}$
1.25×10^{-1}	$3.62 \times 10^{-4} \pm 1.8 \times 10^{-6}$
1.50×10^{-1}	$4.45 \times 10^{-4} \pm 4.0 \times 10^{-6}$
2.00×10^{-1}	$5.49 \times 10^{-4} \pm 4.0 \times 10^{-6}$
2.50×10^{-1}	$7.57 \times 10^{-4} \pm 5.0 \times 10^{-6}$

$[RSNO] = 6.0 \times 10^{-3}$ mol dm^{-3}

$\lambda = 590$ nm

Table 4.13 Kinetic data for the reaction of ascorbic acid with SNAP

$k_2 = 2.9 \times 10^{-3} \pm 1 \times 10^{-4}$ dm^3 mol^{-1} s^{-1}; no significant intercept; r^2 = 0.98.

$[H_2A]$ / mol dm^{-3}	k_{obs} / s^{-1}
3.00×10^{-2}	$1.37 \times 10^{-4} \pm 8.7 \times 10^{-7}$
4.00×10^{-2}	$1.92 \times 10^{-4} \pm 1.6 \times 10^{-6}$
5.00×10^{-2}	$2.33 \times 10^{-4} \pm 1.6 \times 10^{-6}$
6.00×10^{-2}	$2.87 \times 10^{-4} \pm 2.0 \times 10^{-6}$
7.00×10^{-2}	$3.40 \times 10^{-4} \pm 1.8 \times 10^{-6}$
1.00×10^{-1}	$4.20 \times 10^{-4} \pm 3.2 \times 10^{-6}$

$[RSNO] = 2.5 \times 10^{-3}$ mol dm^{-3}

$\lambda = 590$ nm

Table 4.14 Kinetic data for the reaction of ascorbic acid with SNAP

$k_2 = 4.1 \times 10^{-3} \pm 7 \times 10^{-4}$ dm^3 mol^{-1} s^{-1}; $k' = 3.0 \times 10^{-5} \pm 4 \times 10^{-5}$ s^{-1}; r^2 = 0.98.

These data give an average value of $k_2 = 3.5 \times 10^{-3} \pm 8 \times 10^{-4}$ dm^3 mol^{-1} s^{-1}.

- ### *S*-Nitroso homocysteine

$[H_2A]$ / mol dm^{-3}	k_{obs} / s^{-1}
6.00×10^{-2}	$3.24 \times 10^{-4} \pm 2.0 \times 10^{-6}$
8.00×10^{-2}	$3.99 \times 10^{-4} \pm 2.0 \times 10^{-6}$
1.00×10^{-1}	$4.89 \times 10^{-4} \pm 2.0 \times 10^{-6}$
1.20×10^{-1}	$5.43 \times 10^{-4} \pm 6.0 \times 10^{-6}$
1.60×10^{-1}	$6.30 \times 10^{-4} \pm 2.0 \times 10^{-5}$
2.40×10^{-1}	$9.58 \times 10^{-4} \pm 8.0 \times 10^{-6}$

$[RSNO] = 5.0 \times 10^{-3}$ mol dm^{-3}

$\lambda = 545$ nm

Table 4.15 Kinetic data for the decomposition of *S*-nitroso homocysteine

$k_2 = 3.4 \times 10^{-3} \pm 3 \times 10^{-4}$ dm^3 mol^{-1} s^{-1}; no statistically significant intercept; r^2 = 0.99.

- ## S-Nitroso 2-hydroxyethanethiol

[H$_2$A] / mol dm^{-3}	$^a k_{obs}$ / s^{-1}	$^b k_{obs}$ / s^{-1}	$^c k_{obs}$ / s^{-1}
3.00×10^{-2}	$1.08 \times 10^{-4} \pm 6.0 \times 10^{-7}$	-----	$7.64 \times 10^{-5} \pm 6.0 \times 10^{-7}$
3.60×10^{-2}	-----	$8.52 \times 10^{-5} \pm 1.2 \times 10^{-6}$	-----
4.00×10^{-2}	$1.41 \times 10^{-4} \pm 2.0 \times 10^{-6}$	-----	$1.02 \times 10^{-4} \pm 6.0 \times 10^{-7}$
5.00×10^{-2}	-----	-----	$1.23 \times 10^{-4} \pm 8.0 \times 10^{-7}$
6.00×10^{-2}	$2.29 \times 10^{-4} \pm 2.0 \times 10^{-6}$	-----	-----
7.00×10^{-2}	-----	-----	$1.66 \times 10^{-4} \pm 2.0 \times 10^{-6}$
7.20×10^{-2}	-----	$1.62 \times 10^{-4} \pm 4.0 \times 10^{-6}$	-----
1.00×10^{-1}	$3.53 \times 10^{-4} \pm 4.0 \times 10^{-6}$	$2.00 \times 10^{-4} \pm 2.0 \times 10^{-6}$	$2.42 \times 10^{-4} \pm 4.0 \times 10^{-6}$
1.20×10^{-1}	-----	-----	$2.88 \times 10^{-4} \pm 2.0 \times 10^{-6}$
1.40×10^{-1}	$5.01 \times 10^{-4} \pm 4.0 \times 10^{-6}$	-----	-----
1.80×10^{-1}	-----	$2.76 \times 10^{-4} \pm 4.0 \times 10^{-6}$	-----
1.90×10^{-1}	$7.16 \times 10^{-4} \pm 6.0 \times 10^{-6}$	-----	-----
3.06×10^{-1}	-----	$4.56 \times 10^{-4} \pm 4.0 \times 10^{-6}$	-----

[RSNO] = 2.0×10^{-3} mol dm^{-3}

λ = 545 nm

^{a} Gives $k_2 = 3.7 \times 10^{-3} \pm 1 \times 10^{-4}$ dm^3 mol^{-1} s^{-1}; r^2 = 0.99
^{b} Gives $k_2 = 1.3 \times 10^{-3} \pm 1 \times 10^{-4}$ dm^3 mol^{-1} s^{-1}; $k' = 5 \times 10^{-5} \pm 2 \times 10^{-5}$ s^{-1}; r^2 = 0.99
^{c} Gives $k_2 = 2.35 \times 10^{-3} \pm 6 \times 10^{-5}$ dm^3 mol^{-1} s^{-1}; r^2 = 0.99

Table 4.16 Kinetic data for the decomposition of S-nitroso 2-hydroxy-ethanethiol

These data give an average value of $k_2 = 2.4 \times 10^{-3} \pm 1 \times 10^{-3}$ dm^3 mol^{-1} s^{-1}.

- ### S-Nitroso 3-thiopropanoic acid

[H$_2$A] / mol dm^{-3}	$^a k_{obs}$ / s^{-1}	$^b k_{obs}$ / s^{-1}	$^c k_{obs}$ / s^{-1}
5.00×10^{-2}	-----	-----	$1.57 \times 10^{-4} \pm 2.0 \times 10^{-6}$
6.00×10^{-2}	$4.05 \times 10^{-5} \pm 4.0 \times 10^{-7}$	$2.29 \times 10^{-4} \pm 4.0 \times 10^{-6}$	-----
7.50×10^{-2}	-----	-----	$2.26 \times 10^{-4} \pm 4.0 \times 10^{-6}$
1.00×10^{-1}	-----	-----	$2.65 \times 10^{-4} \pm 2.0 \times 10^{-6}$
2.00×10^{-1}	-----	-----	$4.48 \times 10^{-4} \pm 4.0 \times 10^{-6}$
2.40×10^{-1}	$1.29 \times 10^{-4} \pm 8.0 \times 10^{-7}$	$5.09 \times 10^{-4} \pm 8.0 \times 10^{-6}$	-----
3.00×10^{-1}	-----	-----	$6.67 \times 10^{-4} \pm 1.0 \times 10^{-5}$
3.60×10^{-1}	$1.68 \times 10^{-4} \pm 8.0 \times 10^{-7}$	$7.41 \times 10^{-4} \pm 1.0 \times 10^{-5}$	-----
4.20×10^{-1}	$1.99 \times 10^{-4} \pm 8.0 \times 10^{-7}$	$8.40 \times 10^{-4} \pm 1.4 \times 10^{-5}$	-----
4.80×10^{-1}	$2.33 \times 10^{-4} \pm 8.0 \times 10^{-7}$	-----	-----
5.70×10^{-1}	$2.52 \times 10^{-4} \pm 1.4 \times 10^{-6}$	$1.08 \times 10^{-3} \pm 2.0 \times 10^{-5}$	-----

$$[RSNO] = 1.0 \times 10^{-3} \text{ mol dm}^{-3}$$
$$\lambda = 545 \text{ nm}$$

[a] Gives $k_2 = 4.2 \times 10^{-4} \pm 4 \times 10^{-5}$ dm^3 mol^{-1} s^{-1}; $k' = 2.0 \times 10^{-5} \pm 1 \times 10^{-5}$ s^{-1}; r$^2 = 0.99$

[b] Gives $k_2 = 1.69 \times 10^{-3} \pm 7 \times 10^{-5}$ dm^3 mol^{-1} s^{-1}; $k' = 1.2 \times 10^{-4} \pm 3 \times 10^{-5}$ s^{-1}; r$^2 = 0.99$

[c] Gives $k_2 = 2.0 \times 10^{-3} \pm 1 \times 10^{-4}$ dm^3 mol^{-1} s^{-1}; $k' = 7 \times 10^{-5} \pm 2 \times 10^{-5}$ s^{-1}; r$^2 = 0.99$

Table 4.17 Kinetic data for the decomposition of S-nitroso 3-thiopropionic acid

Clearly the data in column *a* of Table 4.17 give a k_2 value that is somewhat erroneous when compared with those obtained from the data in columns *b* and *c*. Averaging these two latter values gives $k_2 = 1.8 \times 10^{-3} \pm 4 \times 10^{-4}$ dm^3 mol^{-1} s^{-1}

- ### S-Nitroso thioglycerol

[H$_2$A] / mol dm^{-3}	k_{obs} / s^{-1}
6.00×10^{-2}	$1.43 \times 10^{-4} \pm 6.0 \times 10^{-7}$
8.00×10^{-2}	$1.88 \times 10^{-4} \pm 8.0 \times 10^{-7}$
1.00×10^{-1}	$2.16 \times 10^{-4} \pm 6.0 \times 10^{-7}$
1.60×10^{-1}	$3.26 \times 10^{-4} \pm 1.2 \times 10^{-6}$
2.40×10^{-1}	$4.00 \times 10^{-4} \pm 6.0 \times 10^{-6}$
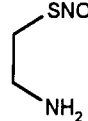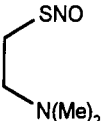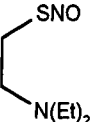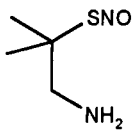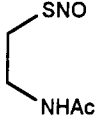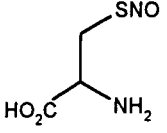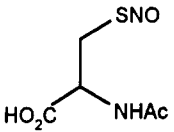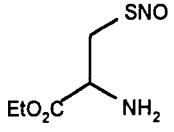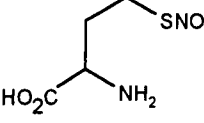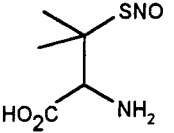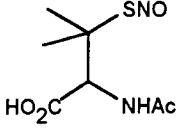
$$[RSNO] = 5.0 \times 10^{-3} \text{ mol dm}^{-3}$$
$$\lambda = 545 \text{ nm}$$

Table 4.18 Kinetic data for the decomposition of S-nitroso thioglycerol

$k_2 = 1.6 \times 10^{-3} \pm 2 \times 10^{-4}$ dm^3 mol^{-1} s^{-1}; $k' = 6 \times 10^{-5} \pm 2 \times 10^{-5}$ s^{-1}; r$^2 = 0.98$.

4.2.3 Summary of k_2 Values

Table 4.19 summarises the k_2 values that have been determined for the copper independent reaction between nitrosothiols and ascorbic acid.

Substrate number	Nitrosothiol	Structure	k_2 / dm^3 mol^{-1} s^{-1}
I	S – nitroso cysteamine		$0.217 \pm 3.0 \times 10^{-3}$
II	S – nitroso 2-(dimethylamino)ethane thiol		$0.59 \pm 9 \times 10^{-3}$
III	S – nitroso 2-(diethylamino)ethane thiol		0.38 ± 0.09
IV	S – nitroso 1-amino-2-methyl-2-propane thiol		1.05 ± 0.06
V	S – nitroso N-acetyl cysteamine		4.3×10^{-3} $\pm 3 \times 10^{-4}$
VI	S – nitroso cysteine		$0.24 \pm 2 \times 10^{-2}$
VII	S-nitroso N-acetylcysteine		2.7×10^{-3} $\pm 2 \times 10^{-4}$
VIII	S – nitroso cysteine ethyl ester		0.28 ± 0.03
IX	S – nitroso homocysteine		3.4×10^{-3} $\pm 3 \times 10^{-4}$
X	S – nitroso penicillamine		1.4 ± 0.1
XI	S – nitroso N-acetyl penicillamine		3.5×10^{-3} $\pm 8 \times 10^{-4}$
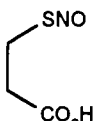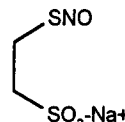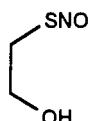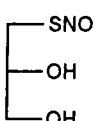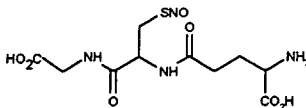
Substrate number	Nitrosothiol	Structure	k_2 / dm^3 mol^{-1} s^{-1}
XII	*S* – nitroso 3-thio-propanoic acid	SNO / CO$_2$H	$1.8 \times 10^{-3} \pm$ 4×10^{-4}
XIII	*S* – nitroso 2-thio-ethanesulfonic acid	SNO / SO$_3$-Na+	$6.7 \times 10^{-3} \pm$ 2×10^{-4}
XIV	*S* – nitroso 2-hydroxyethanethiol	SNO / OH	2.4×10^{-3} $\pm 1 \times 10^{-3}$
XV	*S* – nitroso thioglycerol	SNO / OH / OH	1.6×10^{-3} $\pm 2 \times 10^{-4}$
XVI	*S* – nitroso glutathione	HO$_2$C—NH...SNO...NH$_2$ CO$_2$H	2.0×10^{-2} $\pm 1 \times 10^{-3}$

Table 4.19 Summary of k_2 values for the copper independent decomposition of nitrosothiols by ascorbic acid

Table 4.19 shows that a wide range of k_2 values exists for the reaction between ascorbic acid and *S*-nitrosothiols, extending over four orders of magnitude. Analysis of the structures enables reactivity – structure relationships to be identified.

Examination of entries I to V reveals some interesting features. Comparison of I with the entire table reveals this substrate to be one of the most reactive studied. Modification of the compound by alkylation of the amine moiety gives rise to enhanced reactivity: entries II and III. These alkyl groups increase the electron density on the nitrogen atom, making the substrate more basic. At pH 7.4, II and III exist to a greater extent in the protonated form than I, and therefore one might expect more favourable interaction with the ascorbate anions.

Increasing the steric bulk of the β - nitrogen by acetylation as in V gives rise to a large decrease in reactivity. This effect is also borne out by comparison of VI with VII and X with XI.

Modification of the nitrosothiol structure to include *gem* – dimethyl groups on the carbon atom α to the nitroso group results in increased reactivity, but only in the presence of a free amino group on the β - carbon. This is shown by comparing I,

111

IV, VI and X with VII and XI. Considering that the kinetic analysis suggests nucleophilic attack upon the nitroso group, the increased reactivity of substrates with electron donating methyl groups on the α - carbon is perhaps unexpected. However, recent ^{15}N nmr studies have shown that the *gem* – dimethyl groups lead to an increased chemical shift, indicative of a lower electron density, on the nitroso nitrogen.[7] Lower electron density of this nature is expected to make nucleophilic attack at the nitroso group more favourable.

The presence, absence or modification (e.g. by esterification) of a β - carboxylic acid group does not result in any significant change in reactivity. This is clear from comparison of I with VI and VIII, IV with X, and to a lesser extent V with VII. Substrates possessing only a β - carboxylate, or similar group that is negatively charged at pH 7.4, possess very low reactivity compared with other nitrosothiols, for example XII and XIII.

Comparison of S-nitroso homocysteine, IX, with S – nitroso cysteine, VI, both of which possess a free amino group, reveals the former compound to be considerably less reactive. This suggests that the distance between the nitroso group and reactivity enhancing groups, such as amino groups, is crucial.

The kinetic data have shown that the reactivity of nitrosothiols towards ascorbic acid in the copper independent reaction is higher if positively charged groups are present in the β - position than if only negatively charged groups are present in this position. Increased steric bulk at the β - position also appears to reduce the reactivity of the substrate. These comparisons, considered alongside the results of the pH and temperature dependence studies, enable the formulation of theories concerning the mechanism of the reaction (Section 4.5).

4.3 pH Dependence

pH might affect the rate of reaction between a nitrosothiol and ascorbic acid by changing the proportions of the ascorbic acid forms (H_2A, HA^-, A^{2-}) or the nitrosothiol forms (e.g. β - NH_2, β - NH_3^+) present. Two substrates were chosen for pH dependence studies: S-nitroso glutathione (GSNO) and S-nitroso cysteamine. GSNO was chosen because pH is not expected to modify the molecule

close to the nitroso moiety, so any pH effect will be a consequence of the changing proportions of the three ascorbic acid species. *S*-nitroso cysteamine was chosen in order to attempt to understand the influence of the β - NH_2 group upon the reactivity of nitrosothiols.

A wide pH range was used in these studies, so no one buffer system was suitable to cover the whole range. The buffers used are tabulated in Table 4.20.

pH range	Buffer system	Concentration of primary component / mol dm^{-3}
2.5 – 4.0	Phthalate / HCl	0.15
4.1 – 5.9	Phthalate / NaOH	0.15
6.0 – 8.0	Phosphate / NaOH	0.15
8.1 – 9.4	Tris(hydroxymethyl) amino methane / HCl	0.15
9.5 – 11.0	Bicarbonate / NaOH	0.15
11.1 – 12.0	Phosphate / NaOH	0.15
12.1 -	KCl / NaOH	0.15

Table 4.20 Buffers used in the pH dependence studies

The k_2 values reported in the pH studies were usually obtained in the same way as those given in Section 4.2, i.e. by obtaining k_{obs} values for various excess [ascorbic acid] and calculating the gradient of a plot of k_{obs} versus [ascorbic acid]. For some of the slower, low pH reactions, the values of k_2 were obtained at one [ascorbic acid] by dividing k_{obs} by [ascorbic acid]. Throughout the remainder of the pH dependence section $[H_2A]_\tau$ is used to represent the total concentration of ascorbic acid species, i.e. $[H_2A] + [HA^-] + [A^{2-}]$.

4.3.1 pH Dependence of GSNO Decomposition

The data and k_2 values obtained for the decomposition of GSNO at various pH values are given below. All of the reactions were carried out at 25 °C in the presence of EDTA (1×10^{-3} M). The pH of each solution was measured in order to ensure a constant pH for each plot of k_{obs} versus $[H_2A]_\tau$. For pH values of 9.7 and above the reactions were studied using the stopped flow apparatus: k_{obs} values in these cases are the mean of at least five determinations. Full details of the experimental procedures are in Chapter 6.

- **pH 3.6**

$[H_2A]_\tau$ / mol dm^{-3}	k_{obs} / s^{-1}
1.00×10^{-1}	$3.34 \times 10^{-5} \pm 5.6 \times 10^{-7}$
1.60×10^{-1}	$4.27 \times 10^{-5} \pm 6.0 \times 10^{-7}$
2.00×10^{-1}	$4.85 \times 10^{-5} \pm 5.8 \times 10^{-7}$

$[GSNO] = 2.0 \times 10^{-3}$ mol dm^{-3}

$\lambda = 545$ nm

Table 4.21

$k_2 = 1.51 \times 10^{-4} \pm 5 \times 10^{-6}$ dm^3 mol^{-1} s^{-1}; $k' = 1.83 \times 10^{-5} \pm 9 \times 10^{-7}$ s^{-1}; $r^2 = 0.99$

- **pH 4.6**

$[H_2A]_\tau$ / mol dm^{-3}	k_{obs} / s^{-1}
1.00×10^{-1}	$8.08 \times 10^{-5} \pm 7.6 \times 10^{-7}$
1.60×10^{-1}	$1.05 \times 10^{-4} \pm 8.2 \times 10^{-7}$
2.00×10^{-1}	$1.18 \times 10^{-4} \pm 9.0 \times 10^{-7}$

$[GSNO] = 2.0 \times 10^{-3}$ mol dm^{-3}

$\lambda = 545$ nm

Table 4.22

$k_2 = 3.7 \times 10^{-4} \pm 4 \times 10^{-5}$ dm^3 mol^{-1} s^{-1}; $k' = 4.38 \times 10^{-5} \pm 6.8 \times 10^{-6}$ s^{-1}; $r^2 = 0.99$

- **pH 5.6**

$[H_2A]_\tau$ / mol dm^{-3}	k_{obs} / s^{-1}
4.00×10^{-2}	$4.81 \times 10^{-5} \pm 4 \times 10^{-7}$
8.00×10^{-2}	$8.02 \times 10^{-5} \pm 6 \times 10^{-7}$
1.00×10^{-1}	$9.56 \times 10^{-5} \pm 6 \times 10^{-7}$
1.60×10^{-1}	$1.21 \times 10^{-4} \pm 8 \times 10^{-7}$
2.00×10^{-1}	$1.46 \times 10^{-4} \pm 1.6 \times 10^{-6}$

$[GSNO] = 2.0 \times 10^{-3}$ mol dm^{-3}

$\lambda = 545$ nm

Table 4.23

$k_2 = 5.8 \times 10^{-4} \pm 4 \times 10^{-5}$ dm^3 mol^{-1} s^{-1}; $k' = 3 \times 10^{-5} \pm 1 \times 10^{-5}$ s^{-1}; $r^2 = 0.98$

- ## pH 6.5

$[H_2A]_{\tau}$ / mol dm^{-3}	k_{obs} / s^{-1}
4.00×10^{-2}	$1.71 \times 10^{-4} \pm 2.8 \times 10^{-6}$
8.00×10^{-2}	$2.86 \times 10^{-4} \pm 3.6 \times 10^{-6}$
1.20×10^{-1}	$3.42 \times 10^{-4} \pm 6.0 \times 10^{-6}$
1.60×10^{-1}	$4.22 \times 10^{-4} \pm 6.0 \times 10^{-6}$
2.00×10^{-1}	$4.99 \times 10^{-4} \pm 7.2 \times 10^{-6}$

$[GSNO] = 2.0 \times 10^{-3}$ mol dm^{-3}

$\lambda = 545$ nm

Table 4.24

$k_2 = 2.0 \times 10^{-3} \pm 1 \times 10^{-4}$ dm^3 mol^{-1} s^{-1}; $k' = 1.1 \times 10^{-4} \pm 2 \times 10^{-5}$ s^{-1}; $r^2 = 0.97$

- ## pH 7.3

$[H_2A]_{\tau}$ / mol dm^{-3}	[a] k_{obs} / s^{-1}	[b] k_{obs} / s^{-1}
2.00×10^{-2}	$3.42 \times 10^{-4} \pm 4.0 \times 10^{-6}$	-----
2.40×10^{-2}	-----	$4.49 \times 10^{-4} \pm 3.0 \times 10^{-6}$
4.00×10^{-2}	$6.83 \times 10^{-4} \pm 1.0 \times 10^{-5}$	-----
6.00×10^{-2}	-----	$9.30 \times 10^{-4} \pm 1.2 \times 10^{-5}$
8.00×10^{-2}	$1.27 \times 10^{-3} \pm 2.0 \times 10^{-5}$	$1.14 \times 10^{-3} \pm 1.5 \times 10^{-5}$
1.00×10^{-1}	$1.54 \times 10^{-3} \pm 2.0 \times 10^{-5}$	-----
1.20×10^{-1}	-----	$1.60 \times 10^{-3} \pm 2.4 \times 10^{-5}$
1.60×10^{-1}	$2.15 \times 10^{-3} \pm 2.0 \times 10^{-5}$	$2.03 \times 10^{-3} \pm 4.2 \times 10^{-5}$
2.00×10^{-1}	$2.85 \times 10^{-3} \pm 4.0 \times 10^{-5}$	$2.51 \times 10^{-3} \pm 4.4 \times 10^{-5}$

$[GSNO] = 2.0 \times 10^{-3}$ mol dm^{-3}

$\lambda = 545$ nm

[a] Gives $k_2 = 1.3 \times 10^{-2} \pm 1 \times 10^{-3}$ dm^3 mol^{-1} s^{-1}; $k' = 1.4 \times 10^{-4} \pm 7 \times 10^{-5}$ s^{-1}; $r^2 = 0.99$
[b] Gives $k_2 = 1.15 \times 10^{-2} \pm 3 \times 10^{-4}$ dm^3 mol^{-1} s^{-1}; $k' = 2.1 \times 10^{-4} \pm 4 \times 10^{-5}$ s^{-1}; $r^2 = 0.99$

Table 4.25

These data give an average value of $k_2 = 1.2 \times 10^{-2} \pm 1 \times 10^{-3}$ dm^3 mol^{-1} s^{-1}.

• pH 8.5

$[H_2A]_\tau$ / mol dm^{-3}	k_{obs} / s^{-1}
2.40×10^{-2}	$2.98 \times 10^{-3} \pm 1.0 \times 10^{-4}$
6.00×10^{-2}	$8.61 \times 10^{-3} \pm 2.2 \times 10^{-4}$
1.20×10^{-1}	$1.94 \times 10^{-2} \pm 7.8 \times 10^{-4}$
1.60×10^{-1}	$2.88 \times 10^{-2} \pm 7.0 \times 10^{-4}$
2.00×10^{-1}	$3.42 \times 10^{-2} \pm 1.4 \times 10^{-3}$

$[GSNO] = 2.0 \times 10^{-3}$ mol dm^{-3}

$\lambda = 545$ nm

Table 4.26

$k_2 = 1.8 \times 10^{-1} \pm 1 \times 10^{-2}$ dm^3 mol^{-1} s^{-1}; $r^2 = 0.99$.

• pH 9.7

$[H_2A]_\tau$ / mol dm^{-3}	k_{obs} / s^{-1}
2.50×10^{-2}	$2.67 \times 10^{-2} \pm 2.1 \times 10^{-3}$
5.00×10^{-2}	$4.98 \times 10^{-2} \pm 2.4 \times 10^{-3}$
1.00×10^{-1}	$9.20 \times 10^{-2} \pm 7.5 \times 10^{-3}$
1.60×10^{-1}	$1.56 \times 10^{-1} \pm 6.2 \times 10^{-3}$
2.00×10^{-1}	$2.15 \times 10^{-1} \pm 5.9 \times 10^{-3}$

$[GSNO] = 2.0 \times 10^{-3}$ mol dm^{-3}

$\lambda = 545$ nm

Table 4.27

$k_2 = 1.0 \pm 0.06$ dm^3 mol^{-1} s^{-1}; $r^2 = 0.99$.

In addition, a value of k_{obs} of 0.55 ± 0.02 s^{-1} was obtained for a solution containing 0.199 M ascorbic acid, at pH 10.1, giving a k_2 value of 2.81 ± 0.09 dm^3 mol^{-1} s^{-1}.

• pH 10.8

$[H_2A]_\tau$ / mol dm^{-3}	k_{obs} / s^{-1}
4.00×10^{-2}	0.21 ± 0.006
1.20×10^{-1}	0.64 ± 0.009
2.00×10^{-1}	1.7 ± 0.06

$[GSNO] = 2.0 \times 10^{-3}$ mol dm^{-3}

$\lambda = 545$ nm

Table 4.28

$k_2 = 9.8 \pm 0.2$ dm^3 mol^{-1} s^{-1}; $r^2 = 0.95$

- **pH 11.5**

$[H_2A]_\tau$ / mol dm^{-3}	k_{obs} / s^{-1}
4.04×10^{-2}	1.88 ± 0.10
1.22×10^{-1}	8.74 ± 0.20
2.07×10^{-1}	11.3 ± 0.50

$[GSNO] = 2.0 \times 10^{-3}$ mol dm^{-3}

$\lambda = 545$ nm

Table 4.29

$k_2 = 56 \pm 3$ dm^3 mol^{-1} s^{-1}; $r^2 = 0.93$.

- **pH 12.4**

$[H_2A]_\tau$ / mol dm^{-3}	k_{obs} / s^{-1}
3.00×10^{-2}	4.1 ± 0.13
4.10×10^{-2}	6.2 ± 0.32
8.20×10^{-2}	15 ± 0.44
1.20×10^{-1}	24 ± 3.0
2.00×10^{-1}	34 ± 4.0

$[GSNO] = 2.0 \times 10^{-3}$ mol dm^{-3}

$\lambda = 545$ nm

Table 4.30

$k_2 = 180 \pm 10$ dm^3 mol^{-1} s^{-1}; $r^2 = 0.98$.

- **pH 13.7**

$[H_2A]_\tau$ / mol dm^{-3}	k_{obs} / s^{-1}
4.04×10^{-2}	11.6 ± 0.4
1.26×10^{-1}	41 ± 8
1.98×10^{-1}	62 ± 6

$[GSNO] = 2.0 \times 10^{-3}$ mol dm^{-3}

$\lambda = 545$ nm

Table 4.31

$k_2 = 320 \pm 30$ dm^3 mol^{-1} s^{-1}; $r^2 = 0.99$.

Considering the possibility of nitrosothiol decomposition occurring *via* reaction with any of the three protomers of ascorbic acid, one can derive the expression for k_2 given in Equation 4.9. In this equation k_{H2A}, k_{HA-} and k_{A2-} are the second order rate constants for the reaction of the nitrosothiol with ascorbic acid, ascorbate monoanion and ascorbate dianion respectively. K_{a1} and K_{a2} are the two acid dissociation constants of ascorbic acid. The derivation is included in Appendix 5.

$$k_2 = \frac{k_{H2A}\left[H^+\right]^2 + k_{HA-}K_{a1}\left[H^+\right] + k_{A2-}K_{a1}K_{a2}}{K_{a1}K_{a2} + K_{a1}\left[H^+\right] + \left[H^+\right]^2} \qquad \text{Equation 4.9}$$

The data for GSNO decomposition were fitted to Equation 4.9 by a non – linear least squares method using the Scientist [1] package. Table 4.32 summarises the k_2 values obtained at each pH, and Figure 4.7 shows a plot of log (k_2 / dm^3 mol^{-1} s^{-1}) versus pH with the calculated line superimposed.

pH	k_2 / dm^3 mol^{-1} s^{-1}	log (k_2 / dm^3 mol^{-1} s^{-1}) experimental	log (k_2 / dm^3 mol^{-1} s^{-1}) calculated
3.60	$1.51 \times 10^{-4} \pm 5.4 \times 10^{-6}$	-3.8 ± 0.1	-3.94
4.60	$3.7 \times 10^{-4} \pm 4 \times 10^{-5}$	-3.4 ± 0.4	-3.35
5.60	$5.8 \times 10^{-4} \pm 4 \times 10^{-5}$	-3.2 ± 0.2	-3.13
6.50	$2.0 \times 10^{-3} \pm 1 \times 10^{-4}$	-2.7 ± 0.2	-2.75
7.30	$1.2 \times 10^{-2} \pm 1 \times 10^{-3}$	-1.9 ± 0.2	-2.12
8.50	$1.8 \times 10^{-1} \pm 1 \times 10^{-2}$	-0.74 ± 0.06	-0.89
9.70	1.02 ± 0.06	$8.6 \times 10^{-3} \pm 5 \times 10^{-4}$	0.260
10.1	2.8 ± 0.09	0.45 ± 0.01	0.690
10.8	9.8 ± 0.2	0.99 ± 0.02	1.36
11.5	56 ± 3	1.75 ± 0.09	1.91
12.4	180 ± 10	2.2 ± 0.2	2.25
13.7	320 ± 30	2.5 ± 0.2	2.35

Table 4.32 Summary of rate constants at various pH values for GSNO decomposition
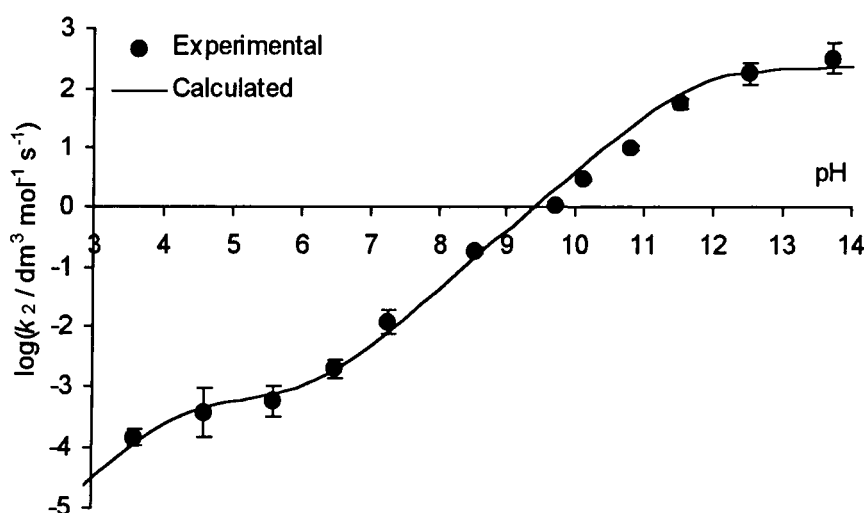
Figure 4.7 log (k_2 / dm^3 mol^{-1} s^{-1}) versus pH for GSNO decomposition

The parameter values obtained from the analysis were:

$k_{H2A} \approx 0$ dm^3 mol^{-1} s^{-1}

$k_{HA^-} = 6.3 \times 10^{-4} \pm 1.0 \times 10^{-5}$ dm^3 mol^{-1} s^{-1}

$k_{A2^-} = 220 \pm 20$ dm^3 mol^{-1} s^{-1}

The parameter values obtained indicate that only the ascorbate anions exhibit significant reactivity, and of these, the dianion is by far the more reactive. Smith *et al*[3] observed the same trend for the reaction between GSNO and ascorbic acid, however their values are not in good agreement with those reported here: k_{HA^-} = 5.23 × 10^{-3} dm^3 mol^{-1} s^{-1}, k_{A2^-} = 1220 dm^3 mol^{-1} s^{-1}. This apparent anomaly probably arises from the inadequate pH range employed in their study: pH 5 – 7.5, which yielded no data close to the pK_a values.

4.3.2 pH Dependence of *S* – Nitroso Cysteamine Decomposition

The k_2 values obtained at each pH for the copper independent decomposition of *S*-nitroso cysteamine by ascorbic acid are tabulated below. Table 4.33 lists the k_2 values calculated from one k_{obs} value.

pH	$[H_2A]_\tau$ / mol dm^{-3}	k_{obs} / s^{-1}	k_2 / dm^3 mol^{-1} s^{-1}
2.8	0.10	1.60×10^{-5}	1.60×10^{-4}
3.0	0.10	1.85×10^{-5}	1.85×10^{-4}
3.1	0.10	2.03×10^{-5}	2.03×10^{-4}
3.3	0.10	2.76×10^{-5}	2.76×10^{-4}
3.5	0.10	3.28×10^{-5}	3.28×10^{-4}
3.8	0.10	9.40×10^{-5}	9.40×10^{-4}
3.9	0.10	1.04×10^{-4}	1.04×10^{-3}
4.1	0.10	1.47×10^{-4}	1.47×10^{-3}
4.2	0.10	8.95×10^{-5}	8.95×10^{-4}
4.5	0.10	1.26×10^{-4}	1.26×10^{-3}
4.6	0.10	2.21×10^{-4}	2.21×10^{-3}
4.7	0.10	2.83×10^{-4}	2.83×10^{-3}
4.9	0.10	3.13×10^{-4}	3.13×10^{-3}
5.5	0.10	3.68×10^{-4}	3.68×10^{-3}
5.8	0.10	7.50×10^{-4}	7.50×10^{-3}

$$[S - \text{nitroso cysteamine}] = 2.0 \times 10^{-3} \text{ mol dm}^{-3}$$
$$\lambda = 545 \text{ nm}$$

Table 4.33 k_2 values for *S*-nitroso cysteamine decomposition at various pH values

The following tables contain the data obtained for the higher pH values, for which k_2 values were obtained by plotting k_{obs} versus $[H_2A]_\tau$.

- **pH 7.4**

$[H_2A]_\tau$ / mol dm^{-3}	k_{obs} / s^{-1}
8.00×10^{-3}	$1.79 \times 10^{-3} \pm 4.0 \times 10^{-5}$
1.00×10^{-2}	$2.02 \times 10^{-3} \pm 4.0 \times 10^{-5}$
2.00×10^{-2}	$3.74 \times 10^{-3} \pm 8.0 \times 10^{-5}$
5.00×10^{-2}	$7.78 \times 10^{-3} \pm 2.0 \times 10^{-4}$
1.00×10^{-1}	$1.25 \times 10^{-2} \pm 2.0 \times 10^{-4}$

$$[S\text{-nitroso cysteamine}] = 5.0 \times 10^{-4} \text{ mol dm}^{-3}$$
$$\lambda = 400 \text{ nm}$$

Table 4.34

$k_2 = 1.2 \times 10^{-1} \pm 1 \times 10^{-2}$ dm^3 mol^{-1} s^{-1}; $r^2 = 0.99$.

• pH 9.5

Data at this pH were obtained using the stopped flow technique, with k_{obs} values calculated as the mean of five determinations.

$[H_2A]_T$ / mol dm^{-3}	k_{obs} / s^{-1}
1.00×10^{-2}	$9.16 \times 10^{-3} \pm 5.7 \times 10^{-4}$
4.00×10^{-2}	$3.06 \times 10^{-2} \pm 3.6 \times 10^{-3}$
6.00×10^{-2}	$4.62 \times 10^{-2} \pm 3.4 \times 10^{-3}$
8.00×10^{-2}	$6.67 \times 10^{-2} \pm 5.5 \times 10^{-3}$
1.00×10^{-1}	$6.42 \times 10^{-2} \pm 6.0 \times 10^{-3}$

$[S\text{-nitroso cysteamine}] = 5.0 \times 10^{-4}$ mol dm^{-3}

$\lambda = 400$ nm

Table 4.35

$k_2 = 6.7 \times 10^{-1} \pm 9 \times 10^{-2}$ dm^3 mol^{-1} s^{-1}; r$^2 = 0.94$.

• pH 10.3

Data at this pH were obtained using the stopped flow technique, with k_{obs} values calculated as the mean of five determinations.

$[H_2A]_T$ / mol dm^{-3}	k_{obs} / s^{-1}
1.22×10^{-2}	$2.38 \times 10^{-2} \pm 2.6 \times 10^{-3}$
4.02×10^{-2}	$5.43 \times 10^{-2} \pm 3.7 \times 10^{-3}$
6.00×10^{-2}	$7.49 \times 10^{-2} \pm 6.2 \times 10^{-3}$
8.00×10^{-2}	$9.22 \times 10^{-2} \pm 4.2 \times 10^{-3}$
1.00×10^{-1}	$1.15 \times 10^{-1} \pm 5.7 \times 10^{-3}$

$[S\text{-nitroso cysteamine}] = 5.0 \times 10^{-4}$ mol dm^{-3}

$\lambda = 400$ nm

Table 4.36

$k_2 = 1.02 \pm 0.04$ dm^3 mol^{-1} s^{-1}; r$^2 = 0.98$.

Table 4.37 illustrates the change in k_2 with pH for the reaction between S-nitroso cysteamine and ascorbic acid.

pH	k_2 / dm^3 mol^{-1} s^{-1}
2.8	1.60×10^{-4}
3.0	1.85×10^{-4}
3.1	2.03×10^{-4}
3.3	2.76×10^{-4}
3.5	3.28×10^{-4}
3.8	9.40×10^{-4}
3.9	1.04×10^{-3}
4.1	1.47×10^{-3}
4.2	8.95×10^{-4}
4.5	1.26×10^{-3}
4.6	2.21×10^{-3}
4.7	2.83×10^{-3}
4.9	3.13×10^{-3}
5.5	3.68×10^{-3}
5.8	7.50×10^{-3}
7.4	1.17×10^{-1}
9.5	6.70×10^{-1}
10.3	1.02

Table 4.37 k_2 at each pH for S-nitroso cysteamine decomposition

Table 4.38 compares the k_2 values for S-nitroso cysteamine decomposition with those for GSNO decomposition over the pH range 4.5 – 10.3. The values in the table reveal that the relative reactivity of GSNO and S-nitroso cysteamine are reversed towards higher pH. The pK_a of the β - amino group on S-nitroso cysteamine is ~10, so over the region covered by the table the proportion of the protonated form of the nitrosothiol will be changing, decreasing towards higher pH. Given that there is no change in the nature of the GSNO over this pH range, it appears that the protonated form of S-nitroso cysteamine is the more reactive form.

pH	k_2 for GSNO / dm^3 mol^{-1} s^{-1}	k_2 for S-nitroso cysteamine / dm^3 mol^{-1} s^{-1}
4.5	3.74×10^{-4}	1.26×10^{-3}
5.5	5.83×10^{-4}	3.68×10^{-3}
7.3	1.24×10^{-2}	1.17×10^{-1}
9.7	1.02	6.70×10^{-1}
10.3	2.81	1.02

Table 4.38 Comparison of k_2 values for GSNO and S-nitroso cysteamine decomposition

Fitting the data for S-nitroso cysteamine decomposition to Equation 4.9 was not successful, probably because the protonated and neutral nitrosothiols have different

reactivities. Modelling the data is not realistically possible because of the number of unknowns. Even if it is assumed that the neutral form of the ascorbic acid doesn't react, there are still four rate constants to determine (for the reaction of the neutral nitrosothiol with HA^- and A^{2-} and the reaction of the protonated nitrosothiol with HA^- and A^{2-}), and the value of the pK_a for the nitrosothiol is not accurately known.

4.3.3 Summary of pH Dependence Studies

The pH dependence studies show that the rate of reaction of nitrosothiols with ascorbic acid increases with pH. The anionic forms of ascorbic acid are the reactive species, reaction through the neutral form being insignificant in comparison. The ascorbate dianion is much more reactive than the monoanion, to the extent that reaction *via* the dianion dominates at pH values well below the pK_a for its formation. These observations are similar to those reported for reactions of ascorbic acid with nitroso benzenes,[8] alkyl nitrites[5] and oral anticancer Pt^{IV} compounds.[6]

Evidence has also been obtained that suggests the protonated form of nitrosothiols possessing a β - amino group is the more reactive form. This implies that an electrostatic interaction between an ascorbate anion and the nitrosothiol might be important in the rate determining step.

4.4 Temperature Dependence Studies

Obtaining kinetic data for a range of temperatures enables the activation parameters to be determined. The relationship between the entropy ($\Delta S^{o\ddagger}$) and enthalpy ($\Delta H^{o\ddagger}$) of activation is formalised in the Eyring Equation, where k_T is the rate constant at temperature T, h is Planck's Constant, k_B is the Boltzmann Constant and R is the gas constant (Equation 4.10).

$$k_T = \frac{k_B T}{h} \exp\left(\frac{\Delta S^{o\ddagger}}{R}\right) \exp\left(-\frac{\Delta H^{o\ddagger}}{RT}\right) \qquad \text{Equation 4.10}$$

Manipulation of Equation 4.10 gives Equation 4.11, hence $\Delta S^{o\ddagger}$ and $\Delta H^{o\ddagger}$ may be obtained from a plot of $\ln(k_T h / k_B T)$ versus T^{-1}, which should be linear.

$$\ln\left(\frac{k_T h}{k_B T}\right) = \frac{\Delta S^{o\ddagger}}{R} - \frac{\Delta H^{o\ddagger}}{RT}$$
     Equation 4.11

- **Activation parameters for *S*-nitroso penicillamine decomposition**

The data obtained for the decomposition of *S*-nitroso penicillamine (5×10^{-4} M) by ascorbic acid (0.005 – 0.2 M) at pH 7.4 are given in Table 4.39. k_2 values were obtained in the same manner as those already reported.

$[H_2A]$ / mol dm^{-3}	k_{obs} / s^{-1}				
	T = 292 K	T = 298 K	T = 303 K	T = 308 K	T = 317 K
5×10^{-3}	3.64×10^{-3} $\pm 1.2 \times 10^{-4}$	7.48×10^{-3} $\pm 4.1 \times 10^{-4}$	1.07×10^{-2} $\pm 2.3 \times 10^{-4}$	1.52×10^{-2} $\pm 5.5 \times 10^{-4}$	5.89×10^{-2} $\pm 5.8 \times 10^{-3}$
1×10^{-2}	6.46×10^{-3} $\pm 2.9 \times 10^{-4}$	1.22×10^{-2} $\pm 2.7 \times 10^{-4}$	1.86×10^{-2} $\pm 4.9 \times 10^{-4}$	2.68×10^{-2} $\pm 4.6 \times 10^{-4}$	1.02×10^{-1} $\pm 5.3 \times 10^{-3}$
2×10^{-2}	1.03×10^{-2} $\pm 2.8 \times 10^{-4}$	1.91×10^{-2} $\pm 2.3 \times 10^{-4}$	3.03×10^{-2} $\pm 1.5 \times 10^{5}$	4.86×10^{-2} $\pm 9.0 \times 10^{-4}$	-----
k_2 / dm^3 mol^{-1} s^{-1}	4.2×10^{-1} $\pm$ 5×10^{-2}	7.6×10^{-1} $\pm$ 8×10^{-2}	1.33 $\pm 8 \times 10^{-2}$	2.30 $\pm 3 \times 10^{-2}$	4.2 $\pm 2 \times 10^{-1}$
$\ln(k_2 h / k_B T.\text{dm}^3$ mol$^{-1})$	-30.3 ± 0.1	-29.7 ± 0.1	-29.2 ± 0.1	-28.7 ± 0.01	-28.1 ± 0.1

Table 4.39 Data for the temperature dependence of *S*-nitroso penicillamine decomposition

The Eyring plot for the data in Table 4.39 is shown in Figure 4.8.
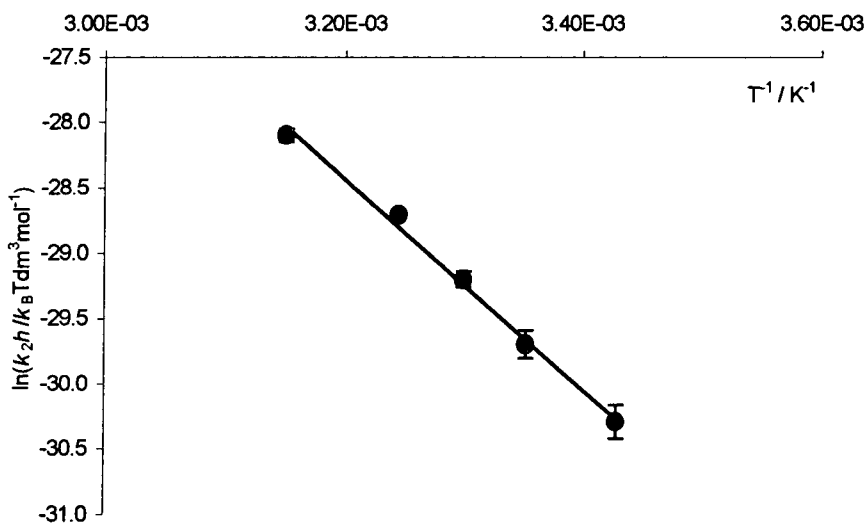
Figure 4.8 Eyring plot for data in Table 4.39

Linear regression on the data enables the activation parameters to be determined as

$\Delta S^{\circ\ddagger} = -21 \pm 9 \; J \; K^{-1} \; mol^{-1}$

$\Delta H^{\circ\ddagger} = 68\,000 \; J \; mol^{-1} = 68 \pm 4 \; kJ \; mol^{-1}$

- **Activation parameters for *S*-nitroso 1-amino-2-methyl-2-propanethiol decomposition**

Data for the reaction of ascorbic acid with *S*-nitroso 1-amino-2-methyl-2-propanethiol (5×10^{-4} M) at pH 7.4 are given in Table 4.40.

[H$_2$A] / mol dm^{-3}	k_{obs} / s^{-1}					
	T = 293 K	T = 299 K	T = 300 K	T = 309 K	T = 313 K	T = 319 K
5×10^{-3}	4.34×10^{-3} $\pm 1.9 \times 10^{-4}$	6.95×10^{-3} $\pm 1.0 \times 10^{-4}$	1.10×10^{-2} $\pm 5.7 \times 10^{-4}$	1.56×10^{-2} $\pm 1.2 \times 10^{-3}$	2.57×10^{-2} $\pm 5.0 \times 10^{-4}$	4.49×10^{-2} $\pm 3.5 \times 10^{-3}$
1×10^{-2}	7.13×10^{-3} $\pm 1.4 \times 10^{-4}$	1.21×10^{-2} $\pm 6.6 \times 10^{-4}$	1.61×10^{-2} $\pm 5.2 \times 10^{-4}$	2.59×10^{-2} $\pm 2.0 \times 10^{-3}$	4.05×10^{-2} $\pm 5.4 \times 10^{-4}$	6.36×10^{-2} $\pm 3.1 \times 10^{-3}$
2×10^{-2}	1.01×10^{-2} $\pm 8.3 \times 10^{-4}$	1.66×10^{-2} $\pm 4.5 \times 10^{-4}$	2.40×10^{-2} $\pm 8.2 \times 10^{-6}$	3.75×10^{-2} $\pm 2.5 \times 10^{-4}$	5.95×10^{-2} $\pm 1.3 \times 10^{-3}$	9.49×10^{-2} $\pm 8.8 \times 10^{-3}$
k_2 / dm^3 mol^{-1} s^{-1}	3.7×10^{-1} $\pm 7 \times 10^{-2}$	6×10^{-1} $\pm 1 \times 10^{-1}$	8.7×10^{-1} $\pm 6 \times 10^{-2}$	1.4 $\pm 2 \times 10^{-1}$	2.2 $\pm 2 \times 10^{-1}$	3.3 $\pm 2 \times 10^{-1}$
$\ln(k_2 h / k_B T.dm^3$ mol^{-1})	-30.4 ± 0.2	-30.0 ± 0.2	-29.6 ± 0.1	-29.1 ± 0.1	-28.7 ± 0.1	-28.3 ± 0.1

Table 4.40 Temperature dependence data for *S*-nitroso 1-amino-2-methyl-2-propanethiol decomposition

The Eyring plot in Figure 4.9 of the data in Table 4.40 is linear. The large errors require a regression analysis that applies more weighting to the points in which there is greater certainty (see Appendix 4).
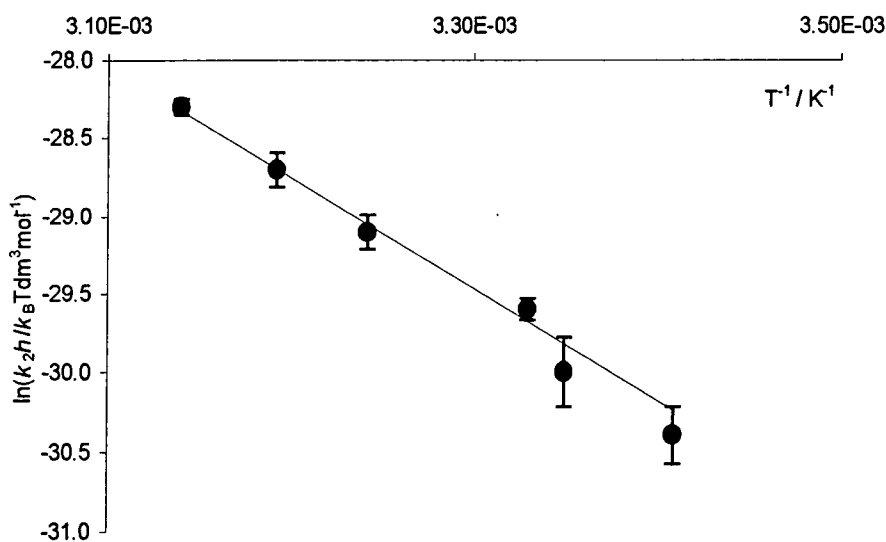
Figure 4.9 Eyring plot for data in Table 4.40

$\Delta S^{\circ\ddagger} = -50 \pm 9$ J K^{-1} mol^{-1}

$\Delta H^{\circ\ddagger} = 59\ 000$ J mol^{-1} = 59 $\pm$ 3 kJ mol^{-1}

- **Activation parameters for GSNO decomposition**

The decomposition of GSNO was studied over a range of temperatures at pH 12.3: the data obtained are in Table 4.41. Under these conditions, only reaction *via* the ascorbate dianion will be a significant contributor to the decomposition.

[H$_2$A] / mol dm^{-3}	k_{obs} / s^{-1}					
	T = 292 K	T = 298 K	T = 303 K	T = 308 K	T = 313 K	T = 318 K
1.0 × 10^{-2}	9.55 × 10^{-1} ± 5.2 × 10^{-3}	1.71 ± 5.8 × 10^{-3}	2.47 ± 1.2 × 10^{-2}	3.55 ± 1.1 × 10^{-1}	5.19 ± 1.4 × 10^{-2}	6.84 ± 1.1 × 10^{-1}
3.0 × 10^{-2}	3.03 ± 1.0 × 10^{-2}	5.07 ± 2.0 × 10^{-2}	7.99 ± 5.5 × 10^{-2}	11.4 ± 5.8 × 10^{-2}	16.5 ± 3.2 × 10^{-1}	22.3 ± 2.5 × 10^{-1}
4.5 × 10^{-2}	4.63 ± 9.2 × 10^{-2}	7.90 ± 1.4 × 10^{-1}	11.9 ± 5.8 × 10^{-2}	17.1 ± 2.1 × 10^{-1}	24.1 ± 1.2 × 10^{-1}	30.6 ± 3.5 × 10^{-1}
6.0 × 10^{-2}	6.24 ± 9.9 × 10^{-2}	10.8 ± 1.0 × 10^{-1}	15.9 ± 3.5 × 10^{-1}	21.8 ± 1.2 × 10^{-1}	31.6 ± 1.7 × 10^{-1}	42.2 ± 3.0 × 10^{-1}
k_2 / dm^3 mol^{-1} s^{-1}	135 ± 2	216 ± 9	302 ± 5	400 ± 20	570 ± 10	730 ± 3
ln(k_2h/k_BT.dm^3 mol^{-1})	-24.5 ± 0.03	-24.1 ± 0.1	-23.8 ± 0.03	-23.5 ± 0.07	-23.2 ± 0.05	-22.9 ± 0.09

Table 4.41 Temperature dependence data for GSNO decomposition

The associated Eyring plot is shown in Figure 4.10
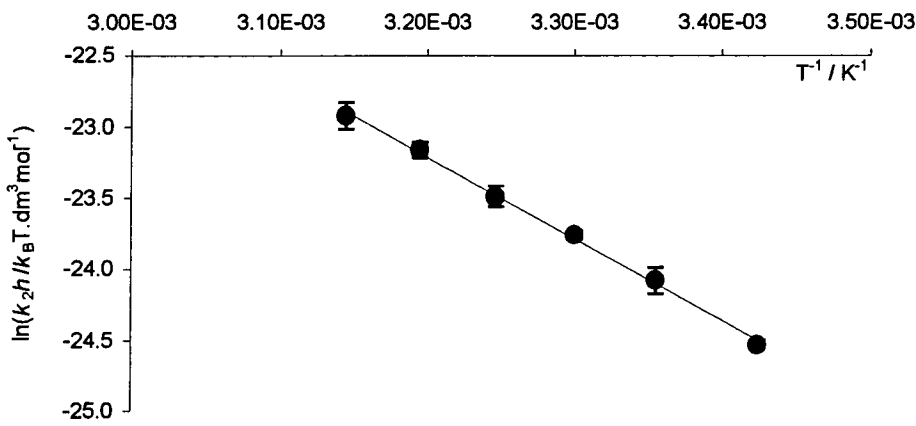
Figure 4.10 Eyring plot for GSNO decomposition

$\Delta S^{\circ\ddagger} = -41 \pm 7$ J K^{-1} mol^{-1}

$\Delta H^{\circ\ddagger} = 48\ 000$ J mol^{-1} = 48 $\pm$ 2 kJ mol^{-1}

4.4.1 Discussion of Activation Parameters

It must be recognised that the activation parameters determined for the decomposition of *S*-nitroso penicillamine and *S*-nitroso 1-amino-2-methyl-2-propanethiol are combinations of the activation parameters for the two reaction pathways: *via* HA^- and A^{2-}. Nevertheless, the expected similarity of the two routes assures that the values obtained are meaningful. The activation parameters obtained for GSNO decomposition will be representative of the reaction *via* A^{2-}.

The activation parameters obtained are consistent with an S_N2 reaction between ascorbate and the nitrosothiol. The entropies of activation are significantly negative, suggesting considerable ordering in the activated complex. The relatively low values of the activation enthalpies indicate that bond breaking and bond formation are probably highly concerted.

Measurements of the activation parameters for the copper independent reaction between ascorbic acid and GSNO reported by Smith and Dasgupta [3] agree that the reaction *via* HA^- has a significantly negative entropy of activation. However, the entropy of activation for the reaction *via* A^{2-} is reported to be significantly positive. Despite this, the mechanism proposed in the study is the same for reaction *via* both HA^- and A^{2-} and involves significant ordering in the activated complex. It is not clear why the entropies of activation should be of opposite sign for reaction *via* HA^- and A^{2-} and no explanation was advanced to account for this apparent anomaly.

Reactions between C – nitrosobenzenes and ascorbic acid, yielding dehydroascorbic acid and the hydroxylamine, also exhibit significantly negative entropies of activation and low enthalpies of activation.[8]

4.5 Proposed Mechanism and Conclusions

This section considers all of the results obtained for the copper independent reaction between nitrosothiols and ascorbic acid, including those presented in Chapter 3.

The rate equation and the results of the temperature dependence studies suggest that the rate – determining step is an S_N2 type process. Attack by ascorbate at the

nitroso nitrogen, expelling thiolate, in a concerted process, accounts for the rate law, activation parameter values and the observation of thiol as one of the products.

The reactivity order A^{2-} > HA^- > H_2A indicates the reactive centre on the ascorbic acid molecule to be oxygen, thus the other product of the nucleophilic substitution will be O-nitroso ascorbate. Homolytic cleavage of the $O - NO$ bond in O-nitroso ascorbate then results in the formation of nitric oxide and the ascorbyl radical.

Studies on the nitrosation of ascorbic acid have failed to observe O-nitroso ascorbate directly, the nitrosation products being dehydroascorbic acid and nitric oxide.[10,11] The spectrophotometric detection of O-nitrosoascorbate was claimed for the nitrosation of ascorbic acid at 70 °C and pH 5.5.[12] The analysis for this reaction was carried out by HPLC / UV spectrophotometry after thirty minutes, and given the rapidity with which NO is detected when ascorbic acid and nitrous acid react, it is unlikely that the O-nitroso species would remain after such time. The spectra were therefore probably assigned mistakenly, and are likely to be due to other products. The high temperature might also have caused side reactions. The reaction between ascorbic acid and alkyl nitrites also yields nitric oxide.[4] The formation of O – nitroso ascorbate is implied by these studies and provides a good explanation of the results.

In order to explain the kinetics observed in the nitrosothiol reactions, it is not a requirement for the decomposition of O-nitroso ascorbate to be faster than the initial nucleophilic attack, because the experiments measure the loss of nitrosothiol. However, the apparent instability of O-nitroso ascorbate suggests that its homolysis is rapid.

The fate of the ascorbyl radical is either disproportionation to ascorbic acid and dehydroascorbic acid, the ascorbic acid then reacting with the nitrosothiol, or direct reaction in a fast step with the nitrosothiol. Both of these situations result in an overall stoichiometry of two nitrosothiol molecules to one of ascorbic acid, as observed experimentally.

A mechanism can therefore be proposed to explain all of the experimental observations, and this is given in Scheme 4.1. Similar schemes have been suggested for the reactions of ascorbic acid with alkyl nitrites [4] and nitrosobenzenes.[8]

$$H_2A$$

$$\Big\updownarrow \begin{array}{l} K_{a1} \\ -H^+ \end{array}$$

$$HA^- + RSNO \xrightarrow{k_{HA^-}} RS^- + A\text{-}NO \longrightarrow A^{\cdot -} + NO + H^+$$

$$\Big\updownarrow \begin{array}{l} K_{a2} \\ -H^+ \end{array}$$

$$A^{2-} + RSNO \xrightarrow{k_{A^{2-}}} RS^- + {}^-A\text{-}NO \longrightarrow A^{\cdot -} + NO$$

$$2\, A^{\cdot -} \longrightarrow H_2A + DA$$

or

$$A^{\cdot -} + RSNO \xrightarrow{fast} RS^- + NO + DA$$

Overall: $2\,RSNO + H_2A \longrightarrow 2\,RSH + 2\,NO + DA$
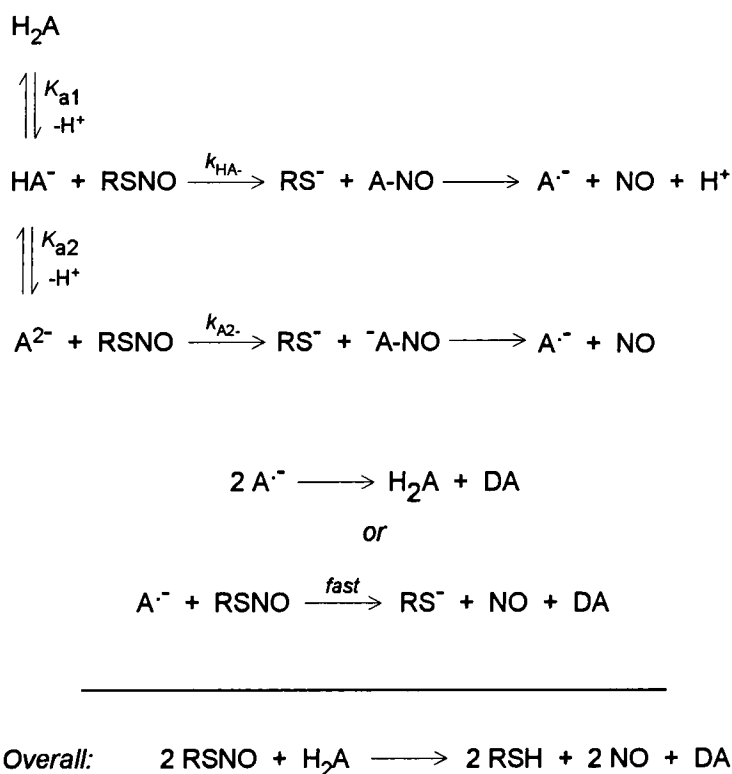
Scheme 4.1 Proposed mechanism for the copper independent decomposition of nitrosothiols by ascorbic acid

There are a number of feasible reasons why the ascorbate dianion is more reactive than the monoanion. The dianion has two O^- sites and therefore there is a statistical factor favouring reaction *via* the dianion. In the monoanion the negative charge is extensively delocalised, whereas in the dianion a more localised charge is present, leading to it possessing a greater nucleophilic character.

The high reactivity of nitrosothiols possessing a β - amino group might be explained by the ability of the dianion to form an ordered complex with the nitrosothiol in which the reactive sites on the two molecules are in close proximity (Figure 4.11). Interaction of this nature between the O^- and ammonium group in the reaction with the monoanion would place the reactive centres much farther apart. It is feasible that the activated complex for the reaction involving the dianion is structurally similar to the complex in Figure 4.11, giving rise to the negative entropy of activation. The formation of a similar complex was proposed for the reaction of ascorbic acid with nitrosobenzenes,[8] for which numerically large, negative values were obtained for the entropy of activation.

The greater reactivity of nitrosothiols possessing both *gem*-dimethyl groups and a *β*-amino group could also be explained in terms of the complex in Figure 4.11. Recent ^{15}N nmr and theoretical analyses have shown that the C-S-N=O *anti* conformation is preferred by nitrosothiols with tertiary *α*-carbons, whereas secondary and primary nitrosothiols favour the *syn* conformation.[13] The *anti* conformer, and therefore nitrosothiols with a statistical preference for this conformer, would be more reactive if a complex such as that in Figure 4.11 is involved.

$$R = CH(OH)CH_2OH$$
$$R' = \text{any group or } H$$
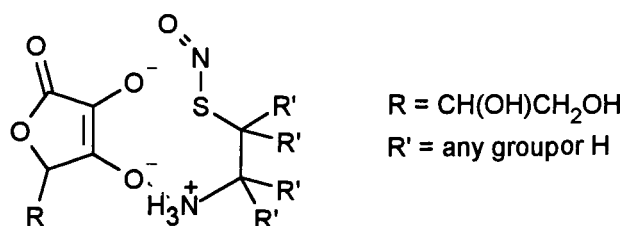
Figure 4.11 Possible complex between ascorbate dianion and *S*-nitroso cysteamine

An alternative mechanism for the decomposition of GSNO by ascorbic acid has been proposed,[3] which proceeds *via* formation of a complex between the nitrosothiol and ascorbate, followed by an outer sphere electron transfer from ascorbate to the nitrosothiol and the rapid dissociation of the resultant complex to products. During the reaction the $GSNO^{\bullet-}$ radical anion is formed, which theoretical studies have predicted to be very unstable with respect to S – N bond cleavage.[14]

The rate law for an electron transfer of this type is first order in [ascorbate] and [nitrosothiol], the second order rate constant being the product of the equilibrium constant for the complex formation and the rate constant for the electron transfer. The superior reducing capability of the ascorbate dianion and the necessity of forming a complex prior to electron transfer leads to the expectation that the dianion will be more reactive than the monoanion and that $\Delta S^{\ddagger}$ will be negative. This mechanism is therefore largely indistinguishable from that proposed in Scheme 4.1. The nucleophilic substitution mechanism in Scheme 4.1 does benefit from its similarity to the accepted mechanism for the nitrosation of ascorbic acid, and transnitrosation reactions in general.

In summary, the copper independent decomposition of nitrosothiols by ascorbate can be explained by rate limiting attack at the nitroso nitrogen by ascorbate, forming thiol and *O*-nitroso ascorbate, followed by homolytic cleavage of the O – NO bond, yielding nitric oxide and the ascorbyl radical. The mechanism in Scheme 4.1 explains fully the stoichiometry, products, kinetics, activation parameters and pH dependence of the reaction.

4.6 References

1. MicroMath® Scientist® for Windows®, Version 2.02

2. Microsoft® Excel 97

3. J. N. Smith and T. P. Dasgupta, *Nitric Oxide: Biol. Chem.*, **4** No. 1, 57 (2000)

4. J. R. Leis and A. Ríos, *J. Chem. Soc., Chem. Commun.*, 169 (1995)

5. J. R. Leis and A. Ríos, *J. Chem. Soc., Perkin Trans. 2*, 857 (1996)

6. K. Lemma, A. M. Sargeson and L. I. Elding, *J. Chem. Soc., Dalton Trans.*, 1167 (2000)

7. K. Wang, Y. Hou, W. Zhang, M. B. Ksebati, M. Xian, J.-P. Cheng and P. G. Wang, *Bioorg. Med. Chem. Lett.*, **9**, 2897 (1999)

8. S. Uršić, V. Vrček, D. Ljubas and I. Vinković, *New J. Chem.*, 221 (1998)

9. J. C. Miller and J. N. Miller, 'Statistics for Analytical Chemistry', 3rd Ed., Ellis Horwood, London, 1993

10. C. A. Bunton, H. Dahn and D. L. Loewe, *Nature*, **183**, 163 (1959)

11. B. D. Beake, R. B. Moodie and D. Smith, *J. Chem. Soc., Perkin Trans. 2*, 1251 (1995)

12. J. B. Fox Jr., R. N. Fiddler and A. E. Wasserman, *J. Food Prot.*, **44** No.1, 28 (1981)

13. M. D. Bartberger, K. N. Houk, S. C. Powell, J. D. Mannion, K. Y. Lo, J. S. Stamler and E. J. Toone, *J. Am. Chem. Soc.*, **122**, 5889 (2000).

14. N. Arulsamy, D. S. Bohle, J. A. Butt, G. J. Irvine, P. A. Jordan and E. Segan, *J. Am. Chem. Soc.*, **121**, 7115 (1999)

Conclusions Regarding the Role of Ascorbic Acid in *S*-Nitrosothiol Decomposition

Chapter 5　Conclusions Regarding the Role of Ascorbic Acid in
S-Nitrosothiol Decomposition

Chapters 3 and 4 presented the results obtained for the studies of S – nitrosothiol decomposition by ascorbic acid. Two pathways for decomposition were identified: the previously identified Cu^+ catalysed[1] route and a copper independent process.

Further studies in the copper reaction enabled the mechanism in Scheme 5.1 to be proposed. The products of the reaction are disulfide and nitric oxide. Only small quantities of ascorbate are required to promote the reaction because the thiolate produced in the second step can assume the reducing role for Cu^{2+}. Ascorbic acid could also be important in releasing and reducing copper from bound sources such as proteins to facilitate nitrosothiol decomposition: this effect was demonstrated for copper complexed by the disulfide of the tripeptide glutathione.

$$H_2A + 2\,Cu^{2+} \longrightarrow DA + 2\,Cu^+$$

$$Cu^+ + RSNO \longrightarrow RS^- + Cu^{2+} + NO$$

$$2\,RS^- + 2\,Cu^{2+} \longrightarrow RSSR + 2\,Cu^+$$
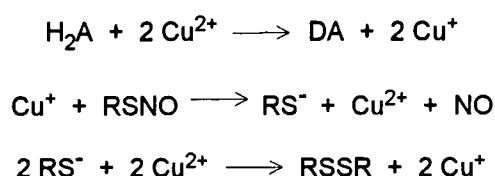
Scheme 5.1　Proposed mechanism for copper catalysed ascorbate promoted decomposition of S - nitrosothiols

The copper independent reaction was more extensively studied, having not been subject to rigorous study previously. Products of this reaction are thiolate and nitric oxide. The stoichiometry was found to be two RSNO: one ascorbic acid. The rate law for the decomposition is first order both in ascorbic acid and the nitrosothiol, the reactive ascorbic acid species being the dianion and, to a much smaller extent the monoanion. Activation parameter analysis suggested a high degree of ordering in the activated complex. Some structure – reactivity factors were identified. The mechanism proposed for this reaction is given in Scheme 5.2.

$$H_2A$$

$$\Updownarrow \; K_{a1}, -H^+$$

$$HA^- + RSNO \xrightarrow{k_{HA^-}} RS^- + A\text{-}NO \longrightarrow A^{\cdot -} + NO + H^+$$

$$\Updownarrow \; K_{a2}, -H^+$$

$$A^{2-} + RSNO \xrightarrow{k_{A2^-}} RS^- + {}^-A\text{-}NO \longrightarrow A^{\cdot -} + NO$$

$$2\,A^{\cdot -} \longrightarrow H_2A + DA$$

or

$$A^{\cdot -} + RSNO \xrightarrow{fast} RS^- + NO + DA$$

Overall: $2\,RSNO + H_2A \longrightarrow 2\,RSH + 2\,NO + DA$
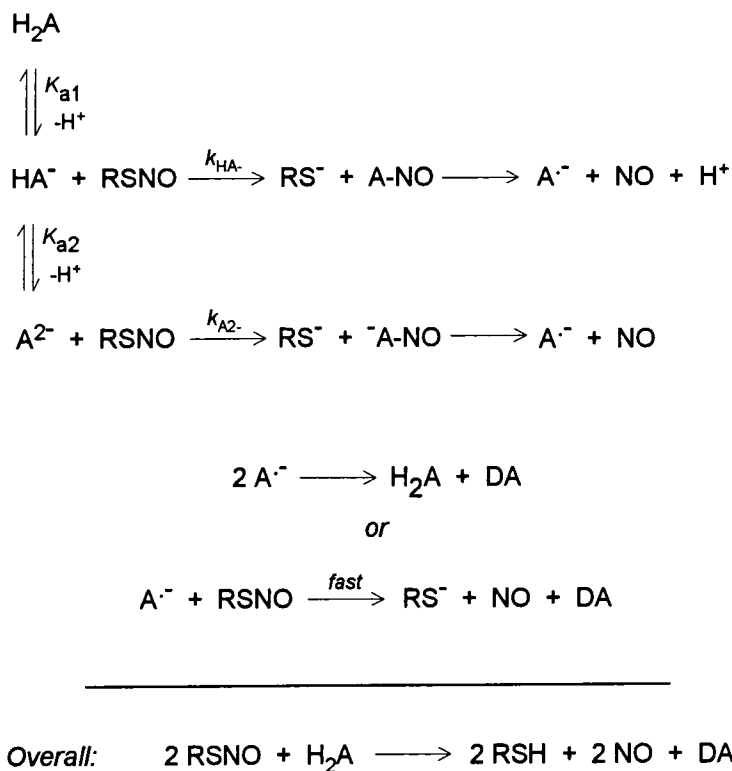
Scheme 5.2 Proposed mechanism for the copper independent reaction between ascorbic acid and S – nitrosothiols

The decomposition of nitrosothiols by ascorbic acid has now been well characterised and similarities between the copper independent pathway and reactions of other compounds with ascorbic acid are observed. Examples of similar reactions include reactions with alkyl nitrites[2], C-nitrosobenzenes [3] and anticancer compounds.[4]

There is also a wider picture to consider, namely the possible physiological importance of ascorbic acid mediated nitrosothiol decomposition. Ascorbic acid could be directly involved in nitric oxide production by promoting the decomposition of nitroso species. Indirect factors might also be relevant in the role of ascorbic acid in physiological processes involving nitric oxide: these are briefly discussed later.

In principle, both the copper dependent and copper independent pathways could occur *in vivo*. The dominant pathway will of course depend upon the prevailing conditions, with factors such as copper availability, ascorbic acid concentration and the structure of the nitrosothiol being important.

Section 3.2.1 shows that, under the conditions of study, the copper pathway predominated for S – nitroso – N – acetyl penicillamine decomposition. However, *in vivo* there is very little free copper,[5] and although nitrosothiols are decomposed by bound copper sources such as the tripeptide Gly – Gly – His and the protein human serum albumin (HSA), the reactions are slower than in the presence of free copper.[5] Both the copper dependent and independent pathways lead to nitric oxide production, so competing reactions of perhaps more relevance are those not yielding nitric oxide.

The second order rate constants observed for nitrosothiol decomposition *via* the copper independent pathway are in general quite small, though when compared with reactions of nitrosothiols with amines [6] and thiols,[7,8,9] also present *in vivo*, could be significant (Table 5.1). The reactions between nitrosothiols and sulfur centred nucleophiles such as sulfide and sulfite have also been studied,[10] and values for the reactions with sulfite are included in Table 5.1 for comparison.

Nitrosothiol	Reaction of nitrosothiol with parent thiol [7] $^a k_2$ / dm^3 mol^{-1} s^{-1}	Reaction with selected N nucleophiles [6] $^b k_2'$ / dm^3 mol^{-1} s^{-1}	Reaction with sulfite [10] $^c k_2'$ / dm^3 mol^{-1} s^{-1}	Reaction with ascorbic acid $^d k_2$ / dm^3 mol^{-1} s^{-1}
S – nitroso penicillamine	0.262	Pyrrolidine 9×10^{-7} Piperidine 3×10^{-7} Morpholine 3×10^{-5} Ethylamine 3×10^{-7} Trimethylamine 1×10^{-6} Azide 1×10^{-2}	376	1.40
S – nitroso cysteine	1.07×10^{-2}	---	468	0.254
S – nitroso glutathione	5.5×10^{-3}	---	96	2.02×10^{-2}

^{a} k_2 in rate $= k_2[\text{RSNO}][\text{RSH}]_\tau$ at pH 7.4, 25 °C

^{b} k_2' calculated for reaction at pH 7.4 from $k_2' = k_2 K_a/(K_a + [\text{H}^+])$ when rate $= k_2[\text{RSNO}][\text{amine free base}]$, 25 °C

^{c} k_2' calculated for reaction at pH 7.4 from $k_2' = k_2 K_a/(K_a + [\text{H}^+])$ when rate $= k_2[\text{RSNO}][\text{SO}_3]$, 25 °C

^{d} k_2 in rate $= k_2[\text{RSNO}][\text{ascorbic acid}]_\tau$ at pH 7.4, 25 °C

Table 5.1 Comparison of nitrosothiol reactions with nucleophiles

Reaction with the same thiol from which the nitrosothiol is derived gives predominantly ammonia[7] whereas reaction with other thiols leads to rapid transnitrosation [8,9] (typical second order rate constants $\sim 10^2$ to 10^3 dm^3 mol^{-1} s^{-1}). In the latter case, the stability of the nitrosothiol produced will govern the outcome. Thiols can of course act as reducing agents in the copper dependent decomposition pathway.[11] The reaction with primary amines produces diazonium ions, and with secondary and tertiary amines, nitrosoamines.

The extent to which ascorbic acid is involved in physiological processes that are dependent upon nitric oxide remains to be established. Few studies regarding the effect of ascorbic acid upon nitric oxide dependent processes have considered the possibility of nitric oxide production by reaction with nitrosothiols.

An example of a study that did consider this possibility involved monitoring the effects upon dog arterial blood pressure of co-administering GSNO and ascorbic acid.[12] The administration of the nitrosothiol was found to lead to a decrease in arterial blood pressure, attributed to vasodilation induced by nitric oxide, the effect being prolonged when ascorbic acid was co-administered. The possibility of nitric oxide release from the nitrosothiol by ascorbic acid was proposed as one possible explanation for the observations.

Research has revealed that nitric oxide formation is enhanced by ascorbic acid in activated macrophages [13] and endothelial cells.[14] In the case of macrophages the enhancement was attributed to ascorbic acid increasing the availability of the inducible nitric oxide synthase enzyme. The results of the endothelial study were interpreted in terms of the protection of nitric oxide by scavenging of superoxide by the ascorbic acid. Neither study considered the possibility that nitrosothiols might be involved.

Ascorbic acid enhances endothelial dependent vasodilation.[14] Once again, these results were attributed to protection of nitric oxide from superoxide by the ascorbic acid. Hypertension (high blood pressure) has been treated by ascorbic acid in clinical trials, though the efficacy [15] and mechanism [16] are subject to debate and more trials are necessary before any conclusions can be drawn.

In summary, the results of Chapters 3 and 4 have demonstrated that there is a role for ascorbic acid in nitrosothiol decomposition, and this might have biological implications.

5.1 References

1. A. P. Dicks, H. R. Swift, D. L. H. Williams, A. R. Butler, H. H. Al-Sa'doni and B. G. Cox, *J. Chem. Soc., Perkin Trans. 2*, 481 (1996)

2. J. R. Leis and A. Ríos, *J. Chem Soc., Chem. Commun.*, 169 (1995)

3. S. Uršić, V. Vrček, D. Ljubas and I. Vinkovuić, *New J. Chem.*, 221 (1998)

4. K. Lemma, A. M. Sargeson and L. I. Elding, *J. Chem. Soc., Dalton Trans.*, 1167 (2000)

5. A. P. Dicks and D. L. H. Williams, *Chem. Biol.*, **3**, 655 (1996)

6. A. P. Munro and D. L. H. Williams, *J. Chem. Soc., Perkin Trans. 2*, 1989 (1999)

7. A. P. Dicks, E. Li, A. P. Munro, H. R. Swift and D. L. H. Williams, *Can. J. Chem.*, **76**, 789 (1998)

8. D. J. Barnett, J. McAninly and D. L. H. Williams, *J. Chem. Soc., Perkin Trans. 2*, 1131 (1994)

9. D. J. Barnett, A. Ríos and D. L. H. Williams, *J. Chem. Soc., Perkin Trans. 2*, 1279 (1995)

10. A. P. Munro and D. L. H. Williams, *J. Chem. Soc., Perkin Trans. 2*, 1794 (2000).

11. A. P. Dicks, P. H. Beloso and D. L. H. Williams, *J. Chem. Soc., Perkin Trans. 2*, 1429 (1997)

12. D. McGowder, D. Ragoobirsingh and T. Dasgupta, *Nitric Oxide: Biol. Chem.*, **3**, No.6, 481 (1999)

13. A. Mizutani, H. Maki, Y. Torii, K. Hitomi and N. Tsukagoshi, *Nitric Oxide Biol. Chem.*, **2**, No. 4, 235 (1998)

14. R. Heller, F. Münscher-Paulig, R. Gräbner and U. Till, *J. Biol. Chem.*, **274**, No. 12, 8254 (1999)

15. A. Ness and J. Sterne, *Lancet*, **355**, 1271 (2000)

16. S. J. Duffy, N. Gokce, M. Holbrook, A. Huang, B. Frei, J. F. Keaney Jr., J. A. Vita, *Lancet*, **354**, 2048 (1999)

Experimental

CHAPTER 6

Chapter 6 Experimental

Experimental details specific to the work in Chapters 3 and 4 are contained in this Chapter. General information regarding the equipment and instrumentation used can be found in Appendix 3.

6.1 Materials

Chemicals were obtained from Sigma-Aldrich, BDH or Lancaster in the highest grade available and were used without further purification. Standard laboratory distilled water was used for all solutions prepared in an aqueous medium. No attempt was made to quantify the levels of contaminants, including copper ions, in the water. HPLC grade solvents were used for chromatography; all other solvents were reagent grade.

6.2 Preparation of Solutions

- **Nitrosothiol solutions**

Nitrosothiol solutions were freshly prepared for each experiment, nitrosating the thiol in a volumetric flask using acidified sodium nitrite, according to the following procedure. The required volume of 0.50 M perchloric acid was placed in the flask and the flask placed in an ice bath. The thiol was then dissolved in the acid. The necessary quantity of sodium nitrite was dissolved in water and added drop-wise to the acidified thiol solution. Usually a two – fold excess of nitrite over the thiol concentration was used to reduce the amount of thiol remaining after nitrosation. The volume was then made up to the line with distilled water. The nitrosothiol solution was protected from light and kept in ice to prevent decomposition. Ten minutes were allowed to elapse before using the solution to ensure the reaction had finished. The final pH of the nitrosothiol solutions was 1 – 2, and the nitrosothiol concentration typically 0.025 M.

• Ascorbic acid solutions

Ascorbic acid solutions were prepared last and were used immediately. The ascorbic acid was weighed, transferred into a suitable foil-covered flask with a tight fitting stopper and small headspace (to minimise decomposition of the ascorbic acid by photolysis / oxidation), and dissolved in water. EDTA was then added to complex metal ions (final concentration $\approx 1 \times 10^{-4}$ M), except when studying the copper dependent reaction when no EDTA was used. Sodium hydroxide solution was then added drop-wise to raise the pH to the required value for the experiment, the pH being measured using a 5 mm diameter electrode that could be washed clean into the solution. This was necessary to ensure the buffer capacity was not exceeded. The solution was then made to the required volume using distilled water.

• Ellman's reagent

Ellman's reagent, 5,5'-dithiobis(2-nitrobenzoic acid), was prepared as a 1.25×10^{-2} M stock solution, using methanol as the solvent.

• EDTA

Stock solutions of ethylenediamineteraacetic acid, EDTA, 2.50×10^{-2} M, were prepared in distilled water. Brief sonication was required to fully dissolve the solid.

6.3 Sample Preparation

• UV / visible spectrophotometric studies

Samples were prepared in stoppered 1 cm pathlength quartz cells, the order of addition being:

a) Copper dependent studies – buffer, water, $CuSO_4$ solution, then thermostatted, then nitrosothiol solution and ascorbic acid solution in quick succession to start the reaction.

b) Copper independent studies – buffer, water, EDTA solution, ascorbic acid solution, then thermostatted, then nitrosothiol solution to start the reaction.

The solutions were kept in the spectrophotometer cell compartment for ten minutes prior to adding the final reagents, to allow thermal equilibrium to be established. Throughout the observation time, the samples were maintained at the required temperature using a circulating water system or an electrical heating/cooling system.

- **Stopped-flow**

The reagents were present in two syringes, separating the nitrosothiol from the other reactants. The syringe compositions were:

Syringe A – water or buffer, EDTA, ascorbic acid

Syringe B – water or buffer, EDTA, nitrosothiol.

The solutions were transferred from the syringes into the sealed solution reservoirs of the stopped-flow apparatus, where they were allowed to reach thermal equilibrium before mixing, the temperature being maintained by means of a circulating water system.

The solutions were studied in a randomised order by selecting the solution number using the random number function of a calculator, or by Dr. (then Miss) Kathryn Brown picking the numbers 'from a hat'. In the case of the temperature dependence studies, the time taken to heat the water system and apparatus cell-block to the required temperatures prevented the use of this system, and the samples were studied in order of increasing temperature.

- **Nitric oxide detection**

Samples were prepared in a two-necked vessel surrounded by a circulating-water jacket, enabling the samples to be maintained at constant temperature. Rapid stirring was provided by means of a magnetic stirrer and follower. The main, vertical, neck was sealed with the rubber stopper supplied with the electrode, through which the electrode was passed. The small, angled, neck was sealed with a rubber septum through which passed the purging-gas inlet and outlet needles. A schematic of the apparatus is included in Appendix 3.

Buffer, water, EDTA (when required), and other reagents excluding the nitrosothiol, were added to the vessel and the vessel sealed (typical final volume $25 - 30$ cm^3).

The electrode was lowered into the vessel such that the tip was 5 mm below the surface of the solution. The solution was purged with high purity nitrogen for 15 minutes, the gas stream being pre-saturated with buffer to reduce mass transfer from the vessel. The purging stream was then switched off and the electrode zeroed and data collection initiated. The final reactant was then injected under the surface of the solution.

Calibration of the electrode was carried out daily using one of the methods outlined in Appendix 3.

6.4 pH Dependence Studies

The pH dependence studies were carried out using both conventional UV / visible spectrophotometry and the stopped-flow technique. The pH of each solution was measured in the cell or, for stopped-flow work, measured on a sample taken from the waste outlet.

When the stopped-flow technique was used, the buffer was generally present in the syringe containing the nitrosothiol. However, for the most basic solutions (pH higher than *ca.* 11), the buffer was present with the ascorbic acid solution because of the instability of the nitrosothiols at these pH values.

For the experiments using conventional UV / visible spectrophotometry the cells were prepared as outlined in Section 6.3.

6.5 Temperature Dependence Studies

Temperature dependence studies were carried out using the stopped-flow technique, the temperature measurements being provided by a thermometer incorporated into the stopped-flow cell. Temperatures > 50 °C were inaccessible, being beyond the upper limit of the thermometer.

The sample solutions were present in syringes as outlined in Section 6.3.

6.6 HPLC Experiments

Solvents were de-gassed before use, by filtration through nylon filters (0.45 μm maximum pore size) under reduced pressure. The eluent was pumped through the column at 0.70 cm^3 min^{-1} until a stable baseline was achieved. The flow was then maintained continuously until the experiments were complete. The sample injection was synchronised with the start of data collection by means of the interfaced computer system. The column was washed through with water, followed by methanol, after use.

6.7 Ionic Strength

The absence of significant curvature in plots of k_{obs} versus [H$_2$A] suggests that the variation in ionic strength does not have a significant effect on values of k_{obs} over the concentration range studied, therefore no attempt was made to maintain the ionic strength at a constant value.

Nitrosation of Thiol Derivatives of Nitrogen Heterocycles

Chapter 7 Nitrosation of Thiol Derivatives of Nitrogen Heterocycles

7.1 Introduction

The results of studies carried out into the nitrosation of heterocyclic thiols are discussed in Chapters 7 and 8. Aspects of the chemistry and physical properties of these compounds are introduced below.

7.1.1 Tautomerism in Heterocyclic Thiols

Heterocyclic compounds such as amino-, hydroxy- and thio- pyridines, pyrimidines and imidazoles can exhibit tautomerism. An example is given in Figure 7.1, which shows the tautomerism of 4-thiopyridine.
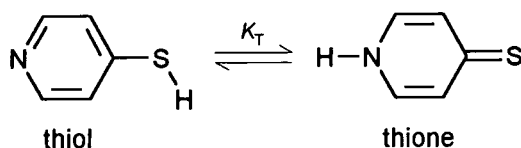
Figure 7.1 Tautomerism of 4-thiopyridine

There have been many studies into tautomerism in heterocyclic thiols, particularly in aqueous solution when the thione form is favoured.[1,2,3,4] For thiones such as 2-thiopyridine, 4-thiopyridine and 2-thiopyrimidine, the preference for the thione form is very large, resulting in the thiol form being undetectable.[1,2]

Several different methods have been employed for establishing the preferred tautomer of heterocyclic compounds. One of the most widely used methods in solution is to compare the UV / visible spectra of methyl derivatives with those of the non-derivatised compounds. For example, for 4-thiopyridine the N-methyl and S-methyl derivatives would be compared with 4-thiopyridine. Adopting the assumption that substitution of the hydrogen by a methyl group leaves the spectrum unchanged, the position of the hydrogen, i.e. whether it resides principally on the nitrogen or on the sulfur, can be established.

Measuring the basicity of thiol-containing heterocycles has also been used to establish the preferred tautomer in aqueous solution.[1] The presence of a hydrogen atom on the ring nitrogen reduces the basicity of the compounds. Thus, the observation that thiopyridines are 0.7 to 3 pK_a units less basic than the

corresponding hydroxy compounds, which are known to exist to a considerable extent in the pyridone tautomer, demonstrates that the thione form is the preferred conformer for the thiopyridines.[2] The preference for the thione over the thiol form is greater than the preference for the pyridone form over the hydroxy form in the corresponding oxygen compounds (Table 7.1).

Compound	K_T
2-thiopyridine	49 000
2-hydroxypyridine	340
4-thiopyridine	35 000
4-hydroxypiridine	2 200

Table 7.1 K_T values for some tautomeric pyridine derivatives in water[2]

[15]N nmr techniques have also been applied to the study of tautomerism in thiopyridines.[5] Infra-red, Raman and photoelectron spectroscopy have been utilised in the gas phase, and in the solid state X-ray data have proved useful. Studies on the solid state structures of thiopyridines revealed that the thione form is favoured; whereas in the gas phase the thiol form dominates.[6,7] Crystals of compounds such as 4-thiopyridine consist of chains of thione tautomers as shown in Figure 7.2.[8]
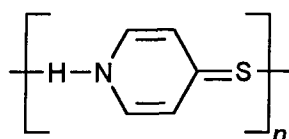
Figure 7.2 Solid state aggregation of 4-thiopyridine

Aggregation of the thione tautomers to form dimers, and in some cases oligomers, has been observed for thiopyridines in aqueous solution.[8,9,10] Heating and dilution of the solutions breaks up the aggregates.[9]

Molecular environment effects have been shown to be very important in thio-heterocycle tautomerism.[6,10] Decreasing the solvent polarity results in the preference for the thione form being reduced, or in some cases replaced by a preference for the thiol form.[9]

The greater preference for the thione in polar solvents has been attributed to the higher dipole moment of the thione relative to the thiol form.[11] Quantitative

models to describe the relationship between the preferred tautomer and solvent polarity have been developed.[11,12,13]

For 3-thiopyridine, for which no thione tautomer is possible, it has been shown that the proton is still present on the nitrogen in aqueous solution: this compound therefore exists as a Zwitterion.[1] The same is true to a lesser extent for the corresponding hydroxy compound.[2]

7.1.2 Nitrosation

Relatively few studies have been made on the nitrosation of thione compounds. The nitrosation of thiourea and its derivatives,[14,15,16,17,18] and the nitrosation of 2-thiopyridine [19] have been examined. The formation of disulfides in the reaction of thiopyrimidines with nitrous acid has also been reported.[20]

The nitrosation of thiourea was introduced in Chapter 1. Nitrosation is observed both at the nitrogen sites and at the sulfur site. Reaction at sulfur results in the formation of a deep yellow compound, which decomposes rapidly to form the disulfide dication C,C'-dithiodiformamidinium.[15]

Equilibrium constants for the formation of =SNO$^+$ derivatives of thioureas have been obtained (K=[SNO$^+$]/[H$^+$][S][HNO$_2$]).[18] The values are generally large, for example: thiourea, 5 000 dm^6 mol^{-2}; N,N'-dimethyl thiourea, 9 400 dm^6 mol^{-2}. The equilibria are acid dependent and therefore not directly comparable to those obtained for thiol S-nitrosation.

The nitrosation of 2-thiopyridine is readily achieved,[19] forming the =SNO$^+$ cation. This species decays under acidic conditions to the corresponding disulfide. Raising the pH indicated that the nitroso species was deprotonated, forming the aromatic – SNO compound, which then undergoes hydrolysis, re-forming the thione.

The equilibrium constant for the S-nitroso species formation from 2-thiopyridine is around 1×10^5 dm^6 mol^{-2}. The nitrosation proceeds at rates approaching the diffusion limit, and is markedly catalysed by chloride and bromide. As expected, the large equilibrium constant for the nitrosation of 2-thiopyridine makes the thione an excellent nitrosation catalyst.

7.1.3 Aims

The aim of the work presented in this Chapter is to expand the range of tautomeric sulfur compounds for which nitrosation reactions have been studied. Nitrosation reactions are reported here for the substrates 4-thiopyridine (4-TP), 2-thiopyrimidine (2-TPM) and 2-thioimidazole (2-TI). The structures of these compounds are given in Figure 7.3, and are shown as the thione tautomers, which are the predominant forms in aqueous solution. It was intended that 3-thiopyridine (3-TP) would also be studied because the absence of tautomerism in this compound would provide interesting comparisons. However, attempts to synthesise this substrate were unsuccessful.
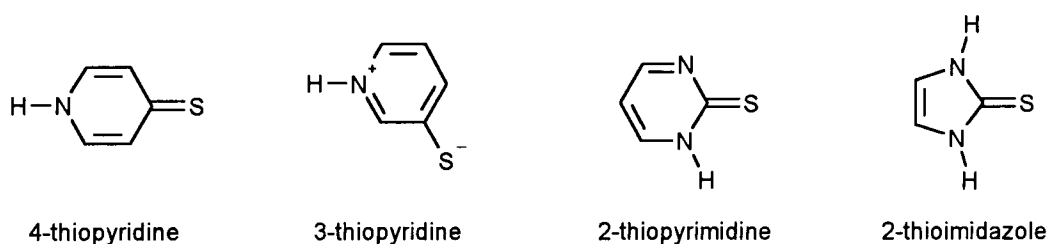

Figure 7.3 Structures of the nitrosation substrates

The nitrosation reactions studied are of particular interest because the compounds are good models for similar biologically relevant compounds, such as ergothioneine (Figure 7.4) and thiopurines.
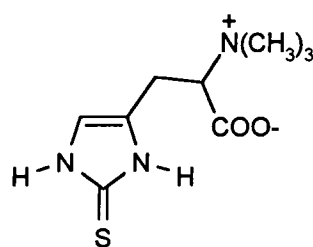
Figure 7.4 Ergothioneine

All of the work presented in this chapter was carried out at 25 °C.

7.2 Thione Spectra and Stability

7.2.1 2-Thioimidazole

The UV / visible spectra of 2-thioimidazole (4×10^{-5} M) were obtained in 0.1 M perchloric acid, water, and 0.1 M sodium hydroxide: these are shown in Figure 7.5.
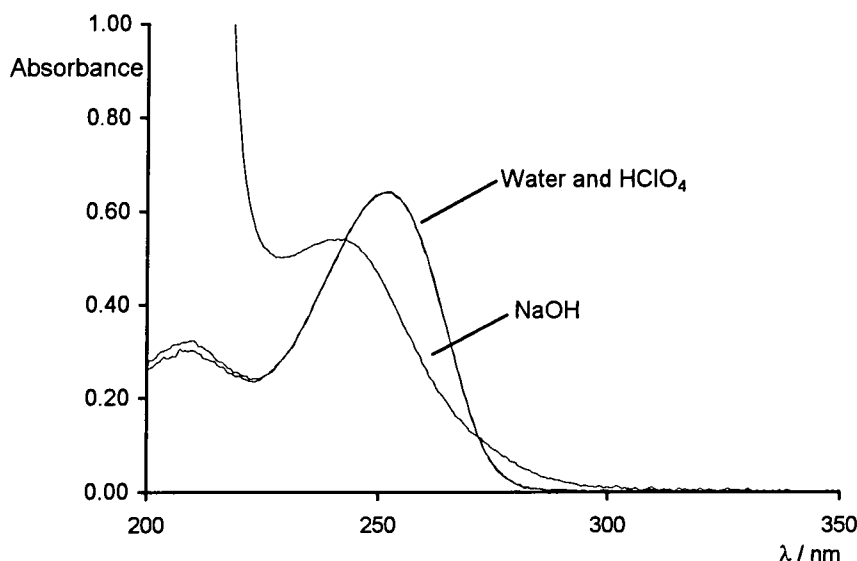
Figure 7.5 UV / visible spectra of 2-thioimidazole

The spectrum in sodium hydroxide is different from that in water and perchloric acid. This indicates the deprotonation occurs in sodium hydroxide, forming the species in Figure 7.6. The pK_a for this process is 11.6 at 21 °C; protonation of 2-thioimidazole has a pK_a value of -1.6 at 21 °C.[21] The low value of the pK_a for protonation probably arises from the nitrogen atoms being *sp2* hybridised with the lone pairs contributing to stabilisation of the molecule by giving the ring aromatic character (six π-electrons).
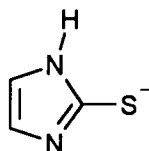
Figure 7.6 2-thioimidazole anion

Data obtained to determine the extinction coefficients of the neutral species, λ_{max} 209 and 252 nm, and the deprotonated species, λ_{max} 242 nm, are in Table 7.2.

153

[2-TI] / mol dm^{-3}	Abs in water		Abs in NaOH
	λ = 209 nm	λ = 252 nm	λ = 242 nm
1.00×10^{-5}	0.067	0.144	0.181
2.00×10^{-5}	0.119	0.284	0.310
4.00×10^{-5}	0.259	0.582	0.550
6.00×10^{-5}	0.410	0.868	0.758
8.00×10^{-5}	0.574	1.17	0.979
1.00×10^{-4}	0.775	1.44	1.21

Table 7.2 Data for 2-TI extinction coefficient determination

Plots of absorbance versus [2-TI] were linear, enabling the extinction coefficients to be determined (Figure 7.7). For the data obtained in sodium hydroxide a small non-zero intercept was obtained. Linear regression analysis using Excel [22] gives

Neutral 2-TI: ε_{209nm} = 7 810 $\pm$ 600 dm^3 mol^{-1} cm^{-1}

ε_{252nm} = 14 500 $\pm$ 150 dm^3 mol^{-1} cm^{-1}

2-TI anion: ε_{242nm} = 11 300 $\pm$ 290 dm^3 mol^{-1} cm^{-1}
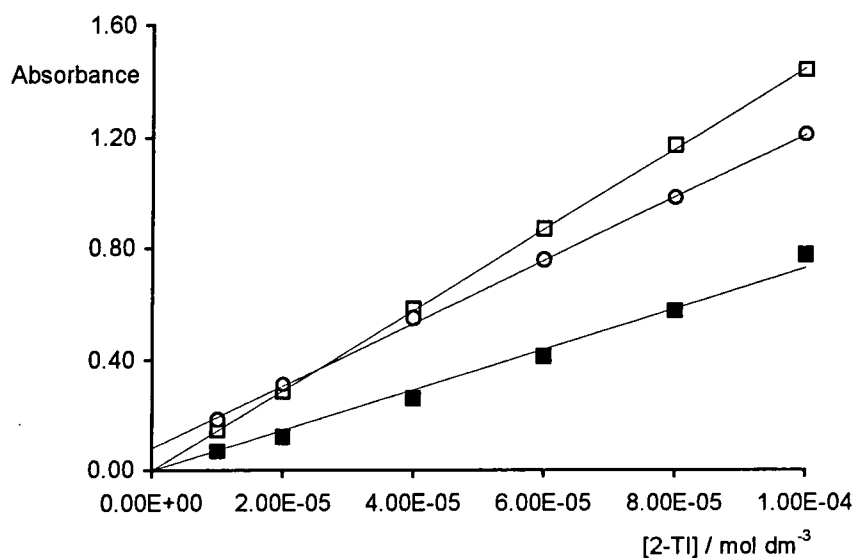
Figure 7.7 Plots of abs versus [2-TI]. ■ = water, 209 nm; □ = water, 252 nm; o = NaOH, 242nm

Repeat scan spectra obtained for samples of 2-thioimidazole (4 $\times$ 10^{-5} M) in water, 0.1 M perchloric acid and 0.1 M sodium hydroxide showed that there was no significant decomposition of the thione in 14 hours.

7.2.2 4-Thiopyridine

The UV / visible spectrum of 4-thiopyridine (4×10^{-5} M) was obtained in 2 M perchloric acid and in water (Figure 7.8). The two spectra are different, indicating that the chromophore is affected by protonation. The pK_a for this process is 1.43, and that for the deprotonation of 4-thiopyridine is 8.83.[2] In the protonated form the positive charge resides partially on the ring nitrogen and partially on the sulfur atom.[1]
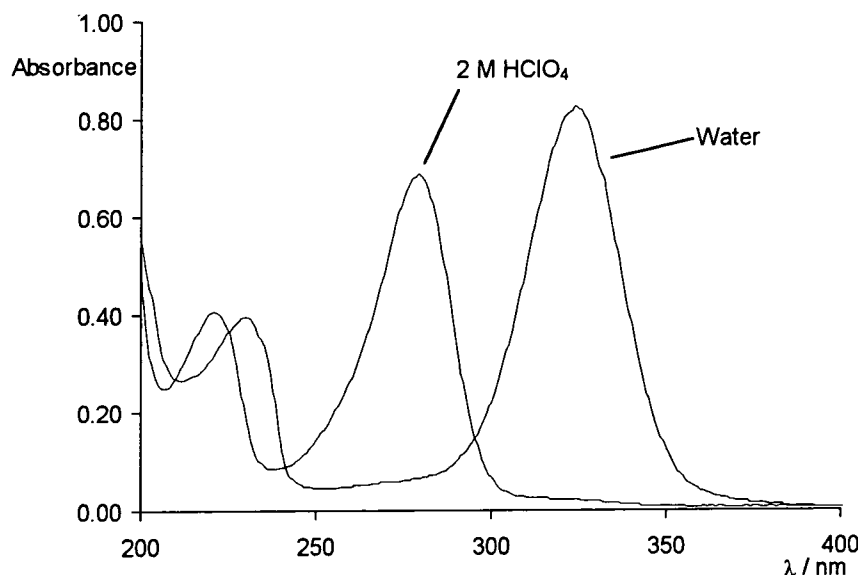
Figure 7.8 UV / visible spectrum of 4-TP (4×10^{-5} M).

A sample of 4-thiopyridine (5.2×10^{-4} M) in pH 7.4 phosphate buffer decomposed slowly, half of the sample being decomposed after ~ 30 hours in the dark. The process occurring was presumably oxidation, and probably proceeds *via* the anion.

The extinction coefficients were measured as described for 2-thioimidazole (Section 7.2.1) and are tabulated alongside the corresponding literature values in Table 7.3.[2]

Protomer	λ_{max} / nm	Measured ε / $dm^3 \, mol^{-1} \, cm^{-1}$	Literature ε / $dm^3 \, mol^{-1} \, cm^{-1}$
Neutral	230	$9\,200 \pm 100$	10 400
	320	$20\,100 \pm 200$	21 900
Cation	220	$9\,000 \pm 100$	7 900
	280	$16\,500 \pm 700$	17 000

Table 7.3 Extinction coefficients for 4-TP

7.2.3 2-Thiopyrimidine

Figure 7.9 shows the spectrum of 2-thiopyrimidine (4×10^{-5} M) in water and in 1 M perchloric acid. The pK_a of this compound is 1.35.[3]
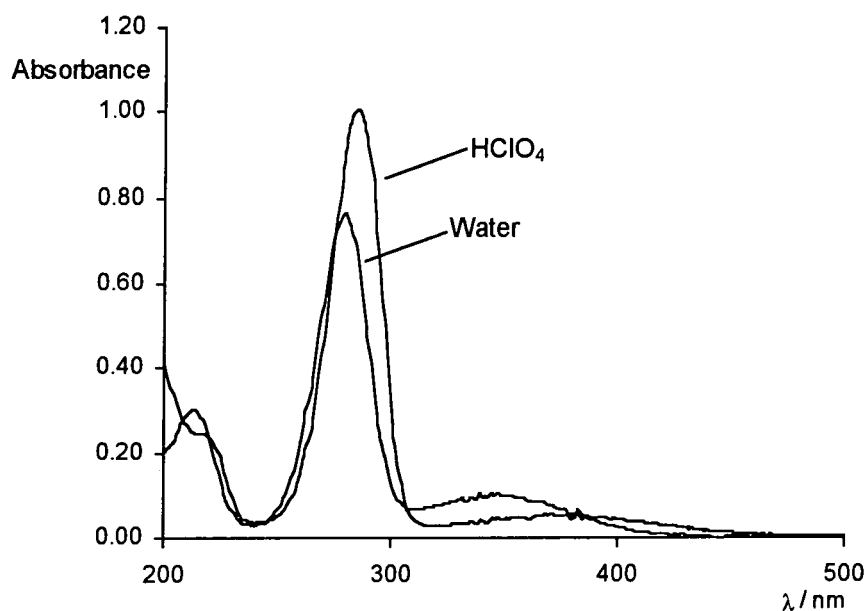
Figure 7.9 Spectra of 2-thiopyrimidine

Repeat spectra obtained over twelve hours revealed that the thione was stable over this time. The extinction coefficient of the protonated form was measured as:

$\varepsilon_{285nm} = 28\ 900 \pm 300\ dm^3\ mol^{-1}\ cm^{-1}$

$\varepsilon_{379nm} = 1\ 600 \pm 100\ dm^3\ mol^{-1}\ cm^{-1}$

For the neutral form the extinction coefficients were determined as:

$\varepsilon_{279nm} = 19\ 000 \pm 500\ dm^3\ mol^{-1}\ cm^{-1}$

$\varepsilon_{351nm} = 2\ 500 \pm 200\ dm^3\ mol^{-1}\ cm^{-1}$

7.3 Initial Nitrosation Studies

Spectral studies were initially carried out to establish whether any reaction occurred between the substrates and nitrous acid. Given that halides usually catalyse nitrosation reactions (Section 1.1.4), bromide was added to some of the solutions to ascertain if the spectral changes observed were accelerated. Various ratios of [HNO$_2$] to [substrate] were used in order to test whether equilibrium processes were being observed.

7.3.1 2-Thioimidazole

Figure 7.10 shows the spectra obtained when 2-thioimidazole (4×10^{-5} M) was reacted in a 1:1 ratio with nitrous acid in 0.1 M perchloric acid. The spectrum of 2-thioimidazole is superimposed for comparison. The spectra show the absorbance decreases at 250 nm and increases above 278 nm, with a tight isosbestic point at 278 nm, indicating that the process does not involve the formation of significant concentrations of any intermediate. The spectrum of 2-thioimidazole does not pass through this isosbestic point, indicating that the spectrum obtained immediately after mixing (t = 5 s) is formed from the 2-thioimidazole, and that this species then decomposes to form the final product.
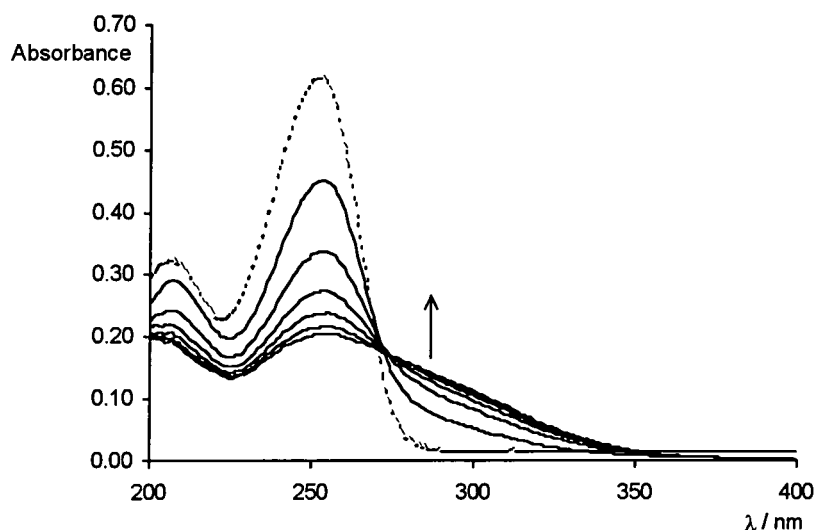
Figure 7.10 Spectra obtained for reaction of 2-TI (4×10^{-5} M) with HNO_2 (4×10^{-5} M) in 0.1 M $HClO_4$. Spectrum represented by dashed line is of 4×10^{-5} M 2-TI. First spectrum, t = 5 s after mixing; subsequent spectra every 60 s.

When similar spectra were obtained with a 2:1 HNO₂: 2-TI ratio the extent of the initial absorbance decrease at 250 nm was greater. The final product had a spectrum identical to that in Figure 7.10.

With a 10:1 ratio of HNO₂: 2-TI the intermediate spectrum exhibited a higher absorbance at 280 nm than the final product spectrum, unlike the 1:1 and 2:1 cases where the reverse was true (Table 7.4).

[HNO$_2$]:[2-TI]	Abs 280 nm t = 5 s	Abs 280 nm Final product
1:1	0.103	0.160
2:1	0.149	0.154
10:1	0.189	0.156

Table 7.4 Comparison of absorbance at 280 nm for different [HNO$_2$]:[2-TI]

An absorbance-time trace obtained at 280 nm for the reaction of 2-thioimidazole (4 × 10^{-5} M) with a ten-fold excess of nitrous acid is shown in Figure 7.11. An initial fast formation is observed, followed by a slower decomposition.
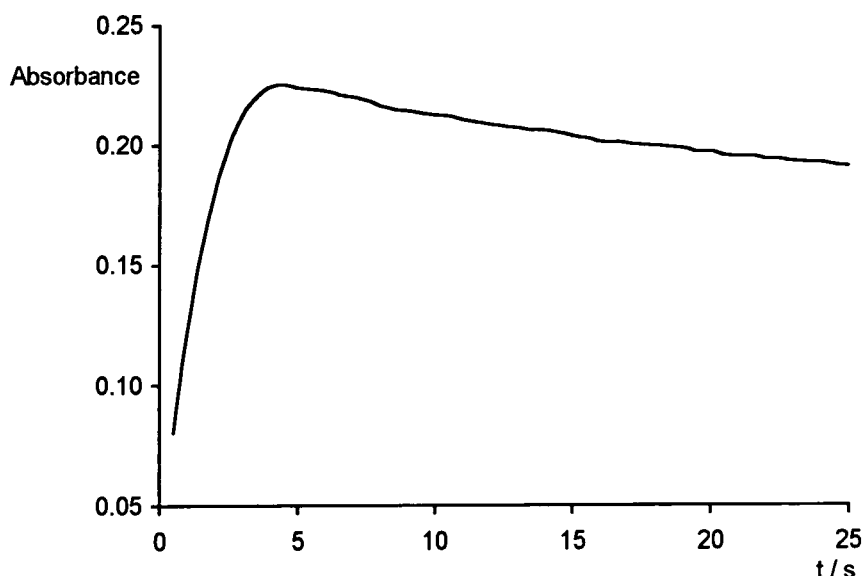
Figure 7.11 Absorbance-time trace obtained at 280 nm for reaction of 2-TI (4 × 10^{-5} M) with HNO$_2$ (4 × 10^{-4} M) in 0.1 M HClO$_4$ at 25 °C.

When 2-thioimidazole (1 × 10^{-3} M) was reacted in a flask with nitrous acid (2 × 10^{-3} M) in 0.1 M HClO$_4$ the solution rapidly turned green/yellow, fading to a paler yellow over time. Gas was evolved, and this was shown to be nitric oxide using the nitric oxide electrode. More nitric oxide was evolved than from a 2 × 10^{-3} M solution of nitrous acid alone after the same time. *S*-Nitrosation of thiones has previously been observed to give rise to green/yellow products that are unstable, decomposing to the corresponding disulfide.[15,19] This suggests that the 2-thioimidazole is *S*-nitrosated, forming a product that quickly decomposes. Further confirmation that *S*-nitrosation occurs came from experiments in which imidazole

was reacted with an equimolar concentration of nitrous acid in 0.1 M HClO₄: no loss of nitrous acid was observed over several minutes.

7.3.2 4-Thiopyridine

When 4-thiopyridine (final concentration 4×10^{-4} M) was added to a 2×10^{-3} M solution of nitrous acid in 0.1 M perchloric acid, the solution rapidly turned yellow. A spectrum of the solution showed a shoulder at 400 nm and a peak at 550 nm ($\varepsilon \approx$ 70 dm³ mol⁻¹ cm⁻¹), which is characteristic of S-nitrosated species.[23] The S-nitroso species decomposed, the process being complete after one hour.

Figure 7.12 shows the spectra of the products of 4-thiopyridine nitrosation carried out with a range of nitrous acid: 4-thiopyridine concentrations. Bromide ion was added to catalyse the reactions, ensuring the spectra of the products could be obtained before any significant decomposition occurred. The difference between the spectrum taken with one equivalent of nitrous acid and that taken with two equivalents of nitrous acid demonstrates that the nitrosation is an equilibrium process. Much higher concentrations of nitrous acid were required to give complete nitrosation at pH 3 (citrate buffer), demonstrating the acid dependence of this equilibrium.
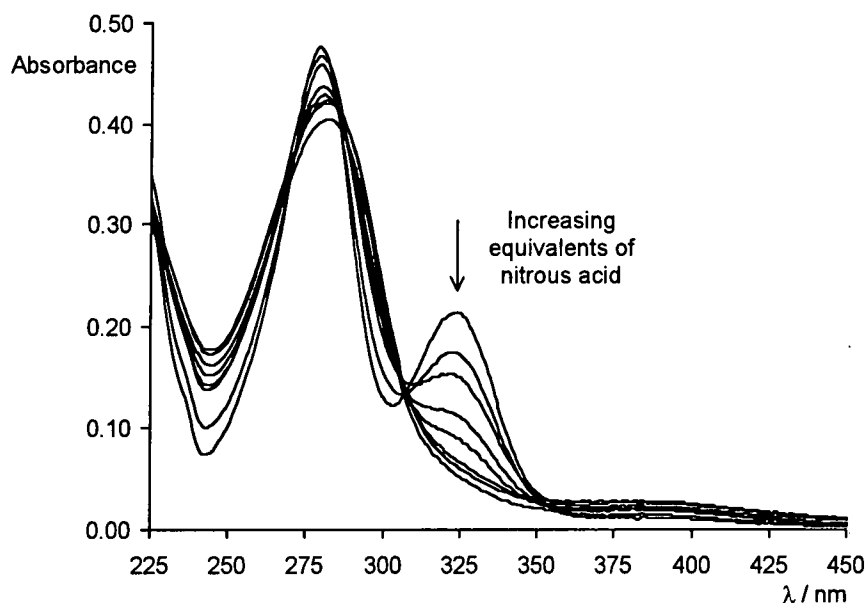
Figure 7.12 Spectra obtained for the nitrosation of 4-TP (4×10^{-5} M) in 0.1 M HClO$_4$ using 0.2, 0.4, 0.6, 0.8, 1, 2, 3 and 5 equivalents of nitrous acid

7.3.3 2-Thiopyrimidine

The nitrosation of 2-thiopyrimidine was found to require large excess concentrations of nitrous acid to give reasonable absorbance changes. The reaction of the thione with nitrous acid gave an initial rapid absorbance decrease at 280 nm, followed by a slower absorbance decrease that presumably represents the decomposition of the product. Figure 7.13 shows the spectral changes occurring when 2-thiopyrimidine is nitrosated.
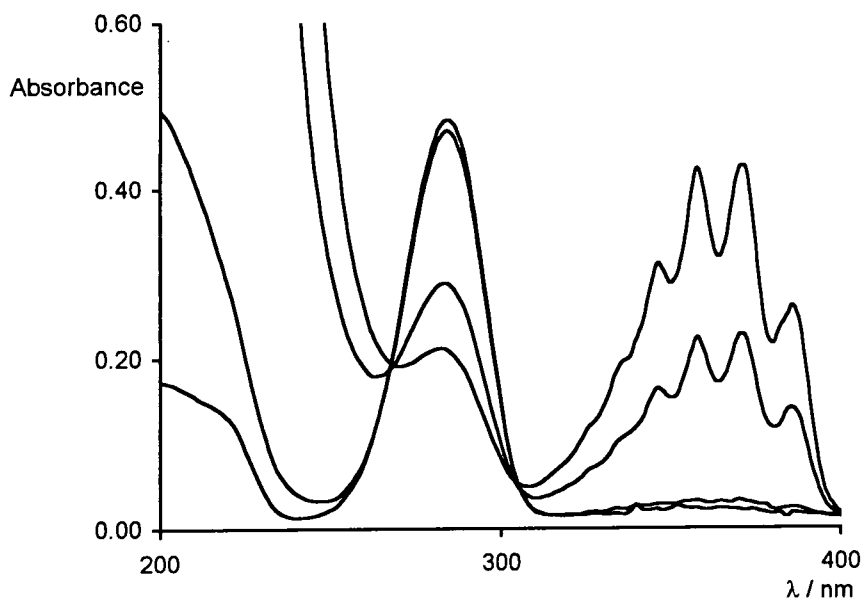
Figure 7.13 Nitrosation of 2-TPM $(2 \times 10^{-5}\ M)$ in 0.1 M perchloric acid by nitrous acid $(2 \times 10^{-5}\ M, 2 \times 10^{-4}\ M, 4 \times 10^{-3}\ M, 8 \times 10^{-3}\ M)$. Higher nitrous acid concentrations give lower absorbance values at 280 nm. Bands centred around 360 nm are due to nitrous acid

7.4 Nitrosation Equilibrium Constants Obtained using Spectral Data

Some of the spectral data discussed in Section 7.3 were used to calculate the equilibrium constants for the formation of the S-nitroso products. Absorbance data from the kinetic work (Section 7.5) were also used in this respect, calculating equilibrium constants from changes in ΔAbs observed as one of the reactant concentrations was changed. Equation 7.1 was used to calculate values of K_N. The equilibrium is acid dependent because the nitroso product $(R^+S=NO)$ does not lose a proton.

$$K_N = \frac{[SNO^+]}{[S][HNO_2][H^+]} \qquad \text{Equation 7.1}$$

The mass balance terms given in Equations 7.2 – 7.4 must be taken into account when applying Equation 7.1. Usually $[H^+]$ is sufficiently high that the corresponding mass balance equation is not required.

$$[S]_r = [S] + [SNO^+] \qquad \text{Equation 7.2}$$

$$[HNO_2]_r = [HNO_2] + [SNO^+] \qquad \text{Equation 7.3}$$

$$[H^+]_r = [H^+] + [HNO_2] \qquad \text{Equation 7.4}$$

7.4.1 2-Thioimidazole

The final absorbance at 280 nm from traces obtained for the kinetic studies in Section 7.5.1.1 (varying $[HNO_2]_\tau$) and Section 7.5.3.2 (varying $[H^+]_\tau$) are given in Table 7.5. Only the *S*-nitroso product absorbs significantly at this wavelength. The change in final absorbance with $[H^+]_\tau$ indicates the equilibrium is acid dependent, and justifies the application of Equation 7.1.

$[HNO_2]_\tau$ / mol dm^{-3}	Final abs at 280 nm	$[H^+]_\tau$ / mol dm^{-3}	Final abs at 280 nm
1.60×10^{-5}	0.052	1.25×10^{-2}	0.098
4.80×10^{-5}	0.099	2.50×10^{-2}	0.158
8.00×10^{-5}	0.147	3.75×10^{-2}	0.200
9.60×10^{-5}	0.150	5.00×10^{-2}	0.232
1.20×10^{-4}	0.165	7.50×10^{-2}	0.279
1.60×10^{-4}	0.190	1.00×10^{-1}	0.311
2.40×10^{-4}	0.210	1.50×10^{-1}	0.354
3.20×10^{-4}	0.220	2.00×10^{-1}	0.383
4.00×10^{-4}	0.229	2.50×10^{-1}	0.403
5.00×10^{-4}	0.232	---	---
1.00×10^{-3}	0.250	---	---

Table 7.5 Absorbance data for K_N determination for *S*-nitrosation of 2-TI (4×10^{-5} M). When $[HNO_2]_\tau$ varied $[H^+] = 0.10$ M; when $[H^+]_\tau$ varied $[HNO_2]_\tau = 4 \times 10^{-4}$ M.

The data were fitted with Scientist,[24] using a model incorporating the relevant mass balance equations, and an expression for the absorbance in terms of the extinction coefficients for the absorbing species, into Equation 7.1. Good fits were obtained, as shown in Figure 7.14 for the data obtained by varying $[HNO_2]_\tau$.
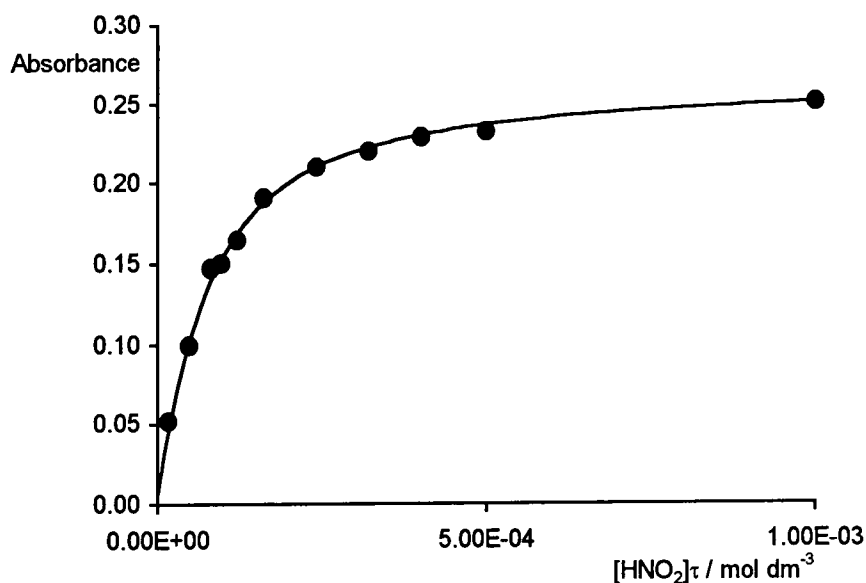
Figure 7.14 Data from Table 7.5 when $[HNO_2]_\tau$ varied. The circles represent the experimental data and the line the calculated values.

The parameter values obtained are tabulated below.

Data set	K_N / dm^6 mol^{-2}	$\varepsilon_{product(280nm)}$ / dm^3 mol^{-1} cm^{-1}
Vary $[HNO_2]_\tau$	$1.70 \times 10^5 \pm 1.6 \times 10^4$	$6\ 200 \pm 270$
Vary $[H^+]_\tau$	$1.30 \times 10^5 \pm 1.5 \times 10^4$	$6\ 700 \pm 560$

Table 7.6 Parameter values obtained from analysis of the data in Table 7.4

The average values are

$K_N = 1.50 \times 10^5 \pm 2 \times 10^4$ dm^6 mol^{-2}

$\varepsilon_{product(280nm)} = 6\ 450 \pm 350$ dm^3 mol^{-1} cm^{-1}

7.4.2 4-Thiopyridine

When the nitrosation is carried out under conditions where both $[H^+]$ and $[HNO_2]_\tau$ remain effectively constant, the expression in Equation 7.5 describes the absorbance due to the thione at 325 nm. These conditions were achieved for 4-thiopyridine by working at pH 3.1 (citrate buffer). At this pH the pK_a of nitrous acid must be taken into account: a value of 3.15 was used.[25] The equation is derived in Appendix 5, and is a formulation of Equation 7.1 including terms to convert concentrations into absorbance values.

$$\frac{1}{\Delta Absorbance} = \frac{K_{a(HNO_2)} + [H^+]}{\left(\varepsilon_{4TP} - \varepsilon_{4TPNO^+}\right) K_N [H^+]^2 [4\text{-}TP]_\tau [HNO_2]_\tau} + \frac{1}{\left(\varepsilon_{4TP} - \varepsilon_{TPNO^+}\right) [4 - TP]_\tau}$$

Equation 7.5

Absorbance data for the nitrosation at pH 3.1 are given in Table 7.7.

$[HNO_2]_\tau$ / mol dm^{-3}	Final absorbance at 325 nm	ΔAbsorbance
0	0.445	---
2.00×10^{-4}	0.191	0.255
3.00×10^{-4}	0.154	0.291
5.00×10^{-4}	0.119	0.326
1.00×10^{-3}	0.078	0.367
1.50×10^{-3}	0.066	0.379
2.00×10^{-3}	0.060	0.389

Table 7.7 Final absorbance when 4-TP was nitrosated (2×10^{-5} M) in the presence of Br$^-$ (2×10^{-3} M) at pH 3.1.

Equation 7.5 predicts that a plot of ($1/\Delta$Absorbance) versus ($1/[HNO_2]_\tau$) should be linear, and Figure 7.15 shows this is the case. Interpretation of the gradient and intercept allows the calculation of K_N:

$K_N = 1.95 \times 10^7 \pm 6 \times 10^5$ dm^6 mol^{-2}
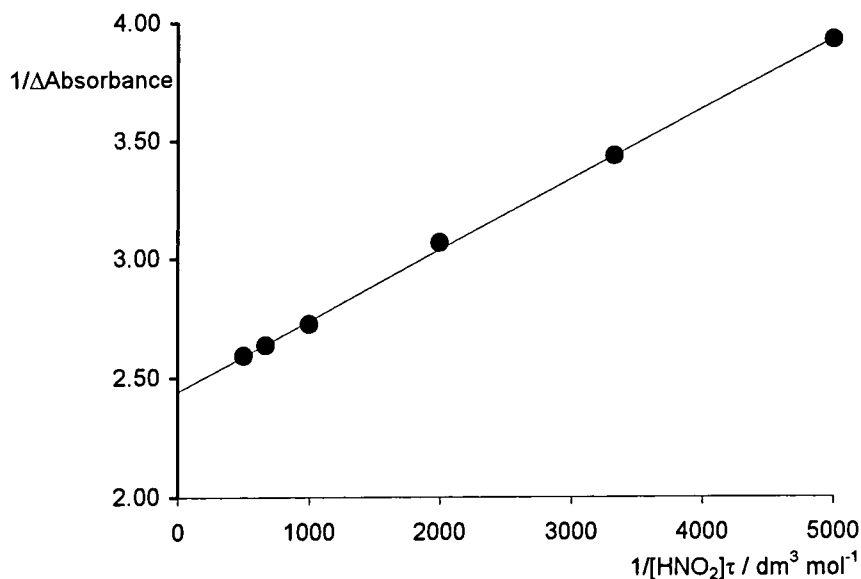
Figure 7.15 Graphical treatment of the data in Table 7.7

In 0.1 M perchloric acid the absorbance data in Table 7.8 was fitted directly as per 2-thioimidazole. This was necessary because it was not possible to use a large excess of nitrous acid, and the pK_a of the substrate had to be taken into account. It was assumed that the reactive form of the substrate in the nitrosation was the neutral form, and this was confirmed in the nitrosation kinetic studies (see Section 7.5.1).

$[HNO_2]_\tau$ / mol dm^{-3}	Final absorbance at 325 nm
8.00×10^{-6}	0.214
1.60×10^{-5}	0.173
2.40×10^{-5}	0.151
3.20×10^{-5}	0.112
4.00×10^{-5}	0.089
8.00×10^{-5}	0.067
1.20×10^{-4}	0.052
2.00×10^{-4}	0.060

Table 7.8 Absorbance data from Figure 7.12 for 4-TP nitrosation

Fitting the data using Scientist [24] gave the parameter values below. The fit is shown in Figure 7.16. $\varepsilon_{4TP(325nm)}$ was taken as 20 100 dm^3 mol^{-1} cm^{-1}.

$K_N = 2.0 \times 10^7 \pm 4 \times 10^6$ dm^6 mol^{-2}

$pK_a = 1.45 \pm 0.02$

The pK_a value obtained agrees well with the literature value of 1.43, and K_N agrees with the value obtained at pH 3.1.

Figure 7.16 The calculated fit for the data in Table 7.7

7.4.3 2-Thiopyrimidine

Absorbance data for the nitrosation of 2-thiopyrimidine $(2 \times 10^{-5}$ M) in 0.10 M $HClO_4$ is given in Table 7.9. Data in the second column is from the spectral work reported in Section 7.3.3; data in the third column is from the kinetic study in Section 7.5.1.2.

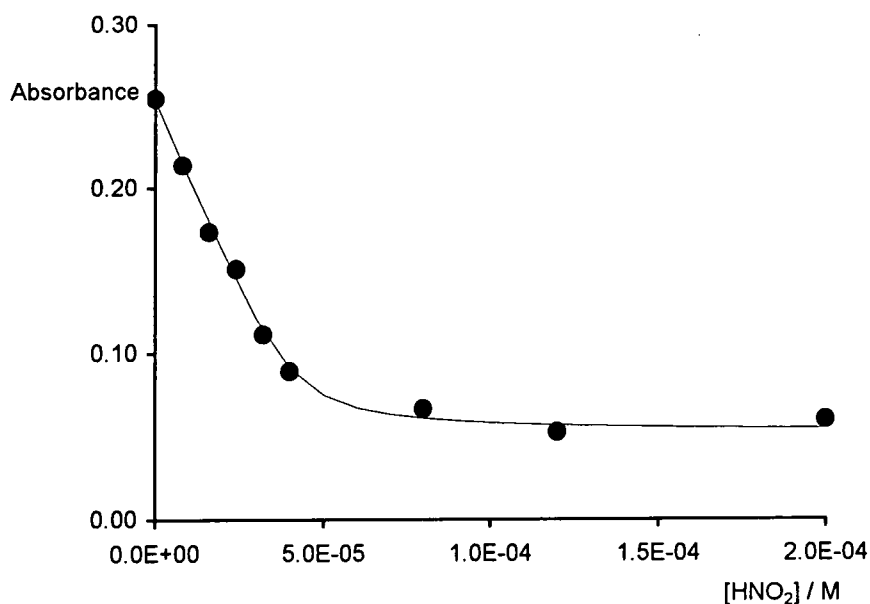| $[HNO_2]_\tau$ / mol dm^{-3}	Final absorbance at 285 nm	Δ absorbance at 285 nm
0.00	0.475	---
2.00×10^{-5}	0.448	---
2.00×10^{-4}	0.434	---
2.00×10^{-4}	0.443	---
4.00×10^{-4}	0.450	0.112
4.00×10^{-4}	0.427	---
6.00×10^{-4}	---	0.159
8.00×10^{-4}	0.399	0.205
1.00×10^{-3}	0.404	0.238
1.60×10^{-3}	0.345	---
2.00×10^{-3}	0.334	---
4.00×10^{-3}	0.276	0.474
8.00×10^{-3}	0.198	0.564
8.00×10^{-3}	0.193	---

Table 7.9 Absorbance data for the nitrosation of 2-thiopyrimidine

Analysis of the absorbance data in the second column using Scientist[24] gives

K_N = 1 700 ± 200 dm^6 mol^{-2}

Plotting (1/Δabsorbance) against (1/$[HNO_2]_\tau$) as per Section 7.4.1 gives a straight line and the value

K_N = 4 300 ± 600 dm^6 mol^{-2}

These values are much lower than the values obtained for 2-TI and 4-TP, and for 2-TP nitrosation which has been previously reported.[19] The values are comparable with those obtained for the nitrosation of some thiourea derivatives.[18]

7.5 Kinetics of *S*-Nitrosation

The kinetics of *S*-nitrosation of the substrates was studied, including the effects of adding nitrosation catalysts such as halides. Unless otherwise stated the stopped-flow technique was used, and the reactions were carried out at 25 °C.

7.5.1 Uncatalysed Nitrosation by Nitrous Acid

7.5.1.1 Varying the Substrate Concentration

Nitrosations were carried out with [H⁺] and [substrate] >> [HNO₂], varying the substrate concentration. The formation of the product was monitored at 280 nm (2-TI) or 400 nm (4-TP). The reaction profiles were fitted to a first order rate equation by applying non-linear least squares analysis using Scientist.[24] Values of the first order rate constants obtained for each substrate are tabulated in Table 7.10.

$[S]_\tau$ / mol dm^{-3}	2-TI k_{obs} / s^{-1}	4-TP k_{obs} / s^{-1}
5.00×10^{-4}	$4.22 \times 10^{-1} \pm 2 \times 10^{-3}$	---
7.50×10^{-4}	$5.84 \times 10^{-1} \pm 1 \times 10^{-2}$	---
1.00×10^{-3}	$8.16 \times 10^{-1} \pm 8 \times 10^{-3}$	---
1.50×10^{-3}	$1.23 \pm 1 \times 10^{-2}$	---
2.00×10^{-3}	$1.64 \pm 4 \times 10^{-3}$	---
3.00×10^{-3}	$2.35 \pm 2 \times 10^{-2}$	---
5.00×10^{-3}	$3.90 \pm 6 \times 10^{-2}$	$1.01 \pm 5 \times 10^{-3}$
6.00×10^{-3}	---	$1.25 \pm 6 \times 10^{-3}$
8.00×10^{-3}	---	$1.59 \pm 6 \times 10^{-3}$
1.00×10^{-2}	---	$2.01 \pm 7 \times 10^{-3}$
1.50×10^{-2}	---	$2.97 \pm 3 \times 10^{-3}$

Table 7.10 First order rate constants for nitrosation varying [substrate]. 2-TI:[H⁺] = 0.1 M, [HNO₂]$_\tau$ = 4 × 10⁻⁵ M. 4-TP:[H⁺] = 0.1 M, [HNO₂]$_\tau$ = 5 × 10⁻⁴ M.

Plots of k_{obs} versus $[S]_\tau$ are linear, as shown in Figure 7.17, demonstrating that the nitrosations are first order in $[S]_\tau$. The data are analysed in Section 7.5.1.4.
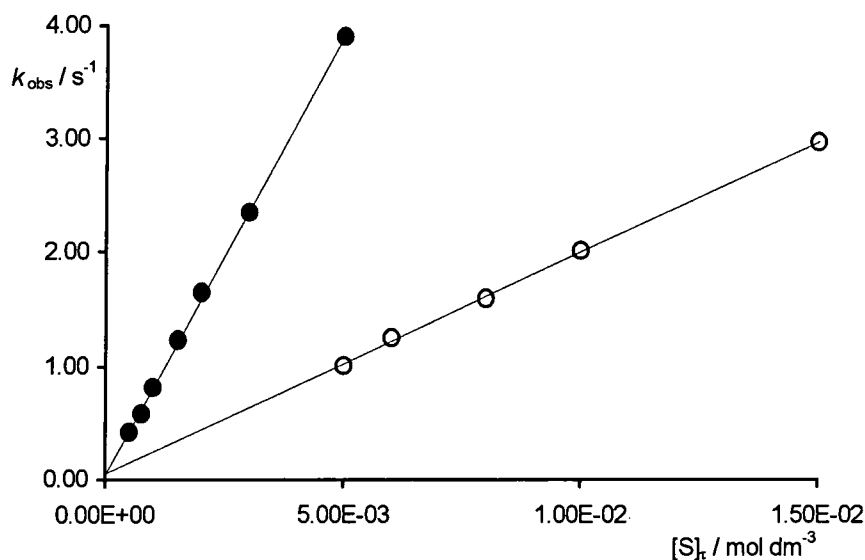
Figure 7.17 Plots of k_{obs} versus $[S]_T$. ● 2-TI, ○ 4-TP

7.5.1.2 Varying the Nitrous Acid Concentration

Experiments were carried out in which $[HNO_2]$ was varied, maintaining $[HNO_2]$ $>>$ $[H^+]$ and $[S]_T$. The product formation was followed at 280 nm for 2-TI. For 4-TP and 2-TPM the reactions were followed by measuring the decomposition of the thione at 325 nm and 285 nm respectively. The absorbance-time profiles obtained for 2-TI and 4-TP were not first-order, as demonstrated for 2-TI in Figure 7.18.
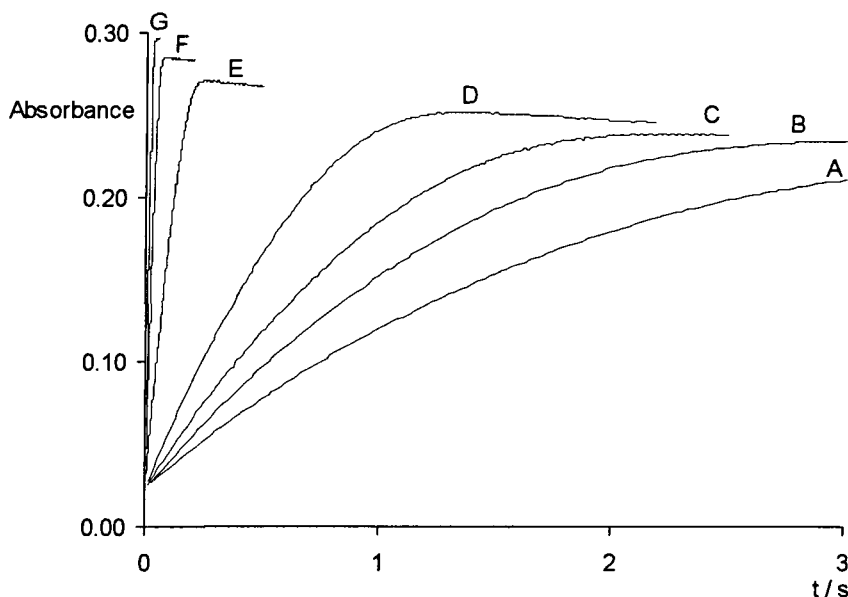
Figure 7.18 Non first-order traces for 2-TI nitrosation in 0.1 M $HClO_4$.
$[2\text{-}TI]_\tau = 4 \times 10^{-5}$ M. $[HNO_2] =$ A, 4×10^{-4} M; B, 5×10^{-4} M; C, 6×10^{-4} M; D, 8×10^{-4} M;
E, 2×10^{-3} M; F, 4×10^{-3} M; G $= 6 \times 10^{-3}$ M

The kinetic order in [A] is related to the way the half-life changes throughout the course of the reaction, and this relationship is formalised in Equation 7.6.[26]

$$\log\left(t_{\frac{1}{2}}\right) = (1 - n)\log[A_o] + \log\left(\frac{2^{n-1} - 1}{(n-1)k}\right) \qquad \text{Equation 7.6}$$

Table 7.11 Shows the change in kinetic order with $[HNO_2]$, calculated using Equation 7.6, observed for the traces in Figure 7.18. As $[HNO_2]$ is increased the kinetic order approaches zero, suggesting the participation of nitrosation by dinitrogen trioxide, with the formation of N_2O_3 being rate-determining (Section 1.1.2).

$[HNO_2]$ / mol dm^{-3}	Kinetic order
4.00×10^{-4}	0.64
5.00×10^{-4}	0.60
6.00×10^{-4}	0.51
8.00×10^{-4}	0.44
2.00×10^{-3}	0.29
4.00×10^{-3}	0.17
6.00×10^{-3}	0.02

Table 7.11 Kinetic order of the traces in Figure 7.18 for 2-TI nitrosation

Due to the intermediate kinetic order observed, analysis of the data is complex and requires either direct fitting using a suitable computer model, or interpretation of the initial rates. Table 7.12 lists the initial rates (v_o) obtained for the nitrosations. These were calculated by dividing the gradient of the initial linear section of the absorbance-time profile by the relevant extinction coefficient (taken from the results of the equilibrium analysis in Section 7.4). These results are analysed in Section 7.5.1.4.

2-TI nitrosation: $\varepsilon_{product(280nm)} = 6\,450 \pm 350$ dm^3 mol^{-1} cm^{-1}

2-TP nitrosation: $\varepsilon_{325nm} = 20\,100 \times \dfrac{K_a}{K_a + [H^+]} = 5\,400 \pm 60$ dm^3 mol^{-1} cm^{-1}

[HNO$_2$] / mol dm^{-3}	2-TI v_o / mol dm^{-3} s^{-1}	4-TP v_o / mol dm^{-3} s^{-1}
2.00×10^{-4}	---	$1.52 \times 10^{-6} \pm 2 \times 10^{-8}$
4.00×10^{-4}	$1.7 \times 10^{-5} \pm 1 \times 10^{-6}$	$5.67 \times 10^{-6} \pm 6 \times 10^{-8}$
5.00×10^{-4}	$2.3 \times 10^{-5} \pm 1 \times 10^{-6}$	---
6.00×10^{-4}	$3.1 \times 10^{-5} \pm 2 \times 10^{-6}$	---
8.00×10^{-4}	$5.1 \times 10^{-5} \pm 3 \times 10^{-6}$	$2.15 \times 10^{-5} \pm 3 \times 10^{-7}$
1.00×10^{-3}	---	$3.56 \times 10^{-5} \pm 4 \times 10^{-7}$
2.00×10^{-3}	$2.5 \times 10^{-4} \pm 1 \times 10^{-5}$	$1.32 \times 10^{-4} \pm 2 \times 10^{-6}$
4.00×10^{-3}	$8.7 \times 10^{-4} \pm 5 \times 10^{-5}$	---
6.00×10^{-3}	$1.8 \times 10^{-3} \pm 1 \times 10^{-4}$	---

Table 7.12 Initial rates for nitrosations when [HNO$_2$] was varied. [H$^+$] = 0.10 M. [2-TI] = 4×10^{-5} M

For 2-thiopyrimidine the disappearance of the thione was followed at 285 nm, and first order traces were observed: these are given in Table 7.13.

[HNO$_2$] / mol dm^{-3}	2-TPM k_{obs} / s^{-1}
4.00×10^{-4}	6.30 ± 0.08
6.00×10^{-4}	8.77 ± 0.07
8.00×10^{-4}	11.8 ± 0.2
1.00×10^{-3}	14.7 ± 0.1
4.00×10^{-3}	103 ± 2
8.00×10^{-3}	432 ± 8

Table 7.13 Kinetic data for the nitrosation of 2-TPM (4×10^{-5} M) by nitrous acid in 0.1 M HClO$_4$

A plot of k_{obs} versus $[HNO_2]$ curved sharply upwards, but a plot of k_{obs} versus $[HNO_2]^2$ was linear, indicating nitrosation by N_2O_3 according to Equation 7.13 in Section 7.5.1.4.

7.5.1.3 Varying [H⁺]

Nitrosations were followed when $[H^+]$ was varied, maintaining $[H^+] >> [S]_\tau$ and $[HNO_2]$. One of $[S]_\tau$ or $[HNO_2]$ was in excess over the other. The reactions were followed at the wavelengths given in Section 7.5.1.1. The observed first order rate constants are in Table 7.14.

$[H^+]$ / mol dm^{-3}	2-TI k_{obs} / s^{-1}	2-TI k_{obs} / s^{-1}	4-TP k_{obs} / s^{-1}
1.00×10^{-2}	$1.74 \times 10^{-1} \pm 5 \times 10^{-2}$	---	---
2.00×10^{-2}	---	$3.12 \times 10^{-1} \pm 2 \times 10^{-3}$	---
4.00×10^{-2}	$9.10 \times 10^{-1} \pm 6 \times 10^{-3}$	$7.17 \times 10^{-1} \pm 2 \times 10^{-2}$	$8.16 \times 10^{-1} \pm 2 \times 10^{-3}$
6.00×10^{-2}	1.47 ± 0.02	1.06 ± 0.02	1.02 ± 0.003
8.00×10^{-2}	2.01 ± 0.02	---	1.20 ± 0.001
1.00×10^{-1}	2.45 ± 0.05	1.86 ± 0.02	1.27 ± 0.006
1.40×10^{-1}	---	2.62 ± 0.03	---
1.50×10^{-1}	3.73 ± 0.04	---	1.43 ± 0.02
1.80×10^{-1}	---	3.43 ± 0.01	---
2.00×10^{-1}	5.19 ± 0.06	---	1.54 ± 0.006
2.50×10^{-1}	---	---	1.63 ± 0.02
3.00×10^{-1}	---	---	1.68 ± 0.008

Table 7.14 Data for 2-TI and 4-TP nitrosation. 2-TI: $[HNO_2] = 4 \times 10^{-5}$ M, $[2\text{-TI}] = 3 \times 10^{-3}$ M (2nd column), 2.28×10^{-3} M (3rd column). 4-TP: $[HNO_2] = 4 \times 10^{-4}$ M, $[4\text{-TP}] = 6 \times 10^{-3}$ M

For 2-thioimidazole plots of k_{obs} versus $[H^+]$ are linear, indicating the nitrosation is first order in $[H^+]$ (see Figure 7.19).
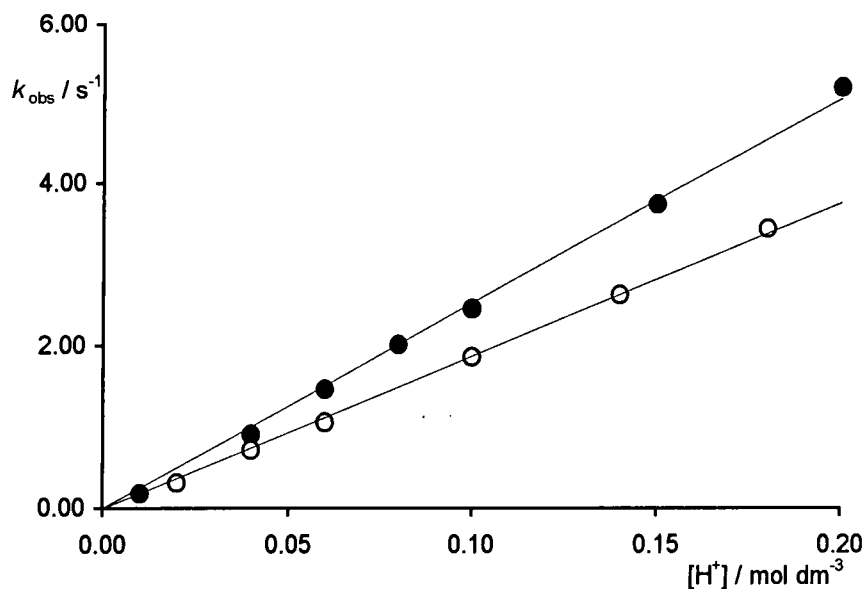
Figure 7.19 k_{obs} versus [H⁺] for 2-TI nitrosation, data from Table 7.14. There were no statistically significant intercepts.

For the nitrosation of 4-thiopyridine the plot of k_{obs} against [H⁺] is curved, indicating that the pK_a for the substrate probably appears in the rate equation (Figure 7.20).
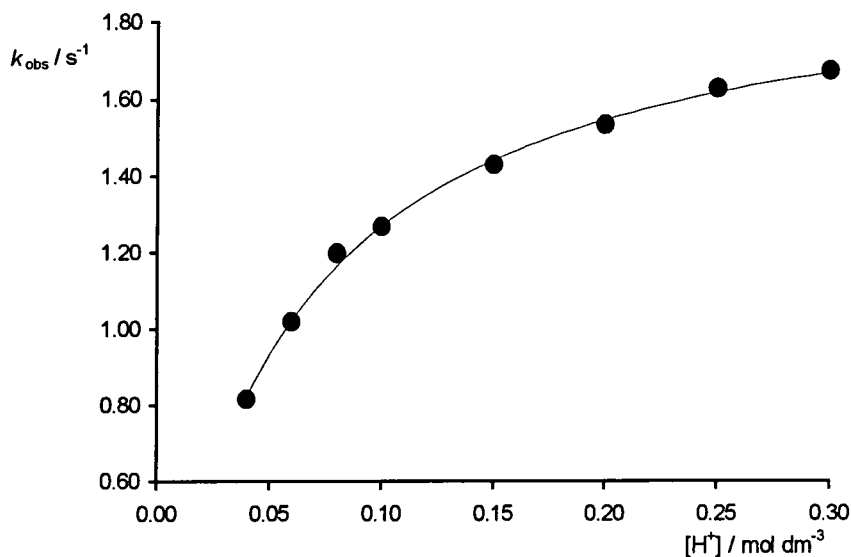
Figure 7.20 Plot of k_{obs} versus [H⁺] for 4-TP nitrosation. The analysis carried out to calculate the fit line is described in Section 7.5.1.4.

7.5.1.4 Analysis

- **Nitrosation by Nitrous Acid**

The general scheme for nitrosation by nitrous acid is shown in Scheme 7.1. The initial deprotonation applies to 4-thiopyridine, for which nitrosation proceeds *via* the deprotonated form.

$$SH^+ \rightleftharpoons S + H^+ \quad K_a = \frac{[S][H^+]}{[SH^+]}$$

$$S + H^+ + HNO_2 \underset{k_{-N}}{\overset{k_N}{\rightleftharpoons}} {}^+SNO + H_2O \quad K_N = \frac{k_N}{k_{-N}}$$

Scheme 7.1 General scheme for the nitrosation of substrate S by nitrous acid

For the data obtained in Section 7.5.1.1, where $[S]_\tau$ and $[H^+]$ are in excess, the expression for k_{obs} is given by Equation 7.7, which is derived in Ap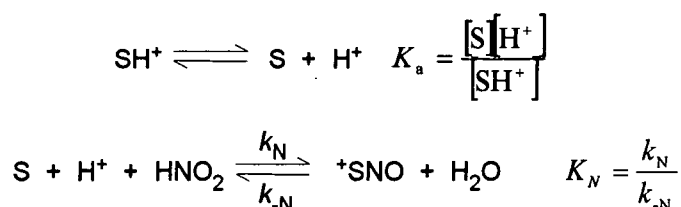pendix 5. For substrates where there is no acid dissociation step involved, i.e. when $K_a \gg [H^+]$, Equation 7.8 applies.

$$k_{obs} = \frac{K_a k_N [H^+][S]_\tau}{K_a + [H^+]} + k_{-N} \qquad \text{Equation 7.7}$$

$$k_{obs} = k_N [H^+][S]_\tau + k_{-N} \qquad \text{Equation 7.8}$$

When $[H^+]$ is constant and $[S]_\tau$ is varied, plots of k_{obs} versus $[S]_\tau$ should be linear, as is the case for the data in Section 7.5.1.1. Applying Equation 7.7 to the 2-TI data and Equation 7.8 to the 4-TP data from Sections 7.5.1.1 and 7.5.1.3 yields the parameter values in Table 7.15. The uncertainty in the small intercepts makes it impossible to determine accurately k_{-N} and K_N from the data.

Substrate	Varied	k_N / $dm^6\ mol^{-2}\ s^{-1}$	k_{-N} / s^{-1}	K_N / $dm^6\ mol^{-2}$
2-TI	$[S]_\tau$	7 730 ± 20	0.04 ± 0.02	$1.8 \times 10^5 \pm 9 \times 10^4$
	$[H^+]$	8 430 ± 200	---	---
	$[H^+]$	8 500 ± 100	---	---
4-TP	$[S]_\tau$	7 500 ± 100	Large error in intercept	---

Table 7.15 Parameter values for the uncatalysed nitrosation reactions

Re-writing Equation 7.7 gives Equation 7.9. From the values of k_N and K_N previously determined it can be seen that both $k_{-N}K_a$ and $k_{-N}[H^+]$ are a lot smaller than $k_N K_a[H^+][S]_\tau$, therefore Equation 7.9 reduces to Equation 7.10.

$$k_{obs} = \frac{k_N K_a [H^+][S]_\tau + k_{-N}K_a + k_{-N}[H^+]}{K_a + [H^+]}$$
Equation 7.9

$$k_{obs} = \frac{k_N K_a [H^+][S]_\tau}{K_a + [H^+]}$$
Equation 7.10

Rearranging Equation 7.10 gives Equation 7.11, from which it can be seen that a plot of $(1/k_{obs})$ versus $(1/[H^+])$ should be linear, enabling K_a and k_N to be determined.

$$\frac{1}{k_{obs}} = \frac{1}{k_N [H^+][S]_\tau} + \frac{1}{k_N K_a [S]_\tau}$$
Equation 7.11

Figure 7.21 shows the corresponding plot for the data in Section 7.5.1.3 (Table 7.14) for 4-TP nitrosation.
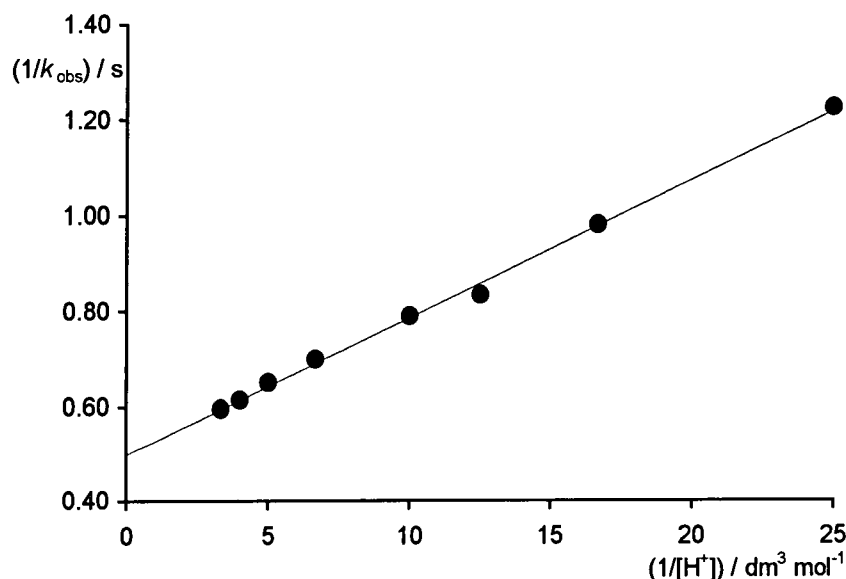
Figure 7.21 Double reciprocal plot for 4-TP nitrosation when $[H^+]$ was varied

The data for 4-TP nitrosation were also fitted directly to Equation 7.10 using Scientist.[24] The fit line obtained can be seen superimposed upon the data in Figure 7.20, section 7.5.1.3. The parameter values obtained from the two analyses are shown in Table 7.16. The pK_a values obtained for 4-thiopyridine compare reasonably well with the literature value of 1.43 at 20 °C.[2]

Substrate	Analysis method	k_N / dm^6 mol^{-2} s^{-1}	pK_a
4-TP	Graphical	5 800 ± 200	1.2 ± 0.1
	Scientist	5 900 ± 300	1.25 ± 0.07

Table 7.16 Parameters obtained when [H$^+$] was varied for 4-TP nitrosation

- **Nitrosation by Dinitrogen Trioxide**

Nitrosation by nitrous acid where the active nitrosating agent is dinitrogen trioxide can exhibit either of the rate laws in Equations 7.12 and 7.13, which follow from applying the limiting cases to Equation 7.14 (see Section 1.1.2). $k_{N_2O_3}$ is the rate constant for N$_2$O$_3$ formation from nitrous acid, $K_{N_2O_3}$ is the equilibrium constant for the same process, and $k_{2N_2O_3}$ is the rate constant for the reaction between the substrate and N$_2$O$_3$.

$$Rate = k_{N_2O_3} [HNO_2]^2 \qquad \text{Equation 7.12}$$

$$Rate = k_{2N_2O_3} K_{N_2O_3} [HNO_2]^2 [S] \qquad \text{Equation 7.13}$$

$$Rate = \frac{k_{N_2O_3} k_{2N_2O_3} [S][HNO_2]^2}{k_{-N_2O_3} + k_{2N_2O_3}[S]} \qquad \text{Equation 7.14}$$

For the experiments with excess [HNO$_2$] (Section 7.5.1.2), if equation 7.13 applies then the absorbance-time profiles would be first order, whereas if Equation 7.12 applies zeroth order traces would be observed. The results in Section 7.5.1.2 for 2-TI and 4-TP can therefore be interpreted in terms of nitrosation *via* N$_2$O$_3$ formation from nitrous acid where the formation of the active nitrosating agent is rate limiting (Equation 7.12). The deviation from zeroth order probably arises because there is some contribution from nitrosation where protonated nitrous acid is the active nitrosating agent. Considering this, it is possible to write Equation 7.15 as the expression for the initial rates of these reactions.[27]

$$v_o = k_{N_2O_3} [HNO_2]^2 + k_N [HNO_2][H^+][S]_r \qquad \text{Equation 7.15}$$

From Equation 7.15 it is possible to write Equation 7.16, which predicts that a plot of (v_o/[HNO$_2$]) versus [HNO$_2$] should be linear. An example of such a plot is given in Figure 7.22.

$$\frac{v_o}{[\text{HNO}_2]} = k_{\text{N}_2\text{O}_3}[\text{HNO}_2] + k_{\text{N}}[\text{H}^+][\text{S}]_r \qquad \text{Equation 7.16}$$
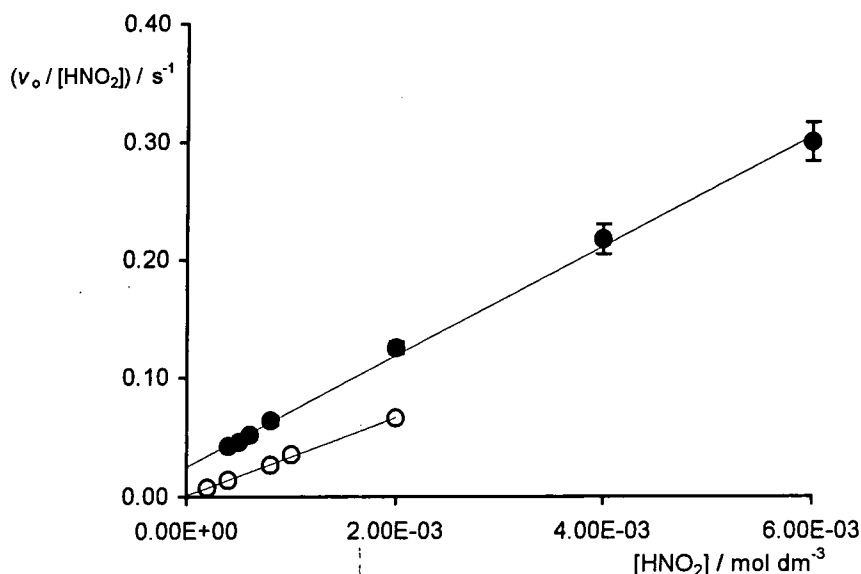
Figure 7.22 Initial rates analysis of the data in Table 7.11 (Section 7.5.1.2). ● 2-TI, ○ 4-TP

The parameter values obtained are in Table 7.17.

Substrate	k_{N} / dm^6 mol^{-2} s^{-1}	$k_{\text{N}_2\text{O}_3}$ / dm^3 mol^{-1} s^{-1}
2-TI	6 400 ± 700	46 ± 2
4-TP	No contribution *via* HNO$_2$ pathway	32 ± 2

Table 7.17 Parameter values obtained when nitrosation occurs *via* N_2O_3

Analysis of the plot of k_{obs} versus $[\text{HNO}_2]^2$ for 2-TPM nitrosation according to Equation 7.13, using $K_{\text{N}_2\text{O}_3} = 3 \times 10^{-3}$ dm^3 mol^{-1},[28] gives

$$k_{2\text{N}_2\text{O}_3} = 2.21 \times 10^9 \pm 5 \times 10^7 \text{ dm}^3 \text{ mol}^{-1} \text{ s}^{-1}.$$

With $K_{\text{N}_2\text{O}_3} = 3 \times 10^{-3}$ dm^3 mol^{-1} and $k_{\text{N}_2\text{O}_3} \sim 40$ dm^3 mol^{-1} s^{-1}, $k_{-\text{N}_2\text{O}_3}$ is $\sim 13\ 000$ s^{-1}.

For Equation 7.13 to apply, $k_{-\text{N}_2\text{O}_3}$ must be much greater than $k_{\text{N}_2\text{O}_3}[\text{S}]$ (see Equation 7.14), which given the value of $k_{2\text{N}_2\text{O}_3}$ above and a substrate concentration of 4 × 10^{-5} M is not true. Therefore, Equation 7.12 should apply and the reaction traces should have been zeroth order, not first order.

7.5.2 Cl⁻ Catalysis in Thione Nitrosations

The catalytic effect of added Cl⁻ upon the nitrosations of the thiones by nitrous acid was studied. Absorbance-time traces were obtained using the stopped-flow technique at the wavelengths given in the previous sections, following the formation of the product or decomposition of the thione.

7.5.2.1 Varying [Cl⁻]

In the experiments where [Cl⁻] was varied, $[H^+]$, $[HNO_2]$ and $[S]_\tau$ were kept constant. Either $[H^+]$ and $[HNO_2]$ or $[H^+]$ and $[S]_\tau$ were in large excess over the third reagent. First order traces were obtained, and the first order rate constants are tabulated below (Tables 7.18 and 7.19). The observation of first order traces when $[HNO_2] \gg [S]_\tau$ confirms that the deviations observed from first order traces for the uncatalysed reaction were due to the intervention of N_2O_3.

[Cl⁻] / mol dm⁻³	2-TI k_{obs} / s⁻¹	2-TI k_{obs} / s⁻¹
2.00×10^{-3}	$6.0 \times 10^{-1} \pm 2 \times 10^{-2}$	---
4.00×10^{-3}	$8.9 \times 10^{-1} \pm 3 \times 10^{-2}$	---
5.00×10^{-3}	---	1.34 ± 0.02
6.00×10^{-3}	1.20 ± 0.02	---
8.00×10^{-3}	---	1.84 ± 0.03
1.00×10^{-2}	1.71 ± 0.01	2.24 ± 0.03
2.00×10^{-2}	2.94 ± 0.03	3.68 ± 0.05
4.00×10^{-2}	5.42 ± 0.04	6.72 ± 0.04
6.00×10^{-2}	---	9.57 ± 0.02
8.00×10^{-2}	---	12.2 ± 0.001

Table 7.18 Data for Cl⁻ catalysed nitrosation of 2-TI. Column 2: $[H^+] = 0.1$ M, $[2\text{-TI}]_\tau = 4 \times 10^{-4}$ M, $[HNO_2] = 4 \times 10^{-5}$ M. Column 3: $[H^+] = 0.1$ M, $[2\text{-TI}]_\tau = 4 \times 10^{-5}$ M, $[HNO_2] = 4 \times 10^{-4}$ M

[Cl⁻] / mol dm⁻³	4-TP k_{obs} / s⁻¹	2-TPM k_{obs} / s⁻¹
2.00×10^{-3}	---	9.3 ± 0.2
4.00×10^{-3}	---	10.7 ± 0.1
8.00×10^{-3}	---	14.1 ± 0.1
1.00×10^{-2}	$3.68 \times 10^{-1} \pm 4 \times 10^{-3}$	15.3 ± 0.2
1.40×10^{-2}	---	17.9 ± 0.4
2.00×10^{-2}	---	22.1 ± 0.5
4.00×10^{-2}	$9.42 \times 10^{-1} \pm 1 \times 10^{-2}$	34.8 ± 0.5
4.90×10^{-2}	---	40.9 ± 0.3
8.00×10^{-2}	1.69 ± 0.02	---
1.00×10^{-1}	2.06 ± 0.02	---
1.50×10^{-1}	3.01 ± 0.02	---

Table 7.19 4-TP: $[H^+] = 0.1$ M, $[4\text{-TP}]_\tau = 2 \times 10^{-5}$ M, $[HNO_2] = 2 \times 10^{-4}$ M. 2-TPM: $[H^+]$ $= 0.1$ M, $[2\text{-TPM}]_\tau = 2 \times 10^{-5}$ M, $[HNO_2] = 1 \times 10^{-3}$ M.

Plots of k_{obs} versus [Cl⁻] give straight lines, as shown in Figure 7.23, indicating that the reaction is catalysed by chloride with a first-order dependence upon [Cl⁻].
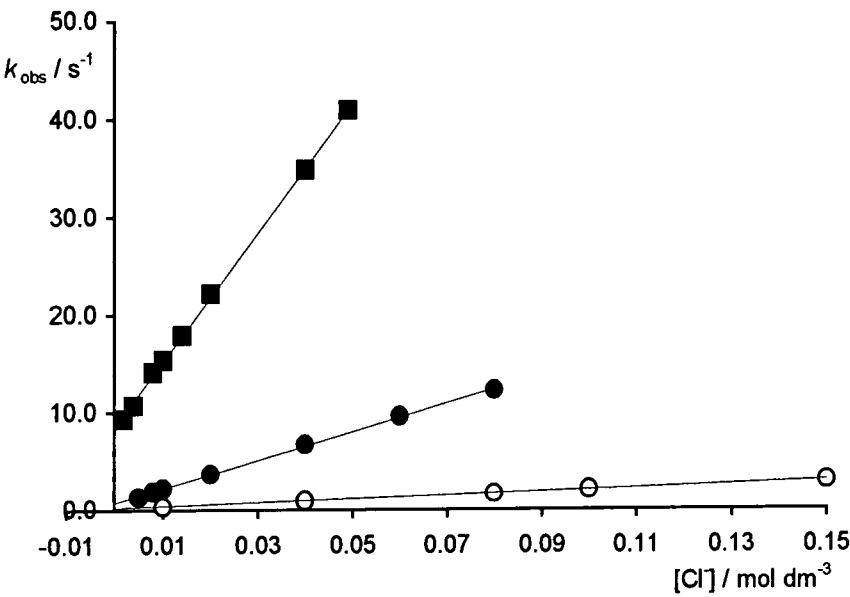

Figure 7.23 Plots of k_{obs} versus [Cl⁻] for the data in tables 7.18 and 7.19. ● = 2-TI, ○ = 4-TP, ■ = 2-TPM

7.5.2.2 Varying [H⁺]

In the experiments where [H⁺] was varied, [Cl⁻], [HNO₂] and [S]$_\tau$ were kept constant. Either [H⁺] and [HNO₂]., or [H⁺] and [S]$_\tau$, were in large excess over the

third reagent. The rate constants from the first order traces obtained are in Table 7.20.

[H$^+$] / mol dm^{-3}	2-TI k_{obs} / s^{-1}	4-TP k_{obs} / s^{-1}	2-TPM k_{obs} / s^{-1}
2.00 × 10^{-2}	---	---	4.79 ± 0.04
2.50 × 10^{-2}	5.0 ± 0.1	---	---
4.00 × 10^{-2}	---	3.05 ± 0.02	7.0 ± 0.2
5.00 × 10^{-2}	7.7 ± 0.1	---	8.10 ± 0.06
6.00 × 10^{-2}	---	3.54 ± 0.04	---
7.50 × 10^{-2}	10.2 ± 0.2	---	---
8.00 × 10^{-2}	---	3.92 ± 0.02	---
1.00 × 10^{-1}	13.3 ± 0.2	4.03 ± 0.08	13.5 ± 0.1
1.50 × 10^{-1}	18.2 ± 0.3	4.39 ± 0.02	---
2.00 × 10^{-1}	23.1 ± 0.5	4.51 ± 0.03	27.1 ± 0.3
2.50 × 10^{-1}	29.3 ± 0.4	4.83 ± 0.05	---
3.00 × 10^{-1}	---	5.02 ± 0.06	46 ± 1

Table 7.20 Data for Cl$^-$ catalysed nitrosations when [H$^+$] was varied. 2-TI: [2-TI]$_\tau$ = 4 × 10^{-5}, [HNO$_2$] = 4 × 10^{-4} M, [Cl$^-$] = 0.08 M. 4-TP: [4-TP]$_\tau$ = 4 × 10^{-5} M, [HNO$_2$] = 4 × 10^{-4} M, [Cl$^-$] = 0.1 M. 2-TPM: [2-TPM]$_\tau$ = 2 × 10^{-5} M, [HNO$_2$] = 1 × 10^{-3} M, [Cl$^-$] = 8 × 10^{-3} M

Graphs of k_{obs} versus [H$^+$] give good straight lines for 2-TI and 2-TPM. As expected, the graph obtained for 4-TP is curved like that shown Figure 7.20 in Section 7.5.1.3.

7.5.2.3 Varying the Nitrous Acid Concentration

[HNO$_2$] was varied whilst keeping [H$^+$], [Cl$^-$] and [S]$_\tau$ constant. [H$^+$] and [HNO$_2$] were always in large excess over [S]$_\tau$. The observed first order rate constants obtained are tabulated below (Table 7.21). Plots of k_{obs} versus [HNO$_2$] were linear, indicating the reactions are first order in [HNO$_2$].

[HNO$_2$] / mol dm^{-3}	2-TI k_{obs} / s^{-1}	2-TPM k_{obs} / s^{-1}
3×10^{-4}	---	9.9 ± 0.2
4×10^{-4}	5.21 ± 0.03	---
5×10^{-4}	6.58 ± 0.06	---
6×10^{-4}	7.89 ± 0.05	12.2 ± 0.5
8×10^{-4}	10.3 ± 0.5	---
1×10^{-3}	14.0 ± 0.6	15.1 ± 0.3
2×10^{-3}	27 ± 1	24.0 ± 0.2
3×10^{-3}	---	34.6 ± 0.2

Table 7.21 Kinetic data for Cl$^-$ catalysed nitrosations when [HNO$_2$] was varied. [2-TI] = 4 × 10^{-5} M, [H$^+$] = 0.1 M, [Cl$^-$] = 3 × 10^{-2} M. 2-TPM: [2-TPM] = 2 × 10^{-5} M, [H$^+$] = 0.1 M, [Cl$^-$] = 0.01 M.

7.5.2.4 Varying the Substrate Concentration

No results were obtained where the substrate concentration was varied, but the fact that first order traces were observed for all of the reactions involving chloride demonstrates that the reactions are first order in the substrate concentration.

7.5.2.5 Analysis of Chloride Catalysis

Nitrosation by nitrous acid catalysed by X$^-$ proceeds according to Scheme 7.2, which also includes a contribution from the uncatalysed reaction that is sometimes significant. The catalysis of nitrosation is discussed in Section 1.1.4.

$$SH^+ \rightleftharpoons S + H^+ \qquad K_a = \frac{[H^+][S]}{[^+SH]}$$

$$H^+ + X^- + HNO_2 \underset{k_{-XNO}}{\overset{k_{XNO}}{\rightleftharpoons}} XNO + H_2O \qquad K_{XNO} = \frac{k_{XNO}}{k_{-XNO}}$$

$$S + XNO \underset{k_{-2XNO}}{\overset{k_{2XNO}}{\rightleftharpoons}} {}^+SNO + X^- \qquad K = \frac{k_{2XNO}}{k_{-2XNO}}$$

$$H^+ + S + HNO_2 \underset{k_{-N}}{\overset{k_N}{\rightleftharpoons}} {}^+SNO + H_2O \qquad K_N = \frac{k_N}{k_{-N}}$$
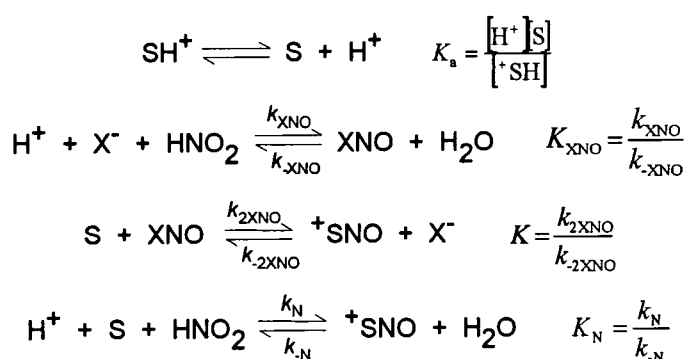
Scheme 7.2 X$^-$ catalysis in nitrosation of S by HNO$_2$

When the formation of XNO is treated as a rapidly established equilibrium, a number of expressions for k_{obs} can be derived, depending upon the conditions used when carrying out investigations into the reactions (for derivations see Appendix 5).

181

When $[HNO_2] >> [S]_\tau$ and $[H^+]$ is in large excess over the other components:

$$k_{obs} = k_N\left([HNO_2][H^+]+\frac{1}{K_N}\right) + k_{2XNO}K_{XNO}\left([HNO_2][H^+]+\frac{1}{K_N}\right)[X^-]$$

Equation 7.17 Applies when $[X^-]$ varied

$$k_{obs} = \frac{k_N + k_{2XNO}K_{XNO}[X^-]}{K_N} + \left(k_{2XNO}K_{XNO}[HNO_2][X^-]+k_N[HNO_2]\right)[H^+]$$

Equation 7.18 Applies when $[H^+]$ varied and no substrate pK_a is relevant

$$k_{obs} = \frac{k_{2XNO}K_{XNO}K_a[X^-][HNO_2][H^+]}{K_a+[H^+]} + k_{-2XNO}[X^-]$$

Equation 7.19 Applies when $[H^+]$ varied and a substrate pK_a is relevant. Assumes negligible uncatalysed reaction

$$k_{obs} = \frac{k_N + k_{2XNO}K_{XNO}[X^-]}{K_N} + \left(k_N[H^+]+k_{2XNO}K_{XNO}[H^+][X^-]\right)[HNO_2]$$

Equation 7.20 Applies when $[HNO_2]$ varied

When $[S]_\tau >> [HNO_2]$ and $[H^+]$ is in large excess over the other components:

$$k_{obs} = k_N\left([S]_\tau[H^+]+\frac{1}{K_N}\right) + k_{2XNO}K_{XNO}\left([S]_\tau[H^+]+\frac{1}{K_N}\right)[X^-].$$

Equation 7.21 Applies when $[X^-]$ varied

- **Analysis of Data where [Cl⁻] was Varied**

Equation 7.17 or 7.21 was used to analyse the data in Section 7.5.2.1, depending upon whether $[S]_\tau$ or $[HNO_2]_\tau$ was in excess. The values of K_N used were those determined in Section 7.4, though for 2-TI and 4-TP, $1/K_N$ is sufficiently small that it can be eliminated from the equations. It can be seen from the equations that the gradient of a plot of k_{obs} versus $[X^-]$ can be used to obtain k_{2XNO}, and the intercept can be used to obtain k_N. A value of 1.1×10^{-3} dm^6 mol^{-2} was used for K_{ClNO}.[28]

The small intercepts observed for many of the plots made accurate determinations of k_N difficult.

In the case of 4-TP the parameter values obtained were corrected to allow for the fact that only the neutral form of the substrate reacts. This correction was achieved by dividing the parameter value obtained from the analysis by the fraction of the substrate present in the reactive form (calculated using Equation 7.22).

$$\text{Fraction} = \frac{K_a}{K_a + [H^+]} \qquad \text{Equation 7.22}$$

The parameter values obtained from the analyses are given in Table 7.22.

Substrate	k_{2ClNO} / dm^3 mol^{-1} s^{-1}	k_N / dm^6 mol^{-2} s^{-1}
2-TI	$2.44 \times 10^9 \pm 8 \times 10^7$	$8\ 800 \pm 1\ 000$
	$2.82 \times 10^9 \pm 8 \times 10^7$	$15\ 000 \pm 4\ 000$
4-TP	$3.23 \times 10^9 \pm 3 \times 10^7$	$9\ 120 \pm 50$
2-TPM	$1.5 \times 10^9 \pm 7 \times 10^8$	$19\ 000 \pm 9\ 000$

Table 7.22 Parameter values obtained from the data in Section 7.5.2.1

- **Analysis of Data where [H$^+$] was Varied**

For the nitrosation of 2-TI and 2-TPM Equation 7.18 was used to analyse the data in Table 7.20. For 2-TI the value of k_N from Section 7.5.1.4 of ~8 000 dm^6 mol^{-2} s^{-1} was used, enabling K_N and k_{2ClNO} to be calculated from the straight line obtained when k_{obs} was plotted against [H$^+$]. For 2-TPM k_N is not known, but is likely to be similar to that obtained for other thiones and was estimated at 8 000 dm^3 mol^{-1} s^{-1}. The parameter values obtained are in Table 7.23.

Substrate	k_{2ClNO} / dm^3 mol^{-1} s^{-1}	K_N / dm^6 mol^{-2}
2-TI	$2.92 \times 10^9 \pm 9 \times 10^7$	$1.1 \times 10^5 \pm 2 \times 10^4$
2-TPM	$1.6 \times 10^{10} \pm 2 \times 10^9$	Error in intercept too large

Table 7.23 Parameter values obtained for Cl$^-$ catalysed nitrosations where [H$^+$] was varied

For 4-TP Equation 7.19 was used to analyse the data. Assuming $k_{-2}[X^-]$ is small compared with the first term in the equation, rearrangement gives Equation 7.23. Plotting $(1/k_{obs})$ versus $(1/[H^+])$ should give a straight line, from which k_{2XNO} and

K_a can be obtained. A straight line was obtained, and the parameter values are given in Table 7.24.

$$\frac{1}{k_{obs}} = \frac{1}{k_2 K_{XNO}[X^-][H^+][HNO_2]} + \frac{1}{k_2 K_{XNO} K_a [X^-][HNO_2]} \qquad \text{Equation 7.23}$$

Substrate	k_{2ClNO} / dm^3 mol^{-1} s^{-1}	pK_a
4-TP	$4.0 \times 10^9 \pm 3 \times 10^8$	1.52 ± 0.05

Table 7.24 Parameter values obtained for 4-TP nitrosation when [H$^+$] was varied

- **Analysis of Data when [HNO₂] was Varied**

The data in Table 7.21 were analysed using Equation 7.20. Approximate values of k_N were taken from Section 7.5.1.4. The parameter values obtained are in Table 7.25.

Substrate	k_{2ClNO} / dm^3 mol^{-1} s^{-1}	K_N / dm^6 mol^{-2}
2-TI	$3.8 \times 10^9 \pm 2 \times 10^8$	Not obtained due to very small intercept
2-TPM	$7.6 \times 10^9 \pm 6 \times 10^8$	$10\ 000 \pm 2\ 000$

Table 7.25 Parameter values obtained from analysis of data in Table 7.21

7.5.3 Bromide Ion Catalysis in the Nitrosation Reactions

Experiments into the catalysis of the nitrosation reactions by Br⁻ were carried out as described for Cl⁻ catalysis in Section 7.5.2.

7.5.3.1 Varying the Bromide Ion Concentration

The observed first order rate constants obtained when [Br⁻] was varied are in Table 7.26. Plots of k_{obs} versus [Br⁻] gave good straight lines for all three substrates.

[Br$^-$] / mol dm^{-3}	2-TI k_{obs} / s^{-1}	4-TP k_{obs} / s^{-1}	2-TPM k_{obs} / s^{-1}
2.00×10^{-4}	---	---	10.1 ± 0.2
5.00×10^{-4}	---	---	20.4 ± 0.7
1.00×10^{-3}	9.44 ± 0.07	1.67 ± 0.02	35.0 ± 0.3
2.00×10^{-3}	19 ± 1	3.16 ± 0.04	66.2 ± 0.7
3.00×10^{-3}	---	---	99 ± 6
4.00×10^{-3}	34.5 ± 0.2	6.04 ± 0.09	---
8.00×10^{-3}	69.9 ± 0.5	12.0 ± 0.2	---
1.00×10^{-2}	88.0 ± 0.7	16.0 ± 0.2	---
1.50×10^{-2}	133 ± 5	---	---
2.00×10^{-2}	177 ± 6	---	---

Table 7.26 Data for the Br$^-$ catalysed nitrosations when [Br$^-$] was varied. 2-TI: [2-TI] = 4 × 10^{-5} M, [H$^+$] = 0.1 M, [HNO$_2$] = 4 × 10^{-4} M. 4-TP: [4-TP] = 2 × 10^{-5} M, [H$^+$] = 0.1 M, [HNO$_2$] = 2 × 10^{-4} M. 2-TPM: [2-TPM] = 2 × 10^{-5} M, [H$^+$] = 0.1 M, [HNO$_2$] = 3 × 10^{-4} M

7.5.3.2 Varying [H$^+$]

When [H$^+$] was varied the first order rate constants in Table 7.27 were observed. For 2-TI and 2-TPM plots of k_{obs} versus [H$^+$] were linear, whereas for 4-TP a curve like that in Figure 7.20 in Section 7.5.1.3 were obtained.

[H$^+$] / mol dm^{-3}	2-TI k_{obs} / s^{-1}	4-TP k_{obs} / s^{-1}	2-TPM k_{obs} / s^{-1}
1.04×10^{-2}	---	---	6.8 ± 0.3
2.00×10^{-2}	---	---	7.45 ± 0.08
2.50×10^{-2}	26.0 ± 0.7	---	---
4.00×10^{-2}	---	4.69 ± 0.03	12.4 ± 0.2
5.00×10^{-2}	42.2 ± 0.8	---	---
6.00×10^{-2}	---	5.66 ± 0.04	---
7.50×10^{-2}	56.9 ± 0.4	---	---
8.00×10^{-2}	---	6.31 ± 0.06	21.2 ± 0.1
1.00×10^{-1}	74.2 ± 0.4	6.81 ± 0.03	---
1.40×10^{-1}	---	---	33.4 ± 0.1
1.50×10^{-1}	104 ± 2	7.58 ± 0.05	---
2.00×10^{-1}	138 ± 4	8.12 ± 0.09	46.9 ± 0.9
2.50×10^{-1}	176 ± 8	8.47 ± 0.09	---
3.00×10^{-1}	---	9.06 ± 0.06	---
4.00×10^{-1}	---	---	116 ± 7

Table 7.27 Data for Br$^-$ catalysis varying [H$^+$]. 2-TI: [2-TI] = 4 × 10^{-5} M, [HNO$_2$] = 4 × 10^{-4} M, [Br$^-$] = 4 × 10^{-3} M. 4-TP: [4-TP] = 4 × 10^{-5} M, [HNO$_2$] = 4 × 10^{-4} M, [Br$^-$] = 2 × 10^{-3} M

7.5.3.3 Varying [HNO₂]

The results of experiments in which the nitrous acid concentration was varied in the presence of bromide are given in Table 7.28. Plots of k_{obs} versus [HNO$_2$] were linear.

[HNO$_2$] / mol dm^{-3}	2-TI k_{obs} / s^{-1}	4-TP k_{obs} / s^{-1}	2-TPM k_{obs} / s^{-1}
3.00×10^{-4}	---	---	19.7 ± 0.8
4.00×10^{-4}	20.1 ± 0.6	7.01 ± 0.03	---
5.00×10^{-4}	---	9.00 ± 0.07	---
6.00×10^{-4}	27.5 ± 0.5	11.0 ± 0.06	22 ± 1
8.00×10^{-4}	37.5 ± 0.4	15.3 ± 0.2	---
1.00×10^{-3}	45.8 ± 0.6	19.5 ± 0.2	25.8 ± 0.4
2.00×10^{-3}	94 ± 2	---	35.9 ± 0.2
3.00×10^{-3}	---	---	75.6 ± 0.2

Table 7.28 k_{obs} values for Br$^-$ catalysis when [HNO$_2$] was varied. 2-TI: [2-TI] = 4 × 10^{-5} M, [H$^+$] =0.10 M, [Br$^-$] = 5 × 10^{-4} M. 4-TP: [4-TP] = 4 × 10^{-5} M, [H$^+$] = 0.10 M, [Br$^-$] = 2 × 10^{-3} M. 2-TPM: [2-TPM] = 2 × 10^{-5} M, [H$^+$] = 0.1 M, [Br$^-$] = 5 × 10^{-4} M.

7.5.3.4 Analysis of Data for Bromide Ion Catalysis

The data for bromide catalysis was analysed as per that for chloride catalysis in Section 7.5.2.5. K_{BrNO} was taken as 0.052 dm^{-6} mol^{-2}.[28]

- **Analysis of Data when [Br⁻] was Varied**

Table 7.29 contains the parameter values obtained from the analyses.

Substrate	k_{2BrNO} / dm^3 mol^{-1} s^{-1}	k_N / dm^6 mol^{-2} s^{-1}
2-TI	$3.64 \times 10^9 \pm 5 \times 10^7$	---
4-TP	$5.4 \times 10^9 \pm 1 \times 10^8$	Error in intercept to large
2-TPM	$1.88 \times 10^9 \pm 4 \times 10^7$	$10\,000 \pm 3\,000$

Table 7.29 Parameter values obtained when [Br⁻] varied

- **Analysis of Data when [H⁺] was Varied**

The results of the analyses are tabulated below (Table 7.30).

Substrate	k_{2BrNO} / dm^3 mol^{-1} s^{-1}	K_N / dm^6 mol^{-2}	pK_a
2-TI	$7.8 \times 10^9 \pm 2 \times 10^8$	$2.0 \times 10^5 \pm 4 \times 10^4$	---
4-TP	$5.3 \times 10^9 \pm 3 \times 10^8$	---	1.32 ± 0.08
2-TPM	$8.1 \times 10^9 \pm 2 \times 10^8$	$5.5 \times 10^4 \pm 1 \times 10^4$	---

Table 7.30 Parameter values for Br⁻ catalysis when [H⁺] varied

- **Analysis of Data when [HNO₂]$_\tau$ was Varied**

Table 7.31 summarises the results.

Substrate	k_{2BrNO} / dm^3 mol^{-1} s^{-1}	K_N / dm^6 mol^{-2}
2-TI	$4.5 \times 10^9 \pm 2 \times 10^8$	---
4-TP	$2.00 \times 10^9 \pm 3 \times 10^7$	Error in intercept too large
2-TPM	$7.6 \times 10^9 \pm 5 \times 10^8$	$1.4 \times 10^4 \pm 2\,000$

Table 7.31 Parameter values obtained when [HNO₂]$_\tau$ was varied

7.5.4 Iodide Ion Catalysis in the Nitrosation Reactions

4-TP (2×10^{-5} M) was reacted with nitrous acid (2×10^{-3} M) in pH 3.1 citrate buffer with added iodide. Table 7.32 and Figure 7.24 clearly show that iodide catalyses the nitrosation reaction. The significant curvature in the plot of k_{obs} versus [I⁻] probably arises from the decomposition to iodine.

[I⁻] / mol dm⁻³	4-TP k_{obs} / s⁻¹
4.0×10^{-3}	2.51 ± 0.01
8.0×10^{-3}	3.78 ± 0.03
1.2×10^{-2}	4.93 ± 0.03
2.0×10^{-2}	6.4 ± 0.2
4.0×10^{-2}	9.9 ± 0.3

Table 7.32 Data for the I⁻ catalysed nitrosation of 4-TP

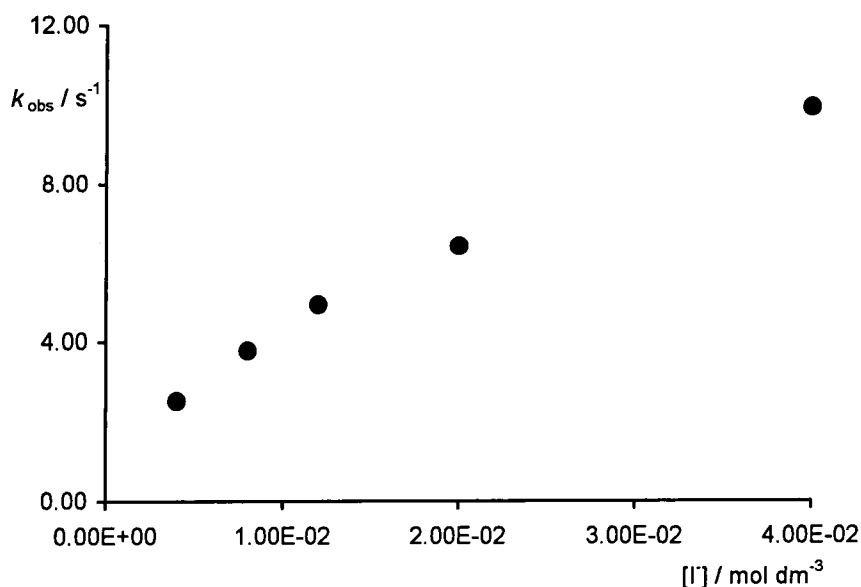

Figure 7.24 k_{obs} versus [I⁻] for the catalysed nitrosation of 4-TP

7.5.5 Thiocyanate Catalysis in the Nitrosation Reactions

Thiocyanate catalysis of the nitrosation of 2-TI and 4-TP was investigated, employing the same techniques used for chloride and bromide catalysis.

7.5.5.1 Experiments where the Thiocyanate Concentration was Varied

When thiocyanate was added as a catalyst, the reaction traces were not first order, but had significant zero order character. This suggests that the formation of ONSCN, the active nitrosating agent, could be rate determining, as has been observed with other substrates (Section 1.1.4). The initial rates observed (calculated as described in Section 7.5.1.2) are given in Table 7.33.

$[SCN^-]$ / mol dm^{-3}	2-TI v_o / mol dm^{-3} s^{-1}	4-TP v_o / mol dm^{-3} s^{-1}
5.00×10^{-5}	$5.3 \times 10^{-5} \pm 1 \times 10^{-6}$	---
1.00×10^{-4}	$9.1 \times 10^{-5} \pm 2 \times 10^{-6}$	$2.3 \times 10^{-5} \pm 1 \times 10^{-6}$
2.00×10^{-4}	---	$5.0 \times 10^{-5} \pm 3 \times 10^{-6}$
3.00×10^{-4}	$2.28 \times 10^{-4} \pm 7 \times 10^{-6}$	---
4.00×10^{-4}	---	$9.1 \times 10^{-5} \pm 2 \times 10^{-6}$
5.00×10^{-4}	$4.7 \times 10^{-4} \pm 2 \times 10^{-5}$	---
8.00×10^{-4}	---	$1.6 \times 10^{-4} \pm 1 \times 10^{-5}$
1.00×10^{-3}	$8.5 \times 10^{-4} \pm 2 \times 10^{-5}$	$2.2 \times 10^{-4} \pm 2 \times 10^{-5}$
2.00×10^{-3}	$1.60 \pm 10^{-3} \pm 5 \times 10^{-5}$	$4.0 \times 10^{-4} \pm 2 \times 10^{-5}$
6.00×10^{-3}	---	---
1.00×10^{-2}	---	---

Table 7.33 2-TI: $[2\text{-TI}] = 4 \times 10^{-5}$ M, $[H^+] = 0.1$ M, $[HNO_2] = 4 \times 10^{-4}$ M.
4-TP: $[4\text{-TP}] = 2 \times 10^{-5}$ M, $[H^+] = 0.1$ M, $[HNO_2] = 2 \times 10^{-4}$ M

7.5.5.2 Experiments where the Substrate Concentration was Varied

For 2-TI the substrate concentration was varied when thiocyanate was present as a catalyst. Traces exhibiting significant zeroth order character were observed, and the initial rates obtained from these are tabulated below (Table 7.34).

$[S]_\tau$ / mol dm^{-3}	2-TI v_o / mol dm^{-3} s^{-1}
2.00×10^{-5}	$3.2 \times 10^{-4} \pm 2 \times 10^{-5}$
4.00×10^{-5}	$3.3 \times 10^{-4} \pm 2 \times 10^{-5}$
6.00×10^{-5}	$3.4 \times 10^{-4} \pm 2 \times 10^{-5}$
8.00×10^{-5}	$3.5 \times 10^{-4} \pm 2 \times 10^{-5}$
1.00×10^{-4}	$3.6 \times 10^{-4} \pm 2 \times 10^{-5}$
2.00×10^{-4}	$4.1 \times 10^{-4} \pm 2 \times 10^{-5}$
4.00×10^{-4}	$5.1 \times 10^{-4} \pm 3 \times 10^{-5}$
6.00×10^{-4}	$6.1 \times 10^{-4} \pm 3 \times 10^{-5}$
8.00×10^{-4}	$7.4 \times 10^{-5} \pm 4 \times 10^{-5}$
1.00×10^{-3}	$8.1 \times 10^{-4} \pm 4 \times 10^{-5}$
1.50×10^{-3}	$1.1 \times 10^{-3} \pm 6 \times 10^{-5}$
2.00×10^{-3}	$1.3 \times 10^{-3} \pm 7 \times 10^{-5}$

Table 7.34 $[H^+] = 0.1$ M, $[HNO_2] = 8 \times 10^{-4}$ M, $[SCN^-] = 2 \times 10^{-4}$ M

7.5.5.3 Analysis of Data for Thiocyanate Catalysis

Considering Scheme 7.2, with the formation of the active nitrosating agent (ONSCN) rate limiting, the expression for the initial rate is given by Equation 7.24. This includes a term for the uncatalysed reaction.

$$v_o = k_{ONSCN}\left[SCN^-\right]\left[H^+\right]\left[HNO_2\right] + k_N\left[H^+\right]\left[HNO_2\right]\left[S\right]_\tau \qquad \text{Equation 7.24}$$

Plotting v_o versus [SCN$^-$] should be linear with an intercept: such a plot is shown in Figure 7.25 for 4-TP nitrosation.
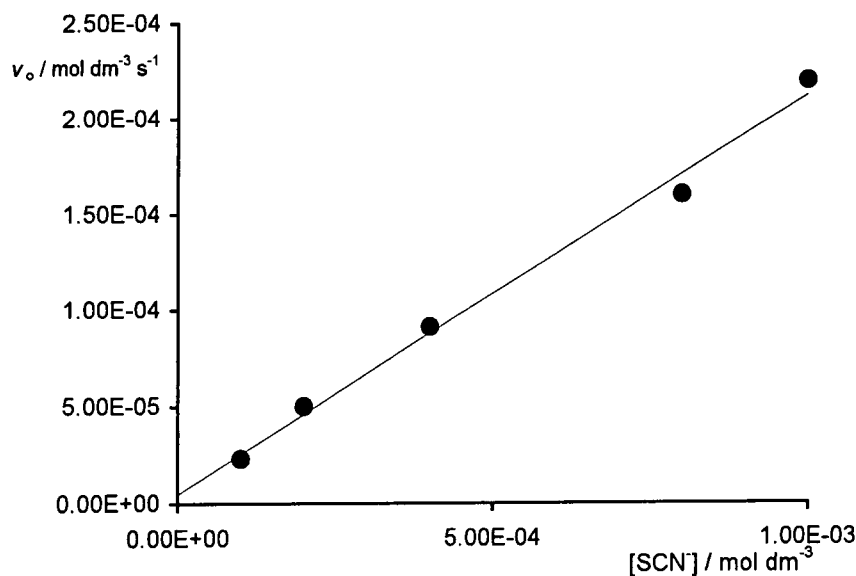

Figure 7.25 v_o versus [SCN$^-$] for 4-TP nitrosation

Figure 7.26 shows v_o plotted against $[2\text{-TI}]_\tau$ for the nitrosation of 2-thioimidazole.
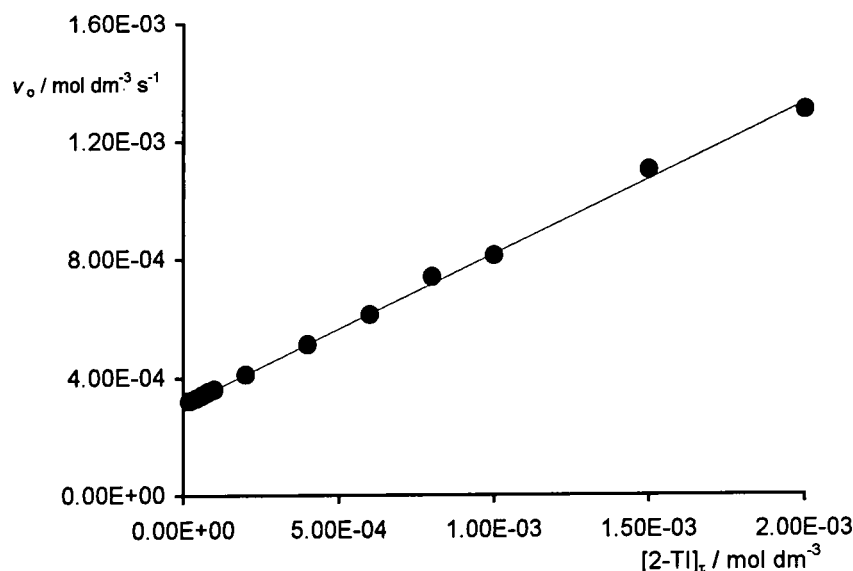

Figure 7.26 v_o versus $[2\text{-TI}]_\tau$ for SCN⁻ catalysed nitrosation of 2-TI

Analysis of the data obtained for thiocyanate catalysis using Equation 7.23 yields the values given in Table 7.35.

Substrate	Varied	k_{ONSCN} / dm³ mol⁻¹ s⁻¹	k_N / dm⁶ mol⁻² s⁻¹
2-TI	[SCN⁻]	19 900 ± 900	Error in intercept too large
	$[2\text{-TI}]_\tau$	18 800 ± 550	2 600 ± 300
4-TP	[SCN⁻]	10 000 ± 1 000	Error in intercept too large

Table 7.35 Parameter values obtained from studies into SCN⁻ catalysis

7.6 Summary and Conclusions

The spectral data obtained for the reaction of nitrous acid with the thiones under acidic conditions indicates that nitrosation occurs. The rapidity of the reactions, yellow colour of the products, and the acid dependence of the nitrosation equilibria indicate that the nitrosation occurs at the sulfur site, resulting in the formation of =SNO⁺ species. The results of the decomposition studies in Chapter 8 show that the nitroso species rapidly decompose to disulfides, confirming the nature of the nitrosation reaction being observed. Nitrosation to form =SNO⁺ cations is expected by analogy with the reactions of thioureas and 2-thiopyridine with nitrous acid.[15,18,19]

Table 7.36 lists the averaged values obtained for each parameter following the analyses in the preceding sections.

Parameter	2-TI	4-TP	2-TPM
K_N / dm^6 mol^{-2}	$1.6 \times 10^5 \pm 3 \times 10^4$	$2.0 \times 10^7 \pm 8 \times 10^5$	$\sim 10^3 - 10^4$
k_N / dm^6 mol^{-2} s^{-1}	$7.9 \times 10^3 \pm 9 \times 10^2$	$7 \times 10^3 \pm 1 \times 10^3$	$\sim 10^4$
k_{2ONCl} / dm^3 mol^{-1} s^{-1}	$2.7 \times 10^9 \pm 2 \times 10^8$	$3.2 \times 10^9 \pm 3 \times 10^7$	$8 \times 10^9 \pm 5 \times 10^9$
k_{2ONBr} / dm^3 mol^{-1} s^{-1}	$4.1 \times 10^9 \pm 4 \times 10^8$	$5.4 \times 10^9 \pm 5 \times 10^7$	$6 \times 10^9 \pm 2 \times 10^9$

Table 7.36 Parameter values for thione nitrosations

Parameter values determined that are independent of the thione studied are:

$$k_{N_2O_3} = 39 \pm 7 \text{ dm}^3 \text{ mol}^{-1} \text{ s}^{-1}$$

$$k_{ONSCN} = 1.6 \times 10^4 \pm 4 \times 10^3 \text{ dm}^6 \text{ mol}^{-2} \text{ s}^{-1}$$

- **Equilibrium Constants**

The value of K_N is greatest for 4-thiopyridine and is probably the largest nitrosation constant known. The value of K_N obtained for 2-TI is similar to the value obtained in a study of the nitrosation of 2-thiopyridine.[19] For 2-TPM, the value of K_N is subject to considerable uncertainty, but is probably 10^3 to 10^4 dm^6 mol^{-2}. This is similar to the values obtained for the nitrosations of thioureas.[18]

- **Uncatalysed Nitrosations**

The values of k_N for the uncatalysed nitrosations are similar for all three substrates, though that for 2-thiopyrimidine has not been determined with great certainty. The nitrosation of thiols and thiones is generally facile, and the values of k_N obtained in this study probably represent reactions with rate constants approaching the diffusion limit.[28] Similar observations have been made regarding the nitrosation of 2-thiopyridine,[19] 2-thiopyridine *N*-oxide,[29] and thiourea.[15]

When the nitrosations were carried out under conditions where [HNO$_2$] was in excess, the active nitrosating agent became N$_2$O$_3$ rather than the nitrous acidium ion. This has been observed previously, including for the nitrosation of 2-thiopyridine.[19] The rate constant obtained for the formation of N$_2$O$_3$ from nitrous

acid was 39 dm^3 mol^{-1} s^{-1}. Values between 13 and 40 dm^3 mol^{-1} s^{-1} have been reported previously.[27]

• **Catalysed Nitrosation**

The results show that the nitrosation of all three substrates can be catalysed by Cl$^-$ and Br$^-$. I$^-$ catalysis also occurs, though this was only examined for 4-TP. The instability of acidified I$^-$ solutions prevented a numerical analysis of the effect of this catalyst. Catalysis by SCN$^-$ was demonstrated for 2-TI and 4-TP, and is also expected to occur for 2-TPM.

Figure 7.27 compares the extent of catalysis of 2-TI nitrosation by Cl$^-$ and Br$^-$. The reaction is clearly catalysed more strongly by bromide than by chloride (gradient for the bromide data is 8824 dm^3 mol^{-1} s^{-1} compared with 145 dm^3 mol^{-1} s^{-1} for chloride), and this is typical for nitrosation reactions.[28] This large difference has its origin not in the relative values of k_{2ONX} but in fact that the equilibrium constant for ONX formation is larger for Br$^-$ than for Cl$^-$.
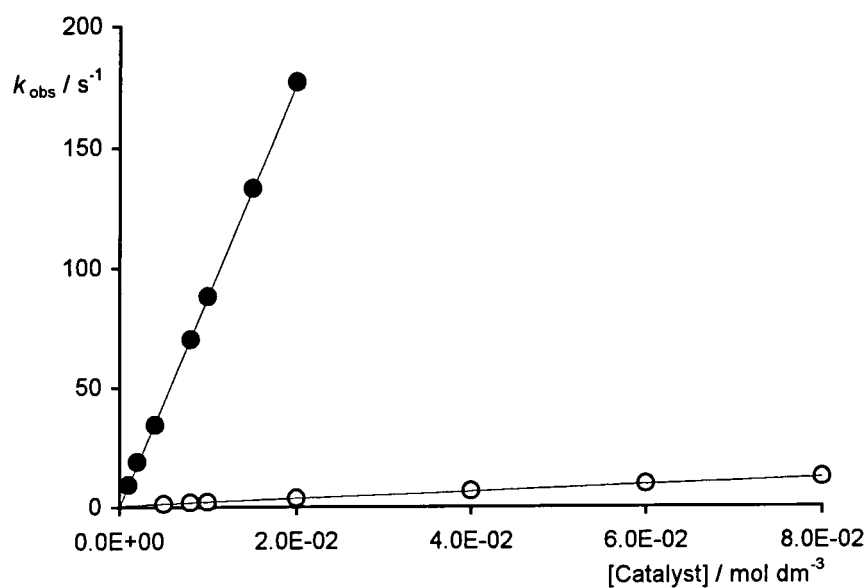

Figure 7.27 Comparison of catalysis of 2-TI nitrosation by Cl$^-$ (o) and Br$^-$ (●)

With Cl$^-$ and Br$^-$ catalysis the rate determining step is the reaction between the substrate and the nitrosyl halide (XNO), and the rate constants obtained for this step probably approach the diffusion limit: this explains why there is no discernable difference between the rate constants obtained.

In the case of thiocyanate catalysis, the rate-determining step was not the reaction between the substrate and nitrosyl thiocyanate, but was the formation of the nitrosyl thiocyanate. The rate constant obtained for the formation of ONSCN was 16 000 dm^6 mol^{-2} s^{-1}, and this compares reasonably favourably with the literature value of 11 000 dm^6 mol^{-2} s^{-1}.[28]

7.7 References

1. R. A. Jones and A. R. Katritzky, *J. Chem. Soc.*, 3610 (1958).

2. A. Albert and G. B. Barlin, *J. Chem. Soc.*, 2384 (1959).

3. A. Albert and G. B. Barlin, *J. Chem. Soc.*, 3129 (1962).

4. D. Bouin-Roubald, J. Kister, M. Rajzmann, L. Bouscasse, *Can. J. Chem.*, **59**, 2883 (1981).

5. L. Stefaniak, G. A. Webb, C. Brevard, M. Bourdonneau, R. Lejeune, L. Thunus and C. L. Lapière, *Mag. Res. Chem.*, **23**, 790 (1985).

6. P. Beak, F. S. Fry, Jr., J. Lee and F. Steele, *J. Am. Chem. Soc.*, **98**, 171 (1976).

7. M. J. Cook, S. El-Abbady, A. R. Katritzky, C. Guimon and G. Pfister-Guillouzo, *J. Chem. Soc., Perkin Trans. 2*, 1652 (1977).

8. M. C. Etter, J. C. MacDonald and R. A. Wanke, *J. Phys. Org. Chem.*, **5**, 191 (1992).

9. P. Beak, J. B. Covington, S. G. Smith, J. M. White and J. M. Zeigler, *J. Org. Chem.*, **45**, 1354 (1980).

10. P. Beak, *Acc. Chem. Res.*, **10**, 186 (1977).

11. M. M. Karelson, A. R. Katritzky, M. Szafran and M. C. Zerner, *J. Org. Chem.*, **54**, 6030 (1989).

12. A. Gordon and A. R. Katritzky, *Tet. Lett.*, **25**, 2767 (1968).

13. P. Beak, J. B. Covington and J. M. White, *J. Org. Chem.*, **45**, 1347 (1980).

14. E. A. Werner, *J. Chem. Soc.*, **101**, 2180 (1912).

15. K. Al-Mallah, P. Collings and G. Stedman, *J. Chem. Soc., Dalton Trans.*, 2469 (1974).

16. P. Collings, M. Garley and G. Stedman, *J. Chem. Soc., Dalton Trans.*, 331 (1981).

17. M. S. Garley, G. Stedman and H. Miller, *J. Chem. Soc., Dalton Trans.*, 1959 (1984).

18. P. Collings, K. Al-Mallah and G. Stedman, *J. Chem. Soc., Perkin Trans. 2*, 1734 (1975).

19. S. Amado, A. P. Dicks and D. L. H. Williams, *J. Chem. Soc., Perkin Trans. 2*, 1869 (1998).

20. D. T. Hurst, S. G. Jones, J. Outram and R. A. Patterson, *J. Chem. Soc., Perkin Trans. 1*, 1688 (1977).

21. D. D. Perrin, 'Dissociation Constants of Organic Bases in Aqueous Solution: Supplement 1972', International Union of Pure and Applied Chemistry, 1972

22. Microsoft® Excel 97.

23. J. Barrett, D. F. Debenham and J. Glauser, *J. Chem. Soc., Chem. Comm.*, 248 (1965).

24. MicroMath® Scientist® for Windows®, Version 2.02.

25. J. Tummavuori and P. Lumme, *Acta. Chem. Scand.*, **22**, 2003 (1968).

26. B. G. Cox, 'Modern Liquid Phase Kinetics', Oxford University Press, Oxford, 1994.

27. M. S. Garley and G. Stedman, *J. Inorg. Nucl. Chem.*, **43**, 2863 (1981).

28. D. L. H. Williams, 'Nitrosation', Chapter 1, Cambridge University Press, Cambridge, 1988.

29. L. Blakelock, 4th Year Research Project, University of Durham, 2000.

Decomposition Reactions of S-Nitrosated Nitrogen Heterocycles

Chapter 8 Decomposition Reactions of *S*-Nitrosated Nitrogen Heterocycles

8.1 Introduction

In Chapter 7 it was demonstrated that the thiones 2-thioimidazole (2-TI), 4-thiopyridine (4-TP) and 2-thiopyrimidine (2-TPM) can be readily nitrosated, resulting in the formation of $=SNO^+$ cations. These are known to be unstable, and have been shown to decompose to disulfides in studies on the nitrosation of thioureas [1,2,3,4] and 2-thiopyridine (2-TP).[5]

This chapter presents the results of studies carried out into the decomposition of the nitroso products described in Chapter 7. Thione concentrations [ ]$_t$ refer to the total thione concentration, including the thione present as the free thione, the nitrosated species, and the corresponding disulfide. All the reactions in this section were carried out at 25 °C.

8.2 *S*-Nitrosated 2-Thioimidazole

In Section 7.3.1 UV / visible spectrophotometric investigations into the nitrosation of 2-thioimidazole revealed the formation of an *S*-nitroso species, which then decomposed. The formation and decomposition reactions were sufficiently well separated to allow kinetic studies to be carried out using the stopped flow technique. However, the decomposition of the nitroso product was often the only process observed in the spectral studies.

The final products of the initial nitrosation studies in Section 7.3.1 exhibited identical spectra irrespective of the nitrous acid concentration employed, and these represent the products of the decomposition of the *S*-nitroso species. Figure 8.1 shows the spectrum obtained after the decomposition of the *S*-nitroso species superimposed upon the spectrum of 2-thioimidazole disulfide. The similarity of the two spectra strongly suggests that *S*-nitrosated 2-thioimidazole decomposes to the disulfide (Figure 8.2), as do other *S*-nitrosated thiones such as 2-thiopyridine.[5]
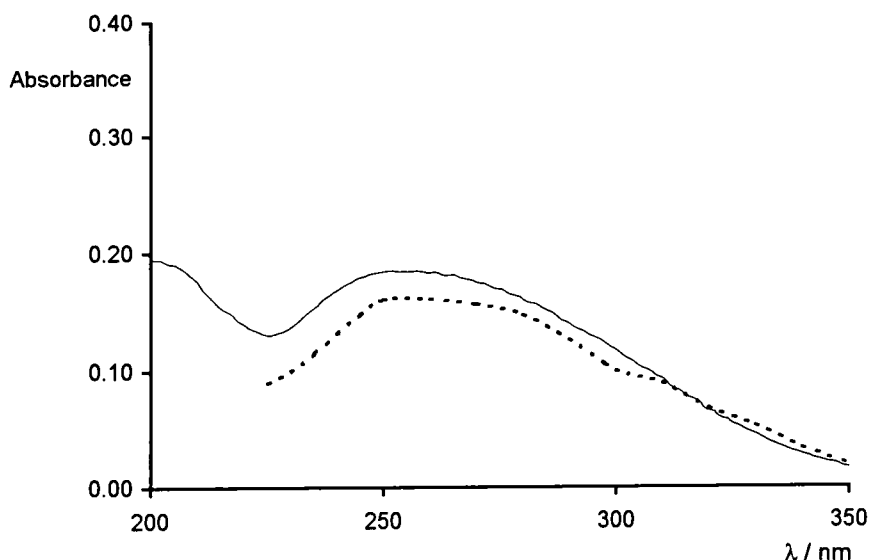
Figure 8.1 Spectra of product of S-nitrosated 2-TI decomposition, solid line ([2-TI]$_\tau$ = 4 ×
10^{-5} M) and of 2-TI disulfide, dashed line, taken from data in reference 6
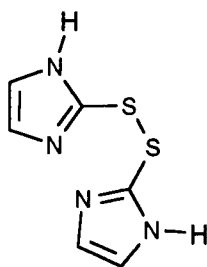([disulfide] ~ 2 × 10^{-5} M)

Figure 8.2 Structure of 2-TI disulfide

Repeat scans of the decomposition product obtained over several hours revealed
that further spectral changes occurred (Figure 8.3). Oxidation of a sample of 2-TI
(1 × 10^{-4} M) by hydrogen peroxide (1 × 10^{-4} M) resulted in the formation of a
species with the same spectrum as that finally obtained in Figure 8.3. These results,
alongside studies reported in the literature on the oxidation of 2-thioimidazole,[6]
suggest that oxidation of the disulfide occurs.
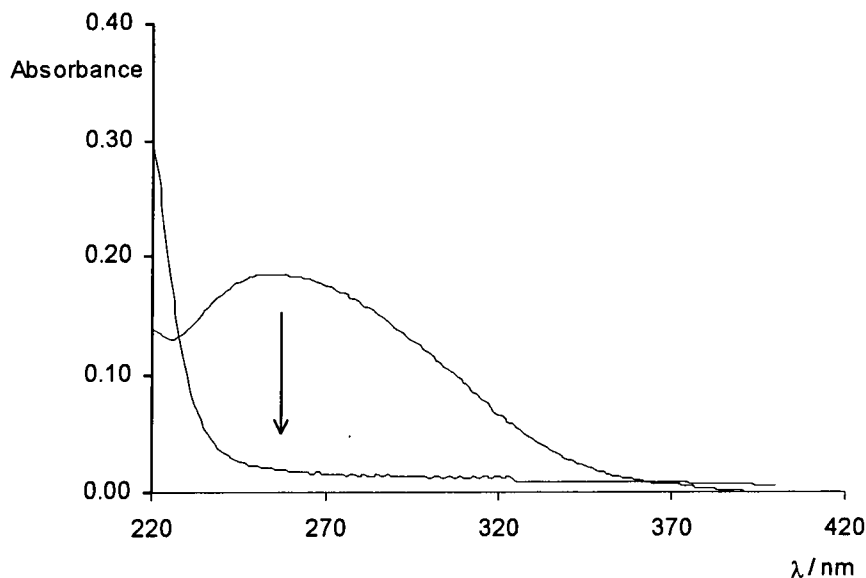
Figure 8.3 Oxidation of the *S*-nitrosated thioimidazole decomposition product
$([2\text{-TI}]_\tau = 4 \times 10^{-5} \text{ M})$

A previous preliminary study into the nitrosation of 2-thioimidazole erroneously assigned the broad spectrum in Figure 8.1 to that of the nitrosated species rather than the disulfide.[7] The decomposition of this was found to result in the formation of a species with a spectrum identical to that produced by the disulfide oxidation in Figure 8.3, and was taken to be the formation of the disulfide from the nitrosated species,[7] but it seems more likely that the oxidation of the disulfide was being observed.

When 2-thioimidazole was nitrosated and an aliquot of the reaction solution quenched into pH 7.4 buffer, the spectral changes in Figure 8.4 were observed. The spectrum of the final product resembles that of the thione, so it was initially thought that the process represented the hydrolysis of the nitrosated species, as observed in 2-thiopyridine nitrosation.[5]
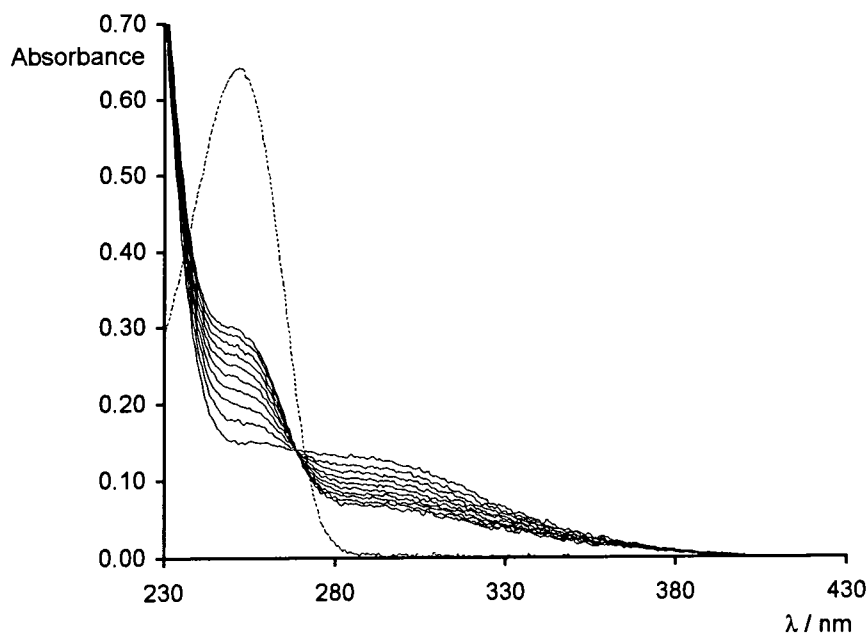
Figure 8.4 2-TI nitrosation solution at pH 7.4 showing reformation of the thione at 250 nm. $[2\text{-TI}]_{\tau} = 4 \times 10^{-5}$ M. $\Delta t = 3$ min. Dashed line represents spectrum of 4×10^{-5} M 2-TI

The facile decomposition of the nitroso species observed in other experiments makes it unlikely that the spectra in Figure 8.4 represent hydrolysis of the nitrosated species. It is more likely that the spectra show the re-formation of the thione from the disulfide. Similar observations have been reported for 2-TI, 4-TP and 2-TPM, where samples of disulfide kept in the dark reverted to the thiones.[8]

The decomposition of *S*-nitrosated 2-thiopyridine under acidic conditions forms the disulfide and nitric oxide.[5] The nitric oxide produced is oxidised under aerobic conditions, eventually forming nitrosating agents such as N_2O_3, which can then nitrosate any excess thione present, thus converting all of the thione initially present to the disulfide. To establish whether this also occurred in 2-thioimidazole nitrosation, 2-TI (8×10^{-5} M) was reacted with nitrous acid (2×10^{-5} M) in 0.1 M perchloric acid. The final spectrum obtained showed no thione peak, and had an absorbance corresponding to a disulfide concentration of 4×10^{-5} M, as expected if all of the thione was converted to the disulfide.

8.2.1 Summary of 2-Thioimidazole Nitrosation

From the results above, and those in Chapter 7 for 2-thioimidazole nitrosation, the reaction scheme in Scheme 8.1 can be proposed.
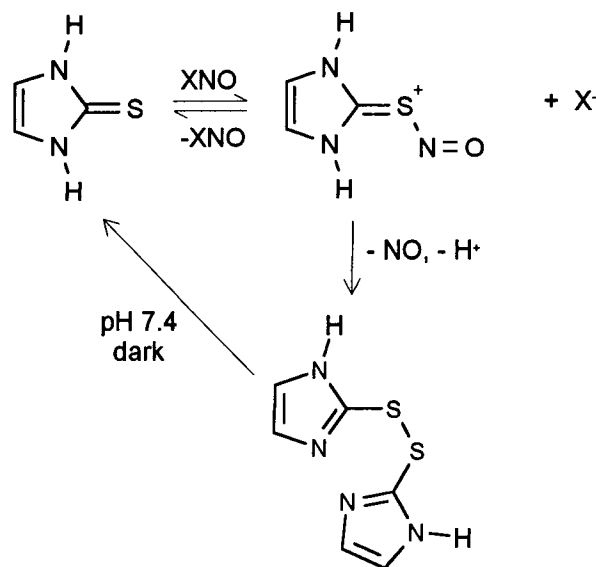
Scheme 8.1 Proposed scheme for the nitrosation reactions observed with 2-TI

8.3 Decomposition of Nitrosated 4-Thiopyridine

8.3.1 Acidic Conditions

At pH 1 the nitrosated species decomposed, the small shoulder at 400 nm and the peak at 550 nm decreasing in intensity. The expected product of the decomposition is the disulfide, as observed during the nitrosation of other thiones. However, at pH 1 the spectrum of the disulfide and the nitrosated species are very similar, making it difficult to distinguish between them. This suggests the disulfide exists as the dication shown in Figure 8.5 (pK_{a1} ~ 4.5, pK_{a2} ~ 5), which would be expected to have a similar spectrum to the nitroso cation in the UV region, but with double the extinction coefficient. This contrasts with 2-thioimidazole where the nitrosated species and the disulfide have different spectra, presumably because the latter is deprotonated.
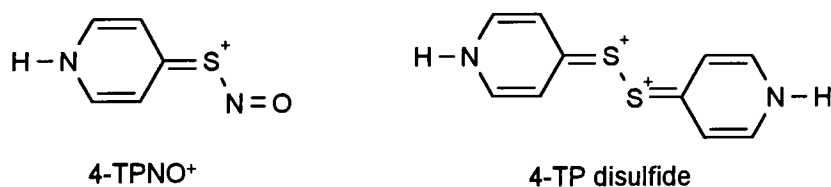

Figure 8.5 Structures of nitrosated 4-TP (4-TPNO⁺) and 4-TP disulfide

Figure 8.6 shows the spectral changes observed when nitrosated 4-TP (prepared at pH 1) was added to a solution of pH 3.1 citrate buffer. The initial spectrum shows

the presence of some thione (λ_{max} 325 nm), the nitrosation equilibrium having adjusted to the new pH regime. Over time, the peak due to the thione decreases in intensity, leading to an increasing absorbance at 278 nm. An isosbestic point is observed at 295 nm. The final spectrum corresponds to that of 4-thiopyridine disulfide, and given the very stable nature of the thione this must be formed by the decomposition of the nitrosated species rather than the oxidation of the thione.
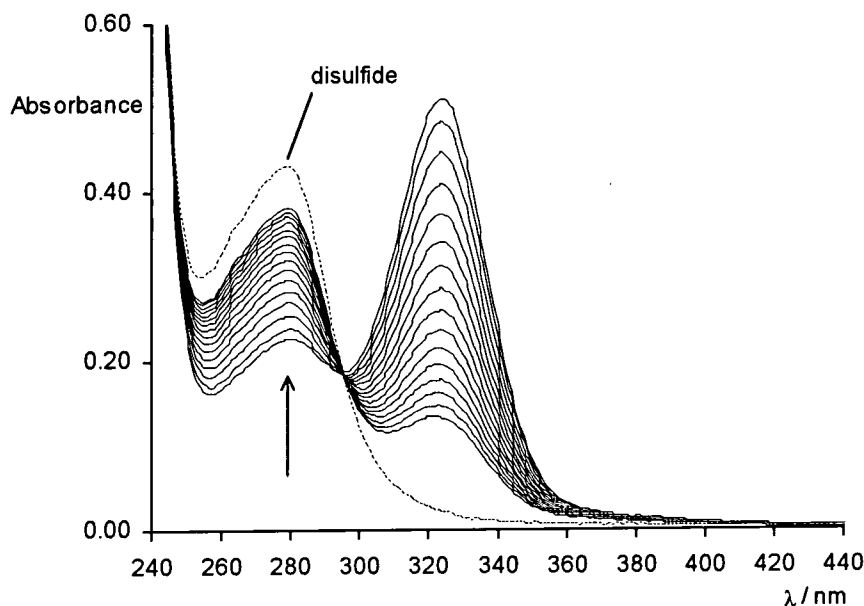

Figure 8.6 Decomposition of nitrosated 4-TP at pH 3.1, spectra taken every 2 minutes. [4-TP]$_\tau$ = 4 × 10^{-5} M. Spectrum of disulfide (2 × 10^{-5} M) is shown for comparison

As with 2-thioimidazole nitrosation, nitrosation of 4-thiopyridine in the presence of a lower concentration of nitrous acid leads to quantitative disulfide formation from the thione.

8.3.1.1 Decomposition Studies Using the Nitric Oxide Electrode

In Chapter 7, decomposition of nitrosated 2-thioimidazole was shown to produce nitric oxide, and similar observations have been made for the nitrosation of 2-thiopyridine [5] and thiourea.[1] The decomposition of nitrosated 4-thiopyridine under acidic conditions yields the disulfide (see above), and the other product is therefore expected to be nitric oxide.

In situ nitrosation of 4-thiopyridine was carried out in the nitric oxide electrode apparatus using a large excess of 4-thiopyridine. The reasons for the use of excess 4-thiopyridine were:

- To ensure complete conversion of the nitrous acid to the nitroso product

- To ensure rapid nitrosation whilst maintaining a low enough theoretical nitric oxide yield to be measured

- To enhance the rate of nitrosated product decomposition (studies on *S*-nitroso thiourea decomposition showed that the rate of decomposition was enhanced by adding thiourea)[2]

The required quantity of 4-thiopyridine was weighed out and placed into the nitric oxide electrode apparatus. Perchloric acid and water were then added to give a final $[H^+]$ of 0.1 M, and the thione dissolved by stirring. The solution was purged with nitrogen for 15 minutes, after which the nitrogen stream was turned off and the electrode zeroed and data collection initiated. The appropriate quantity of a solution of sodium nitrite was then injected, maintaining stirring continuously. The yields of nitric oxide produced, and the rate constants for its formation are given in Table 8.1.

$[\text{4-TP}]_t$ / mol dm^{-3}	NO yield / %	k_{obs} / s^{-1}
2.00×10^{-3}	99	0.047
4.00×10^{-3}	98	0.099
4.00×10^{-3}	100	0.10

Table 8.1 Nitric oxide yields from nitrosated 4-TP decomposition in 0.1 M HClO$_4$. $[\text{4-TPNO}^+] = 3 \times 10^{-6}$ M.

When the experiment was carried out without excess 4-TP, injecting an aliquot of nitrosated 4-TP (prepared with a 1:1 ratio of HNO$_2$: 4-TP and allowing one minute for the nitrosation to reach completion) into a solution of 0.1 M perchloric acid, nitric oxide was detected, but its formation was slow.

8.3.2 Decomposition at pH 7.4

When an aliquot of nitrosated 4-thiopyridine (prepared at pH 1 using a ten-fold excess of nitrous acid) was quenched into pH 7.4 buffer the thione was reformed (Figure 8.7). This was also observed in the case of 2-thiopyridine nitrosation.[5]
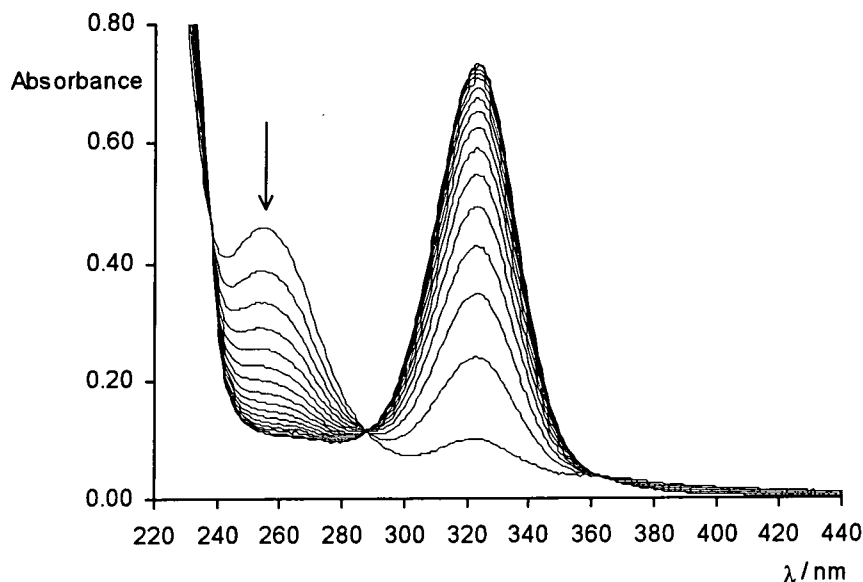

Figure 8.7 Nitrosated 4-TP decomposition at pH 7.4, spectra acquired every 2 minutes.
$[4\text{-TP}]_t = 4 \times 10^{-5}$ M.

The initial spectrum in Figure 8.7 has a peak at 255 nm and 325 nm (the latter due to the thione). The nitrosated species 4-TPNO$^+$ absorbs at 280 nm, so the peak at 255 nm must be due to another species: probably the deprotonated S-nitroso species 4-TPNO (Scheme 8.2). Similar observations were made when 2-thiopyridine was nitrosated.[5]
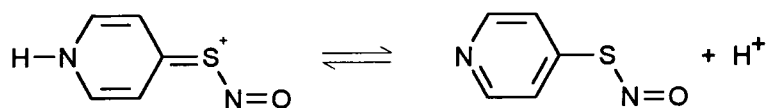
Scheme 8.2 Deprotonation of 4-TPNO$^+$

When a solution of nitrosated 4-thiopyridine was raised to pH 7.4, the 280 nm peak was replaced by the 255 nm peak. Lowering the pH back to pH 1 reformed the 280 nm peak and eliminated the 255 nm peak, demonstrating the reversibility of the deprotonation in Scheme 8.2. The pK_a for this process was estimated at 4.5 by obtaining spectra at a range of pH values.
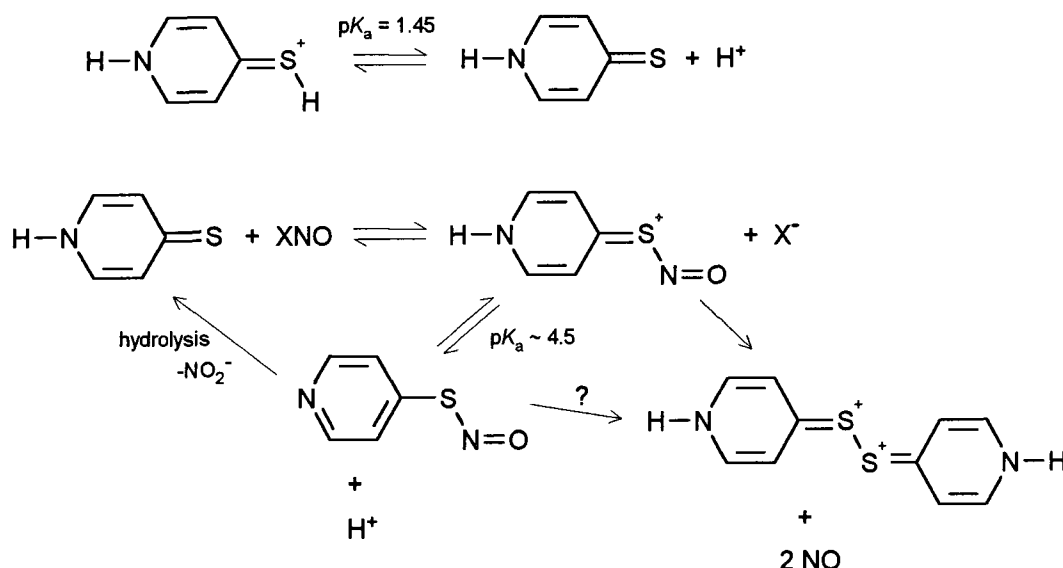
Further studies on the decomposition of nitrosated 4-thiopyridine at pH 7.4 shown in Figure 8.7 revealed that 68 % of [4-TP]$_\tau$ was converted to the thione, and the rest to the disulfide. This was established by subtracting the spectra obtained from various ratio mixtures of the thione and disulfide from the decomposition product spectrum until a level zero baseline was obtained. When solutions of the nitrosated species were allowed to stand at pH 1 before being quenched to pH 7.4, the final product composition changed, with more disulfide being produced when the standing time was longer (Table 8.2). This shows that much of the disulfide is formed by decomposition in the pH 1 solution prior to addition to the pH 7.4 solution.

Standing time / minutes	% [4-TP]$_\tau$ detected as thione	% [4-TP]$_\tau$ detected as disulfide
2	73	37
7	60	45
12	53	50

Table 8.2 Products of nitrosated 4-TP decomposition as a feature of standing time in acid prior to addition to pH 7.4 solution

8.3.3 Summary of 4-Thiopyridine Nitrosation

The reactions which have been identified during 4-TP nitrosation are in Scheme 8.3.

Scheme 8.3 Nitrosation of 4-TP

8.4 Further Studies on Nitrosated 4-Thiopyridine

8.4.1 Role of Copper Sources in Nitrosated 4-Thiopyridine Decomposition

The role of copper sources in the decomposition of nitrosated 4-thiopyridine at pH 7.4 was investigated. The ability of 4-thiopyridine to reduce Cu^{2+} to Cu^+ was tested by using the specific Cu^+ chelator neocuproine to detect any Cu^+ produced, the Cu(1)-neocuproine complex formed absorbs at 450 nm.[9] Ascorbic acid was used as a control reducing agent. The results are in Table 8.3 and show that 4-thiopyridine will reduce Cu^{2+} to Cu^+.

Reductant	$[Cu^{2+}]$ / mol dm^{-3}	[Reductant] / mol dm^{-3}	[Neocuproine] / mol dm^{-3}	Absorbance at 450 nm
None	5×10^{-5}	---	5.6×10^{-4}	0.01
Ascorbic acid	5×10^{-5}	5×10^{-5}	5.6×10^{-4}	0.37
4-thiopyridine	5×10^{-5}	5×10^{-5}	5.6×10^{-4}	0.33
4-thiopyridine	5×10^{-5}	1×10^{-4}	5.6×10^{-4}	0.40

Table 8.3 Production of Cu^+ from Cu^{2+} reduction by ascorbic acid and 4-TP at pH 7.4

The decomposition of nitrosated 4-thiopyridine at pH 7.4 was studied spectrophotometrically in the presence of various concentrations of $[Cu^{2+}]$. 4-thiopyridine was nitrosated in 0.1 M perchloric acid, allowing two minutes for the nitrosation to reach completion. The nitrosated species was then added to solutions containing pH 7.4 buffer, and the decomposition of the nitrosated species followed at 255 nm, 25 °C. The rate constants obtained for the decomposition showed no variation with the copper concentration (Table 8.4), therefore the decomposition observed was due to the hydrolysis of the nitroso species, rather than a copper catalysed route.

$[Cu^{2+}]$ added / mol dm^{-3}	k_{obs} / s^{-1}
$0 + 1 \times 10^{-4}$ M EDTA	$1.30 \times 10^{-3} \pm 5 \times 10^{-6}$
5.00×10^{-6}	$1.23 \times 10^{-3} \pm 4 \times 10^{-6}$
1.00×10^{-5}	$1.21 \times 10^{-3} \pm 3 \times 10^{-6}$
2.00×10^{-5}	$1.27 \times 10^{-3} \pm 4 \times 10^{-6}$
4.00×10^{-5}	$1.24 \times 10^{-3} \pm 4 \times 10^{-6}$
1.00×10^{-4}	$1.24 \times 10^{-3} \pm 5 \times 10^{-6}$

Table 8.4 Rate constants for the decomposition of nitrosated 4-TP at pH 7.4 in the presence of added $[Cu^{2+}]$

Figure 8.8 shows the traces obtained when nitrosated 4-thiopyridine decomposition was monitored using the nitric oxide electrode in the presence of various copper sources. The traces show that Cu^+ will promote nitric oxide release from nitrosated 4-TP, and that copper metal also promotes nitric oxide release, though the active form of the copper is unknown. EDTA prevents the nitric oxide production.
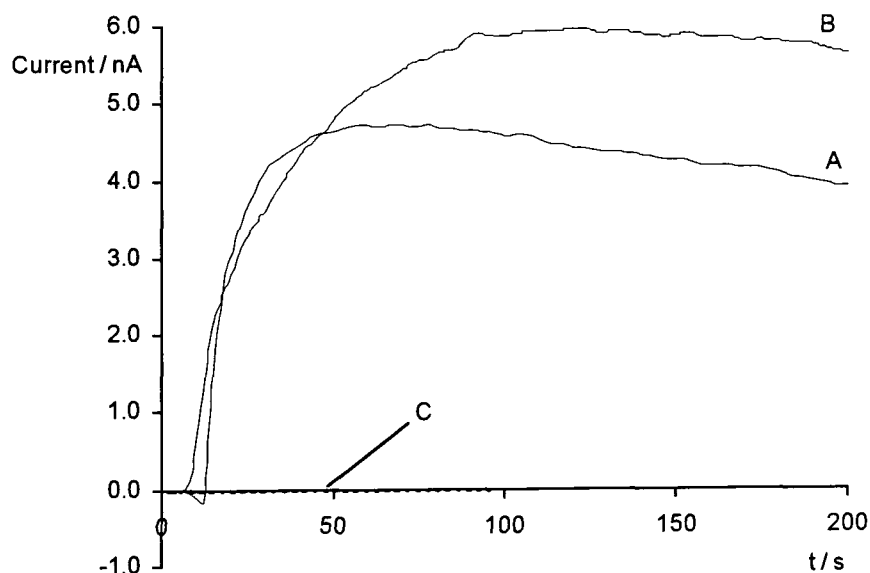

Figure 8.8 NO production from 4-TPNO decomposition. A: $[4\text{-TP}]_\tau = 3 \times 10^{-6}$ M, 2 mg Cu(I)Cl. B: $[4\text{-TP}]_\tau = 3 \times 10^{-6}$ M, 1 cm $\times$ 1 cm Cu strip. C: As A but with 0.1 M EDTA

8.4.2 Role of Ascorbic Acid in Nitrosated 4-Thiopyridine Decomposition

The possibility of decomposition of nitrosated 4-thiopyridine by the copper ion independent ascorbic acid pathway (Chapters 3 – 6) was investigated. Figure 8.9 shows the spectral changes observed when ascorbic acid (4 $\times$ 10^{-5} M) was reacted with nitrosated 4-thiopyridine ($[4\text{-TP}]_\tau = 4 \times 10^{-5}$ M, nitrosated at pH 1 with 1: 1 HNO_2: 4-TP). The reaction was carried out in pH 7.4 buffer with 1 $\times$ 10^{-4} M EDTA present to complex out metal ions, and shows instantaneous loss of ascorbic acid accompanied by formation of the thione (325 nm).
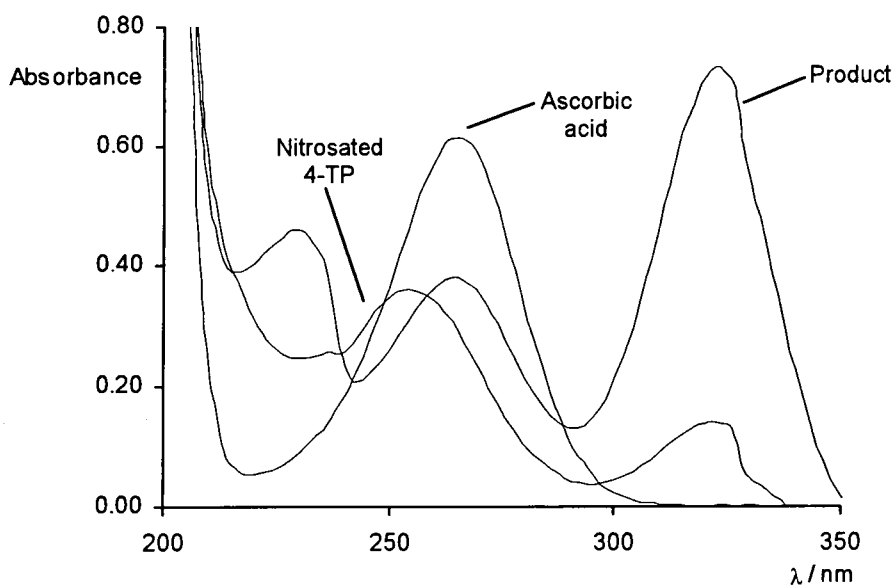
Figure 8.9 Reaction between ascorbic acid and nitrosated 4-TP at pH 7.4

Following the formation of nitric oxide using the nitric oxide electrode showed that the rate of nitric oxide production was dependent upon the ascorbic acid concentration, and the reaction traces were first order. The observed first order rate constants are given in Table 8.5.

$[H_2A]_\tau$ / mol dm^{-3}	k_{obs} / s^{-1}
2×10^{-6}	$1.3 \times 10^{-2} \pm 2 \times 10^{-4}$
3×10^{-6}	$1.9 \times 10^{-2} \pm 3 \times 10^{-4}$
4×10^{-6}	$2.5 \times 10^{-2} \pm 4 \times 10^{-4}$
8×10^{-6}	$4.2 \times 10^{-2} \pm 9 \times 10^{-4}$
1.2×10^{-5}	$1.2 \times 10^{-1} \pm 4 \times 10^{-4}$

Table 8.5 Rate constants for NO production in the reaction between nitrosated 4-thiopyridine ($[4\text{-TP}]_\tau = 2 \times 10^{-7}$ M) and ascorbic acid with EDTA (1×10^{-4} M) at pH 7.4, 25 °C

A plot of k_{obs} versus $[H_2A]_\tau$ was linear, and assuming that the attack of the ascorbic acid upon the nitrosated species is rate limiting, can be interpreted in terms of Equation 8.1.

$$Rate = k_2 [\text{nitrosated species}][H_2A]_\tau \qquad \text{Equation 8.1}$$

Analysis of the data gives:

$k_2 = 4\ 500 \pm 300$ dm^3 mol^{-1} s^{-1}

209

This value is considerably larger than any of the values obtained for other *S*-nitroso species (see Chapter 4).

8.5 Conclusions

In Chapter 7 it was shown that the thiones 2-thioimidazole, 4-thiopyridine and 2-thiopyrimidine could be readily *S*-nitrosated using acidified solutions of nitrous acid.

The results in this chapter have shown that the decomposition of the *S*-nitrosated species under acidic conditions results in the formation of disulfides and nitric oxide. Only the *S*-nitrosated 4-thiopyridine was sufficiently stable to allow its use in further studies.

At pH 7.4, decomposition of nitrosated 4-thiopyridine proceeded *via* hydrolysis, re-forming the thione. Evidence for deprotonation of the nitroso species, with a pK_a value of about 4.5, was observed, and the reaction was demonstrated to be reversible.

S-Nitrosated 4-thiopyridine undergoes facile decomposition with Cu$^+$ (added as Cu(I)Cl) and with copper metal. It also reacts rapidly with ascorbic acid in the absence of metal ions, producing nitric oxide and the thione.

The *S*-nitrosation, and subsequent decomposition reactions of the products, of the three thiones studied here possess many similarities to the nitrosations of other thiones such as thioureas and 2-thiopyridine.

8.6 References

1. K. Al-Mallah, P. Collings and G. Stedman, *J. Chem. Soc., Dalton Trans.*, 2469 (1974).

2. P. Collings, M. Garley and G. Stedman, *J. Chem. Soc., Dalton Trans.*, 331 (1981).

3. M. S. Garley, G. Stedman and H. Miller, *J. Chem. Soc., Dalton Trans.*, 1959 (1984).

4. P. Collings, K. Al-Mallah and G. Stedman, *J. Chem. Soc., Perkin Trans. 2*, 1734 (1975).

5. S. Amado, A. P. Dicks and D. L. H. Williams, *J. Chem. Soc., Perkin Trans. 2*, 1869 (1998).

6. A. Suszka, *Pol. J. Chem.*, **54**, 2289 (1980).

7. A. P. Dicks, PhD Thesis, University of Durham, 1997.

8. S. Stoyanov, I. Petkov, L. Antonov, T. Stoynova, *Can. J. Chem.*, **68**, 1482 (1990).

9. G. F. Smith and W. H. McCurdy, *Anal. Chem*, **24**, 371 (1952).

Experimental

Chapter 9 Experimental

Experimental details specific to the work in Chapters 7 and 8 are contained in this Chapter. General information regarding the equipment and instrumentation used can be found in Appendix 3.

9.1 Materials

Chemicals were obtained from Sigma-Aldrich or Lancaster in the highest grade available and were used without further purification. Standard laboratory distilled water was used for all solutions prepared in an aqueous medium.

9.2 Stock Solutions

- **Perchloric Acid**

Stock solutions of perchloric acid were prepared by appropriate dilution of a commercial solution. Typical stock concentrations were $5 \times 10^{-1} - 2$ M.

- **Sodium Hydroxide**

Sodium hydroxide solutions were prepared by dissolving sodium hydroxide pellets in distilled water.

- **Sodium Nitrite**

Sodium nitrite solutions were prepared in distilled water, and were made fresh for each experiment.

- **Thiones**

Stock solutions of the thiones were prepared in distilled water, typical concentrations were $5 \times 10^{-3} - 1 \times 10^{-2}$ M. The solutions were prepared fresh for each experiment and were protected from light by wrapping the flask in aluminium foil.

- ## Chloride, Bromide and Thiocyanate Solutions

Appropriate concentration solutions of the catalysts used in the nitrosation reactions were prepared in distilled water. Typical stock concentrations were $1 \times 10^{-2} - 2.5 \times 10^{-1}$ M.

- ## Iodide Solution

For the nitrosation of 4-thiopyridine catalysed by iodide a stock solution of sodium iodide was prepared in distilled water and used immediately.

- ## Neocuproine

The specific copper(I) chelator neocuproine was prepared as a stock solution in methanol.

- ## EDTA

Stock solutions of ethylenediaminetetraacetic acid, EDTA, 2.50×10^{-2} M, were prepared in distilled water. Brief sonication was required to dissolve the solid fully.

9.3 Thione Spectra and Stability Studies

These studies were carried out using conventional UV / visible spectrophotometry. The spectrophotometer was zeroed against air or water, and a reference cell containing the appropriate solvent system was used. Water, water/pH 7.4 buffer, water/HClO$_4$ or water/NaOH were added to quartz cuvettes. Aliquots of a solution of the thione being studied were added to the cuvettes and the solutions mixed. The solutions were then thermostatted for ten minutes to allow the temperature to equilibrate to 25 °C prior to obtaining the spectra. During the stability studies, the cells remained in the spectrophotometer for the whole period of study, and so were not exposed to light.

9.4 Initial Nitrosation Spectral Studies

Conventional spectrophotometry was used in these studies. Water, HClO$_4$, thione, and bromide where appropriate, were added to quartz cuvettes. A reference cuvette was prepared containing water, HClO$_4$, and bromide where appropriate. The spectrophotometer was zeroed against water or air. The reference and sample

cuvettes were then placed in the spectrophotometer and allowed to reach thermal equilibrium. An aliquot of sodium nitrite was then added, and the acquisition of spectra initiated.

9.5 Kinetics of Nitrosation

Kinetic studies into the nitrosation of the thiones were carried out using the stopped flow technique. The spectrophotometer was zeroed against water, except for experiments where large excess concentrations of the substrates caused high initial absorbencies, when the spectrophotometer was zeroed against the appropriate concentration of acidified thione solution. The reagents were contained in two syringes, which were discharged into the solution reservoirs and allowed to reach thermal equilibrium before initiating mixing and data collection.

The reaction traces obtained in the experiments were fitted to the appropriate rate equation using the software package supplied with the spectrophotometer. Each trace was obtained by averaging at least three runs, and at least three of these averages were obtained for each sample.

- **Uncatalysed Nitrosation**

Syringe A contained: $HClO_4$, water, thione

Syringe B contained: water, sodium nitrite

- **Catalysed Nitrosations**

Syringe A contained: $HClO_4$, water, thione

Syringe B contained: water, sodium nitrite, catalyst

9.6 Decomposition Reactions of *S*-Nitrosated Thiones

The decomposition reactions of the *S*-nitrosated thiones were studied using conventional UV / visible spectrophotometry, or by measuring nitric oxide release with the nitric oxide electrode.

- **Spectral Studies**

For experiments carried out at pH 1, cuvettes were prepared as described in Section 9.4, using bromide as a nitrosation catalyst. After addition of the sodium nitrite,

spectra were obtained over time to monitor the decomposition of the nitrosated species.

For the experiments carried out at pH 3.1 or pH 7.4, cuvettes were prepared containing the appropriate buffer solution and thermostatted in the sample chamber. The nitrosated thione was then prepared in a volumetric flask (typically 5 or 10 cm^3). This contained HClO$_4$ (final concentration 0.1 M), the thione, and water to make the volume to the line. A small aliquot of sodium nitrite (volume no more than 0.1 cm^3) was added to the flask and the solution shaken. One minute was allowed for the nitrosation to reach completion, after which an aliquot of the nitrosated thione was immediately added to the cuvette, and spectra acquisition started. Fresh solutions of the nitrosated species were prepared for each cuvette.

- **Nitric Oxide Electrode Studies in the Absence of Copper Sources**

For the reactions where the nitrosation was carried out in the nitric oxide electrode apparatus, HClO$_4$, thione and water were added to the apparatus and the solution stirred. The nitric oxide electrode was then placed in the solution and the vessel sealed. Nitrogen was then passed through the solution for 15 minutes to remove oxygen. The nitrogen stream was then switched off, and the electrode zeroed and data collection started. An aliquot of sodium nitrite solution was then injected into the solution, and the production of nitric oxide followed using the electrode.

When the nitrosated thione was prepared separately and then injected into the nitric oxide electrode apparatus, a different procedure was used. The appropriate solvent, for example water or buffer, and any reagents other than the nitrosated species, were added to the nitric oxide electrode apparatus and the solution stirred. The solution was then purged with nitrogen for fifteen minutes, after which the nitrogen stream was turned off, and the electrode zeroed and data collection initiated. The nitrosated species was prepared as described above for the spectral studies, and an aliquot injected into the sample solution.

- **Nitric Oxide Electrode Studies in the Presence of Copper Sources**

pH 7.4 buffer and the appropriate copper source (CuSO$_4$, copper metal, but not Cu(I)Cl powder) were added to the nitric oxide electrode apparatus, and the solution stirred. Nitrogen was passed through the solution for fifteen minutes prior to

zeroing the electrode and starting data collection. At this point Cu(I)Cl powder was added if required. With the nitrogen stream switched off, an aliquot of the nitrosated thione was injected into the solution.

Appendices
1 – 6

Appendix 1 Abbreviations

A1.1 Chemical Compounds

R	A chemical moiety forming part of an organic compound
H_2A	Ascorbic acid
HA^-	Ascorbate monoanion
A^{2-}	Ascorbate dianion
$A^{\bullet-}$	Ascorbyl radical
DA	Dehydroascorbic acid
RSH	Thiol
GSH	Glutathione
Cys	Cysteine
RSSR	Disulfide
GSSG	Gluthathione disulfide
RSNO	S-nitrosothiol
GSNO	S-nitroso glutathione
SNAP	S-nitroso N-acetyl penicillamine
SNAC	S-nitroso N-acetyl cysteine
SNCys	S-nitroso cysteine
SNPen	S-nitroso penicillamine
2-TP	2-thiopyridine
2-TPNOx	2-thiopyridine-N-oxide
3-TP	3-thiopyridine
4-TP	4-thiopyridine
2-TPM	2-thiopyrimidine
2-TI	2-thioimidazole
RONO	Alkyl nitrite
RN_2^+	Diazonium ion
EDTA	Ethylenediaminetetraacetic acid
DTNB	5,5'-dithiobis(2-nitrobenzoic acid)
TNB^{2-}	2-nitro-5-thiobenzoic acid dianion

The structures of most of these compounds can be found in Appendix 2

A.1.2 Chemical and Physical Parameters

[ ]   Concentration term

$[\ ]_T$ Total concentration of a species in all of its different forms, e.g.

$$[H_2A]_T = [H_2A] + [HA^-] + [A^{2-}]$$

M   mol dm^{-3}

pH $-\log_{10}([H^+] / \text{mol dm}^{-3})$

pK_a $-\log_{10}(K_a / \text{mol dm}^{-3})$

k Rate constant

k_{obs} Observed rate constant

K Equilibrium constant

Subscripts used to indicate rate and equilibrium constants for specific reactions are introduced at the appropriate place in the text.

UV   Ultraviolet

λ Wavelength

Abs   Absorbance

ε Extinction coefficient. Subscripts are sometimes used to indicate the wavelength at which the value was obtained

HPLC   High-performance liquid chromatography

h Planck's Constant = 6.626×10^{-34} J s

k_B Boltzmann Constant = 1.381×10^{-23} J K^{-1}

R   Gas constant = 8.314 J K^{-1} mol^{-1}

$\Delta H^{\ddagger}$ Enthalpy of activation

$\Delta S^{\ddagger}$ Entropy of activation

T   Temperature

Å 10^{-10} m

t   Time

min   Minute
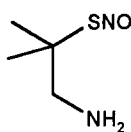
A1.3 Mathematical Parameters
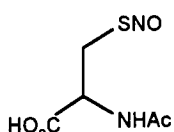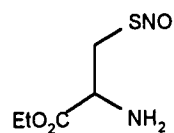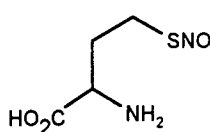
ln $\log_e$
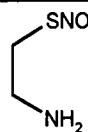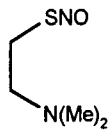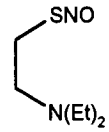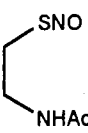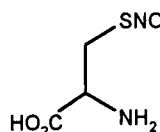
log $\log_{10}$

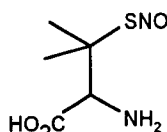r^2 correlation coefficient obtained from statistical analysis

x_i value of data point i

$\bar{x}$ mean value

σ_i standard deviation in i

s_i standard error in i

p probability

w_i weighting applied to i

n sample size

Q Q value in Dixon's Q test

x_i value of data point i

$\bar{x}$ mean value

σ_i standard deviation in i

Appendix 2 Chemical Structures

A2.1 *S*-Nitrosothiol Structures

The table below includes the structures of all the *S*-nitrosothiols discussed in this thesis.

Nitrosothiol	Structure	Abbreviation if used
S – nitroso cysteamine		~
S – nitroso 2-(dimethylamino)ethane thiol		~
S – nitroso 2-(diethylamino)ethane thiol		~
S – nitroso 1-amino-2-methyl-2-propane thiol		~
S – nitroso *N*-acetyl cysteamine		~
S – nitroso cysteine		SNCys
S-nitroso *N*-acetylcysteine		SNAC
S – nitroso cysteine ethyl ester		~
S – nitroso homocysteine		~
S – nitroso penicillamine		SNPen
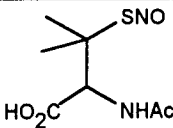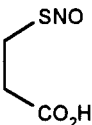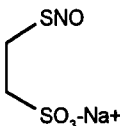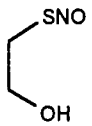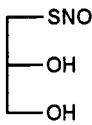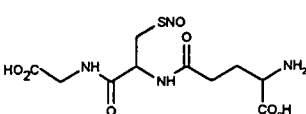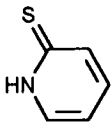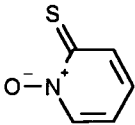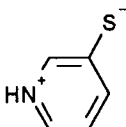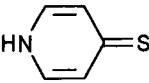
Nitrosothiol	Structure	Abbreviation if used
S – nitroso *N*-acetyl penicillamine		SNAP
S – nitroso 3-thio-propanoic acid		~
S – nitroso 2-thio-ethanesulfonic acid		~
S – nitroso 2-hydroxyethanethiol		~
S – nitroso thioglycerol		~
S – nitroso glutathione		GSNO

Table A2.1 Nitrosothiol Structures

A2.2 Thione Structures

Structures of the thiones discussed in this thesis are shown below

Thione	Structure	Abbreviation if used
2-thiopyridine (pyridine-2(1*H*)-thione)		2-TP
2-thiopyridine *N*-oxide		2-TPNOx
3-thiopyridine (pyridine-3(1*H*)-thione		3-TP
4-thiopyridine (pyridine-4(1*H*)-thione)		4-TP
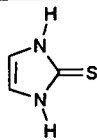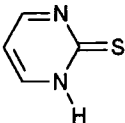
Thione	Structure	Abbreviation if used
2-thioimidazole		2-TI
2-thiopyrimidine		2-TPM

Table A2.2 Thione structures

A2.3 Other Compounds

Structures of other compounds referred to in this thesis are shown below.
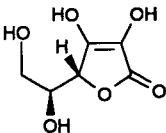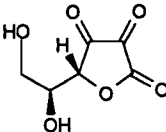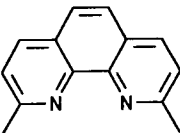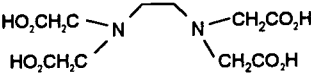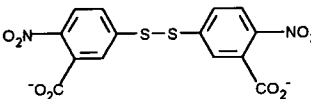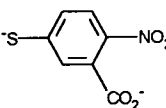
Compound	Structure	Abbreviation if used
Ascorbic acid		H_2A
Dehydroascorbic acid		DA
Neocuproine		Nc
Ethylenediaminetetraacetic acid		EDTA
Ellman's Reagent 5,5'-dithiobis (2-nitrobenzoic acid)		DTNB
2-nitro-5-thiobenzoic acid		TNB^{2-}

Table A2.3 Structures of other compounds

A3 Instrumentation

A3.1 UV / Visible Spectrophotometry

Conventional UV/ visible spectrophotometry was used to obtain spectra and absorbance – time data for reactions of greater than ten minutes duration; faster reactions were studied using the stopped-flow technique (Section A3.2). Double beam instruments were used, with one beam passing through the sample and the other through a suitable reference. The spectrophotometers were zeroed prior to use by obtaining a background reading against air or reference cells containing the appropriate solvent.

Sample solutions were contained in 1 cm path-length cells with tight fitting stoppers. Typical sample volumes were 2.5 – 3 cm³. All solutions were thermostatted at the appropriate temperature.

A3.1.1 Perkin-Elmer Instruments

Perkin-Elmer λ2 and λ12 spectrophotometers equipped with six-cell sample changers were used. The samples were thermostatted by means of a circulating water system. The λ2 was interfaced to a PC operating PECSS version 3.2 software; the λ12 was interfaced to a PC operating UV-Winlab version 1.21 software.

A3.1.2 Shimadzu Instrument

A Shimadzu UV-2101 spectrophotometer equipped with a single-cell sample holder was used when appropriate, the temperature being controlled by an electrical heating / cooling system. The spectrophotometer was interfaced to a PC.

A3.2 Stopped-flow Spectrophotometry

Stopped-flow spectrophotometry was used for reactions of less than ten minutes duration. The spectrophotometer used was an Applied Photophysics DX.17MV BioSequential instrument interfaced to an Acorn A3000 computer.

Samples were contained in two solution reservoirs, thus keeping the reactants separate until mixing. Mixing was automated and was complete in less than 5 ms.

Data recording was instigated automatically by a trigger mechanism fitted in the drive system. A cell path-length of 1 cm was used and the samples were thermostatted by means of a circulating water system. The spectrophotometer was zeroed against the appropriate solvent before use.

A3.2.1 Using the Stopped-Flow to Obtain Spectra

For fast reactions and unstable species, spectral work was carried out using the stopped-flow system rather than conventional spectrophotometry. For spectra within the range 300 – 700 nm the diode array attachment was used. However, for lower wavelengths (down to ~ 220 nm) the diode array attachment was not suitable (detection using this equipment is only possible down to 275 nm). Spectra were instead obtained using the kinetic spectra technique: absorbance – time plots were obtained at a series of wavelengths and then combined to produce a series of time-resolved spectra.

A3.3 Nitric Oxide Electrode

A WPI MK I or MK II nitric oxide electrode interfaced to a PC operating Duo.18 version 1.1 software was used for nitric oxide measurement.

The nitric oxide electrode is a modified Clark-type electrode surrounded by a protective metal sheath. A special membrane encloses the end of the sheath and allows only small gases to pass through to the electrode surface, thus preventing false readings. The only species so far identified as giving rise to false signals is hydrogen. The electrode potential is maintained at 868 mV by the associated electronics.

Samples were contained in the special apparatus described in Section A3.3.1 (the design of which is acknowledged to Dr. D. R. Noble and the manufacture acknowledged to the in-house glass-blowing service).

A3.3.1 Nitric Oxide Electrode Apparatus

A schematic of the electrode set-up is shown in Figure A3.1.
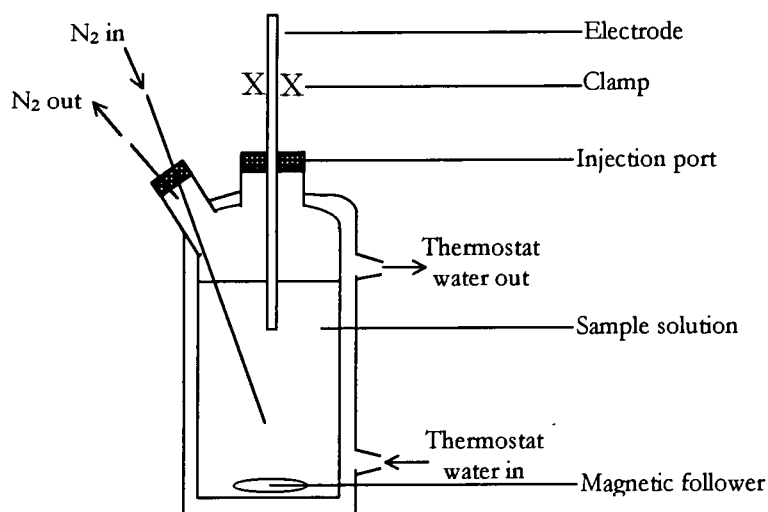
Figure A3.1 The set-up used for nitric oxide measurements

The purging gas (nitrogen) was pre-saturated with the appropriate solvent to reduce mass transfer from the vessel. Solutions were de-oxygenated with the nitrogen stream for fifteen minutes before measurements were made. The electrode was zeroed and used with the nitrogen stream turned off. Vigorous stirring was maintained throughout.

A3.3.2 Calibration of the Nitric Oxide Electrode

The electrode was calibrated using either the ascorbic acid / sodium nitrite method or the H_2SO_4 / KI / $NaNO_2$ method. Details of these methods are outlined below.

- **Ascorbic acid / sodium nitrite method**

30 cm^3 of 0.10 M ascorbic acid solution was placed into the electrode apparatus and de-oxygenated. After 15 minutes of purging with nitrogen, the purging gas stream was switched off and the electrode zeroed. Data collection was then started. A 50 μL aliquot of a sodium nitrite solution (typically 6×10^{-4} M) was then added. As soon as the electrode-current value reached a plateau, another 50 μL aliquot was added. Additions were continued in this manner until six or more aliquots had been added. The electrode response was then calculated from the gradient of a plot of

227

the current against the nitric oxide concentration (equal to the added sodium nitrite concentration). The volume change resulting from the additions was taken into account when calculating the nitric oxide concentration.

The reaction occurring during the calibration is outlined in Scheme A3.1.

$$\text{ascorbic acid} + 2\,HNO_2 \longrightarrow \text{dehydroascorbic acid} + 2\,NO$$
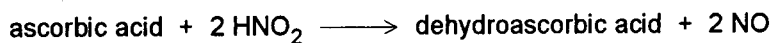
Scheme A3.1 Ascorbic acid calibration of the nitric oxide electrode

- **H₂SO₄ / KI / NaNO₂ method**

The procedure outlined above was used except 30 cm³ of a solution 0.10 M in H_2SO_4 and 0.10 M in KI was used in place of the ascorbic acid solution. The reaction occurring during the calibration is outlined in Scheme A3.2.

$$4\,H^+ + 2\,NO_2^- + 2\,I^- \longrightarrow 2\,NO + I_2 + 2\,H_2O$$

Scheme A3.2 H_2SO_4 / KI / $NaNO_2$ calibration of the nitric oxide electrode

A3.4 HPLC

A Gilson model 620 HPLC fitted with a UV detection unit and interfaced to an Apple IIC computer was used for the HPLC analysis.

A3.5 pH Meter

pH measurements were undertaken using a Jenway 3020 pH meter fitted with a BDH Gelplas general purpose electrode of either 5 or 10 mm diameter. The meter was calibrated for alkaline measurements using standard pH 7 and pH 10 buffers. For acidic measurements, the electrode was calibrated using standard pH 7 and pH 4 buffers. Samples were contained in a thermostat tank at 25 °C.

A3.6 Balance

An open top-pan balance was used for measuring masses greater than 30 g. For smaller masses, an enclosed top-pan balance was used, which weighed to $\pm$ 0.001 g. The balance was calibrated weekly using a standard 20.000 g mass.

A3.7 Volume Measurement

Standard solutions were prepared in volumetric flasks, the liquid level being carefully made up to the line. Small volumes (0.020 – 1.00 cm^3) were measured using Gilson Pippetteman dispensers with disposable tips. These were calibrated prior to each use by measuring the mass of water dispensed. When injection through septa was necessary, Hamilton syringes were used. Graduated glass pipettes were used for volumes in the range 0.50 – 20 cm^3. Larger volumes were dispensed from appropriate bulb pipettes.

A4 Statistics

Further information on the topics covered by this appendix can be found in: J. C. Miller and J. N. Miller, 'Statistics for Analytical Chemistry', 3rd ed., Ellis Horwood, Chichester, 1993.

A4.1 Rounding

When performing calculations, values were not rounded at each stage but only at the final stage. Numbers ending in 5 were rounded to the nearest even number, e.g. 2.45 becomes 2.4. The number of significant figures quoted for a particular value is dependent upon the uncertainty of the value.

A4.2 Averages

Averages are mean ($\bar{x}$) values unless otherwise indicated. The standard deviation in $\bar{x}$ (denoted σ_i) was calculated using Equation A4.1, where n is the sample size.

$$\sigma_i = \sqrt{\frac{\sum_i (x_i - \bar{x})^2}{(n-1)}} \qquad \text{Equation A4.1}$$

A4.3 Fitting

Two fitting methods were used depending upon the mathematical relationship being tested: linear least squares fitting and non-linear least squares fitting. The former was used to obtain the gradient and intercept from straight line plots, the latter to obtain parameters for any non-linear relationship, e.g. first order reaction profiles.

Weighted fits were sometimes used when the uncertainties in values were large (see Section A.4.3.2). Least squares analysis was carried out using either the Excel or Scientist programs, the latter being capable of non-linear fitting.* In all cases the fit line was superimposed upon the data and subjected to visual inspection: often the best indication of goodness of fit (Section A4.3.3).

---

* Microsoft® Excel 97; MicroMath® Scientist® for Windows®, Version 2.02

A4.3.1 Outliers

To establish whether a suspect value in a series was a statistical outlier, and therefore could be excluded from the analysis, Dixon's Q test was used. Q was calculated using Equation A4.2, then compared with tabulated values for Q at the p=0.05 level. If Q exceeded the tabulated value, the suspect value was excluded from the analysis.

$$Q = \frac{|\text{suspect value} - \text{nearest value}|}{\text{largest value} - \text{smallest value}} \qquad \text{Equation A4.2}$$

A4.3.2 Weighted Fits

For cases where the uncertainties in the values to be fitted are large, it is necessary to take account of the uncertainties in each value when calculating the fitted curve. This was done by applying a weighting (w_i) to point i, larger weightings being given to points whose values were known with more certainty. These weightings were calculated according to Equation A4.3 and the fitting was carried out using the Scientist Program.

$$w_i = \frac{s_i^{-2}}{\sum_i \frac{s_i^{-2}}{n}} \qquad \text{Equation A4.3}$$

A4.3.3 Goodness of Fit

The goodness of a fit was gauged by a combination of methods. The correlation coefficient (r^2) was used to judge the extent of deviation of the data points from the fit line. r^2 ranges from 0 to 1, a value of 1 indicating that the data points lie exactly on the fit line. It must be recognised that a high value for the correlation coefficient does not indicate that the points follow the same trend as the fit line, only that they lie close to it: data forming a gentle curve fitted to a straight line gives a high r^2 value, but the points do not form a straight line. In order to avoid mistakes of this nature, a visual inspection was made to check that the fit line followed the trend in the data points.

For straight line fits the significance of the intercept was determined by using the p value output by the statistical package. p values lie in the range $0 - 1$, a value of 1

indicating that there is no significant intercept in a straight line plot. The 95 % probability level was used as the cut-off, so $p < 0.05$ indicated a significant intercept.

A4.4 Errors

The errors discussed here are random errors. Systematic errors are difficult to analyse mathematically, as their source is often unknown.

The error values quoted are derived from two sources. When more than one determination of a value was made (e.g. by repeating the experiment or using more than one analysis method) the error quoted is twice the standard deviation, calculated using Equation A4.1.

Errors quoted after application of a particular model or analysis method to one set of data represent the errors in the fit. The quoted values are twice the standard error output by the fitting program.

No attempt was made to propagate the errors involved in making measurements (e.g. pipetting) through to the final values. The spread of the data about the fit line will arise partly from these types of error.

A4.4.1 Propagation of Random Errors

The propagation of random errors was carried out using the following equations.

- **Linear combinations**

If $y = c_0 + c_1 x_1 + c_2 x_2$

where c_i are constants and x_i are data values, then

$$\sigma_y = \sqrt{\left(c_1 \sigma_{x1}\right)^2 + \left(c_2 \sigma_{x2}\right)^2}$$

- **Multiplicative expressions**

If $y = k \dfrac{x_1 x_2}{x_3}$

then $\sigma_y = y \sqrt{\left(\dfrac{\sigma_{x1}}{x_1}\right)^2 + \left(\dfrac{\sigma_{x2}}{x_2}\right)^2 + \left(\dfrac{\sigma_{x3}}{x_3}\right)^2}$

A5 Derivations

A5.1 Chapter 4, Equation 4.9

The three forms of ascorbic acid are H_2A, HA^- and A^{2-} and are related by the acid dissociation constants K_{a1} and K_{a2}. If each form of ascorbic acid reacts with the nitrosothiol in a process which is first order in the nitrosothiol and first order in the ascorbic acid species then Equation A5.1 holds.

$$Rate = k_{H_2A}[H_2A][RSNO] + k_{HA^-}[HA^-][RSNO] + k_{A^{2-}}[A^{2-}][RSNO] \qquad \text{Equation A5.1}$$

Equations A5.2 and A5.3 are obtained from the acid dissociation constants.

$$K_{a1} = \frac{[HA^-][H^+]}{[H_2A]} \Rightarrow [HA^-] = \frac{K_{a1}[H_2A]}{[H^+]} \qquad \text{Equation A5.2}$$

$$K_{a2} = \frac{[A^{2-}][H^+]}{[HA^-]} \Rightarrow [A^{2-}] = \frac{K_{a2}[HA^-]}{[H^+]} \qquad \text{Equation A5.3}$$

Substituting for [HA⁻] from Equation A5.2 in Equation A5.3 gives Equation A5.4.

$$[A^{2-}] = \frac{K_{a1}K_{a2}[H_2A]}{[H^+]^2} \qquad \text{Equation A5.4}$$

Substituting for [HA⁻] from A5.2 and [A²⁻] from A5.4 in Equation A5.1 gives Equation A5.5.

$$Rate = \left(k_{H_2A}[H_2A] + \frac{k_{HA^-}K_{a1}[H_2A]}{[H^+]} + \frac{k_{A^{2-}}K_{a1}K_{a2}[H_2A]}{[H^+]^2} \right)[RSNO] \qquad \text{Equation A5.5}$$

The total ascorbic acid concentration is given by Equation A5.6.

$$[H_2A]_T = [H_2A] + [HA^-] + [A^{2-}] \qquad \text{Equation A5.6}$$

Substituting for [A²⁻] from A5.4 and [HA⁻] from A5.2 in Equation A5.6:

$$[H_2A]_T = [H_2A] + \frac{K_{a1}[H_2A]}{[H^+]} + \frac{K_{a1}K_{a2}[H_2A]}{[H^+]^2}$$

$$\Rightarrow [H_2A]_T = [H_2A]\left(1 + \frac{K_{a1}}{[H^+]} + \frac{K_{a1}K_{a2}}{[H^+]^2} \right)$$

$$[H_2A] = \frac{[H_2A]_T [H^+]^2}{[H^+]^2 + K_{a1}[H^+] + K_{a1}K_{a2}} \qquad \text{Equation A5.7}$$

Substituting for [H₂A] from A5.7 in A5.5 gives Equation A5.8.

$$Rate = \left(\frac{k_{H_2A}[H^+]^2 + k_{HA^-}.K_{a1}[H^+] + k_{A^{2-}}.K_{a1}K_{a2}}{K_{a1}K_{a2} + K_{a1}[H^+] + [H^+]^2} \right)[H_2A]_r[RSNO] \qquad \text{Equation A5.8}$$

Comparing A5.8 with the established rate equation for reaction between ascorbic acid and the nitrosothiol (Equation A5.9) shows that the full expression for k_2 in given by Equation A5.10, which is identical to Equation 4.9 in Chapter 4.

$$Rate = k_2[H_2A]_r[RSNO] \qquad \text{Equation A5.9}$$

$$k_2 = \frac{k_{H_2A}[H^+]^2 + k_{HA^-}.K_{a1}[H^+] + k_{A^{2-}}.K_{a1}K_{a2}}{K_{a1}K_{a2} + K_{a1}[H^+] + [H^+]^2} \qquad \text{Equation A5.10}$$

A5.2 Chapter 7, Equation 7.5

Equation 7.1 in Chapter 7 is shown as Equation A5.11 below.

$$K_N = \frac{[4 - TPNO^+]}{[H^+][HNO_2][4 - TP]} \qquad \text{Equation A5.11}$$

The pK_a of 4-TP is 1.43, therefore at pH 3.1 all of the 4-TP is present as the neutral form. However, the pK_a of nitrous acid is 3.15 and must therefore be taken into account (Equation A5.12).

$$K_{a(HNO_2)} = \frac{[NO_2^-][H^+]}{[HNO_2]} \qquad \text{Equation A5.12}$$

The mass balance equation for HNO₂ is given in Equation A5.13

$$[HNO_2]_r = [NO_2^-] + [HNO_2] + [4 - TPNO^+] \qquad \text{Equation A5.13}$$

If [HNO₂]$_\tau$ >> [4-TP]$_\tau$ then Equation A5.13 becomes Equation A5.14

$$[HNO_2]_r = [HNO_2] + [NO_2^-] \qquad \text{Equation A5.14}$$

Substituting for [NO₂⁻] from Equation A5.14 in Equation A5.12 gives

$$K_{a(HNO_2)} = \frac{[H^+][HNO_2]_r - [H^+][HNO_2]}{[HNO_2]} \qquad \text{Equation A5.15}$$

Rearranging Equation A5.15 gives Equation A5.16

$$[HNO_2] = \frac{[H^+][HNO_2]_r}{K_{a(HNO_2)} + [H^+]}$$ Equation A5.16

Substituting for [HNO₂] from A5.16 in Equation A5.11 gives Equation A5.17

$$K_N = \frac{[4 - TPNO^+](K_{a(HNO_2)} + [H^+])}{[H^+]^2[4 - TP][HNO_2]_r}$$ Equation A5.17

Rearranging gives Equation A5.18

$$[4 - TPNO^+] = \frac{K_N[H^+]^2[4 - TP][HNO_2]_r}{K_{a(HNO_2)} + [H^+]}$$ Equation A5.18

The absorbance change at 325 nm (4-TP λ_{max}) upon nitrosation is given by Equation A5.19

$$\Delta A = A_{initial} - A_{final} = \varepsilon_{4-TP}[4 - TP]_r - (\varepsilon_{4-TP}[4 - TP] + \varepsilon_{4-TPNO^+}[4 - TPNO^+])$$

Equation A5.19

Substituting for [4-TPNO⁺] from Equation A5.18 in Equation A5.19 gives

$$\Delta A = \varepsilon_{4-TP}[4 - TP]_r - \varepsilon_{4-TP}[4 - TP] - \frac{\varepsilon_{4-TPNO^+}K_N[H^+]^2[4 - TP][HNO_2]_r}{K_{a(HNO_2)} + [H^+]}$$

Equation A5.20

The mass balance for 4-TP is in Equation A5.21

$$[4 - TP]_r = [4 - TP] + [4 - TPNO^+]$$ Equation A5.21

Equation A5.17 can therefore be re-written as Equation A5.22

$$K_N = \frac{([4 - TP]_r - [4 - TP])(K_{a(HNO_2)} + [H^+])}{[H^+]^2[4 - TP][HNO_2]_r}$$ Equation A5.22

Rearranging gives Equation A5.23

$$[4 - TP] = \frac{[4 - TP]_r(K_{a(HNO_2)} + [H^+])}{K_N[H^+]^2[HNO_2]_r + K_{a(HNO_2)} + [H^+]}$$ Equation A5.23

Substituting for [4-TP] from Equation A5.23 in Equation A5.20 gives Equation A5.24

$$\Delta A = \varepsilon_{4\text{-TP}}[4\text{-TP}]_r - \frac{\varepsilon_{4\text{-TP}}[4\text{-TP}]_r\left(K_{a(\text{HNO}_2)} + [\text{H}^+]\right)}{K_N[\text{H}^+]^2[\text{HNO}_2]_r + K_{a(\text{HNO}_2)} + [\text{H}^+]} - \frac{\varepsilon_{4\text{-TPNO}^+}K_N[\text{H}^+]^2[\text{HNO}_2]_r[4\text{-TP}]_r}{K_N[\text{H}^+]^2[\text{HNO}_2]_r + K_{a(\text{HNO}_2)} + [\text{H}^+]}$$

<div align="center">Equation A5.24</div>

Rearranging and cancelling gives Equation A5.25

$$\Delta A = \frac{\left(\varepsilon_{4\text{-TP}} - \varepsilon_{4\text{-TPNO}^+}\right)[4\text{-TP}]_r K_N[\text{H}^+]^2[\text{HNO}_2]_r}{K_N[\text{H}^+]^2[\text{HNO}_2]_r + K_{a(\text{HNO}_2)} + [\text{H}^+]}$$ Equation A5.25

Inverting Equation A5.25 and rearranging gives Equation A5.26, which is identical to Equation 7.5 in Chapter 7

$$\frac{1}{\Delta\text{Absorbance}} = \frac{1}{\left(\varepsilon_{4\text{-TP}} - \varepsilon_{4\text{-TPNO}^+}\right)[4\text{-TP}]_r} + \frac{K_{a(\text{HNO}_2)} + [\text{H}^+]}{\left(\varepsilon_{4\text{-TP}} - \varepsilon_{4\text{-TPNO}^+}\right)[4\text{-TP}]_r[\text{H}^+]^2[\text{HNO}_2]_r K_N}$$

<div align="center">Equation A5.26</div>

A5.3 Chapter 7, Equation 7.7 and Equation 7.8

For uncatalysed nitrosation of substrate S by nitrous acid the rate equation is given by Equation A5.27

$$Rate = k_N[\text{HNO}_2][\text{H}^+][\text{S}] - k_{-N}[\text{SNO}^+]$$ Equation A5.27

When [H$^+$] and [HNO$_2$] are both a lot greater than [S], Equation A5.27 becomes Equation A5.28, where $k_N' = k_N[\text{HNO}_2][\text{H}^+]$.

$$Rate = k_N'[\text{S}] - k_{-N}[\text{SNO}^+]$$ Equation A5.28

At equilibrium [S] = [S]$_e$ and [SNO$^+$] = [SNO$^+$]$_e$, so for a position approaching equilibrium

$$Rate = k_N'\left([\text{S}]_e + x\right) - k_{-N}\left([\text{SNO}^+]_e - x\right) = k_N'[\text{S}]_e + k_N'x - k_{-N}[\text{SNO}^+]_e + k_{-N}x$$

<div align="center">Equation A5.29</div>

At equilibrium the rate of the forward and reverse reactions are equal, therefore $k_N'[\text{S}]_e = k_{-N}[\text{SNO}^+]$ and Equation A5.29 becomes Equation A5.30.

$$Rate = (k_N' + k_{-N})x$$ Equation A5.30

Therefore k_{obs} is given by Equation A5.31, which is identical to Equation 7.8 in Chapter 7.

$$k_{obs} = k_N[H^+][S] + k_{-N} \qquad \text{Equation A5.31}$$

The pK_a of the substrate and the relevant mass balance expression are given by Equations A5.32 and A5.33

$$K_a = \frac{[S][H^+]}{[SH^+]} \qquad \text{Equation A5.32}$$

$$[S]_r = [S] + [SH^+] \qquad \text{Equation A5.33}$$

Combining Equations A5.32 and A5.33, and incorporating them into Equation A5.31 gives Equation A5.34, which is identical to Equation 7.7 in Chapter 7.

$$k_{obs} = \frac{k_N K_a [H^+][S]_r}{K_a + [H^+]} + k_{-N} \qquad \text{Equation A5.34}$$

A5.4 Chapter 7, Equations 7.16 – Equations 7.20

Scheme 7.2 in Chapter 7 describes nitrosation catalysed by X^-, from which it is possible to write Equation A5.35, which includes terms for the uncatalysed reaction.

$$Rate = k_N[HNO_2][H^+][S] - k_{-N}[SNO^+] + k_{2XNO}K_{XNO}[HNO_2][H^+][S][X^-] - k_{-2XNO}[SNO^+][X^-]$$

$$\text{Equation A5.35}$$

When the reactions are carried out under conditions where [HNO$_2$], [H$^+$] and [X$^-$] are effectively constant, k_{obs} is given by Equation A5.36

$$k_{obs} = k_N[HNO_2][H^+] + k_{-N} + k_{2XNO}K_{XNO}[HNO_2][H^+][X^-] + k_{-2XNO}[X^-]$$

$$\text{Equation A5.36}$$

Incorporating the expressions given in Equations A5.37 and A5.38 into Equation A5.36 gives Equation A5.39.

$$K_N = \frac{k_N}{k_{-N}} \Rightarrow k_{-N} = \frac{k_N}{K_N} \qquad \text{Equation A5.37}$$

$$K_N = K_{XNO}\frac{k_{2XNO}}{k_{-2XNO}} \Rightarrow k_{-2XNO} = \frac{K_{XNO}k_{2XNO}}{K_N} \qquad \text{Equation A5.38}$$

$$k_{obs} = k_N[HNO_2][H^+] + \frac{k_N}{K_N} + k_{2XNO}K_{XNO}[HNO_2][H^+][X^-] + \frac{K_{XNO}k_{2XNO}}{K_N}[X^-]$$

Equation A5.39

Rearranging Equation A5.39 according to the concentration term being varied yields Equations 7.16, 7.17 and 7.19 in Chapter 7. Assuming the uncatalysed reaction is negligible, and incorporating the relevant pK_a and mass balance terms for the substrate gives Equation 7.18 in Chapter 7.

When the reactions are carried out under conditions where [S], [H$^+$] and [X$^-$] are effectively constant, Equation A5.40 can be obtained from Equation A5.35

$$k_{obs} = k_N[S][H^+] + \frac{k_N}{K_N} + k_{2XNO}K_{XNO}[S][H^+][X^-] + \frac{k_{2XNO}K_{XNO}}{K_N}[X^-]$$

Equation A5.40

From Equation A5.40, Equation 7.20 in Chapter 7 can be written.

A6 Training, Conferences and Seminars

A6.1 Training

Training was made available as listed below:

Safety matters, including fire fighting, use of breathing apparatus, COSHH, departmental safety regulations

Handling of heavy equipment

Electrical appliances

Research resources and practicalities

Library resources and methods

Computing

Glassblowing services

High pressure operations

Mass spectrometry

Nuclear magnetic resonance

Analytical services

A6.2 Conferences Attended

* = poster presented

= oral presentation

RSC, Organic Reactivity, Huddersfield, September 1998 *

European Winter School in Organic Reactivity, Bressanone, Italy, January 1999 *

European Symposium on Organic Reactivity VII, Ulm, Germany, August 1999 *

RSC, Organic Reactivity, Welwyn Garden City, September 1999 *

University of Durham Graduate Symposium, June 2000 #

A6.3 Seminars

The following seminars were arranged by the Chemistry Department at the University of Durham during the tuition period in which the work in this thesis was carried out:

1997

October 8   Professor E. Atkins, Department of Physics, University of Bristol
              Advances in the Control of Architecture for Polyamides:
              From nylons to genetically engineered silks to monodisperse oligoamides

October 15   Dr. R. M. Ormerod, Department of Chemistry, Keele University
              Studying Catalysts in Action

October 21   Professor A. F. Johnson, IRC, Leeds
              Reactive Processing of Polymers: Science and Technology

October 22   Professor R. J. Puddephatt (RSC Endowed Lecture),
              University of Western Ontario
              Organoplatinum Chemistry and Catalysis

October 23   Professor M. R. Bryce, University of Durham, Inaugural Lecture
              New Tetrathiafulvalene Derivatives in Molecular,
              Supramolecular and Macromolecular Chemistry:
              Controlling the Electronic Properties of Organic Solids

October 29   Professor R. Peacock, University of Glasgow
              Probing Chirality with Circular Dichroism

October 28   Professor A. P. de Silva, The Queen's University, Belfast
              Luminescent Signalling Systems

November 5   Dr. M. Hii, Oxford University
              Studies of the Heck reaction

November 11   Professor V. Gibson, Imperial College, London
              Metallocene Polymerisation

November 12   Dr. J. Frey, Department of Chemistry, Southampton University
              Spectroscopy of Liquid Interfaces:
              From Bio-organic Chemistry to Atmospheric Chemistry

November 19   Dr. G Morris, Department of Chemistry, Manchester University
              Pulsed field Gradient NMR Techniques:
              Good News for the Lazy and DOSY

November 20   Dr. L. Spiccia, Monash University, Melbourne, Australia
              Polynuclear Metal Complexes

November 25   Dr. R. Withnall, University of Greenwich
              Illuminated Molecules and Manuscripts

November 26　Professor R. W Richards, University of Durham, Inaugural Lecture
　　　　　　　A Random Walk in Polymer Science

December 2　Dr. C. J. Ludman, University of Durham
　　　　　　　Explosions

December 3　Professor A. P. Davis, Department of Chemistry, Trinity College Dublin.
　　　　　　　Steroid-based Frameworks for Supramolecular Chemistry

December 10　Sir G. Higginson,
　　　　　　　Former Professor of Engineering in Durham and retired
　　　　　　　Vice-Chancellor of Southampton University.
　　　　　　　1981 and all that.

December 10　Professor M. Page, Department of Chemistry, University of Huddersfield
　　　　　　　The Mechanism and Inhibition of Beta-lactamases

October 27　Professor W. Roper FRS. University of Auckland, New Zealand

1998

January 14　Professor D. Andrews, University of East Anglia
　　　　　　　Energy Transfer and Optical Harmonics in Molecular Systems

January 20　Professor J. Brooke, University of Lancaster
　　　　　　　What's in a Formula? Some Chemical Controversies of the 19th Century

January 21　Professor D. Cardin, University of Reading

January 27　Professor R. Jordan, Dept. of Chemistry, University of Iowa, USA.
　　　　　　　Cationic Transition Metal and Main Group Metal Alkyl Complexes in
　　　　　　　Olefin Polymerisation

January 28　Dr. S. Rannard, Courtaulds Coatings (Coventry)
　　　　　　　The Synthesis of Dendrimers Using Highly Selective Chemical Reactions

February 3　Dr. J. Beacham, ICI Technology
　　　　　　　The Chemical Industry in the 21st Century

February 4　Professor P. Fowler, Department of Chemistry, Exeter University
　　　　　　　Classical and Non-classical Fullerenes

February 11　Professor J. Murphy, Dept of Chemistry, Strathclyde University

February 17　Dr. S. Topham, ICI Chemicals and Polymers
　　　　　　　Perception of Environmental Risk; The River Tees, Two Different Rivers

February 18　Professor G. Hancock, Oxford University
　　　　　　　Surprises in the Photochemistry of Tropospheric Ozone

February 24　Professor R. Ramage, University of Edinburgh
　　　　　　　The Synthesis and Folding of Proteins

February 25   Dr. C. Jones, Swansea University
Low Coordination Arsenic and Antimony Chemistry

March 4   Professor T. C. B. McLeish, IRC of Polymer Science Technology,
Leeds University
The Polymer Physics of Pyjama Bottoms (or the Novel Rheological Characterisation of Long Branching in Entangled Macromolecules)

March 11   Professor M. J. Cook, Dept of Chemistry, UEA
How to Make Phthalocyanine Films and what to do with them.

March 17   Professor V. Rotello, University of Massachusetts
The Interplay of Recognition & Redox Processes - from Flavoenzymes to Devices

March 18   Dr. J. Evans, Oxford University
Materials which Contract on Heating
(From Shrinking Ceramics to Bullet-proof Vests)

October 7   Dr. S. Rimmer, University of Lancaster
New Polymer Colloids

October 9   Professor M. F. Hawthorne, Department Chemistry & Biochemistry,
UCLA, USA
RSC Endowed Lecture

October 21   Professor P. Unwin, Department of Chemistry, Warwick University
Dynamic Electrochemistry: Small is Beautiful

October 23   Professor J. C. Scaiano, Department of Chemistry,
University of Ottawa, Canada
In Search of Hypervalent Free Radicals, RSC Endowed Lecture

October 26   Dr. W. Peirs, University of Calgary, Alberta, Canada
Reactions of the Highly Electrophilic Boranes $HB(C_6F_5)_2$ and $B(C_6F_5)_3$ with Zirconium and Tantalum Based Metallocenes

October 27   Professor A. Unsworth, University of Durham
What's a Joint Like this Doing in a Nice Girl Like You?
In Association with The North East Polymer Association

October 28   Professor J. P. S. Badyal, Department of Chemistry, University of Durham
Tailoring Solid Surfaces, Inaugural Lecture

November 4   Dr. N. Kaltscoyannis, Department of Chemistry, UCL, London
Computational Adventures in d & f Element Chemistry

November 3   Dr. C. J. Ludman, Chemistry Department, University of Durham
Bonfire night Lecture

November 10   Dr. J. S. O. Evans, Chemistry Department, University of Durham
Shrinking Materials

November 11   Dr. M. Wills, Department of Chemistry, University of Warwick
              New Methodology for the Asymmetric Transfer Hydrogen of Ketones

November 12   Professor S. Loeb, University of Windsor, Ontario, Canada
              From Macrocycles to Metallo-Supramolecular Chemistry

November 17   Dr. J. McFarlane
              Nothing but Sex and Sudden Death!

November 18   Dr. R. Cameron, Department of Materials Science & Metallurgy,
              Cambridge University
              Biodegradable Polymers

November 24   Dr. B. G. Davis, Department of Chemistry, University of Durham
              Sugars and Enzymes

December 1   Professor N. Billingham, University of Sussex
              Plastics in the Environment - Boon or Bane
              In association with The North East Polymer Association.

December 2   Dr. M. Jaspers, Department of Chemistry, University of Aberdeen
              Bioactive Compounds Isolated from Marine Inverterates and Cyanobacteria

December 9   Dr. M. Smith Department of Chemistry, Warwick University
              Multinuclear Solid-state Magnetic Resonance Studies of Nanocrystalline
              Oxides and Glasses

1999

January 19   Dr. J. Mann, University of Reading
              The Elusive Magic Bullet and Attempts to find it?

January 20   Dr. A. Jones, Department of Chemistry, University of Edinburgh
              Luminescence of Large Molecules:
              From Conducting Polymers to Coral Reefs

January 27   Professor K. Wade, Department of Chemistry, University of Durham
              Foresight or Hindsight? Some Borane Lessons and Loose Ends

February 3   Dr. C. Schofield, University of Oxford
              Studies on the Stereoelectronics of Enzyme Catalysis

February 9   Professor D. J. Cole-Hamilton, St. Andrews University
              Chemistry and the Future of Life on Earth

February 10   Dr. C. Bain, University of Oxford
              Surfactant Adsorption and Marangoni Flow at Expanding Liquid Surfaces

February 17   Dr. B. Horrocks, Department of Chemistry, Newcastle University
              Microelectrode Techniques for the Study of Enzymes
              and Nucleic Acids at Interfaces

February 23   Dr. C. Viney, Heriot-Watt
               Spiders, Slugs and Mutant Bugs

February 24   Dr. A.-K Duhme, University of York
               Bioinorganic Aspects of Molybdenum Transport in
               Nitrogen-Fixing Bacteria

March 3   Professor B. Gilbert, Department of Chemistry, University of York
               Biomolecular Damage by Free Radicals:
               New Insights through ESR Spectroscopy

March 9   Dr. Michael Warhurst, Chemical Policy issues, Friends of the Earth
               Is the Chemical Industry Sustainable?

March 10   Dr. A. Harrison, Department of Chemistry, The University of Edinburgh
               Designing Model Magnetic Materials

March 17   Dr. J. Robertson, University of Oxford
               Recent Developments in the Synthesis of Heterocyclic Natural Products

May 11   Dr. John Sodeau, University of East Anglia
               Ozone Holes and Ozone Hills

May 12   Dr. Duncan Bruce, Exeter University
               The Synthesis and Characterisation of Liquid-Crystalline
               Transition Metal Complexes

October 12   Dr. S. Beckett (Nestlé)
               Chocolate for the Next Millennium

October 13   Professor G. Fleet, University of Oxford
               Sugar Lactone and Amino Acids

October 19   Professor K. Gloe, TU Dresden, Germany
               Tailor Made Molecules for the Selective Binding of Metal Ions

October 20   Professor S. Lincoln, University of Adelaide
               Aspects of Complexation and Supramolecular Chemistry

October 25   Professor S. Collins, University of Waterloo, Canada
               Methacrylate Polymerization Using Zirconium Enolate Initiators:
               Polymerization Mechanisms and Control of Polymer Tacticity

October 26   Dr. D. Hughes (AstraZeneca)
               Perspectives in Agrochemistry

October 27   Dr. C. Braddock, Imperial College
               Novel Catalysts for Atom Economic Transformations

November 3   Professor D.W. Smith, University of Waikato, NZ
               The Strengths of C-C and C-H Bonds in Organic and Organometallic
               Molecules: Empirical, Semi-empirical and Ab Initio Calculations

November 10   Dr. I. Samuel, Department of Physics, University of Durham
              Improving Organic Light Emitting Diodes by Molecular,
              Optical and Device Design

November 16   Professor A. Holmes (not me!)
              Conjugated Polymers for the Market Place

November 17   Dr. J. Rourke, University of Warwick
              C-H Activation Induced by Water

November 18   Dr. G. Siligardi, Kings College London
              The Use of Circular Dichrosim to Detect and Characterise Biomolecular
              Interactions in Solution.

November 23   Professor B. Caddy
              Trace evidence - a Challenge for the Forensic Scientist

November 24   Professor T. Jones, Imperial College
              Atomic and Molecular Control of Inorganic and Organic Semiconductor
              Thin Films

November 30   Rev. R. Lancaster
              Principles and Practice

December 8   Professor D. Crout, Department of Chemistry, University of Warwick
              More than Simply Sweet: Carbohydrates in Medicine and Biology

2000

January 12   Professor D. Haddleton, Department of Chemistry, University of Warwick
              Atom Transfer Polymerisation - What's all the Hype About?

January 19   Dr. P. R. Fielden, UMIST
              Miniaturised Chemical Analysis (Lab-on-a-Chip):
              Functional or Merely Fashionable?

January 25   Professor B. Meijer
              From Supramolecular Architecture Towards Functional Materials

January 26   Professor S. Flisch, University of Edinburgh
              The Challenges Involved in Protein Glycosylation - Synthesis of Glycan
              Chains and Selective Attachment to Proteins

February 2   Chick Wilson, Head of Crytallography, ISIS, Rutherford Appleton Lab
              Protons in Motion? Neutron Diffraction Studies of Hydrogen Atoms in
              Organic Crystal Structures.

February 9   Dr. S. Moratti, University of Cambridge
              Shape and Stereoselectivity in Polymer

February 15   Professor D. Phillips
              A Little Light Relief

February 16   Professor Kocienski, University of Glasgow
                  Asymmetric Synthesis Using Planar Chiral TT-Allyl Cationic Complexes

February 23   Dr. N. Clarke, UMIST
                  The Flow of Polymer Blends

February 22   Professor G. Stuart
                  Brewing - Evolution from a Craft into a Technology

March 1   Professor D. Tildsley, Unilever (Head of Research)
                  Computer Simulation of Interfaces: Fact and Friction

March 7   Professor Motherwell, University College, London
                  Curiosity and Simplicity:
                  Essential Ingredients for the Discovery of New Reactions

March 8   Professor J. Courtieu, Universite de Paris-Sud, Orsay
                  Chiral Recognition Through NMR in Liquid Crystal Solvents:
                  An Order Affair

March 9   Dr. Antony Fairbanks, Dyson-Perrins Laboratory, Oxford
                  Selectivity in Glycoside Formation

March 20   Professor S. Marder, Professor of Chemistry and Optical Sciences,
                  University of Arizona
                  Design of Molecules for Two-Photon Absorption and their Application to
                  3D Polymerization and Imaging

March 21   Professor E. Rizzardo, CSIRO Mol. Sci. Victoria, Australia
                  Designed Polymers by Free Radical Addition-Fragmentation Processes

May 5   Professor R. Hochstrasser, University Pennsylvania, USA
                  Ultrafast Molecular and Protein Dynamics seen through their Vibrations